G7 & CALA

ABSTRACT

EFFECTS OF PSEUDOSONIC AND ELECTROACOUSTIC WAVES ON ANTENNA RADIATION

By

Garth Maxam

The purpose of this investigation is to study the properties of radiating systems immersed in hot lossy plasma media. Specifically, the dissertation considers two problems: (1) a spherical antenna coated with a finite layer of hot lossy plasma, and (2) a cylindrical antenna immersed in an infinite, hot, lossy plasma.

In the first problem, a spherical antenna, covered with a layer of plasma described by the linearized hot electron and ion equations, is studied theoretically. It is found that in the layer of hot plasma, a pseudosonic wave, an electroacoustic wave, and an electromagnetic wave can be excited by the antenna. The effects of these waves on the radiated power and input admittance of the plasmacoated antenna are investigated. Significant findings are the resonances due to the pseudosonic and electroacoustic waves and the enhanced radiation phenomenon which implies that under certain conditions a plasma-coated

antenna will radiate more power than the same antenna in free space.

In the second problem, we study theoretically and experimentally the input impedance of a cylindrical antenna immersed in an infinite, hot, lossy plasma. The theoretical development is based on the linearized hot electron equations and considers the ions to be motionless. An integral equation is developed for the current on the antenna surface. A zeroth order current distribution is assumed and a zeroth order input impedance is derived.

An experiment is performed to measure the input impedance of a cylindrical antenna in a laboratory plasma and the results are found to be in good qualitative agreement with theoretical results.

EFFECTS OF PSEUDOSONIC AND ELECTROACOUSTIC WAVES ON ANTENNA RADIATION

Ву

 ${\tt Garth}_{{\it N}}^{\overleftarrow{L}}{\tt Maxam}$

A THESIS

Submitted to
Michigan State University
in partial fulfillment of the requirements
for the degree of

DOCTOR OF PHILOSOPHY

Department of Electrical Engineering

ACKNOWLEDGMENTS

The author is eternally grateful to his major professor, Dr. K. M. Chen, for his guidance and encouragement throughout the course of this work.

He also wishes to thank the other members of the guidance committee, Dr. J. Asmussen, Dr. M. M. Gordon, Dr. G. Kemeny, and Dr. D. P. Nyquist for their time and interest in this work.

A special note of thanks is extended to the Office of Education, U.S. Department of Health, Education, and Welfare, for the National Defense Graduate Fellowship which allowed the author to complete this study. The research reported in this dissertation was supported in part by the National Science Foundation under Grant GK-2952.

Finally, the author wishes to thank his wife, Rosemary, for her encouragement, understanding, and patience throughout his graduate training program.

TABLE OF CONTENTS

									Page
LIST O	F FIGURES .		•	• •		•	•	•	vi
		PSEUDOS EXCITED SPHER		PLASM	AA-COA		JST	C	
Chapte	•								
ı.	INTRODUCTIO	ON AND BA	SIC E	QUATIO	ons .	•	•	•	1
	1.1 Motiva 1.2 Linear 1.3 Dielec	rized Hyd	rodyna			ions	•	•	1 4 14
II.	LONGITUDINA	AL WAVES	IN A I	HOT PI	LASMA	•	•	•	16
		al Relati rential E ron and I	quatio	ons fo		•	•	•	16
	Densi	ties	•				·	•	17
		and ni.					LOIIS	,	19
	2.4 Physic	cal Inter	preta	tion o	of n ₁	and	n ₂	•	23
III.	RADIATION A SPHERICAL A LAYER OF HO	ANTENNA S	URROUI	NDED E			re •	•	30
		ment of t	he Pro	oblem	and M	letho	od		2.0
		alysis .	looba		• • •		•	•	30 33
	•	n I: Die n II: Pl						•	39
		n III: PI				•	•	•	58
	3.5 Impos	ition of	Bounda	ary Co		ons	at	•	
	Inter:		and i		. Admit	· ·tan	•	•	59 71
	Jau Kaula	LEG FUWEL	auu .				- E	_	, ,

Chapte	er	Page
IV.	NUMERICAL TECHNIQUES AND RESULTS	75
	4.1 Numerical Techniques	75
	4.2 Numerical Results	81
	4.3 Conclusions	90
	PART II. RADIATION OF A CYLINDRICAL ANTENNA IN A COMPRESSIBLE PLASMA INCLUDING THE EFFECT OF AN ELECTROACOUSTIC WAVE	A.
v.	INTRODUCTION	112
	5.1 Historical Development	112
	5.2 Outline of the Investigation	115
	5.2 Outline of the investigation	113
VI.	THEORETICAL DEVELOPMENT OF THE INTEGRAL EQUATION FOR THE CURRENT ON A LINEAR ANTENNA IN A HOT LOSSY PLASMA AND THE ZEROTH ORDER SOLUTION FOR THE CURRENT DISTRIBUTION AND INPUT IMPEDANCE	116
	6.1 Geometry and Basic Equations	116
	6.2 Integral Equation Formulation	120
	6.3 Zeroth Order Current and Input	120
	Impedance	135
VII.	NUMERICAL AND EXPERIMENTAL RESULTS	138
	7.1 Numerical Techniques	138
	7.2 Numerical Results	143
	7.3 Experimental Results	148
	7.2 Numerical Results	152
REFERE	ENCES	175
APPEND	DICES	
Append	lix	
A.	Uncoupling the Differential Equations for	
	the Electrons and the Ions	180
В.	Some Properties of Legendre Functions	194

Append	lix	Page
c.	Method of the Auxiliary Integral	197
D.	The Input Resistance of a Very Thin Cylindrical Antenna in a Hot Lossless Plasma	199

LIST OF FIGURES

Figure		Page
2.1	Plot of Various Parameters Obtained in Uncoupling Equations (2.3.1) and (2.3.2). The Plasma (Oxygen Atoms) is Assumed to be Hot ($V_e/C = 0.01$, $T_e = T_i$) and Lossless ($\gamma_e = \gamma_i = 0$)	22
2.2	Phase Velocity of n_1 and n_2 in a Hot Lossless ($V_e/C = 0.01$, $T_e = T_i$, $\gamma_e = \gamma_i = 0.0$) Plasma as a Function of the Plasma Frequency Squared Over the Source Frequency Squared. The Plasma is Assumed to Consist of Oxygen	
	Atoms	25
3.1	A Spherical Antenna Covered by a Hot, Lossy Plasma	31
4.1	Theoretical Power Radiated by a Spherical Antenna in a Hot ($V_e/C=0.01$) Plasma as a Function of Plasma Density for Various Collision Frequencies	92
4.2	Theoretical Input Conductance of a Spherical Antenna in a Hot ($V_e/C = 0.01$) Plasma as a Function of Plasma Density for Various Collision Frequencies	93
4.3	Theoretical Input Susceptance of a Spherical Antenna in a Hot ($V_e/C = 0.01$) Plasma as a Function of Plasma Density for Various Collision Frequencies	94
4.4	Theoretical Power Radiated by a Small Spherical Antenna in a Hot ($V_e/C = 0.01$), Lossy, ($\gamma_e/\omega = 0.01$, $\gamma_i/\omega = 0.0000584$) Plasma as a Function of Plasma Density for Various Thicknesses of the Plasma Layer.	

Figure		Page
4.5	Theoretical Power Radiated by a Spherical Antenna in a Hot ($V_e/C=0.01$), Lossy ($\gamma_e/\omega=0.01$, $\gamma_i/\omega=0.0000584$) Plasma as a Function of Plasma Density for Various Thicknesses of the Plasma Layer	96
4.6	Theoretical Power Radiated by a Large Spherical Antenna in a Hot ($V_e/C = 0.01$), Lossy ($\gamma_e/\omega = 0.01$, $\gamma_i/\omega = 0.0000584$) Plasma as a Function of Plasma Density for Various Thicknesses of the Plasma Layer	97
4.7	Theoretical Power Radiated by a Spherical Antenna in a Hot ($V_e/C=0.01$), Lossy ($\gamma_e/\omega=0.1$, $\gamma_i/\omega=0.000584$) Plasma as a Function of Plasma Density	98
4.8	Comparison of Experimental Values by Lin and Chen [2,3] with Our Theoretical Radiation of a Spherical Antenna (a = 2.54 cm) in a Hot Lossy Plasma Driven at Various Frequencies as a Function of Plasma Density	99
4.9	Comparison of Experimental Values by Lin and Chen [2,3] with Our Theoretical Radiation of a Spherical Antenna (a = 1.27 cm) in a Hot Lossy Plasma Driven at Various Frequencies as a Function of Plasma Density	100
4.10	Theoretical Power Radiated by a Spherical Antenna in a Hot ($V_{\rm e}/{\rm C}=0.01$) Plasma as a Function of Plasma Density for Various Electron Collision Frequencies with the Ion Collision Frequency Set Equal to Zero	101
4.11	Theoretical Power Radiated by a Spherical Antenna in a Hot ($V_e/C = 0.01$) Plasma as a Function of Plasma Density for Various Collision Frequencies	102
4.12	Theoretical Input Conductance of a Spherical Antenna in a Hot $(V_e/C=0.01)$ Plasma as a Function of Plasma Density for Various Collision Frequencies	103
4.13	Theoretical Input Susceptance of a Spherical Antenna in a Hot (V _e /C = 0.01) Plasma as a Function of Plasma Density for Various	104
	Collision Frequencies	104

Figure		Page
4.14	Theoretical Power Radiated by a Spherical Antenna in a Hot ($V_e/C=0.01$), Lossy ($\gamma_e/\omega=0.01$, $\gamma_i/\omega=0.0000584$) Plasma as a Function of Plasma Density for Various Thicknesses of the Plasma Layer	105
4.15	Theoretical Power Radiated by a Spherical Antenna in a Hot ($V_e/C = 0.01$), Lossy ($\gamma_e/\omega = 0.01$, $\gamma_i/\omega = 0.0000584$) Plasma as a Function of Plasma Density for Different Size Antennas	106
4.16	Theoretical Power Radiated by a Spherical Antenna in a Hot ($V_e/C = 0.01$) Lossy ($\gamma_e/\omega = 0.01$, $\gamma_i/\omega = 0.0000584$) Plasma as a Function of Dielectric Layer Thickness for Various Plasma Densities	107
4.17	Theoretical Input Conductance of a Spherical Antenna in a Hot ($V_e/C = 0.01$) Lossy ($\gamma_e/\omega = 0.01$, $\gamma_i/\omega = 0.0000584$) Plasma as a Function of Dielectric Layer Thickness for Various Plasma Densities	108
4.18	Theoretical Input Susceptance of a Spherical Antenna in a Hot ($V_e/C = 0.01$) Lossy ($\gamma_e/\omega = 0.01$, $\gamma_i/\omega = 0.0000584$) Plasma as a Function of Dielectric Layer Thickness for Various Plasma Densities	109
4.19	Theoretical Power Radiated by a Small Spherical Antenna Surrounded by a Thin Layer of a Hot ($V_e/C=0.01$) Plasma as a Function of Plasma Density for Various Collision Frequencies	110
4.20	Theoretical Power Radiated by a Spherical Antenna Surrounded by a Thin Layer of a Hot $(V_e/C=0.01)$ Plasma as a Function of Plasma Density for Various Collision Frequencies	111
6.1	A Cylindrical Antenna of Radius a and Half Length h Immersed in an Unbounded Hot Lossy Plasma	117
6.2	Source and Field Points on or Near the Surface of the Antenna	126

Figure			Page
7.1	Experimental Setup for the Measurement of Impedance of a Cylindrical Antenna	•	150
7.2	Theoretical Input Impedance of a Monopole $(h/\lambda_O=0.147,\ a/\lambda_O=0.008)$ in a Hot $(V_e/C=0.01)$ Lossy Plasma as a Function of Plasma Density	•	154
7.3	Current Distributions on a Dipole with $h/\lambda_0=0.147$ and $a/\lambda_0=0.0072$ for Various Values of ω_e^2/ω^2 and γ/ω as a Function of z/h	•	155
7.4	Theoretical Input Impedance of a Monopole $(h/\lambda_O=0.192,\ a/\lambda_O=0.0072)$ in a Hot $(V_e/C=0.01)$ Lossy Plasma as a Function of Plasma Density	•	156
7.5	Current Distributions on a Dipole with $h/\lambda_O = 0.192$ and $a/\lambda_O = 0.0072$ for Various Values of ω_e^2/ω^2 and γ/ω as a Function of z/h	•	157
7.6	Theoretical Input Impedance of a Monopole $(h/\lambda_O=0.251,\ a/\lambda_O=0.0064)$ in a Hot $(V_e/C=0.01)$ Lossy Plasma as a Function of Plasma Density	•	158
7.7	Current Distributions on a Dipole with $h/\lambda_0=0.251$ and $a/\lambda_0=0.0064$ for Various Values of ω_e^2/ω^2 and γ/ω as a Function of z/h	•	159
7.8	Theoretical Input Impedance of a Monopole $(h/\lambda_O=0.313,\ a/\lambda_O=0.008)$ in a Hot $(V_e/C=0.01)$ Lossy Plasma as a Function of Plasma Density	•	160
7.9	Current Distributions for a Dipole with $h/\lambda_0=0.313$ and $a/\lambda_0=0.008$ for Various Values of ω_e^2/ω^2 and γ/ω as a Function of z/h	•	161
7.10	Antenna Resistance of a Cylindrical Antenna (Half Length = 0.25 $\lambda_{\rm O}$, Radius = 0.001 $\lambda_{\rm O}$) in a Hot (V _e /C = 0.01) Lossless Plasma as a Function of Plasma Density	•	162

Figure		Page
7.11	Antenna Reactance of a Cylindrical Antenna (Half Length = 0.25 $\lambda_{\rm O}$, Radius = 0.001 $\lambda_{\rm O}$) in a Hot (V _e /C = 0.01) Lossless Plasma as a Function of Plasma Density	163
7.12	Comparison of Theoretical and Experimental Current Distributions on a Monopole with $\beta oh=1.54$ and $a=0.615$ cm for Various Values of ω_e^2/ω^2 . The Driving Frequency in the Experiment was 1.25 GHz	164
7.13	Input Impedance of a Dipole of Half Length $h/\lambda_0=0.25$ Normalized to 100Ω . Normalized Electron Density (ω_e^2/ω^2) Values are Indicated	165
7.14	Input Impedance of a Dipole of Half Length $h/\lambda_0=0.12$ Normalized to 100Ω . Normalized Electron Density (ω_e^2/ω^2) Values are Indicated	166
7.15	Input Impedance of a Short Dipole Antenna in a Hot ($V_e/C = 0.001$) Lossless Plasma as a Function of Plasma Density	167
7.16	Input Impedance of a Short Dipole Antenna in a Hot ($V_e/C = 0.001$) Lossless Plasma as a Function of Plasma Density	168
7.17	Input Admittance (y = G + jH) of a Dipole Antenna in a Hot (V_e/C = 0.001) Lossless Plasma as a Function of the Plasma Density .	169
7.18	Experimental and Theoretical Input Impedance of a Monopole ($h/\lambda_O = 0.117$, $a/\lambda_O = 0.0064$) in a Hot Lossy Plasma as a Function of Plasma Density	170
7.19	Experimental and Theoretical Input Impedance of a Monopole ($h/\lambda_0 = 0.132$, $a/\lambda_0 = 0.0072$) in a Hot Lossy Plasma as a Function of	
7.20	Plasma Density	170
	in a Hot Lossy Plasma as a Function of Plasma Density	171

Figure		Page
7.21	Experimental and Theoretical Input Impedance of a Monopole ($h/\lambda_O=0.171$, $a/\lambda_O=0.0064$) in a Hot Lossy Plasma as a Function of Plasma Density	171
7.22	Experimental and Theoretical Input Impedance of a Monopole (h/λ_0 = 0.192, a/λ_0 = 0.0072) in a Hot Lossy Plasma as a Function of Plasma Density	172
7.23	Experimental and Theoretical Input Impedance of a Monopole (h/λ_0 = 0.213, a/λ_0 = 0.008) in a Lossy Hot Plasma as a Function of Plasma Density	172
7.24	Experimental and Theoretical Input Impedance of a Monopole ($h/\lambda_O=0.251$, $a/\lambda_O=0.0064$) 0.0064) in a Hot Lossy Plasma as a Function of Plasma Density	173
7.25	Experimental and Theoretical Input Impedance of a Monopole ($h/\lambda_0=0.282$, $a/\lambda_0=0.0072$) in a Hot Lossy Plasma as a Function of Plasma Density	173
7.26	Experimental and Theoretical Input Impedance of a Monopole ($h/\lambda_0 = 0.313$, $a/\lambda_0 = 0.008$) in a Hot Lossy Plasma as a Function of Plasma Ponsity	174

PART I

PSEUDOSONIC AND ELECTROACOUSTIC WAVES EXCITED BY A PLASMA-COATED SPHERICAL ANTENNA

CHAPTER I

INTRODUCTION AND BASIC EQUATIONS

The research described in this part of the dissertation is concerned with the radiation of a spherical antenna through a concentric layer of a compressible plasma surrounding the antenna. The antenna is assumed to be separated from the plasma by a thin sheath region which is also concentric with the sphere.

In this chapter we motivate the above problem and give some of the historical background dealing with this problem. Also, the linearized hydrodynamic equations are developed and discussed.

1.1 Motivation and Background

The study of an antenna surrounded by a finite layer of plasma is motivated by two important unsolved problems:

(1) the well-known "blackout" phenomenon which occurs when a satellite reënters the atmosphere, and (2) the audible noise generated by power lines when a corona forms on the conductors of the line.

The conventional approach to solve the blackout phenomenon is to raise the antenna frequency to a level above the electron plasma frequency of the surrounding plasma medium. This approach is usually hampered by the practical limitation of available high-frequency sources.

In this dissertation it will be shown that under certain conditions the radiation of a spherical antenna covered by a concentric spherical layer of plasma can be enhanced if the antenna frequency is adjusted to be much lower than the electron plasma frequency.

The phenomenon of enhanced radiation from a small antenna covered by a cold collisionless plasma layer was first studied by Messian and Vandenplas [1] in 1967. Lin [2] and Lin and Chen [3] later studied the same problem and extended it to include the electroacoustic wave and collisional losses in the plasma. The electroacoustic wave consists of a longitudinal compression of the electron fluid with the ions forming a uniform positive background necessary for overall charge neutrality.

In this work the same problem is again studied but this time, effects due to the finite temperature of the ions are included. It is shown that a psuedosonic wave may propagate in the plasma for antenna frequencies much less than the electron plasma frequency of the medium.

Pseudosonic waves are longitudinal compression waves in a plasma which are quite analogous to sound waves

in a gas. The election and ion fluids are constrained to move very nearly in phase by the requirement that the plasma remain nearly neutrally charged.

Pseudosonic waves were first predicted theoretically by Tonks and Langmuir [4] in 1929 and probably first observed experimentally by Revans [5] in 1933. Since 1933 pseudosonic waves have been observed by many other workers in the area such as Barrett and Little [6] and Alexeff, Jones, and Lonngren [7].

Cook and Buchanan [8] have shown that a significant amount of power may be radiated in the pseudosonic wave into an infinite plasma above a ground plane. The excitation they use is an infinitesimal slot in the ground plane.

When an antenna on a reëntry vehicle is covered by a plasma layer and suffers blackout, a possible scheme of overcoming this problem will be to reduce the antenna frequency to a value which will excite the pseudosonic wave in plasma. The pseudosonic wave will excite an electromagnetic wave at the outer surface of the plasma and, thus, radio contact with the space vehicle may be maintained.

The second problem stated earlier, that of the audible noise generated by power lines in the presence of a corona, is not solved here but the mechanisms discussed may be those involved in that problem. More needs to be done to verify this.

The remainder of this chapter is devoted to a discussion of the basic linearized hydrodynamic equations to be used later. Chapter II studies the pseudosonic and the electroacoustic waves in an infinite plasma while Chapter III applies the results of Chapter II to the specific problem of a spherical antenna covered by a spherical layer of compressible plasma. Chapter IV discusses the techniques used to numerically solve the problem in Chapter III and discusses some specific numerical results.

1.2 Linearized Hydrodynamic Equations

It is necessary to specify a mathematical model to describe the antenna and the plasma in order to determine their interaction. The hydrodynamic model of the plasma which is used throughout this investigation is presented in this section. A discussion of the models used for the spherical antenna is presented in later chapters.

Basically there are two ways of describing a plasma: a microscopic gas-kinetic treatment using the Boltzmann equation together with Maxwell's equations of electrodynamics; or a macroscopic, hydrodynamic approach using the momentum transport equations together with Maxwell's equations. The kinetic theory treatment is generally much more difficult mathematically and requires serious physical restrictions be placed on the model to make the

problem tractable. For this reason the hydrodynamic equations together with Maxwell's equations are used throughout this investigation. It must be noted that the hydrodynamic equations do not describe Landau damping which is included in the more general kinetic theory. Thus, in following investigation, caution should be exercised when the phase velocity of the waves is nearly equal to the average thermal velocity of the plasma components because in this range Landau damping can be significant [9].

A plasma consists of electrons, ions, and neutral particles. The neutral particles contribute to the dynamics of the plasma by collisions with the charged particles and are considered by including a neutral particle collision frequency for the electrons and the ions. Thus, in our investigation, the plasma consists of two fluids, the electrons and the ions.

The basic equations may be written in such a general way that both the problem in this part and the problem in Part II are included as special cases. Gravitational forces, static electrical and magnetic fields, and macroscopic gradients of density and temperature are not included in this analysis. The plasma is assumed to be macroscopically neutral and consists, on the average, of n_{o} electrons per meter³, and of the same number of singly ionized ions.

Let \tilde{E} and \tilde{H} be the time varying electrical and magnetic fields and let \tilde{V}_{e} and \tilde{V}_{i} represent the average fluid velocities of the electrons and the ions. The universal constants are the elementary charge (electron charge: -e); the electron and ion masses m_{e} and m_{i} ; the permeability of free space μ_{o} ; and the permittivity of free space ϵ_{o} . The MKS system of units is used throughout.

The hydrodynamic equations of motion for electrons and ions are [10]

$$\frac{\partial}{\partial t} \overset{\nabla}{\nabla}_{e} + (\overset{\nabla}{\nabla}_{e} \cdot \nabla) \overset{\nabla}{\nabla}_{e} = -\frac{e}{m_{e}} [\overset{E}{\Sigma} + \overset{\nabla}{\nabla}_{e} \times \overset{B}{\Sigma}]$$

$$-\frac{1}{N_{e}m_{e}} \overset{\nabla}{\nabla}_{e} - \gamma_{e} \overset{\nabla}{\nabla}_{e}$$

$$\frac{\partial}{\partial t} \overset{\nabla}{\nabla}_{i} + (\overset{\nabla}{\nabla}_{i} \cdot \nabla) \overset{\nabla}{\nabla}_{i} = \frac{e}{m_{i}} [\overset{E}{\Sigma} + \overset{\nabla}{\nabla}_{i} \times \overset{B}{\Sigma}]$$

$$-\frac{1}{m_{i}N_{i}} \overset{\nabla}{\nabla}_{i} - \gamma_{i} \overset{\nabla}{\nabla}_{i}. \qquad (1.2.2)$$

These equations include a damping term proportional to the velocities where γ_e and γ_i are termed the mean electron-neutral particle collision frequency and the mean ion-neutral particle collision frequency. P_e and P_i are scalar pressures for electrons and ions. The gradients of these pressures are discussed in detail later. The equations of continuity are

$$\nabla \cdot (N_{e} \nabla_{e}) + \frac{\partial}{\partial t} N_{e} = 0 \qquad (1.2.3)$$

$$\nabla \cdot (N_i \nabla_i) + \frac{\partial}{\partial t} N_i = 0 \qquad (1.2.4)$$

The Maxwell equations become

$$\nabla \times E = - u_0 \frac{\partial H}{\partial t}$$
 (1.2.5)

$$\nabla \times H = J^{S} + e(N_{i}V_{i} - N_{e}V_{e}) + \varepsilon_{o} \frac{\partial E}{\partial t}$$
 (1.2.6)

$$\nabla \cdot \mathbf{H} = \mathbf{0}$$

where $\rho^{\mbox{S}}$ and $\mbox{J}^{\mbox{S}}$ are externally supplied sources and are related by

$$\frac{\partial \rho^{S}}{\partial t} + \nabla \cdot J^{S} = 0 \tag{1.2.7}$$

Equations (1.2.1) through (1.2.7) are nonlinear and hence are very difficult to solve exactly. In order to simplify the equations, a small signal excitation is assumed. That is, the various field quantities are assumed to be of the form

$$E(r,t) = E_{DC}(r) + E_{AC}(r,t)$$
 (1.2.8)

$$H(r,t) = H_{DC}(r) + H_{AC}(r,t)$$
 (1.2.9)

$$v_{e}(r,t) = v_{eo}(r) + v_{e}(r,t)$$
 (1.2.10)

e;

Sţ CC

$$v_{i}(r,t) = v_{io}(r) + v_{i}(r,t)$$
 (1.2.11)

$$N_e(r,t) = N_{eo}(r) + n_e(r,t)$$
 (1.2.12)

$$N_{i}(r,t) = N_{io}(r) + n_{i}(r,t)$$
 (1.2.13)

where E_{DC} , E_{DC} , E_{DC} , E_{OC} ,

In this investigation it is assumed that the average electron and ion densities are equal and do not vary with position

$$N_{eO} (r) \equiv n_{O} \equiv N_{iO} (r)$$
 (1.2.14)

and that the average electron and ion velocities are zero since allowing V_{eo} and V_{io} to be finite introduces no new physical results but it does seriously complicate the mathematics [11]. In addition in this investigation externally applied static fields are not considered and static electric fields set up in sheath regions are not considered hence

$$H_{DC}(r) = E_{DC}(r) = 0.$$
 (1.2.15)

In general the ion and the electron fluids can be considered to act as neutral particle gaseous media with one main difference. The interactions of particles in an ion or electron fluid are over much larger distances than those for neutral particles.

For both fluids we will later be concerned with ∇P where P is the pressure of the fluid.

If we are concerned with a static pressure (D.C. case), the pressure is established by an isothermal process. That is, the temperature of the gas is fixed throughout the volume of interest, then

$$P = n k T$$
 (1.2.17)

where T is the fixed temperature of the fluid, n is the number density of the fluid and k is Boltzmann's constant.

If an external force disturbs n, such that

$$n(r,t) = n_0(r) + n_1(r,t)$$
 (1.2.18)

and n is a fast function of time such as a high frequency disturbance, then the temperature of the gas is not fixed simply due to the fact that there is not enough time for the exchanging of energies in the gas to keep the temperature fixed. In this type of problem, the adiabatic law should be used, that is

$$Pn^{-\gamma} = constant$$
 (1.2.19)

where γ is the ratio of specific heats such that

$$\gamma = \frac{C_{\rm P}}{C_{\rm V}} = \frac{m + 2}{m} \tag{1.2.20}$$

where m is the degrees of freedom of the gas.

For high frequency plasma oscillations, the motion of the electrons is usually in one direction only, so we can assume m=1, so that $\gamma=3$.

Now for the case of a small r.f. perturbation, as in eqn. (1.2.18), the relationship between pressure and election density is

$$Pn^{-\gamma} = P_O n_O^{-\gamma} = constant$$
 (1.2.20)

since $P = P_0$ and $n = n_0$ initially. Then

$$P = P_O \left(\frac{n}{n_O}\right)^{\gamma} . \qquad (1.2.21)$$

Remembering that the static pressure is established by an isothermal process, we have

$$P_{O} = n_{O} k T$$
 (1.2.22)

Therefore

$$\begin{split} \nabla P &= \nabla \left[P_{O} \left(\frac{n}{n_{O}} \right)^{\gamma} \right] \\ &= \left(\frac{n}{n_{O}} \right)^{\gamma} \nabla P_{O} + P_{O} \nabla \left(\frac{n}{n_{O}} \right)^{\gamma} \\ &= \left(1 + \frac{n_{1}}{n_{O}} \right)^{\gamma} \nabla P_{O} + P_{O} \nabla \left[1 + \frac{n_{1}}{n_{O}} \right]^{\gamma} \\ &= \left(1 + \frac{n_{1}}{n_{O}} \right)^{\gamma} k T \nabla n_{O} + k T n_{O} \left[\gamma \left(1 + \frac{n_{1}}{n_{O}} \right)^{\gamma - 1} \nabla \left(\frac{n_{1}}{n_{O}} \right) \right] \\ &= \left(1 + \frac{n_{1}}{n_{O}} \right)^{\gamma} k T \nabla n_{O} + k T n_{O} \left[\gamma \left(1 + \frac{n_{1}}{n_{O}} \right)^{\gamma - 1} \frac{n_{O} \nabla n_{1} - n_{1} \nabla n_{O}}{n_{O}^{2}} \right] \\ &= k T \left[\left(1 + \frac{n_{1}}{n_{O}} \right)^{\gamma} - \gamma \left(1 + \frac{n_{1}}{n_{O}} \right)^{\gamma - 1} \frac{n_{1}}{n_{O}} \right] \nabla n_{O} \\ &+ \gamma k T \left(1 + \frac{n_{1}}{n_{O}} \right)^{\gamma - 1} \nabla n_{1} \end{split}$$

or since n₁ << n₀

$$\nabla P = kT \nabla n_0 + \gamma kT \nabla n_1. \qquad (1.2.23)$$

For the case of a uniform average electron density, n_0 ,

$$\nabla n_{O} = 0, \qquad (1.2.24)$$

so that

$$\nabla P = \gamma k T \nabla n_1. \qquad (1.2.25)$$

For our case of a two fluid gas, we have

$$\nabla P_e = 3kT_e \nabla n_e(r) \qquad (1.2.26)$$

and

$$\nabla P_{i} = 3kT_{i} \nabla n_{i} (r). \qquad (1.2.27)$$

Assuming an $e^{j\omega t}$ suppressed time dependence along with the above assumptions and neglecting products of small perturbation quantities, the linearized hydrodynamic equations and Maxwell's equations in a plasma media are

$$\nabla \times E_{AC} = -j\omega u_{O} H_{AC} \qquad (1.2.28)$$

$$\nabla \times H_{AC} = J^{S} + j\omega \varepsilon_{O} E_{AC} + en_{O}(v_{i} - v_{e}) \qquad (1.2.29)$$

$$n_{O} \nabla \cdot v_{e} + j \omega n_{e} = 0 \qquad (1.2.30)$$

$$n_0 \nabla \cdot v_i + j \omega n_i = 0 \qquad (1.2.31)$$

$$(j\omega + \gamma_e)_{e}^{v} = -\frac{e}{m_e} E - \frac{3kT_e}{n_o m_e} \nabla n_e$$
 (1.2.32)

$$(j\omega + \gamma_{i})v_{i} = \frac{e}{m_{i}} E - \frac{3kT_{i}}{n_{0}m_{i}} \nabla n_{i}$$
 (1.2.33)

Equations (1.2.28) thru (1.2.33) are a complete set of equations which along with the source continuity equation, equation (1.2.7), completely describe the fields in a plasma medium.

In a study of plasma media, certain characteristic parameters appear frequently. It is convenient to make the following symbolic definitions. ω_e , the electron plasma frequency or simply the electron frequency is defined by

$$\omega_e^2 = \frac{n_o e^2}{m_e \varepsilon_o} \tag{1.2.34}$$

while $\boldsymbol{\omega}_{\text{i}}\text{,}$ the ion plasma frequency is

$$\omega_{i}^{2} = \frac{m_{e}}{m_{i}} \omega_{e}^{2} = \frac{n_{o}e^{2}}{m_{i}\varepsilon_{o}}$$
 (1.2.35)

Another pair of parameters, the thermal velocities, of the electrons $\mathbf{V}_{\mathbf{e}}$ and of the ions $\mathbf{V}_{\mathbf{i}}$ are defined by

$$v_e^2 = \frac{3kT_e}{m_e}$$
 (1.2.36)

$$v_i^2 = \frac{3kT_i}{m_i}$$
 (1.2.37)

The definitions (1.2.36) and (1.2.37) are debatable, but other commonly used definitions lead to the same order of magnitude result as long as the linearized equations are used [11]. Therefore, these definitions are used in this investigation. Characteristic lengths in a plasma are often measured in terms of the Debye lengths, which for the electrons is

$$(\lambda_{D})_{e}^{2} = \frac{\varepsilon_{O}^{kT}_{e}}{n_{O}e^{2}}$$
 (1.2.38)

and for the ions is

$$(\lambda_D)_i^2 = \frac{\varepsilon_0^{kT_i}}{n_0^{e^2}}.$$
 (1.2.39)

Physically the Debye length is range of effectiveness of any electrostatic fields due either to a surface at some nonzero potential or to a charge within a plasma.

1.3 Dielectric Sheath

When a conducting solid is placed in an otherwise homogeneous plasma medium, a transition region between the main body of the plasma and the solid is formed. If the potential of the object is allowed to float, the object will acquire a negative potential and the electrical neutrality of the plasma will be disturbed in the vicinity of the object. Due to the high thermal velocity of the electrons with respect to the ions, the object will become negatively charged so that at equilibrium, equal numbers of electrons and ions will hit the object per unit time. The potential distribution in the vicinity of the object causes a perturbation of the number densities of the electrons and the ions. The electron density in this transition region is less than the ion density and, thus, the transition region for such a situation is called an

ion sheath region. From an electrical viewpoint, this sheath behaves as a vacuum sheath, or simply as a dielectric sheath.

In this investigation, the sheath region will be considered as an electron depletion layer, or a vacuum adjacent to the antenna. It is assumed that the outer boundary of the sheath is rigid to the elections and ions in the plasma and, thus, it reflects all particles that come into contact with it. Also, the sheath layer is taken to be a few Debye lengths in thickness [12].

CHAPTER II

LONGITUDINAL WAVES IN A HOT PLASMA

In this chapter we devote our attention to two purely longitudinal waves that are excited in an infinite hot lossy plasma by a source current $\mathbf{J}^{\mathbf{S}}$ and source charge density $\rho^{\mathbf{S}}$. The plasma is considered to be a weakly ionized gas so that linearized hydrodynamic equations developed in Chapter I may be used.

2.1 General Relations

The source terms are related by the continuity equation

$$\nabla \cdot J^{S} + j\omega \rho^{S} = 0 \qquad (2.1.1)$$

From Chapter I the linearized equations of motion for the electrons are

$$j\omega n_{e} + n_{o} \nabla \cdot v_{e} = 0 \qquad (2.1.2)$$

$$(j\omega + \gamma_e)_{e}^{v} = -\frac{e}{m_e} - \frac{v_e^2}{n_o} \nabla n_e$$
 (2.1.3)

and the linearized equations of motion for the ions are

$$j\omega n_{i} + n_{O} \nabla \cdot v_{i} = 0 \qquad (2.1.4)$$

$$(j\omega + \gamma_{i})v_{i} = + \frac{e}{m_{i}} \frac{E}{c} - \frac{v_{i}^{2}}{n_{o}} \nabla n_{i}$$
 (2.1.5)

The fields E and H in the plasma satisfy Maxwell's equations which from Chapter I are

$$\nabla \times \mathbf{E} = -j\omega \mathbf{u}_{\mathbf{O}}^{\mathbf{H}} \tag{2.1.6}$$

$$\nabla \times H = J^{S} + en_{O}(v_{i} - v_{e}) + j\omega \varepsilon_{O^{c}}$$
 (2.1.7)

2.2 <u>Differential Equations for the Electron</u> and Ion Perturbation Densities

Rearranging equations (2.1.2) and (2.1.4), we have

$$\nabla \cdot \mathbf{v}_{e} = -\frac{\mathbf{j}\omega}{\mathbf{n}_{o}} \mathbf{n}_{e} \tag{2.2.1}$$

$$\nabla \cdot \mathbf{v}_{i} = -\frac{\mathbf{j}\omega}{\mathbf{n}_{0}} \mathbf{n}_{i}. \tag{2.2.2}$$

Taking the divergence of equation (2.1.7) yields

$$0 = \nabla \cdot J^{S} + en_{O}(\nabla \cdot v_{i} - \nabla \cdot v_{e}) + j\omega \varepsilon_{O} \nabla \cdot E \quad (2.2.3)$$

or using equations (2.2.1) and (2.2.2) and rearranging,

$$\nabla \cdot \mathbf{E} = \frac{\mathbf{j}}{\omega \varepsilon_{0}} \left[\nabla \cdot \mathbf{J}^{S} - \mathbf{j} \omega e (\mathbf{n}_{i} - \mathbf{n}_{e}) \right]. \tag{2.2.4}$$

Taking the divergences of equations (2.1.3) and (2.1.5) gives

$$(j\omega + \gamma_e)\nabla \cdot v_e = -\frac{e}{m_e}\nabla \cdot E - \frac{v_e^2}{n_o}\nabla^2 n_e$$
 (2.2.5)

and

$$(j\omega + \gamma_{i}) \nabla \cdot v_{i} = \frac{e}{m_{i}} \nabla \cdot E - \frac{v_{i}^{2}}{n_{o}} \nabla^{2} n_{i}. \qquad (2.2.6)$$

Putting equations (2.2.1) and (2.2.4) into equation (2.2.5) and multiplying through by $-n_O/V_e^2$ and rearranging yields

$$\nabla^{2} n_{e} + \frac{\omega^{2}}{v_{e}^{2}} \left[1 - \frac{\omega e^{2}}{\omega^{2}} - \frac{j \gamma_{e}}{\omega} \right] n_{e} + \frac{\omega_{e}^{2}}{v_{e}^{2}} n_{i}$$

$$= - j \frac{\omega_e^2}{V_e^2 e \omega} \nabla \cdot J^S \qquad (2.2.7)$$

where $\omega_e = \sqrt{n_e^2/m_e \epsilon_o}$ is the electron plasma frequency. Using the equation of continuity for the sources and setting

$$\beta_{e}^{2} = \frac{\omega_{e}^{2}}{V_{e}^{2}} \left[1 - \frac{\omega_{e}^{2}}{\omega^{2}} - j \frac{\gamma_{e}}{\omega} \right]. \qquad (2.2.8)$$

we get

$$\nabla^{2} n_{e} + \beta_{e}^{2} n_{e} + \frac{\omega_{e}^{2}}{v_{e}^{2}} n_{i} = -\frac{\omega_{e}^{2}}{v_{e}^{2}} \frac{\rho^{S}}{e}$$
 (2.2.9)

By a similar procedure starting with equations (2.2.2), (2.2.4), and (2.2.6) we obtain

$$\nabla^{2} n_{i} + \beta_{i}^{2} n_{i} + \frac{\omega_{i}^{2}}{v_{i}^{2}} n_{e} = \frac{\omega_{i}^{2}}{v_{i}^{2}} \frac{\rho^{S}}{e}$$
 (2.2.10)

where

$$\beta_{i}^{2} = \frac{\omega^{2}}{v_{i}^{2}} \left[1 - \frac{\omega^{2}}{\omega_{i}^{2}} - j \frac{\gamma_{i}}{\omega} \right]$$
 (2.2.11)

and $\omega_i = \sqrt{n_0 e^2/m_i \epsilon_0}$ is the ion plasma frequency.

Equations (2.2.9) and (2.2.10) are two coupled differential equations for the electron and ion perturbation densities.

Multiplying equation (2.2.9) by V_e/ω_e and equation (2.2.10) by V_i/ω_i , we obtain

$$\nabla^{2} \left[\frac{\mathbf{v}_{e}}{\omega_{e}} \, \mathbf{n}_{e} \right] + \beta_{e}^{2} \left[\frac{\mathbf{v}_{e}}{\omega_{e}} \, \mathbf{n}_{e} \right] + \frac{\omega_{e}^{\omega_{i}}}{\mathbf{v}_{e}^{V_{i}}} \left[\frac{\mathbf{v}_{i}}{\omega_{i}} \, \mathbf{n}_{i} \right] = - \frac{\omega_{e}}{\mathbf{v}_{e}} \, \frac{\rho^{S}}{e}$$
(2.3.1)

and

$$\nabla^{2} \left(\frac{\mathbf{v_{i}}}{\omega_{i}} \, \mathbf{n_{i}} \right) + \beta_{i}^{2} \left(\frac{\mathbf{v_{i}}}{\omega_{i}} \, \mathbf{n_{i}} \right) + \frac{\omega_{e}^{\omega_{i}}}{\mathbf{v_{e}^{v_{i}}}} \left(\frac{\mathbf{v_{e}}}{\omega_{e}} \, \mathbf{n_{e}} \right) = \frac{\omega_{i}}{\mathbf{v_{i}}} \, \frac{\rho^{S}}{e} . \tag{2.3.2}$$

Equations (2.3.1) and (2.3.2) can be written compactly as the matrix equation

$$\nabla^{2}_{n} + \beta_{n} = \frac{\rho^{S}}{e} S \qquad (2.3.3)$$

where

$$\tilde{n} = \begin{bmatrix} \frac{V_{e}}{\omega_{e}} & n_{e} \\ \frac{V_{i}}{\omega_{i}} & n_{i} \end{bmatrix}$$

$$\tilde{\beta} = \begin{bmatrix} \tilde{\beta}_{e}^{2} & \frac{\omega_{e}^{\omega_{i}}}{V_{e}V_{i}} \\ \frac{\omega_{e}^{\omega_{i}}}{V_{e}V_{i}} & \tilde{\beta}_{i}^{2} \end{bmatrix}$$

$$\tilde{S} = \begin{bmatrix} -\frac{\omega_{e}}{V_{e}} \\ \frac{\omega_{i}}{V_{e}} \end{bmatrix}$$
(2.3.4)

In Appendix A it is shown that equations (2.3.1) and (2.3.2) can be uncoupled resulting in two differential equations which describe two new waves n_1 , an ion wave and an electron wave denoted by n_2 . The differential equations that describe n_1 and n_2 are

$$\nabla^2 n_1 + k_1^2 n_1 = s_1 \frac{\rho^S}{e}$$
 (2.3.5)

$$\nabla^2 n_2 + k_2^2 n_2 = S_2 \frac{\rho_S}{e}$$
 (2.3.6)

where

$$k_1^2 = \frac{1}{2} \left[\beta_e^2 + \beta_i^2 + \sqrt{(\beta_i^2 - \beta_e^2)^2 + 4 \frac{\omega_e^2 \omega_i^2}{v_e^2 v_i^2}} \right]$$
 (2.3.7)

and

$$k_2^2 = \frac{1}{2} \left[\beta_e^2 + \beta_i^2 - \sqrt{\beta_i^2 - \beta_e^2 + 4 \frac{\omega_e^2 \omega_i^2}{v_e^2 v_i^2}} \right]$$
 (2.3.8)

and s_1 and s_2 are defined in Appendix A. s_1 and s_2 are linear combinations of s_2 and s_3

$$n_e = \frac{\omega_e}{V_A} (T_{11}^{n_1} + T_{12}^{n_2})$$
 (2.3.9)

$$n_{i} = \frac{\omega_{i}}{V_{i}} (T_{21}^{n_{1}} + T_{22}^{n_{2}})$$
 (2.3.10)

where T₂₂, T₁₂, T₂₁, and T₁₁ are given in Appendix A. Equations (2.3.5) thru (2.3.10) provide a complete solution for the electron perturbation density and the ion perturbation density in an infinite homogeneous plasma.

Figure 2.1 is a plot of the coefficients relating n_e and n_1 to n_1 and n_2 and of S_1 and S_2 versus ω_e^2/ω^2 .

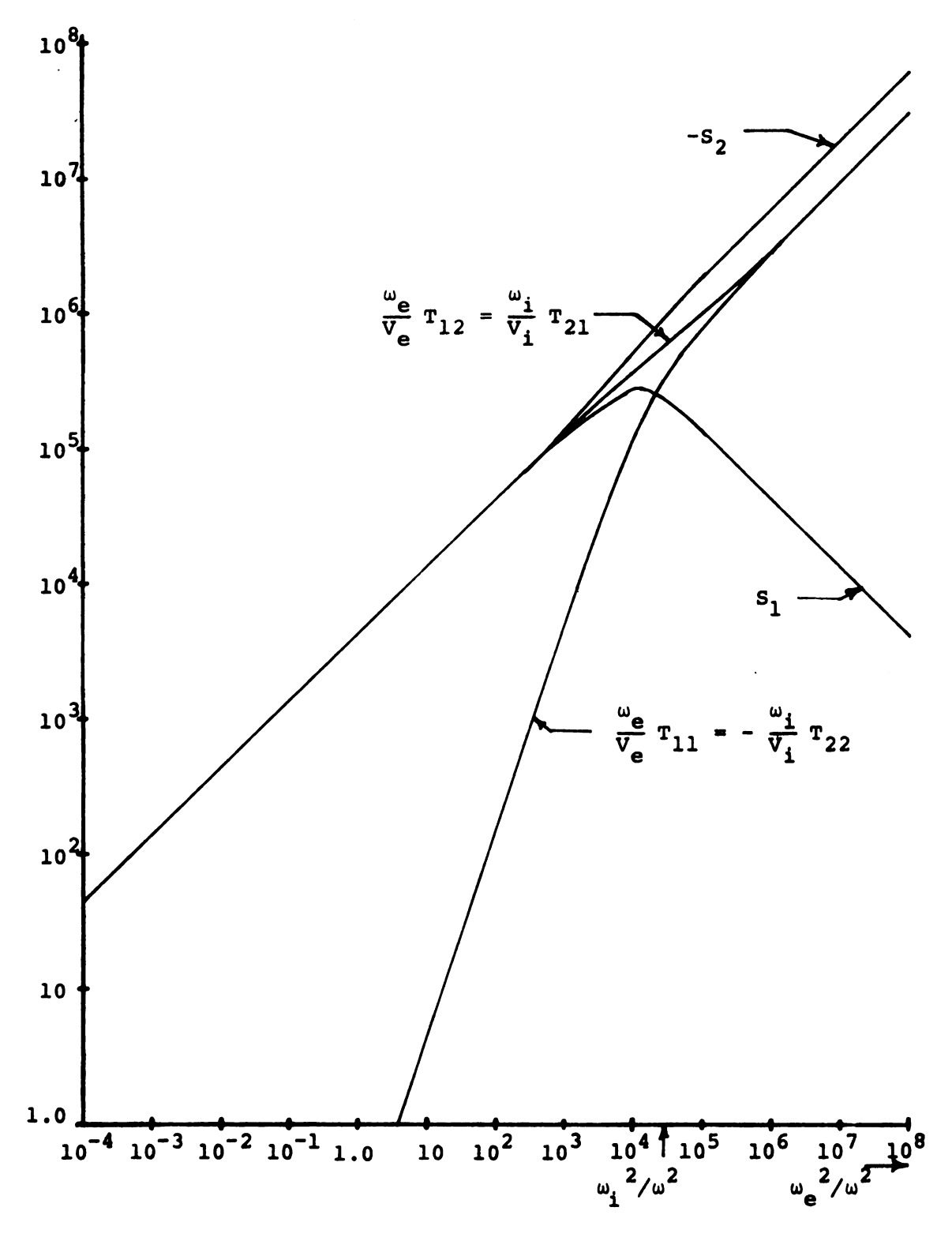


Figure 2.1. Plot of various parameters obtained in uncoupling Equations (2.3.1) and (2.3.2). The plasma (oxygen atoms) is assumed to be hot $(V_e/C=0.01,\,T_e=T_i)$ and lossless $(\gamma_e=\gamma_i=0)$.

٩Ŋ

2.4 Physical Interpretation of n₁ and n₂

In order to discuss n_1 and n_2 in more detail it is necessary to specialize equations (2.1.2) thru (2.1.5) to the specific case of a monochromatic plane wave which propagates in the positive z direction in a cartesian coordinate system. The variables describing the wave are expressed in the form:

$$A = A_0 e^{j(\omega t - kz)}$$
 (2.4.1)

where $A_{\sim O}$ is, in general, a complex coefficient.

We use the following linear operator:

$$\nabla = - j \underset{\sim}{k}$$
 (2.4.2)

where k is the propagation vector in the z direction.

Equations (2.1.2) and (2.1.4) can be written as

$$n_{e} = n_{O}kv_{ez}/\omega \tag{2.4.3}$$

$$n_{i} = n_{O}kv_{i,z}/\omega \qquad (2.4.4)$$

and the z components of equations (2.1.3) and (2.1.5) are

$$(j\omega + \gamma_e)v_{ez} = -\frac{e}{m_e}E_z + j\frac{v_e^2}{n_o}kn_e$$
 (2.4.5)

$$(j\omega + \gamma_i)v_{iz} = \frac{e}{m_i}E_z + j\frac{v_i^2}{n_0}kn_i.$$
 (2.4.6)

Specializing equations (2.4.5) and (2.4.6) to a collision-less plasma ($\gamma_e = \gamma_i = 0$) and solving for v_{ez} and v_{iz} yields

$$v_{ez} = -j \frac{e}{m_e} \frac{\omega}{k^2 v_e^2 - \omega^2} E_z$$
 (2.4.7)

$$v_{iz} = j \frac{e}{m_i} \frac{\omega}{k^2 V_i^2 - \omega^2} E_z.$$
 (2.4.8)

The electron and ion average velocities are seen to be 90° out of phase with the electric field. In addition the simple theory predicts singularities at $k = \omega/V_e$ and $k = \omega/V_e$ due to the use of the linearized equations.

Two other useful quantities are the phase velocities of n_1 and n_2

$$v_{ph_1} = \frac{\omega}{k_1} \tag{2.4.9}$$

$$v_{ph_2} = \frac{\omega}{k_2} \tag{2.4.10}$$

for a collisionless plasma. Figure 2.2 shows a plot of $V_{\rm ph_1}$ and $V_{\rm ph_2}$ versus $\omega_{\rm e}^{\,2}/\omega^{\,2}$ for a weakly ionized collisionless hydrogen gas at equilibrium $(T_{\rm e} = T_{\rm i})$. A study of Figure 2.2 indicates that n_1 propagates at all frequencies but that n_2 propagates only when $\omega > \omega_{\rm e}$. It must be noted that this theory does not include collisionless or Landau

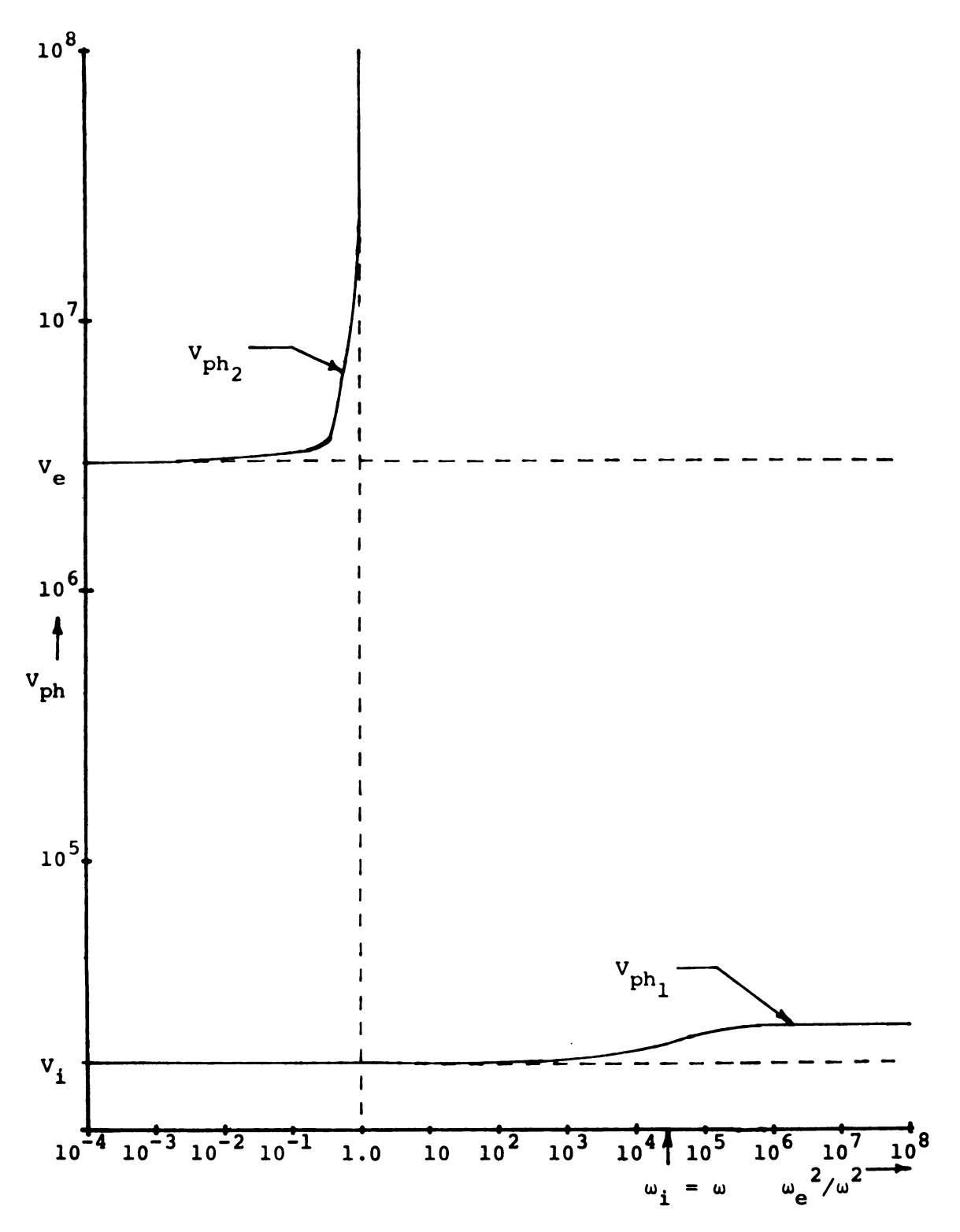


Figure 2.2. Phase velocity of n_1 and n_2 in a hot lossless ($V_e/C = 0.01$, $T_e = T_i$, $\gamma_e = \gamma_i = 0.0$) plasma as a function of the plasma frequency squared over the source frequency squared. The plasma is assumed to consist of oxygen atoms.

damping which damps n_1 when $v_{ph_1} \approx v_i$ and n_2 when $v_{ph_2} = v_e$.

Some physical insight into the nature of n_1 and n_2 can be obtained by studying these waves in the high and low frequency limits. Using the parameter

$$\frac{v_{iz}}{v_{ez}} = -\frac{m_e}{m_i} \frac{k^2 v_e^2 - \omega^2}{k^2 v_i^2 - \omega^2}$$
 (2.4.11)

and choosing freely from limit forms of the parameters k_1 , k_2 , T_{11} , T_{12} , T_{21} , and T_{22} calculated in Appendix A, this will now be done.

(a) Electron Waves, n₂

In the high frequency limit $(\omega^2 > \omega_e^2 >> \omega_i^2)$

$$k_2 \stackrel{\sim}{=} \frac{\omega}{V_e} \left[1 - \frac{\omega_e^2}{\omega^2} \right]^{\frac{1}{2}}$$
 (2.4.12)

and

$$n_2 \approx -\frac{v_e}{\omega_e} n_e \qquad (2.4.13)$$

and
$$\frac{v_{iz}}{v_{ez}} = -\frac{m_e}{m_i} \frac{\omega_e^2}{\omega^2}$$
. (2.4.14)

Result (2.4.14) shows that in the electron wave in the high frequency limit the ions are essentially immobile. This agrees with equation (2.4.13) which says that in the high frequency limit, the electron wave n_2 consists only of

electron oscillations. Equation (2.4.14) also shows that in the electron wave, the ions and electrons oscillate out of phase. From equation (2.4.12) it can be seen that V_{ph_2} ,

$$v_{ph_2} \approx v_e / \sqrt{1 - \omega_e^2 / \omega^2},$$
 (2.4.15)

is always greater than the thermal velocity of the electrons and that in the very high frequency limit $(\omega^2 >> \omega_e^2)$ the phase velocity of n_2 tends to V_e .

In the low frequency limit (in fact for all $\omega < \omega_e$) k_2 is purely imaginary and the electron wave does not propagate.

(b) Ion Waves, n₁

For the ion wave, the phase velocity is always in the range

$$v_i < v_{ph_1} < v_S$$
 (2.4.16)

where V_S is the low frequency limit of the phase velocity of the ion wave:

$$v_S = \sqrt{\frac{3k(T_e + T_i)}{m_i}}$$
 (2.4.17)

On the other hand, the electron temperature is, in most cases, equal to or greater than the ion temperature. Hence \mathbf{V}_{S} is much smaller than \mathbf{V}_{e} , giving

$$v_{ph_1} \ll v_e.$$
 (2.4.18)

In the high frequency limit

$$\begin{vmatrix} v_{iz} \\ v_{ez} \end{vmatrix} \longrightarrow \infty \tag{2.4.19}$$

indicating the electron velocity is much smaller than the ion velocity. In the high frequency limit \mathbf{n}_1 consists mainly of the motion of ions justifying calling \mathbf{n}_1 an ion wave.

In the low frequency limit

$$\frac{v_{iz}}{v_{ez}} = -\frac{m_e}{m_i} \frac{\frac{v_e^2}{v_i^2 + \frac{m_e}{m_i}} v_e^2 - 1}{\frac{v_i^2}{v_i^2 + \frac{m_e}{m_i}} v_e^2 - 1}$$

$$= - \frac{m_e}{m_i} \frac{v_e^2 - v_i^2 - \frac{m_e}{m_i} v_e^2}{v_i^2 - v_i^2 - \frac{m_e}{m_i} v_e^2}$$

$$= 1 - \frac{v_i^2}{v_e^2} - \frac{m_e}{m_i}$$

$$\approx 1$$
 (2.4.20)

and

$$k_1 \approx \omega / \left(v_i^2 + \frac{m_e}{m_i} v_e^2 \right)^{l_2}$$
 (2.4.21)

and

$$n_{1} \approx \frac{1}{\sqrt{2}} \left[\frac{v_{e}}{\omega_{e}} n_{e} + \frac{v_{i}}{\omega_{i}} n_{i} \right]. \qquad (2.4.22)$$

for an equilibrium plasma $(T_e = T_i)$.

From the above equations we can conclude that in the low frequency limit the ion waves consist of electrons and ions moving in phase with approximately equal velocities and the medium remains practically neutral. However, this is rigorously true only in limit of $\omega \to 0$. For finite values of ω there exists a slight deviation from neutrality; the ion oscillations are slightly larger than those of the electrons. Even though this deviation is weak, an electric field resulting from the space charge produces a coupling between the aggregate motion of the elections and ions.

Hereafter, we shall refer to the electron wave in the high frequency range as the electroacoustic wave and the ion wave will be called the pseudosonic wave in the low frequency range. These are the regions of interest for the two waves and the properties discussed above will be used later in the solution of a specific problem.

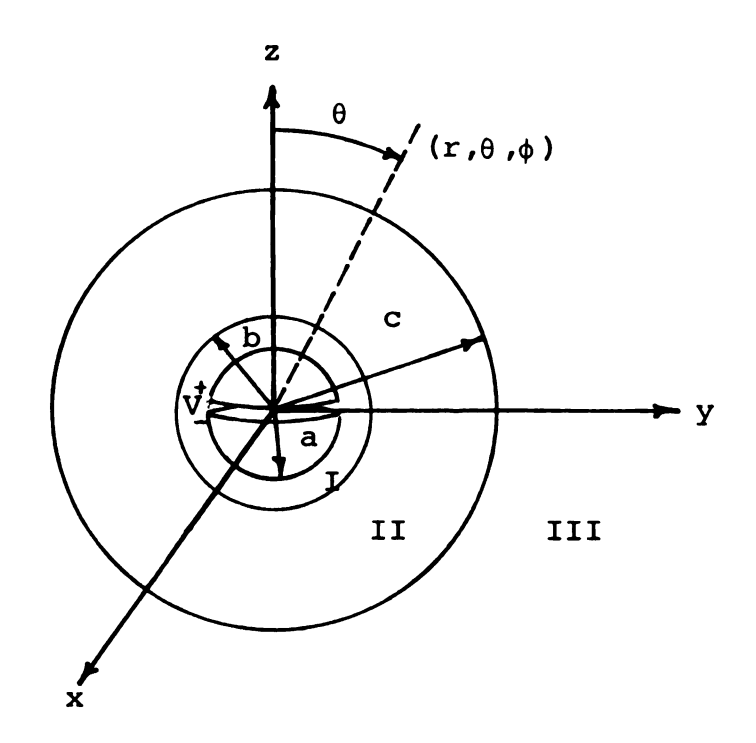
CHAPTER III

RADIATION AND INPUT ADMITTANCE OF A SPHERICAL ANTENNA SURROUNDED BY A FINITE LAYER OF HOT, LOSSY PLASMA

In this chapter the radiation and input admittance of a spherical antenna surrounded by a finite layer of a hot lossy plasma is studied. In addition to the electromagnetic wave, two longitudinal waves, an electroacoustic wave and a pseudosonic wave, may propagate in a hot plasma. These are included in the following analysis. In addition, a thin dielectric sheath is assumed to surround the spherical antenna and separates it from the plasma layer.

3.1 Statement of the Problem and Method of Analysis

The geometrical configuration is shown in Figure 3.1 using a spherical coordinate system (r, θ, ϕ) . A spherical antenna of radius a is centered at the origin and is covered by a thin dielectric sheath of outer radius b. The permittivity of the sheath is ϵ_d and the permeability is taken as the free space permeability, μ_O . The sheath is covered by spherical layer of hot lossy plasma which has an outer



dielectric coating (μ_{o}, ϵ_{D}) Region I:

Region II: hot lossy plasma

free space (μ_O,ε_O) Region III:

Figure 3.1. A spherical antenna covered by a hot, lossy plasma.

radius of C. The plasma is assumed to be a weakly ionized gas so that the linearized hydrodynamic equations apply. It can be regarded as consisting of two fluids, the ions and the electrons with the neutral particles being taken into account by assuming finite collision frequencies between the ions and the neutral particles and between the electrons and the neutral particles.

As an idealized approximation the sheath is considered to be a lossless coating which is perfectly rigid to the inward radial flow of the ions and the electrons. It is also necessary to impose a boundary condition on the outward flow of the ions and electrons at the outer surface of the plasma layer. To make the problem tractable it is assumed that the outer boundary of the plasma is rigid to the outward radial flow of ions and electrons. Without these assumptions a solution to this problem would be very difficult.

The spherical antenna is perfectly conducting except for a narrow equatorial gap between $\pi/2 - \theta_1 \leq \theta \leq \pi/2 + \theta_1$. Across the gap the antenna is driven by a constant voltage generator with a voltage, V, and an angular frequency, ω . The total space excluding the antenna is divided into three regions. Region I is the dielectric coating, Region II is the hot, lossy plasma layer and Region III is an infinite free space region.

1

1

w: is ti

đe,

We aim to solve for the fields in all three regions and the ion and electron densities in Region II. The solutions contain nine arbitrary constants. These constants can be evaluated by matching the tangential electric field in the dielectric region to that on the antenna, by matching the tangential electric and magnetic fields across the boundaries at r = b and r = c, and by requiring that the radial velocities of the ions and the electrons go to zero at r = b and r = c as discussed earlier. This procedure gives us a complete solution to our rather idealized problem.

In this study rationalized MKS units are used. Rotational symmetry and an infinitesimal driving gap are assumed. Furthermore, $\exp(j\omega t)$ time dependence is assumed for the generator and all the fields.

3.2 Region I: Dielectric Sheath Region

The basic equations which govern Region I (dielectric layer, a \leq r \leq b) are Maxwell's equations

$$\nabla \times E_{1}(\mathbf{r}) = -j\omega\mu_{0} H_{1}(\mathbf{r}) \qquad (3.2.1)$$

$$\nabla \times H_1(r) = j\omega \varepsilon_d E_1(r)$$
 (3.2.2)

where \mathbf{E}_1 and \mathbf{H}_1 are the electric and magnetic fields, μ_0 is the permeability of free space, and \mathbf{E}_d is the permittivity of the dielectric medium. The suppressed time dependence is $\exp(j\omega t)$.

From the symmetry of the antenna it can be seen that there is no variation in the ϕ direction and that the magnetic field has only a ϕ component. Thus equations (3.2.1) and (3.2.2) can easily be reduced to three scalar equations such as

$$\frac{\partial}{\partial \mathbf{r}}(\mathbf{r}\mathbf{E}_{1\theta}) - \frac{\partial \mathbf{E}_{1\mathbf{r}}}{\partial \theta} = -j\omega\mu_{0}\mathbf{r}\mathbf{H}_{1\phi}$$
 (3.2.3)

$$\frac{1}{r \sin \theta} \frac{\partial}{\partial \theta} (\sin \theta H_{1\phi}) = j \omega \epsilon_{d}^{E} E_{1r}$$
 (3.2.4)

$$\frac{\partial}{\partial \mathbf{r}} (\mathbf{r} \mathbf{H}_{1\phi}) = \mathbf{j} \omega \varepsilon_{\mathbf{d}} \mathbf{r} \mathbf{E}_{1\theta}. \tag{3.2.5}$$

Differentiating equations (3.2.4) and (3.2.5) and substituting them into equation (3.2.3) leads to a partial differential equation

$$\frac{\partial^{2}}{\partial r^{2}} (rH_{1\phi}) + \frac{1}{r^{2}} \frac{2}{\partial \theta} \left[\frac{1}{\sin \theta} \frac{2}{\partial \theta} \left[\sin \theta \ rH_{1\phi} \right] \right] + \beta_{d}^{2} (rH_{1\phi}) = 0$$
(3.2.6)

where $\beta_d^2 = \omega^2 \mu_0 \epsilon_d$. To solve equation (3.2.6), we use the method of the separation of variables. Since $H_{1\phi}$ is independent of ϕ we can assume

$$rH_{1\phi} = R(r) \bigoplus (\theta)$$
 (3.2.7)

su

eq

Equa Lege

where R is a function of r alone and H is a function of θ only. The substitution of equation (3.2.7) into equation (3.2.6) leads to

$$\frac{r^2}{R} \frac{d^2 R}{dr^2} + k^2 r^2 = -\frac{1}{\hat{H}} \frac{d}{d\theta} \left[\frac{1}{\sin \theta} \frac{d}{d\theta} (\hat{H}) \sin \theta \right] = n(n+1)$$
(3.2.8)

where n(n+1) is the separation constant. Equation (3.2.8) generates two ordinary differential equations

$$\frac{d}{d\theta} \left[\frac{1}{\sin\theta} \frac{d}{d\theta} (\hat{\mathbf{H}} \sin\theta) \right] + n(n+1) \hat{\mathbf{H}} = 0$$
 (3.2.9)

$$\frac{r^2}{R} \frac{d^2R}{dr^2} + \beta_d^2 r^2 - n(n+1) = 0. \qquad (3.2.10)$$

Let us consider equation (3.2.9) first. Making the substitutions,

$$u = \cos\theta$$
 , $\sqrt{1 - u^2} = \sin\theta$, $\frac{d}{d\theta} = -\sqrt{1 - u^2} \frac{d}{du}$,

equation (3.2.9) can be reduced to

$$(1 - u^{2}) \frac{d^{2} \oplus du^{2}}{du^{2}} - 2u \frac{d \oplus du}{du} + \left[n(n+1) - \frac{1}{1 - u^{2}} \right] \oplus 0$$
(3.2.11)

Equation (3.2.11) is a special case of the associated Legendre's equation,

$$(1-x^2) \frac{d^2y}{dx^2} - 2x \frac{dy}{dx} + \left[n(n+1) - \frac{m^2}{1-x^2} \right] y = 0$$
(3.2.12)

which has a solution, $y = P_n^m(x)$, which is called an associated Legendre function of the first kind of order n and degree m.

In order to have finite solutions on the interval $-1 \le x \le 1$ the parameter n must be zero or a positive integer and m must take on only values -n, -(n-1),...,0,...,n-1,n, i.e., n > |m|.

Thus a solution to equation (3.2.11) is

where n must be a positive integer.

Note that only one solution for this second order differential equation (3.2.11) has been considered. The other solution diverges on the θ = 0 and θ = 180° axes and so it must be excluded from the solution.

Some other properties of the associated and ordinary Legendre functions that will be useful to us in later developments and in the numerical calculations are tabulated in Appendix B.

We must now solve the other differential equation, equation (3.2.10). With the substitution

$$R = R_1 r^{\frac{1}{2}} ag{3.2.14}$$

equation (3.2.10) becomes

$$\frac{d^2R_1}{dr^2} + \frac{1}{r}\frac{dR_1}{dr} + \left[\beta_d^2 - \frac{(n+\frac{1}{2})}{r^2}\right]R_1 = 0. \qquad (3.2.15)$$

Equation (3.2.15) is a form of Bessel's equation which has a solution

$$R_1 = A_n H_{n+\frac{1}{2}}^{(2)}(\beta_d r) + B_n H_{n+\frac{1}{2}}^{(1)}(\beta_d r)$$
 (3.2.16)

where A_n and B_n are arbitrary constants and $H_{n+\frac{1}{2}}^{(1)}(\beta_d r)$ and $H_{n+\frac{1}{2}}^{(2)}(\beta_d r)$ are Hankel functions of the first and second kinds with order $n+\frac{1}{2}$, which represent radially inward and outward traveling waves respectively.

Combining equations (3.2.7), (3.2.13), (3.2.14), and (3.2.16) we have

$$H_{1\phi} = \frac{1}{\sqrt{r}} \sum_{n=1}^{\infty} P_n^1(\cos\theta) \left[A_n H_{n+\frac{1}{2}}^{(2)}(\beta_d r) + B_n H_{n+\frac{1}{2}}^{(1)}(\beta_d r) \right].$$
(3.2.17)

The r and θ components of the electric field can now be found using equations (3.2.4) and (3.2.5).

Substituting equation (3.2.17) into equation (3.2.4) and using the identities (B-7) and (B-8) from Appendix B yields

$$E_{1r} = \frac{j}{\omega \varepsilon_{d} r^{3/2}} \sum_{n=1}^{\infty} n(n+1) P_{n}(\cos \theta) \left[A_{n} H_{n+\frac{1}{2}}^{(2)}(\beta_{d} r) + B_{n} H_{n+\frac{1}{2}}^{(1)}(\beta_{d} r) \right].$$
(3.2.18)

To derive $\mathbf{E}_{1\theta}$, we need two differentiation formulas for Hankel functions

$$\frac{d}{dx} H_{n+\frac{1}{2}}^{(1)}(x) = -\frac{n+\frac{1}{2}}{x} H_{n+\frac{1}{2}}^{(1)}(x) + H_{n-\frac{1}{2}}^{(1)}(x)$$
 (3.2.19)

$$\frac{d}{dx} H_{n+\frac{1}{2}}^{(2)}(x) = -\frac{n+\frac{1}{2}}{x} H_{n+\frac{1}{2}}^{(2)}(x) + H_{n-\frac{1}{2}}^{(2)}(x)$$
 (3.2.20)

The substitution of equation (3.2.17) into equation (3.2.6) and using equations (3.2.19) and (3.2.20) leads to

$$E_{1\theta} = -\frac{j}{\omega \epsilon_{d} r^{3/2}} \sum_{n=1}^{\infty} P_{n}^{1}(\cos \theta) \left\{ A_{n} \left[n H_{n+\frac{1}{2}}^{(2)}(\beta_{d} r) - \beta_{d} r H_{n-\frac{1}{2}}^{(2)}(\beta_{d} r) \right] \right\}$$

+
$$B_n \left[n H_{n+\frac{1}{2}}^{(1)}(\beta_d r) - \beta_d r H_{n-\frac{1}{2}}^{(1)}(\beta_d r) \right]$$
 (3.2.21)

The solutions for the fields in Region I can thus be summarized as follows:

$$H_{1\phi} = \frac{1}{\sqrt{r}} \sum_{n=1}^{\infty} P_{n}^{1}(\cos\theta) \left[A_{n} H_{n+\frac{1}{2}}^{(2)}(\beta_{d}r) + B_{n} H_{n+\frac{1}{2}}^{(1)}(\beta_{d}r) \right]$$
(3.2.22)

$$E_{1r} = \frac{j}{\omega \varepsilon_{d} r^{3/2}} \sum_{n=1}^{\infty} n(n+1) P_{n}(\cos \theta) \left[A_{n} H_{n+\frac{1}{2}}^{(2)}(\beta_{d} r) + B_{n} H_{n+\frac{1}{2}}^{(1)}(\beta_{d} r) \right]$$

$$= -\frac{j}{\omega \varepsilon_{d} r^{3/2}} \sum_{n=1}^{\infty} P_{n}^{1}(\cos \theta) \left\{ A_{n} \left[n H_{n+\frac{1}{2}}^{(2)}(\beta_{d} r) - \beta_{d} r H_{n-\frac{1}{2}}^{(2)}(\beta_{d} r) \right] + B_{n} \left[n H_{n+\frac{1}{2}}^{(1)}(\beta_{d} r) - \beta_{d} r H_{n-\frac{1}{2}}^{(1)}(\beta_{d} r) \right] \right\}$$

$$= + B_{n} \left[n H_{n+\frac{1}{2}}^{(1)}(\beta_{d} r) - \beta_{d} r H_{n-\frac{1}{2}}^{(1)}(\beta_{d} r) \right]$$

$$= + B_{1} \left[n H_{n+\frac{1}{2}}^{(1)}(\beta_{d} r) - \beta_{d} r H_{n-\frac{1}{2}}^{(1)}(\beta_{d} r) \right]$$

$$= + B_{1} \left[n H_{n+\frac{1}{2}}^{(1)}(\beta_{d} r) - \beta_{d} r H_{n-\frac{1}{2}}^{(1)}(\beta_{d} r) \right]$$

$$= + B_{1} \left[n H_{n+\frac{1}{2}}^{(1)}(\beta_{d} r) - \beta_{d} r H_{n-\frac{1}{2}}^{(1)}(\beta_{d} r) \right]$$

$$= + B_{1} \left[n H_{n+\frac{1}{2}}^{(1)}(\beta_{d} r) - \beta_{d} r H_{n-\frac{1}{2}}^{(1)}(\beta_{d} r) \right]$$

$$= + B_{1} \left[n H_{n+\frac{1}{2}}^{(1)}(\beta_{d} r) - \beta_{d} r H_{n-\frac{1}{2}}^{(1)}(\beta_{d} r) \right]$$

$$= + B_{1} \left[n H_{n+\frac{1}{2}}^{(1)}(\beta_{d} r) - \beta_{d} r H_{n-\frac{1}{2}}^{(1)}(\beta_{d} r) \right]$$

$$= + B_{1} \left[n H_{n+\frac{1}{2}}^{(1)}(\beta_{d} r) - \beta_{d} r H_{n-\frac{1}{2}}^{(1)}(\beta_{d} r) \right]$$

$$= + B_{1} \left[n H_{n+\frac{1}{2}}^{(1)}(\beta_{d} r) - \beta_{d} r H_{n-\frac{1}{2}}^{(1)}(\beta_{d} r) \right]$$

$$= + B_{1} \left[n H_{n+\frac{1}{2}}^{(1)}(\beta_{d} r) - \beta_{d} r H_{n-\frac{1}{2}}^{(1)}(\beta_{d} r) \right]$$

$$= + B_{1} \left[n H_{n+\frac{1}{2}}^{(1)}(\beta_{d} r) - \beta_{d} r H_{n-\frac{1}{2}}^{(1)}(\beta_{d} r) \right]$$

$$= + B_{1} \left[n H_{n+\frac{1}{2}}^{(1)}(\beta_{d} r) - \beta_{d} r H_{n-\frac{1}{2}}^{(1)}(\beta_{d} r) \right]$$

$$= + B_{1} \left[n H_{n+\frac{1}{2}}^{(1)}(\beta_{d} r) - \beta_{d} r H_{n-\frac{1}{2}}^{(1)}(\beta_{d} r) \right]$$

3.3 Region II: Plasma Layer

In Region II (plasma layer, b \leq r \leq c), the plasma medium is considered to be a two component, ion-electron fluid. That is, both the ions and the electrons are allowed to be mobile. The plasma is also assumed to be a weakly ionized gas having average number densities of n_0 electrons and n_0 singularly ionized atoms which are assumed to be constant in the plasma layer. The deviation of the electron density from the mean density, n_0 , is denoted by n_e and the average induced velocity of the electrons is denoted by n_e . The collision frequency of the electrons with the neutral particles is denoted by n_e . Similiarly defined quantities for the ions are given by n_i , n_i and n_i . Electron-electron, electron-ion and ion-ion collisions are

assumed to be negligible in a weakly ionized gas and thus they are ignored.

In its unperturbed state the plasma is assumed to be homogeneous and neutrally charged and the perturbation of the plasma is assumed to be sufficiently small, i.e., $n_{e} << n_{o} \text{ and } n_{i} << n_{o}, \text{ so that the linearized hydrodynamic equations discussed in Chapter I apply. No static electric or magnetic fields are present.}$

For a harmonic time dependence of $\exp(j\omega t)$ the basic equations in the plasma layer are Maxwell's equations

$$\nabla \times \mathbb{E}_{2}(\mathbf{r}) = - j\omega \mu_{0} \mathbb{H}_{2}(\mathbf{r})$$
 (3.3.1)

$$\nabla \times H_{2}(r) = - en_{0}[v_{e}(r) - v_{i}(r)] + j\omega \epsilon_{0} E_{2}(r)$$
 (3.3.2)

$$\nabla \cdot \mathbf{E}_{2}(\mathbf{r}) = -\frac{\mathbf{e}}{\varepsilon_{0}} \left[\mathbf{n}_{\mathbf{e}}(\mathbf{r}) - \mathbf{n}_{\mathbf{i}}(\mathbf{r}) \right]$$
 (3.3.3)

$$\nabla \cdot H_2(\mathbf{r}) = 0 \tag{3.3.4}$$

and the linearized continuity and force equations for electrons

$$n_{o}[\nabla \cdot v_{e}(r)] + j\omega n_{e}(r) = 0$$
 (3.3.5)

$$(\gamma_e + j\omega) v_e(r) = -\frac{e}{m_e} E_2(r) - \frac{v_e^2}{n_o} \nabla n_e(r)$$
 (3.3.6)

and the linearized continuity and force equations for the ions

$$n_{o}[\nabla \cdot v_{i}(r)] + j\omega n_{i}(r) = 0$$
 (3.3.7)

$$(\gamma_{i} + j\omega) \underbrace{v_{i}}_{i}(\underline{r}) = \frac{e}{m_{i}} \underbrace{E_{2}}_{i}(\underline{r}) - \frac{\underbrace{v_{i}^{2}}_{i}}{n_{o}} \nabla n_{i}(\underline{r})$$
(3.3.8)

where -e and m_e are the electronic charge and mass of the electrons, e and m_i are the electronic charge and mass of the ions, μ_o and ϵ_o are the permeability and permittivity of free space, and V_e and V_i are the thermal velocities of the electrons and the ions, respectively.

It should be noted that the last terms on the right hand side of equations (3.3.6) and (3.3.8) represent the force due to a pressure gradient and the definitions given for V_e and V_i in Chapter I are valid under the assumption of an adiabatic pressure variation and a one-dimensional compression.

In our formulation there are fourteen scalar unknowns, E_2 , H_2 , n_e , n_i , v_e , and v_i . We will determine H_2 , n_e , and n_i first and then calculate E_2 , v_e , and v_i .

It has been shown in Chapter II that n_e and n_i are solutions to a pair of coupled differential equations

$$\nabla^{2} n_{e} + \beta_{e}^{2} n_{e} + \frac{\omega_{e}^{2}}{v_{e}^{2}} n_{i} = -\frac{\omega_{e}^{2}}{v_{e}^{2}} \frac{\rho^{S}}{e}$$
 (3.3.9)

$$\nabla^{2} n_{i} + \beta_{i}^{2} n_{i} + \frac{\omega_{i}^{2}}{v_{i}^{2}} n_{e} = \frac{\omega_{i}^{2}}{v_{i}^{2}} \frac{\rho^{S}}{e}$$
 (3.3.10)

where

$$\beta_e^2 = \frac{\omega^2}{v_e^2} \left[1 - \frac{\omega_e^2}{\omega^2} - j \frac{\gamma_e}{\omega} \right]$$
 (3.3.11)

$$\beta_{i}^{2} = \frac{\omega^{2}}{v_{i}^{2}} \left[1 - \frac{\omega_{i}^{2}}{\omega^{2}} - j \frac{\gamma_{i}}{\omega} \right]$$
 (3.3.12)

and ρ^S is the imposed source charge density. In Appendix A equations (3.3.9) and (3.3.10) are algebraically uncoupled to obtain solutions for n_e and n_i

$$n_{e} = \frac{\omega_{e}}{V_{e}} (T_{11}n_{1} + T_{12}n_{2})$$
 (3.3.13)

$$n_{i} = \frac{\omega_{i}}{V_{i}} (T_{21}n_{1} + T_{22}n_{2})$$
 (3.3.14)

where

$$T_{11} = \frac{1}{\sqrt{1 + \frac{1}{4} \frac{v_e^2 v_i^2}{\omega_e^2 \omega_i^2} [\beta_e^2 - \beta_i^2 - A_o]^2}}$$
(3.3.15)

$$T_{21} = -\frac{1}{2} \frac{v_e v_i}{\omega_e^{\omega_i}} \frac{\beta_e^2 - \beta_i^2 - A_o}{\sqrt{1 + \frac{1}{4} \frac{v_e^2 v_i^2}{\omega_e^2 \omega_i^2} [\beta_e^2 - \beta_i^2 - A_o]^2}}$$
(3.3.16)

$$T_{12} = \frac{1}{\sqrt{1 + \frac{1}{4} \frac{v_e^2 v_i^2}{\omega_e^2 \omega_i^2} [\beta_e^2 - \beta_i^2 + A_o]^2}}$$
(3.3.17)

$$T_{22} = -\frac{1}{2} \frac{v_e v_i}{\omega_e \omega_i} \frac{\beta_e^2 - \beta_i^2 + A_o}{\sqrt{1 + \frac{1}{4} \frac{v_e^2 v_i^2}{\omega_e^2 \omega_i^2} [\beta_e^2 - \beta_i^2 + A_o]^2}}$$
(3.3.18)

and

$$A_{O} = \sqrt{(\beta_{e}^{2} - \beta_{i}^{2})^{2} + 4 \frac{\omega_{e}^{2}\omega_{i}^{2}}{v_{e}^{2}v_{i}^{2}}}$$
 (3.3.19)

and n_1 and n_2 are solutions to the differential equations

$$\nabla^2 n_1 + k_1^2 n_1 = S_1 \frac{\rho^S}{e}$$
 (3.3.20)

$$\nabla^{2} n_{2} + k_{2}^{2} n_{2} = S_{2} \frac{\rho^{S}}{e}$$
 (3.3.21)

where

$$k_1^2 = \frac{1}{2}(\beta_e^2 + \beta_i^2 + A_0) \tag{3.3.22}$$

$$k_2^2 = \frac{1}{2}(\beta_e^2 + \beta_i^2 - A_0)$$
 (3.3.23)

$$s_1 = \frac{\omega_i}{V_i} T_{12} + \frac{\omega_e}{V_e} T_{22}$$
 (3.3.24)

$$s_2 = -\left[\frac{\omega_e}{v_e} T_{21} + \frac{\omega_i}{v_i} T_{11}\right].$$
 (3.3.25)

In a sourceless region like Region II under consideration, equations (3.3.20) and (3.3.21) become

$$\nabla^2 n_1 + k_1^2 n_1 = 0 ag{3.3.26}$$

$$\nabla^2 n_2 + k_2^2 n_2 = 0 (3.3.27)$$

Both equations (3.3.26) and (3.3.27) are of the form

$$\nabla^2 n + k^2 n = 0 (3.3.28)$$

which will now be solved by the method of the separation of variables.

Due to the rotational symmetry, (no ϕ dependence), the Laplacian of the scalar field n can be expressed in spherical coordinates as

$$\nabla^2 n = \frac{1}{r^2} \frac{\partial}{\partial r} \left(r^2 \frac{\partial n}{\partial r} \right) + \frac{1}{r^2 \sin \theta} \frac{\partial}{\partial \theta} \left(\sin \frac{\partial n}{\partial \theta} \right). \quad (3.3.29)$$

Since

$$\frac{\partial}{\partial \mathbf{r}} \left(\mathbf{r}^2 \frac{\partial \mathbf{n}}{\partial \mathbf{r}} \right) = \mathbf{r} \frac{\partial^2}{\partial \mathbf{r}^2} (\mathbf{r} \mathbf{n}) \tag{3.3.30}$$

and using equation (3.3.29), equation (3.3.28) can be reduced to a partial differential equation

w.

er

дŊ

the

$$\frac{\partial^{2}}{\partial r^{2}}(rn) + \frac{1}{r^{2} \sin \theta} \frac{\partial}{\partial \theta} \left[\sin \theta \frac{\partial}{\partial \theta}(rn) \right] + k^{2}(rn) = 0$$
(3.3.31)

Since n is independent of ϕ , we can assume

$$rn = R(r) (H) (\theta)$$
 (3.3.32)

where R is a function r alone and H is a function of θ only. The substitution of equation (3.3.32) into equation (3.3.31) leads to

$$\frac{r^2}{R} \frac{d^2R}{dr^2} + k^2r = -\frac{1}{H} \frac{1}{\sin\theta} \frac{d}{d\theta} (\sin\theta \frac{dH}{d\theta}) = \ell(\ell+1) \quad (3.3.33)$$

where l is an integer and l(l+1) is the separation constant. Equation (3.3.33) generates two ordinary differential equations,

$$\frac{1}{\sin\theta} \frac{d}{d\theta} (\sin\theta \frac{d\theta}{d\theta}) + \ell(\ell+1) (\theta) = 0$$
 (3.3.34)

and

$$r^{2} \frac{d^{2}R}{dr^{2}} + k^{2}r^{2}R - \ell(\ell+1) R = 0.$$
 (3.3.35)

Let us consider equation (3.3.34) first. Making the substitutions

$$u = \cos\theta$$
, $\sqrt{1 - u^2} = \sin\theta$, $\frac{d}{d\theta} = -\sqrt{1 - u^2} \frac{d}{du}$,

eq

Eq:

sol

whe

has axes

cal

as e

Where

equat

Theref

equation (3.3.34) and be reduced to

$$(1 - u^2) \frac{d^2 H}{du^2} - 2u \frac{d H}{du} + \ell(\ell+1) H = 0.$$
 (3.3.36)

Equation (3.3.36) is the standard form of the ordinary Legendre's equation. This equation has the standard solution

$$\mathbf{\hat{H}} = \mathbf{P}_{\ell} (\mathbf{u}) = \mathbf{P}_{\ell} (\cos \theta) \tag{3.3.37}$$

where & is zero or a positive integer. Note that only one solution for this second-order differential equation has been considered. The other solution diverges on the axes and so it can be excluded from the solution on physical grounds.

Since equation (3.3.35) is in exactly the same form as equation (3.2.10), its solution can be written as

$$R = \sqrt{r} \left[C_{\ell} H_{\ell+\frac{1}{2}}^{(2)}(kr) + D_{\ell} H_{\ell+\frac{1}{2}}^{(1)}(kr) \right]$$
 (3.3.38)

where C_{ℓ} and D_{ℓ} are arbitrary constants. Combining equations (3.3.32), (3.3.37) and (3.3.38), we have

$$n = \frac{1}{\sqrt{r}} \sum_{\ell=0}^{\infty} P_{\ell}(\cos\theta) \left[C_{\ell} H_{\ell+\frac{1}{2}}^{(2)}(kr) + D_{\ell} H_{\ell+\frac{1}{2}}^{(1)}(kr) \right].$$
(3.3.39)

Therefore n_1 and n_2 can be written as follows:

$$n_{1} = \frac{1}{\sqrt{r}} \sum_{\ell=0}^{\infty} P_{\ell}(\cos\theta) \left[C_{1\ell} H_{\ell+\frac{1}{2}}^{(2)}(k_{1}r) + D_{1\ell} H_{\ell+\frac{1}{2}}^{(1)}(k_{1}r) \right]$$
(3.3.40)

$$n_{2} = \frac{1}{\sqrt{r}} \sum_{\ell=0}^{\infty} P_{\ell}(\cos\theta) \left[C_{2\ell} H_{\ell+\frac{1}{2}}^{(2)}(k_{2}r) + D_{2\ell} H_{\ell+\frac{1}{2}}^{(1)}(k_{2}r) \right]$$
(3.3.41)

 n_1 and n_2 are the perturbations due to the pseudosonic and the electroacoustic waves respectively. Substitution of equations (3.3.40) and (3.3.41) into equations (3.3.13) and (3.3.14) yields explicit representations of n_e and n_i .

We must now determine the magnetic field $\frac{H_2}{2}$ in Region II. Taking the curl of equations (3.3.2), (3.3.6) and (3.3.8), we obtain

$$\nabla \times \nabla \times H_{2} = -\operatorname{en}_{O}(\nabla \times v_{e} - \nabla \times v_{i}) + j\omega \varepsilon_{O} \nabla \times E_{2}$$
(3.3.42)

$$\nabla \times \nabla_{e} = -\frac{e}{m_{e}(\gamma_{e} + j\omega)} \nabla \times E_{2}$$
 (3.3.43)

and

$$\nabla \times v_{i} = \frac{e}{m_{i} (\gamma_{i} + j\omega)} \nabla \times E_{2}. \qquad (3.3.44)$$

The substitution of equations (3.3.43), (3.3.44), and (3.3.1) into equation (3.3.42) gives

$$\nabla \times \nabla \times \frac{H}{2} = \omega^{2} \mu_{0} \varepsilon_{0} \left[1 + \frac{\omega_{e}^{2}}{j\omega (\gamma_{e} + j\omega)} + \frac{\omega_{i}^{2}}{j\omega (\gamma_{i} + j\omega)} \right]_{\sim 2}^{H}.$$
(3.3.45)

Using the vector identity of

$$\nabla \times \nabla \times H_2 = \nabla (\nabla \cdot H_2) - \nabla^2 H_2$$
 (3.3.46)

and equation (3.3.4), equation (3.3.45) can be reduced to a homogeneous wave equation

$$(\nabla^2 + k_e^2)_{\approx 2}^{H} = 0 (3.3.47)$$

where k_e is the complex propagation constant of the electromagnetic wave in a two fluid plasma given by

$$k_e^2 = \omega^2 \mu_O \xi$$
 (3.3.48)

where ξ is the equivalent complex permittivity defined by

$$\xi = \varepsilon_{0} \left[1 + \frac{\omega_{e}^{2}}{j\omega(\gamma_{e} + j\omega)} + \frac{\omega_{i}^{2}}{j\omega(\gamma_{i} + j\omega)} \right]$$

$$= \varepsilon_{0} \left[1 - \frac{\omega_{e}^{2}}{\omega^{2} + \gamma_{e}^{2}} - \frac{\omega_{i}^{2}}{\omega^{2} + \gamma_{i}^{2}} - j \left(\frac{\omega_{e}^{2}\gamma_{e}}{\omega(\omega^{2} + \gamma_{e}^{2})} + \frac{\omega_{i}^{2}\gamma_{i}}{\omega(\omega^{2} + \gamma_{i}^{2})} \right) \right]. \tag{3.3.49}$$

e

in

eq

From the symmetry of the antenna it can be seen that there is no variation in the ϕ direction, i.e., $\partial/\partial \phi = 0$ and the magnetic field has only a ϕ component. Thus the Laplacian of the vector magnetic field in spherical coordinates takes the form

$$\nabla^{2} H_{2} = \hat{\phi} (\nabla^{2} H_{2\phi} - \frac{1}{r^{2}} \csc^{2} \theta H_{2\phi})$$

$$= \hat{\phi} \left[\frac{1}{r^{2}} \frac{\partial}{\partial r} \left(r^{2} \frac{\partial^{H}_{2\phi}}{\partial r} \right) + \frac{1}{r^{2} \sin \theta} \frac{\partial}{\partial \theta} \left(\sin \theta \frac{\partial^{H}_{2\phi}}{\partial \theta} \right) - \frac{1}{r^{2}} \csc^{2} \theta H_{2\phi} \right]$$

$$(3.3.50)$$

where $\hat{\phi}$ is the unit vector in the ϕ direction. Using equations (3.3.30), (3.3.50) and the following identity

$$\frac{1}{\sin\theta} \frac{\partial}{\partial \theta} \left[\sin\theta \frac{\partial^{H}_{2\phi}}{\partial \theta} \right] - \csc^{2}\theta H_{2\phi} = \frac{\partial}{\partial \theta} \left[\frac{1}{\sin\theta} \frac{\partial}{\partial \theta} \left(\sin\theta H_{2\phi} \right) \right]$$
$$= \frac{\partial^{2}H_{2\phi}}{\partial \theta^{2}} + \cot\theta \frac{\partial^{H}_{2\phi}}{\partial \theta} - \csc^{2}\theta H_{2\phi} \qquad (3.3.51)$$

in equation (3.3.47) leads to a partial differential equation,

$$\frac{\partial^{2}}{\partial r^{2}} (rH_{2\phi}) + \frac{1}{r^{2}} \frac{\partial}{\partial \theta} \left[\frac{1}{\sin \theta} \frac{\partial}{\partial \theta} \left[\sin \theta rH_{2\phi} \right] \right] + k_{e}^{2} (rH_{2\phi}) = 0$$
(3.3.52)

which is in exactly the same form as equation (3.2.6). Thus the solution to equation (3.3.52) can be written as

$$H_{2\phi}(r,\theta) = \frac{1}{\sqrt{r}} \sum_{n=1}^{\infty} P_n^{1}(\cos\theta) \left[E_n H_{n+\frac{1}{2}}^{(2)}(k_e r) + F_n H_{n+\frac{1}{2}}^{(1)}(k_e r) \right]$$
(3.3.53)

where E_n and F_n are arbitrary constants.

 H_2 , n_e , and n_i have been determined explicitly and are expressed in equations (3.3.13), (3.3.14), (3.3.40), (3.3.41), and (3.3.53). We now must express E_2 , v_e , and v_i in terms of these known quantities.

From equations (3.3.6) and (3.3.8) we easily get

$$v_e = -\frac{e}{m_e (\gamma_e + j\omega)} E_2 - \frac{v_e^2}{n_O (\gamma_e + j\omega)} \nabla n_e$$
 (3.3.54)

$$v_{i} = \frac{e}{m_{i} (\gamma_{i} + j\omega)} \sum_{i=2}^{E} - \frac{v_{i}^{2}}{n_{o} (\gamma_{i} + j\omega)} \nabla n_{i}. \qquad (3.3.55)$$

The substitution of equations (3.3.54) and (3.3.55) into equation (3.3.2) leads to

$$E_{2} = \frac{1}{j\omega\xi} \nabla x_{2}^{H} - \frac{e V_{e}^{2}}{j\omega\xi(\gamma_{e}+j\omega)} \nabla n_{e} + \frac{e V_{i}^{2}}{j\omega\xi(\gamma_{i}+j\omega)} \nabla n_{i}$$
(3.3.56)

where ξ is given in equation (3.3.49). The substitution of equation (3.3.56) into equations (3.3.54) and (3.3.55) yields

$$v_{e} = -\frac{e}{m_{e}(\gamma_{e}+j\omega)} \frac{1}{j\omega\xi} \nabla x_{e}^{H_{2}} - \frac{\varepsilon_{o}V_{e}^{2}}{\xi n_{o}(\gamma_{e}+j\omega)} \left[1 - \frac{\omega_{i}^{2}}{\omega^{2}+\gamma_{i}^{2}}\right]$$

$$-\frac{j\gamma_{i}\omega_{i}^{2}}{\omega(\omega^{2}+\gamma_{i}^{2})} \nabla n_{e} + \frac{j\omega_{e}^{2}\varepsilon_{o}V_{i}^{2}}{n_{o}\xi\omega(\gamma_{i}+j\omega)(\gamma_{e}+j\omega)} \nabla n_{i} \quad (3.3.57)$$

$$v_{i} = \frac{e}{m_{i}(\gamma_{i}+j\omega)} \frac{1}{j\omega\xi} \nabla x_{e}^{H_{2}} - \frac{\varepsilon_{o}V_{i}^{2}}{\xi n_{o}(\gamma_{i}+j\omega)} \left[1 - \frac{\omega_{e}^{2}}{\omega^{2}+\gamma_{e}^{2}}\right]$$

$$-\frac{j\gamma_{e}\omega_{e}^{2}}{\omega(\omega^{2}+\gamma_{e}^{2})} \nabla n_{i} + \frac{j\omega_{i}^{2}\varepsilon_{o}V_{e}^{2}}{n_{o}\xi\omega(\gamma_{i}+j\omega)(\gamma_{e}+j\omega)} \nabla n_{e}. \quad (3.3.58)$$

Under rotational symmetry the two vector differential operators in spherical coordinates can be expressed as

$$\nabla \times H_2 = \hat{r} \frac{1}{r \sin \theta} \frac{\partial}{\partial \theta} (\sin \theta H_{2\phi}) - \hat{\theta} \frac{1}{r} \frac{\partial}{\partial r} (rH_{2\phi}) \quad (3.3.59)$$

and

$$\nabla n = \hat{r} \frac{\partial n}{\partial r} + \hat{\theta} \frac{1}{r} \frac{\partial n}{\partial \theta}$$
 (3.3.60)

where \hat{r} and $\hat{\theta}$ are unit vectors in the r and θ directions respectively. Combining equations (3.3.56) to (3.3.60), we obtain

$$E_{2r} = \frac{1}{j\omega\xi} \frac{1}{r \sin\theta} \frac{\partial}{\partial\theta} (\sin\theta \ H_{2\phi}) + \frac{j e V_e^2}{\omega\xi (\gamma_e + j\omega)} \frac{\partial n_e}{\partial r}$$

$$- j \frac{e V_i^2}{\omega \xi (\gamma_i + j\omega)} \frac{\partial n_i}{\partial r}$$
 (3.3.61)

$$E_{2\theta} = -\frac{1}{j\omega\xi} \frac{1}{r} \frac{\partial}{\partial r} (rH_{2\phi}) + j \frac{e v_e^2}{\omega\xi (\gamma_e + j\omega)} \frac{1}{r} \frac{\partial n_e}{\partial \theta}$$

$$- j \frac{e V_i^2}{\omega \xi (\gamma_i + j\omega)} \frac{1}{r} \frac{\partial n_i}{\partial \theta}$$
 (3.3.62)

$$v_{er} = -\frac{e}{m_e(\gamma_e + j\omega)} \frac{1}{j\omega\xi} \frac{1}{r \sin\theta} \frac{\partial}{\partial\theta} (\sin\theta H_{2\phi})$$

$$-\frac{\varepsilon_{o} v_{e}^{2}}{\xi n_{o} (\gamma_{e} + j\omega)} \left[1 - \frac{\omega_{i}^{2}}{\omega^{2} + \gamma_{i}^{2}} - j \frac{\gamma_{i} \omega_{i}^{2}}{\omega (\omega^{2} + \gamma_{i}^{2})} \right] \frac{\partial n_{e}}{\partial r}$$

+ j
$$\frac{\omega_e^2 \varepsilon_o V_i^2}{n_o \xi \omega (\gamma_i + j \omega) (\gamma_e + j \omega)} \frac{\partial n_i}{\partial r}$$
 (3.3.63)

$$v_{e\theta} = \frac{e}{m_e (\gamma_e + j\omega)} \frac{1}{j\omega\xi} \frac{1}{r} \frac{\partial}{\partial r} (rH_{2\phi})$$

$$-\frac{\varepsilon_{o} v_{e}^{2}}{\xi n_{o} (\gamma_{e} + j\omega)} \left[1 - \frac{\omega_{i}^{2}}{\omega^{2} + \gamma_{i}^{2}} - j \frac{\gamma_{i} \omega_{i}^{2}}{\omega_{i} (\omega^{2} + \gamma_{i}^{2})} \right] \frac{1}{r} \frac{\partial n_{e}}{\partial \theta}$$

$$+ j \frac{\omega_e^2 \varepsilon_o^{V_i^2}}{n_0 \xi \omega (\gamma_i + j\omega) (\gamma_0 + j\omega)} \frac{1}{r} \frac{\partial n_i}{\partial \theta}$$
 (3.3.64)

$$v_{ir} = \frac{e}{m_{i} (\gamma_{i} + j\omega)} \frac{1}{j\omega\xi} \frac{1}{r \sin\theta} \frac{\partial}{\partial\theta} (\sin\theta H_{2\phi})$$

$$- \frac{\varepsilon_{o} V_{i}^{2}}{\xi n_{o} (\gamma_{i} + j\omega)} \left[1 - \frac{\omega_{e}^{2}}{\omega^{2} + \gamma_{e}^{2}} - j \frac{\omega_{e}^{2} \gamma_{e}}{\omega (\omega^{2} + \gamma_{e}^{2})} \right] \frac{\partial n_{i}}{\partial r}$$

$$+ j \frac{\omega_{i}^{2} \varepsilon_{o} V_{e}^{2}}{n_{o} \xi \omega (\gamma_{i} + j\omega) (\gamma_{e} + j\omega)} \frac{\partial n_{e}}{\partial r} \qquad (3.3.65)$$

$$v_{i\theta} = - \frac{e}{m_{i} (\gamma_{i} + j\omega)} \frac{1}{j\omega\xi} \frac{1}{r} \frac{\partial}{\partial r} (rH_{2\phi})$$

$$- \frac{\varepsilon_{o} V_{i}^{2}}{\xi n_{o} (\gamma_{i} + j\omega)} \left[1 - \frac{\omega_{e}^{2}}{\omega^{2} + \gamma_{e}^{2}} - j \frac{\omega_{e}^{2} \gamma_{e}}{\omega (\omega^{2} + \gamma_{e}^{2})} \right] \frac{1}{r} \frac{\partial n_{i}}{\partial \theta}$$

$$+ j \frac{\omega_{i}^{2} \varepsilon_{o} V_{e}^{2}}{n_{o} \xi \omega (\gamma_{i} + j\omega) (\gamma_{i} + j\omega)} \frac{1}{r} \frac{\partial n_{e}}{\partial \theta} \qquad (3.3.66)$$

(3.3.66)

Using equations (3.3.13), (3.3.14), (3.3.40), and (3.3.41) to express n_e and n_i explicitly, we obtain

$$n_{e} = \frac{\omega_{e}}{V_{e}} \frac{1}{\sqrt{r}} \sum_{n=0}^{\infty} P_{n}(\cos\theta) \left\{ T_{11} \left[C_{1n} H_{n+\frac{1}{2}}^{(2)}(k_{1}r) + D_{1n} H_{n+\frac{1}{2}}^{(1)}(k_{1}r) \right] + T_{12} \left[C_{2n} H_{n+\frac{1}{2}}^{(2)}(k_{2}r) + D_{2n} H_{n+\frac{1}{2}}^{(1)}(k_{2}r) \right] \right\}$$

$$(3.3.67)$$

$$n_{i} = \frac{\omega_{i}}{V_{i}} \frac{1}{\sqrt{r}} \sum_{n=0}^{\infty} P_{n}(\cos\theta) \left\{ T_{21} \left[C_{1n} H_{n+\frac{1}{2}}^{(2)}(k_{1}r) + D_{1n} H_{n+\frac{1}{2}}^{(1)}(k_{1}r) \right] + T_{22} \left[C_{2n} H_{n+\frac{1}{2}}^{(2)}(k_{2}r) + D_{2n} H_{n+\frac{1}{2}}^{(1)}(k_{2}r) \right] \right\}$$

$$(3.3.68)$$

where T_{11} , T_{12} , T_{21} , and T_{22} are given by equations (3.3.15) thru (3.3.18). Using equations (3.2.19), (3.2.20), (3.3.67), and (3.3.68) we can get

$$\frac{\partial n_{e}}{\partial r} = -\frac{\omega_{e}}{V_{e}} \frac{1}{r^{3/2}} \sum_{n=0}^{\infty} P_{n}(\cos\theta) \left\{ T_{11} C_{1n} \left[(n+1) H_{n+\frac{1}{2}}^{(2)}(k_{1}r) \right] - k_{1}r H_{n-\frac{1}{2}}^{(2)}(k_{1}r) \right] + T_{11} D_{1n} \left[(n+1) H_{n+\frac{1}{2}}^{(1)}(k_{1}r) \right] - k_{1}r H_{n-\frac{1}{2}}^{(1)}(k_{1}r) \right] + T_{12} C_{2n} \left[(n+1) H_{n+\frac{1}{2}}^{(2)}(k_{2}r) \right] - k_{2}r H_{n-\frac{1}{2}}^{(2)}(k_{2}r) \right] + T_{12} D_{2n} \left[(n+1) H_{n+\frac{1}{2}}^{(1)}(k_{2}r) \right] - k_{2}r H_{n-\frac{1}{2}}^{(1)}(k_{2}r) \right\}$$

$$(3.3.69)$$

and

$$\frac{\partial n_{i}}{\partial r} = -\frac{\omega_{i}}{V_{i}} \frac{1}{r^{3/2}} \sum_{n=0}^{\infty} P_{n}(\cos\theta) \left\{ T_{21} C_{1n} \left[(n+1)H_{n+\frac{1}{2}}^{(2)}(k_{1}r) - k_{1}rH_{n-\frac{1}{2}}^{(2)}(k_{1}r) \right] + T_{21} D_{1n} \left[(n+1)H_{n+\frac{1}{2}}^{(1)}(k_{1}r) - k_{1}rH_{n-\frac{1}{2}}^{(1)}(k_{1}r) \right] + T_{22} C_{2n} \left[(n+1)H_{n+\frac{1}{2}}^{(2)}(k_{2}r) - k_{2}rH_{n-\frac{1}{2}}^{(2)}(k_{2}r) \right] + T_{22} D_{2n} \left[(n+1)H_{n+\frac{1}{2}}^{(1)}(k_{2}r) - k_{2}rH_{n-\frac{1}{2}}^{(2)}(k_{2}r) \right] \right\}.$$
(3.3.70)

From the definition of the associated Legendre functions and the ordinary Legendre functions we can derive the identity

$$P_{n}^{1} (\cos \theta) = \frac{d}{d\theta} P_{n} (\cos \theta). \qquad (3.3.71)$$

Using equations (3.3.67), (3.3.68), and (3.3.71) we have

$$\frac{\partial n_{e}}{\partial \theta} = \frac{\omega_{e}}{V_{e}} \frac{1}{\sqrt{r}} \sum_{n=1}^{\infty} P_{n}^{1} (\cos \theta) \left\{ T_{11} \left[C_{1n} H_{n+\frac{1}{2}}^{(2)} (k_{1}r) + D_{1n} H_{n+\frac{1}{2}}^{(1)} (k_{1}r) \right] + T_{12} \left[C_{2n} H_{n+\frac{1}{2}}^{(2)} (k_{2}r) + D_{2n} H_{n+\frac{1}{2}}^{(1)} (k_{2}r) \right] \right\}$$
(3.3.72)

and

$$\frac{\partial n_{i}}{\partial \theta} = \frac{\omega_{i}}{V_{i}} \frac{1}{\sqrt{r}} \sum_{n=1}^{\infty} P_{n}^{1}(\cos\theta) \left\{ T_{21} \left[C_{1n} H_{n+\frac{1}{2}}^{(2)}(k_{1}r) + D_{1n} H_{n+\frac{1}{2}}^{(1)}(k_{1}r) \right] + T_{22} \left[C_{2n} H_{n+\frac{1}{2}}^{(2)}(k_{2}r) + D_{2n} H_{n+\frac{1}{2}}^{(1)}(k_{2}r) \right] \right\}$$
(3.3.73)

because $P_0^1(\cos\theta) = 0$. Equations (3.3.61) thru (3.3.66) can now be expressed explicitly. The first terms on the right hand sides of equations (3.3.61) thru (3.3.66) can be obtained using the same procedures as those used in Section 3.2 and the other terms can be derived using equations (3.3.69), (3.3.70), (3.3.72), and (3.3.73). Since we are interested in $E_{2\theta}$, v_{er} , and v_{ir} for later development, only equations (3.3.62), (3.3.63), and (3.3.65) are expressed more explicitly as follows:

$$\begin{split} \mathbf{E}_{2\theta} &= -\frac{\mathbf{j}}{\omega \xi r^{3/2}} \sum_{n=1}^{\infty} \mathbf{P}_{n}^{1} (\cos \theta) \left\{ \mathbf{E}_{n} \left[\mathbf{n} \mathbf{H}_{n+\frac{1}{2}}^{(2)} (\mathbf{k}_{e} \mathbf{r}) - \mathbf{k}_{e} \mathbf{r} \mathbf{H}_{n-\frac{1}{2}}^{(2)} (\mathbf{k}_{e} \mathbf{r}) \right] \right. \\ &+ \left. \mathbf{F}_{n} \left[\mathbf{n} \mathbf{H}_{n+\frac{1}{2}}^{(1)} (\mathbf{k}_{e} \mathbf{r}) - \mathbf{k}_{e} \mathbf{r} \mathbf{H}_{n-\frac{1}{2}}^{(1)} (\mathbf{k}_{e} \mathbf{r}) \right] \right. \\ &- \left. \frac{\omega_{e} \mathbf{V}_{e} \mathbf{e}}{\gamma_{e} + \mathbf{j} \omega} \left[\mathbf{T}_{11} \mathbf{C}_{1n} \mathbf{H}_{n+\frac{1}{2}}^{(2)} (\mathbf{k}_{1} \mathbf{r}) + \mathbf{T}_{11} \mathbf{D}_{1n} \mathbf{H}_{n+\frac{1}{2}}^{(1)} (\mathbf{k}_{1} \mathbf{r}) \right. \\ &+ \left. \mathbf{T}_{12} \mathbf{C}_{2n} \mathbf{H}_{n+\frac{1}{2}}^{(2)} (\mathbf{k}_{2} \mathbf{r}) + \mathbf{T}_{12} \mathbf{D}_{2n} \mathbf{H}_{n+\frac{1}{2}}^{(1)} (\mathbf{k}_{2} \mathbf{r}) \right] + \end{split}$$

$$\begin{split} \frac{\omega_{1}V_{1}e}{\gamma_{1}+j\omega} & \mathbb{I}_{21}^{C} C_{1n}^{H}_{n+l_{2}}^{(2)}(k_{1}r) + \mathbb{I}_{21}^{D} C_{1n}^{H}_{n+l_{2}}^{(1)}(k_{1}r) \\ & + \mathbb{I}_{22}^{C} C_{2n}^{H}_{n+l_{2}}^{(2)}(k_{2}r) + \mathbb{I}_{22}^{D} C_{2n}^{H}_{n+l_{2}}^{(1)}(k_{2}r) \bigg] \bigg\} \qquad (3.3.74) \\ v_{er} & = \frac{e}{m_{e}(\gamma_{e}+j\omega)} \frac{1}{j\omega\xi} \frac{1}{r^{3/2}} \sum_{n=1}^{\infty} n(n+1) P_{n}(\cos\theta) \left[\mathbb{E}_{n}^{H}_{n+l_{2}}^{(2)}(k_{e}r) \right] \\ & + \mathbb{E}_{n}^{H}_{n+l_{2}}^{(1)}(k_{e}r) \right] + \frac{\varepsilon_{o}}{n_{o}\xi(\gamma_{e}+j\omega)} \frac{1}{r^{3/2}} \sum_{n=0}^{\infty} P_{n}(\cos\theta) \\ & \times \left[\left\{ C_{1n} \left[(n+1) H_{n+l_{2}}^{(2)}(k_{1}r) - k_{1}r H_{n-l_{2}}^{(2)}(k_{1}r) \right] \right\} \left\{ \omega_{e}V_{e}T_{11} \right[1 \\ & + \mathbb{E}_{n}^{2} \left[(n+1) H_{n+l_{2}}^{(1)}(k_{1}r) - k_{1}r H_{n-l_{2}}^{(1)}(k_{1}r) \right] \right\} \left\{ \omega_{e}V_{e}T_{11} \right[1 \\ & - \frac{\omega_{1}^{2}}{\omega^{2}+\gamma_{1}^{2}} - j \frac{\gamma_{1}\omega_{1}^{2}}{\omega(\omega^{2}+\gamma_{1}^{2})} \right] - j \frac{\omega_{e}^{2}\omega_{1}V_{1}}{\omega(\gamma_{1}+j\omega)} T_{21} \bigg\} \\ & + \left\{ C_{2n} \left[(n+1) H_{n+l_{2}}^{(2)}(k_{2}r) - k_{2}r H_{n-l_{2}}^{(2)}(k_{2}r) \right] \right\} \left\{ \omega_{e}V_{e}T_{12} \right[1 \\ & - \frac{\omega_{1}^{2}}{\omega^{2}+\gamma_{1}^{2}} - j \frac{\gamma_{1}\omega_{1}^{2}}{\omega(\omega^{2}+\gamma_{1}^{2})} \right] - j \frac{\omega_{e}^{2}\omega_{1}V_{1}}{\omega(\gamma_{1}+j\omega)} T_{22} \bigg\} \\ & - \frac{\omega_{1}^{2}}{\omega^{2}+\gamma_{1}^{2}} - j \frac{\gamma_{1}\omega_{1}^{2}}{\omega(\omega^{2}+\gamma_{1}^{2})} - j \frac{\omega_{e}^{2}\omega_{1}V_{1}}{\omega(\gamma_{1}+j\omega)} T_{22} \bigg\} \end{aligned}$$

3.

Spa

$$\begin{split} \mathbf{v}_{ir} &= -\frac{\mathbf{e}}{m_{i} (\gamma_{i} + j \omega)} \frac{1}{j \omega \xi} \frac{1}{r^{3/2}} \sum_{n=1}^{\infty} n (n + 1) P_{n} (\cos \theta) \left[\mathbb{E}_{n} \mathbf{H}_{n + \frac{1}{2}}^{(2)} (k_{e} r) \right] \\ &+ F_{n} \mathbf{H}_{n + \frac{1}{2}}^{(1)} (k_{e} r) \right] + \frac{\varepsilon_{o}}{n_{o} \xi (\gamma_{i} + j \omega)} \frac{1}{r^{3/2}} \sum_{n=0}^{\infty} P_{n} (\cos \theta) \\ &\times \left[\left\{ C_{1n} \left[(n + 1) \mathbf{H}_{n + \frac{1}{2}}^{(2)} (k_{1} r) - k_{1} r \mathbf{H}_{n - \frac{1}{2}}^{(2)} (k_{1} r) \right] \right. \\ &+ D_{1n} \left[(n + 1) \mathbf{H}_{n + \frac{1}{2}}^{(1)} (k_{1} r) - k_{1} r \mathbf{H}_{n - \frac{1}{2}}^{(1)} (k_{1} r) \right] \right\} \left\{ \omega_{i} \mathbf{V}_{i} \mathbf{T}_{21} \right[1 \\ &- \frac{\omega_{e}^{2}}{\omega^{2} + \gamma_{e}^{2}} - \mathbf{j} \frac{\omega_{e}^{2} \gamma_{e}}{\omega (\omega^{2} + \gamma_{e}^{2})} \right] - \mathbf{j} \frac{\omega_{i}^{2} \omega_{e} \mathbf{V}_{e}}{\omega (\gamma_{e} + j \omega)} \mathbf{T}_{11} \right\} \\ &+ \left\{ C_{2n} \left[(n + 1) \mathbf{H}_{n + \frac{1}{2}}^{(1)} (k_{2} r) - k_{2} r \mathbf{H}_{n - \frac{1}{2}}^{(2)} (k_{2} r) \right] \right. \\ &+ D_{2n} \left[(n + 1) \mathbf{H}_{n + \frac{1}{2}}^{(1)} (k_{2} r) - k_{2} r \mathbf{H}_{n - \frac{1}{2}}^{(1)} (k_{2} r) \right] \left\{ \omega_{i} \mathbf{V}_{i} \mathbf{T}_{22} \right[1 \\ &- \frac{\omega_{e}^{2}}{\omega^{2} + \gamma_{e}^{2}} - \mathbf{j} \frac{\omega_{e}^{2} \gamma_{e}}{\omega (\omega^{2} + \gamma_{e}^{2})} \right] - \mathbf{j} \frac{\omega_{i}^{2} \omega_{e} \mathbf{V}_{e}}{\omega (\gamma_{e} + j \omega)} \mathbf{T}_{12} \right\} \end{aligned}$$

$$(3.3.76)$$

3.4 Region III: Free Space

The basic equations which govern Region III (free space, $r \geqslant c$) are Maxwell's equations

$$\nabla \times E_3(r) = -j\omega\mu_0H_3(r) \qquad (3.4.1)$$

$$\nabla \times \underset{\sim}{H_3}(\underline{r}) = j\omega \varepsilon_0 \underbrace{\varepsilon_3}(\underline{r}). \tag{3.4.2}$$

Since Region III is unbounded, no reflected or inward traveling wave exists in this region. Following an analysis similar to that in Section 3.2, the solutions to Maxwell's equations in this region can be written as

$$H_{3\phi} = \frac{1}{\sqrt{r}} \sum_{n=1}^{\infty} G_n P_n^1(\cos\theta) H_{n+\frac{1}{2}}^{(2)}(\beta_0 r)$$
 (3.4.3)

$$E_{3r} = \frac{j}{\omega \epsilon_0 r^{3/2}} \sum_{n=1}^{\infty} G_n n(n+1) P_n(\cos\theta) H_{n+\frac{1}{2}}^{(2)}(\beta_0 r)$$
(3.4.4)

$$E_{3\theta} = -\frac{j}{\omega \epsilon_0 r^{3/2}} \sum_{n=1}^{\infty} G_n P_n^1 (\cos \theta) \left[n H_{n+\frac{1}{2}}^{(2)} (\beta_0 r) \right]$$

$$-\beta_{0}r H_{n-\frac{1}{2}}^{(2)}(\beta_{0}r)$$
 (3.4.5)

and

$$H_{3r} = H_{3\theta} = E_{3\phi} = 0$$
 (3.4.6)

where G_n is an arbitrary constant, n is a positive integer, and $\beta_0 = \omega \sqrt{\mu_0 \epsilon_0}$.

3.5 <u>Imposition of Boundary</u> Conditions at Interfaces

In order to determine the arbitrary constants A_n , B_n , C_{1n} , D_{1n} , C_{2n} , D_{2n} , E_n , E_n , E_n , and G_n , the boundary conditions at r = a, r = b, and r = c are applied.

The voltage across the gap of the spherical antenna is given by

$$V = \int_{\frac{\pi}{2} - \theta_1}^{\frac{\pi}{2} + \theta_1} E_{1\theta}(a,\theta) ad\theta = \int_{0}^{\pi} E_{1\theta}(a,\theta) ad\theta \qquad (3.5.1)$$

because $E_{1\theta}$ is zero on the surface of the conducting sphere except at the gap $\pi/2 - \theta_1 \le \theta \le \pi/2 + \theta_1$. Since the ordinary Legendre functions form a complete set of orthogonal functions, any function f(x) on the interval $-1 \le x \le 1$ can be expanded in terms of them. Thus the electric field on the surface of the sphere can be represented as

$$E_{1\theta}(a,\theta) = \sum_{n=1}^{\infty} b_n P_n^{1}(\cos\theta)$$
 (3.5.2)

where

$$b_n = \frac{2n+1}{2n(n+1)} \int_{0}^{\pi} E_{1\theta}(a,\theta) P_n^{1}(\cos\theta) \sin\theta d\theta.$$
 3.5.3)

If the gap between the two halves of the sphere is assumed to be small, then

$$\begin{cases}
P_n^1(\cos\theta) \approx P_n^1(0) \\
\sin\theta \approx 1
\end{cases}$$

$$\frac{\pi}{2} - \theta_1 \leq \theta \leq \frac{\pi}{2} + \theta_1 \\
\theta_1 \text{ is small.}$$
(3.5.4)

Combining equations (3.5.1), (3.5.3), and (3.5.4), we have

$$b_{n} = \frac{(2n+1) P_{n}^{1}(0) V}{2n(n+1) a} . \qquad (3.5.5)$$

From equation (3.2.21)

$$E_{1\theta}(a,\theta) = -\frac{j}{\omega \varepsilon_{d} a^{3/2}} \sum_{n=1}^{\infty} P_{n}^{1}(\cos \theta) \left\{ A_{n} \left[n \ H_{n+\frac{1}{2}}^{(2)}(\beta_{d} a) \right] - \beta_{d} a H_{n-\frac{1}{2}}^{(2)}(\beta_{d} a) \right] + B_{n} \left[n \ H_{n+\frac{1}{2}}^{(1)}(\beta_{d} a) \right] - \beta_{d} a \ H_{n-\frac{1}{2}}^{(1)}(\beta_{d} a) \right\}.$$

$$(3.5.6)$$

Combining equations (3.5.2), (3.5.5), and (3.5.6) we have

$$M_{11} A_n + M_{12} B_n = S V$$
 (3.5.7)

where

$$M_{11} = n H_{n+\frac{1}{2}}^{(2)}(\beta_{d}a) - \beta_{d}a H_{n-\frac{1}{2}}^{(2)}(\beta_{d}a)$$

$$M_{12} = n H_{n+\frac{1}{2}}^{(1)}(\beta_{d}a) - \beta_{d}a H_{n-\frac{1}{2}}^{(1)}(\beta_{d}a)$$

$$S = j\omega\epsilon_{d}a^{\frac{1}{2}} P_{n}^{1}(0) \frac{2n+1}{2n(n+1)}.$$
(3.5.8)

The M_{ij} , i,j = 1,2,...,8,9 refer to position in a matrix to be set up later.

The continuity of the tangential components of \mathbf{E} and \mathbf{H} at the dielectric-plasma interface (r=b) requires that

$$E_{1\theta}(b,\theta) = E_{2\theta}(b,\theta)$$
 (3.5.9)

$$H_{1\phi}(b,\theta) = H_{2\phi}(b,\theta).$$
 (3.5.10)

Using equations (3.2.21) and (3.3.74), equation (3.5.9) gives

$$M_{21}^{A}_{n} + M_{22}^{B}_{n} + M_{23}^{C}_{1n} + M_{24}^{D}_{1n} + M_{25}^{C}_{2n}$$

 $+ M_{26}^{D}_{2n} + M_{27}^{E}_{n} + M_{28}^{F}_{n} = 0$ (3.5.11)

where

$$\begin{split} &\mathsf{M}_{21} = \frac{\xi}{\varepsilon_{\mathbf{d}}} \left[\mathbf{n} \ \ \mathsf{H}_{\mathbf{n}+\mathbf{i}_{2}}^{(2)}(\beta_{\mathbf{d}} \mathbf{b}) \ - \ \beta_{\mathbf{d}} \mathbf{b} \ \ \ \mathsf{H}_{\mathbf{n}-\mathbf{i}_{2}}^{(2)}(\beta_{\mathbf{d}} \mathbf{b}) \right] \\ &\mathsf{M}_{22} = \frac{\xi}{\varepsilon_{\mathbf{d}}} \left[\mathbf{n} \ \ \mathsf{H}_{\mathbf{n}+\mathbf{i}_{2}}^{(1)}(\beta_{\mathbf{d}} \mathbf{b}) \ - \ \beta_{\mathbf{d}} \mathbf{b} \ \ \ \mathsf{H}_{\mathbf{n}-\mathbf{i}_{2}}^{(1)}(\beta_{\mathbf{d}} \mathbf{b}) \right] \\ &\mathsf{M}_{23} = \mathbf{e} \left[\frac{\omega_{\mathbf{e}} \mathbf{V}_{\mathbf{e}}}{\gamma_{\mathbf{e}}+\mathbf{j}\omega} \ \mathbf{T}_{11} \ - \ \frac{\omega_{\mathbf{i}} \mathbf{V}_{\mathbf{i}}}{\gamma_{\mathbf{i}}+\mathbf{j}\omega} \ \mathbf{T}_{21} \right] \mathsf{H}_{\mathbf{n}+\mathbf{i}_{2}}^{(2)}(\mathbf{k}_{1} \mathbf{b}) \\ &\mathsf{M}_{24} = \mathbf{e} \left[\frac{\omega_{\mathbf{e}} \mathbf{V}_{\mathbf{e}}}{\gamma_{\mathbf{e}}+\mathbf{j}\omega} \ \mathbf{T}_{11} \ - \ \frac{\omega_{\mathbf{i}} \mathbf{V}_{\mathbf{i}}}{\gamma_{\mathbf{i}}+\mathbf{j}\omega} \ \mathbf{T}_{21} \right] \mathsf{H}_{\mathbf{n}+\mathbf{i}_{2}}^{(1)}(\mathbf{k}_{1} \mathbf{b}) \\ &\mathsf{M}_{25} = \mathbf{e} \left[\frac{\omega_{\mathbf{e}} \mathbf{V}_{\mathbf{e}}}{\gamma_{\mathbf{e}}+\mathbf{j}\omega} \ \mathbf{T}_{12} \ - \ \frac{\omega_{\mathbf{i}} \mathbf{V}_{\mathbf{i}}}{\gamma_{\mathbf{i}}+\mathbf{j}\omega} \ \mathbf{T}_{22} \right] \mathsf{H}_{\mathbf{n}+\mathbf{i}_{2}}^{(2)}(\mathbf{k}_{2} \mathbf{b}) \\ &\mathsf{M}_{26} = \mathbf{e} \left[\frac{\omega_{\mathbf{e}} \mathbf{V}_{\mathbf{e}}}{\gamma_{\mathbf{e}}+\mathbf{j}\omega} \ \mathbf{T}_{12} \ - \ \frac{\omega_{\mathbf{i}} \mathbf{V}_{\mathbf{i}}}{\gamma_{\mathbf{i}}+\mathbf{j}\omega} \ \mathbf{T}_{22} \right] \mathsf{H}_{\mathbf{n}+\mathbf{i}_{2}}^{(1)}(\mathbf{k}_{2} \mathbf{b}) \\ &\mathsf{M}_{27} = - \left[\mathbf{n} \ \ \mathsf{H}_{\mathbf{n}+\mathbf{i}_{2}}^{(2)}(\mathbf{k}_{\mathbf{e}} \mathbf{b}) \ - \ \mathbf{k}_{\mathbf{e}} \mathbf{b} \ \ \mathsf{H}_{\mathbf{n}-\mathbf{i}_{2}}^{(2)}(\mathbf{k}_{\mathbf{e}} \mathbf{b}) \right] \end{split}$$

$$M_{28} = -\begin{bmatrix} n & H_{n+\frac{1}{2}}^{(1)}(k_eb) - k_eb & H_{n-\frac{1}{2}}^{(1)}(k_eb) \end{bmatrix}$$

From equations (3.2.22) and (3.3.53), equation (3.5.10) can be expressed as

$$M_{31}A_n + M_{32}B_n + M_{37}E_n + M_{38}F_n = 0$$
 (3.5.13)

where

$$M_{31} = H_{n+\frac{1}{2}}^{(2)}(\beta_d b)$$

$$M_{32} = H_{n+\frac{1}{2}}^{(1)}(\beta_d b)$$

(3.5.14)

$$M_{37} = -H_{n+\frac{1}{2}}^{(2)}(k_eb)$$

$$M_{38} = -H_{n+\frac{1}{2}}^{(1)}(k_eb).$$

The continuity of the tangential components of the E and H fields at the plasma-free space interface (r=c) leads to the boundary conditions

$$E_{2\theta}(c,\theta) = E_{3\theta}(c,\theta)$$
 (3.5.15)

$$H_{2\phi}(c,\theta) = H_{3\phi}(c,\theta)$$
. (3.5.16)

Using equations (3.3.74) and (3.4.5), equation (3.5.15) gives

$$^{M}_{43}^{C}_{1n} + ^{M}_{44}^{D}_{1n} + ^{M}_{45}^{C}_{2n} + ^{M}_{46}^{D}_{2n} + ^{M}_{47}^{E}_{n}$$
 $+ ^{M}_{48}^{F}_{n} + ^{M}_{49}^{G}_{n} = 0$ (3.5.17)

where

$$\begin{split} &\mathsf{M}_{43} = \mathbf{e} \left[\frac{\omega_{e} \mathsf{V}_{e}}{\mathsf{Y}_{e}^{+j\omega}} \; \mathsf{T}_{11} - \frac{\omega_{i} \mathsf{V}_{i}}{\mathsf{Y}_{i}^{+j\omega}} \; \mathsf{T}_{21} \right] \mathsf{H}_{n+l_{2}}^{(2)}(\mathsf{k}_{1}c) \\ &\mathsf{M}_{44} = \mathbf{e} \left[\frac{\omega_{e} \mathsf{V}_{e}}{\mathsf{Y}_{e}^{+j\omega}} \; \mathsf{T}_{11} - \frac{\omega_{i} \mathsf{V}_{i}}{\mathsf{Y}_{i}^{+j\omega}} \; \mathsf{T}_{21} \right] \mathsf{H}_{n+l_{2}}^{(1)}(\mathsf{k}_{1}c) \\ &\mathsf{M}_{45} = \mathbf{e} \left[\frac{\omega_{e} \mathsf{V}_{e}}{\mathsf{Y}_{e}^{+j\omega}} \; \mathsf{T}_{12} - \frac{\omega_{i} \mathsf{V}_{i}}{\mathsf{Y}_{i}^{+j\omega}} \; \mathsf{T}_{22} \right] \; \mathsf{H}_{n+l_{2}}^{(2)}(\mathsf{k}_{2}c) \\ &\mathsf{M}_{46} = \mathbf{e} \left[\frac{\omega_{e} \mathsf{V}_{e}}{\mathsf{Y}_{e}^{+j\omega}} \; \mathsf{T}_{12} - \frac{\omega_{i} \mathsf{V}_{i}}{\mathsf{Y}_{i}^{+j\omega}} \; \mathsf{T}_{22} \right] \; \mathsf{H}_{n+l_{2}}^{(1)}(\mathsf{k}_{2}c) \\ &\mathsf{M}_{47} = - \left[\mathsf{n} \; \; \mathsf{H}_{n+l_{2}}^{(2)}(\mathsf{k}_{e}c) - \mathsf{k}_{e}c \; \; \mathsf{H}_{n-l_{2}}^{(2)}(\mathsf{k}_{e}c) \right] \\ &\mathsf{M}_{48} = - \left[\mathsf{n} \; \; \mathsf{H}_{n+l_{2}}^{(1)}(\mathsf{k}_{e}c) - \mathsf{k}_{e}c \; \; \mathsf{H}_{n-l_{2}}^{(1)}(\mathsf{k}_{e}c) \right] \\ &\mathsf{M}_{49} = \frac{\xi}{\varepsilon_{o}} \left[\mathsf{n} \; \; \mathsf{H}_{n+l_{2}}^{(2)}(\mathsf{k}_{o}c) - \mathsf{k}_{o}c \; \; \mathsf{H}_{n-l_{2}}^{(2)}(\mathsf{k}_{o}c) \right] . \end{split}$$

From equations (3.3.53) and (3.4.3), equation (3.5.16) can be expressed as

$$M_{57}E_n + M_{58}F_n + M_{59}G_n = 0$$
 (3.5.19)

where

$$M_{57} = -H_{n+\frac{1}{2}}^{(2)}(k_{e}c)$$

$$M_{58} = -H_{n+\frac{1}{2}}^{(1)}(k_{e}c)$$
(3.5.20)

$$M_{59} = H_{n+\frac{1}{2}}^{(2)}(\beta_0 c).$$

In the present analysis, it is assumed that the normal components of the mean electron and ion velocities vanish at the interfaces at r=b and r=c. These rigid boundary conditions require that

$$v_{er}(b,\theta) = 0$$
 (3.5.21)

$$v_{er}(c,\theta) = 0$$
 (3.5.22)

$$v_{ir}(b,\theta) = 0$$
 (3.5.23)

$$v_{ir}(c,\theta) = 0.$$
 (3.5.24)

Using equation (3.3.75), equations (3.5.21), and (3.5.22) give

$$^{M}_{63}^{C}_{1n} + ^{M}_{64}^{D}_{1n} + ^{M}_{65}^{C}_{2n} + ^{M}_{66}^{D}_{2n} + ^{M}_{67}^{E}_{n}$$

$$+ ^{M}_{68}^{F}_{n} = 0$$
 (3.5.25)

and

$$^{M}73^{C}_{1n} + ^{M}74^{D}_{1n} + ^{M}75^{C}_{2n} + ^{M}76^{D}_{2n} + ^{M}77^{E}_{n}$$
 $+ ^{M}78^{F}_{n} = 0$ (3.5.26)

where

$$\begin{split} \mathsf{M}_{63} &= \mathsf{je} \left[(\mathsf{n}+1) \, \mathsf{H}_{\mathsf{n}+\frac{1}{2}}^{(2)} (\mathsf{k}_1 \mathsf{b}) \, - \, \mathsf{k}_1 \mathsf{b} \, \, \mathsf{H}_{\mathsf{n}-\frac{1}{2}}^{(2)} (\mathsf{k}_1 \mathsf{b}) \right] \left[\omega_e \, \mathsf{V}_e \, \mathsf{T}_{11} \right[1 \\ &- \frac{\omega_1^2}{\omega^2 + \gamma_1^2} \, - \, \mathsf{j} \, \frac{\gamma_1 \omega_1^2}{\omega (\omega^2 + \gamma_1^2)} \right] \, - \, \mathsf{j} \, \frac{\omega_e^2 \omega_1 \, \mathsf{V}_1}{\omega (\gamma_1 + \mathsf{j} \omega)} \, \mathsf{T}_{21} \\ \mathsf{M}_{64} &= \, \mathsf{je} \left[(\mathsf{n}+1) \, \mathsf{H}_{\mathsf{n}+\frac{1}{2}}^{(1)} (\mathsf{k}_1 \mathsf{b}) \, - \, \mathsf{k}_1 \mathsf{b} \, \mathsf{H}_{\mathsf{n}-\frac{1}{2}}^{(1)} (\mathsf{k}_1 \mathsf{b}) \right] \left[\omega_e \, \mathsf{V}_e \, \mathsf{T}_{11} \right[1 \\ &- \frac{\omega_1^2}{\omega^2 + \gamma_1^2} \, - \, \mathsf{j} \, \frac{\gamma_1 \omega_1^2}{\omega (\omega^2 + \gamma_1^2)} \right] \, - \, \mathsf{j} \, \frac{\omega_e^2 \omega_1 \, \mathsf{V}_1}{\omega (\gamma_1 + \mathsf{j} \omega)} \, \mathsf{T}_{21} \\ \mathsf{M}_{65} &= \, \mathsf{je} \left[(\mathsf{n}+1) \, \mathsf{H}_{\mathsf{n}+\frac{1}{2}}^{(2)} (\mathsf{k}_2 \mathsf{b}) \, - \, \mathsf{k}_2 \mathsf{b} \, \mathsf{H}_{\mathsf{n}-\frac{1}{2}}^{(2)} (\mathsf{k}_2 \mathsf{b}) \right] \left[\omega_e \, \mathsf{V}_e \, \mathsf{T}_{12} \right[1 \\ &- \frac{\omega_1^2}{\omega^2 + \gamma_1^2} \, - \, \mathsf{j} \, \frac{\gamma_1 \omega_1^2}{\omega (\omega^2 + \gamma_1^2)} \right] \, - \, \mathsf{j} \, \frac{\omega_e^2 \omega_1 \, \mathsf{V}_1}{\omega (\gamma_1 + \mathsf{j} \omega)} \, \mathsf{T}_{22} \\ \mathsf{M}_{66} &= \, \mathsf{je} \left[(\mathsf{n}+1) \, \mathsf{H}_{\mathsf{n}+\frac{1}{2}}^{(1)} (\mathsf{k}_2 \mathsf{b}) \, - \, \mathsf{k}_2 \mathsf{b} \, \mathsf{H}_{\mathsf{n}-\frac{1}{2}}^{(1)} (\mathsf{k}_2 \mathsf{b}) \right] \left[\omega_e \, \mathsf{V}_e \, \mathsf{T}_{12} \right[1 \\ &- \frac{\omega_1^2}{\omega^2 + \gamma_1^2} \, - \, \mathsf{j} \, \frac{\gamma_1 \omega_1^2}{\omega (\omega^2 + \gamma_1^2)} \right] \, - \, \mathsf{j} \, \frac{\omega_e^2 \omega_1 \, \mathsf{V}_1}{\omega (\gamma_1 + \mathsf{j} \omega)} \, \mathsf{T}_{22} \\ \mathsf{M}_{67} &= \, \mathsf{n} \, (\mathsf{n}+1) \, \frac{\omega_e^2}{\omega} \, \, \mathsf{H}_{\mathsf{n}+\frac{1}{2}}^{(2)} (\mathsf{k}_e \mathsf{b}) \end{split}$$

$$M_{68} = n(n+1) \frac{\omega_e^2}{\omega} H_{n+\frac{1}{2}}^{(1)}(k_e^b)$$

and the expressions for M_{7i} , i = 3,4,5,6,7,8 can be obtained by replacing b with c in the corresponding M_{6i} . Using equation (3.3.76), equations (3.5.23), and (3.5.24) can be represented as

$$^{M}83^{C}_{1n} + ^{M}84^{D}_{1n} + ^{M}85^{C}_{2n} + ^{M}86^{D}_{2n} + ^{M}87^{E}_{n}$$
 $+ ^{M}88^{F}_{n} = 0$ (3.5.28)

and

$$^{M}93^{C}_{1n} + ^{M}94^{D}_{1n} + ^{M}95^{C}_{2n} + ^{M}96^{D}_{2n} + ^{M}97^{E}_{n}$$
 $+ ^{M}98^{F}_{n} = 0$ (3.5.29)

where

$$M_{83} = je \left[(n+1)H_{n+\frac{1}{2}}^{(2)}(k_{1}b) - k_{1}bH_{n-\frac{1}{2}}^{(2)}(k_{1}b) \right] \left[\omega_{i}V_{i}T_{21} \left(1 - \frac{\omega_{e}^{2}}{\omega^{2} + \gamma_{e}^{2}} - j \frac{\omega_{e}^{2}\gamma_{e}}{\omega(\omega^{2} + \gamma_{e}^{2})} \right) - j \frac{\omega_{i}^{2}\omega_{e}V_{e}}{\omega(\gamma_{e}^{+}j\omega)} T_{11} \right]$$

$$M_{84} = je \left[(n+1)H_{n+\frac{1}{2}}^{(1)}(k_{1}b) - k_{1}bH_{n-\frac{1}{2}}^{(1)}(k_{1}b) \right] \left[\omega_{i}V_{i}T_{21} \left(1 - \frac{\omega_{e}^{2}}{\omega^{2} + \gamma_{e}^{2}} - j \frac{\omega_{e}^{2}\gamma_{e}}{\omega(\omega^{2} + \gamma_{e}^{2})} \right) - j \frac{\omega_{i}^{2}\omega_{e}V_{e}}{\omega(\gamma_{e}^{+}j\omega)} T_{11} \right]$$

$$\begin{split} \mathbf{M}_{85} &= \mathbf{je} \left[(\mathbf{n} + \mathbf{1}) \mathbf{H}_{\mathbf{n} + \frac{1}{2}}^{(2)} (\mathbf{k}_{2} \mathbf{b}) - \mathbf{k}_{2} \mathbf{b} \mathbf{H}_{\mathbf{n} - \frac{1}{2}}^{(2)} (\mathbf{k}_{2} \mathbf{b}) \right] \left[\omega_{i} \mathbf{V}_{i} \mathbf{T}_{22} \right[\mathbf{1} \\ &- \frac{\omega_{e}^{2}}{\omega^{2} + \gamma_{e}^{2}} - \mathbf{j} \frac{\omega_{e}^{2} \gamma_{e}}{\omega (\omega^{2} + \gamma_{e}^{2})} \right] - \mathbf{j} \frac{\omega_{i}^{2} \omega_{e} \mathbf{V}_{e}}{\omega (\gamma_{e} + \mathbf{j} \omega)} \mathbf{T}_{12} \\ \mathbf{M}_{86} &= \mathbf{je} \left[(\mathbf{n} + \mathbf{1}) \mathbf{H}_{\mathbf{n} + \frac{1}{2}}^{(1)} (\mathbf{k}_{2} \mathbf{b}) - \mathbf{k}_{2} \mathbf{b} \mathbf{H}_{\mathbf{n} - \frac{1}{2}}^{(1)} (\mathbf{k}_{2} \mathbf{b}) \right] \left[\omega_{i} \mathbf{V}_{i} \mathbf{T}_{22} \right[\mathbf{1} \\ &- \frac{\omega_{e}^{2}}{\omega^{2} + \gamma_{e}^{2}} - \mathbf{j} \frac{\omega_{e}^{2} \gamma_{e}}{\omega (\omega^{2} + \gamma_{e}^{2})} \right] - \mathbf{j} \frac{\omega_{i}^{2} \omega_{e} \mathbf{V}_{e}}{\omega (\gamma_{e} + \mathbf{j} \omega)} \mathbf{T}_{12} \end{split}$$

(3.5.30)

$$M_{87} = -n(n+1) \frac{\omega_i^2}{\omega} H_{n+\frac{1}{2}}^{(2)}(k_eb)$$

$$M_{88} = -n(n+1) \frac{\omega_i^2}{\omega} H_{n+\frac{1}{2}}^{(1)}(k_eb)$$

and the expressions M_{9i} , i = 3,4,5,6,7,8 can be obtained by replacing b with c in the corresponding M_{8i} . It should be noted that the summation of the second term on the right hand side of equations (3.3.75) and (3.3.76) can be changed from Σ to Σ because the n=0 term makes no n=0 n=1 contribution to the series. Thus equations (3.3.75) and (3.3.76) can be written as single summations and the rigid boundary conditions may be imposed to yield equations (3.5.25), (3.5.26), (3.5.28), and (3.5.29).

By imposing the above boundary conditions, we obtain nine algebraic equations for the nine unknown coefficients.

For convenience these equations may be written as a single matrix equation:

$$\begin{bmatrix} A_{n} \\ B_{n} \\ C_{1n} \\ D_{1n} \\ C_{2n} \\ D_{2n} \\ D_{2n} \\ D_{n} \\ C_{n} \\ C_{n}$$

where [M] is the matrix

where [M] is the matrix
$$\begin{bmatrix} M_{11} & M_{12} & 0 & 0 & 0 & 0 & 0 & 0 & 0 \\ M_{21} & M_{22} & M_{23} & M_{24} & M_{25} & M_{26} & M_{27} & M_{28} & 0 \\ M_{31} & M_{32} & 0 & 0 & 0 & 0 & M_{37} & M_{38} & 0 \\ 0 & 0 & M_{43} & M_{44} & M_{45} & M_{46} & M_{47} & M_{48} & M_{49} \\ 0 & 0 & 0 & 0 & 0 & 0 & M_{57} & M_{58} & M_{59} \\ 0 & 0 & M_{63} & M_{64} & M_{65} & M_{66} & M_{67} & M_{68} & 0 \\ 0 & 0 & M_{73} & M_{74} & M_{75} & M_{76} & M_{77} & M_{78} & 0 \\ 0 & 0 & M_{83} & M_{84} & M_{85} & M_{86} & M_{87} & M_{88} & 0 \\ 0 & 0 & M_{93} & M_{94} & M_{95} & M_{96} & M_{97} & M_{98} & 0 \end{bmatrix}$$

(3.5.32)

From equation (3.5.31) we obtain a solution for the arbitrary constants as

$$\begin{bmatrix} A_{n} \\ B_{n} \\ C_{1n} \\ D_{1n} \\ C_{2n} \\ D_{2n} \\ E_{n} \\ E_{n} \\ E_{n} \\ G_{n} \end{bmatrix}^{-1} \begin{bmatrix} SV \\ 0 \\ 0 \\ 0 \\ 0 \\ 0 \\ 0 \end{bmatrix}$$

$$(3.3.33)$$

where $[M_{ij}]^{-1}$ is the matrix inverse of $[M_{ij}]$.

Equations (3.2.22) thru (3.2.25), (3.3.53), (3.3.61), (3.3.62), (3.3.67), (3.3.68), (3.4.3) thru (3.4.6), and (3.5.33) completely determine the fields in Regions I, II, III as functions of r and θ .

Using the first result from Appendix B it is seen that S = 0 for even n. Thus, from (3.5.33), the arbitrary constants are all zero when n is even. This means that the summations for the fields in all three regions may be changed from Σ to Σ . The fields in Region III are n=1 n=1 n odd

of most interest to us and so they will be reproduced here as follows:

$$H_{3\phi} = \frac{1}{\sqrt{r}} \sum_{n=1}^{\infty} G_n P_n^1(\cos\theta) H_{n+\frac{1}{2}}^{(2)}(\beta_0 r)$$
 (3.5.34)

$$E_{3r} = \frac{j}{\omega \varepsilon_{0} r^{3/2}} \sum_{n=1}^{\infty} G_{n} \quad n(n+1) \quad P_{n}(\cos \theta) \quad H_{n+\frac{1}{2}}^{(2)}(\beta_{0} r)$$
n odd
(3.5.35)

$$E_{3\theta} = -\frac{j}{\omega \varepsilon_0 r^{3/2}} \sum_{\substack{n=1\\ n \text{ odd}}}^{\infty} G_n P_n^1(\cos\theta) \left[n H_{n+\frac{1}{2}}^{(2)}(\beta_0 r) \right]$$

$$-\beta_{0}r H_{n-\frac{1}{2}}^{(2)}(\beta_{0}r)$$
 (3.5.36)

and

$$H_{3r} = H_{3\theta} = H_{3\phi} = 0$$
 (3.5.37)

3.6 <u>Radiated Power and Input</u> Admittance

Two important quantities that we will use extensively in the next chapter on numerical results are the power radiated by the spherical antenna together with its surrounding plasma layer and the input admittance to the spherical antenna. These quantities are derived below for the specific problem which we are studying.

The power radiated from a large sphere is defined as

$$P = \lim_{r \to \infty} Re \left[\oint_{S} P_{e} \cdot dS \right]$$
 (3.6.1)

where $\underset{\sim}{P}_{e}$ is the complex Poynting vector defined by

$$P_{e} = \frac{1}{2} E \times H^*$$
 (3.6.2)

and dS is a vector quantity, which points in the outward radial direction, associated with a differential area on the spherical surface. The integration is over a large closed spherical surface.

Thus the radiated power can be written as

$$P = \lim_{r \to \infty} \frac{1}{2} \int_{0}^{2\pi} \int_{0}^{\pi} \operatorname{Re}\left[\mathbf{E} \times \mathbf{H}^{*} \cdot \hat{\mathbf{r}}\right] r^{2} \sin\theta \ d\theta d\phi.$$
(3.6.3)

In Region III in our problem

$$\times \left[mH_{m+\frac{1}{2}}^{(2)}(\beta_{O}r) - \beta_{O}rH_{m-\frac{1}{2}}^{(2)}(\beta_{O}r) \right] H_{n+\frac{1}{2}}^{(2)*}(\beta_{O}r)$$
(3.6.4)

where a superscripted * denotes complex conjugation. In the far zone $(r+\infty)$, the asymptotic expansion for large argument for the second of Hankel function is

$$\lim_{x \to \infty} H_{\alpha}^{(2)}(x) = \sqrt{\frac{2}{\pi x}} e^{-j(x-\frac{1}{2}\alpha\pi - \frac{1}{4}\pi)}.$$
 (3.6.5)

Thus, neglecting terms of the order $1/r^3$ and higher we get

$$\lim_{r\to\infty} \mathbb{E}_{3} \times \mathbb{H}_{3}^{*} \cdot \hat{r} = \frac{2}{\pi} \frac{1}{\omega \varepsilon_{0} r^{2}} \sum_{m=1}^{\infty} \sum_{n=1}^{\infty} G_{m}G_{n} P_{m}^{1}(\cos\theta)$$

$$\times P_{n}^{1}(\cos\theta) = \int_{0}^{\pi} (\frac{m-n}{2})^{\pi}. \qquad (3.3.6)$$

Therefore we obtain

$$P = \frac{1}{\pi} \frac{1}{\omega \varepsilon_{o}} \sum_{m=1}^{\infty} \sum_{n=1}^{\infty} \operatorname{Re} \left[G_{m} G_{n}^{*} \exp \left[j \left(m-n \right) \frac{\pi}{2} \right] \int_{O}^{2\pi} \int_{O}^{\pi} P_{m}^{1} \left(\cos \theta \right) \right]$$
m odd n odd

$$\times P_{n}^{1}(\cos\theta)\sin\theta d\theta d\phi$$

$$= \frac{2}{\omega \varepsilon_{0}} \sum_{m=1}^{\infty} \sum_{n=1}^{\infty} \operatorname{Re} \left[G_{m} G_{n}^{*} \exp \left[j (m-n) \frac{\pi}{2} \right] \int_{-1}^{1} P_{m}^{1}(x) P_{n}^{1}(x) dx \right].$$
m odd n odd

(3.6.7)

Using result (B-3) from Appendix B, the radiated power becomes

$$P = \frac{2}{\omega \epsilon_{0}} \sum_{n=1}^{\infty} |G_{n}|^{2} \frac{2n(n+1)}{2n+1}$$
(3.6.8)

The input admittance is defined [13] as

$$Y = 2\pi a \sin\theta [H_{\phi}]$$

$$r=a$$

$$\theta = \pi/2$$
(3.6.9)

which for our problem is

$$Y = 2\pi\sqrt{a} \sum_{n=1}^{\infty} P_n^{1}(0) \left[A_n H_{n+\frac{1}{2}}^{(2)}(\beta_d a) + B_n H_{n+\frac{1}{2}}^{(1)}(\beta_d a) \right]$$
(3.6.10)

It is noted that because of the assumption of a delta function driver only the real part of the series for Y converges. Infeld [14] has suggested that the imaginary part be calculated at some angle slightly different from $\theta = 90^{\circ}$. He suggests using the angle that a real physical gap would make with the $\theta = 90^{\circ}$ axis. In our case this means we must evaluate the susceptance at $\theta = \frac{\pi}{2} - \theta_1$. This is the procedure used in Chapter IV.

CHAPTER IV

NUMERICAL TECHNIQUES AND RESULTS

4.1 Numerical Techniques

In order to complete the solution for the fields in Regions I, II, and III of Figure 3.1, it is necessary to solve the matrix equation (3.5.31), i.e.,

$$\begin{bmatrix} A_n \\ B_n \\ C_{1n} \\ D_{1n} \\ C_{2n} \\ D_{2n} \\ D_{2n} \\ D_{3n} \\ D_{3n$$

for the arbitrary constants A_n , B_n , C_{1n} , D_{1n} , C_{2n} , D_{2n} , E_n , F_n , and G_n where the elements of M and S are given in equations (3.5.8), (3.5.12), (3.5.14), (3.5.18),

(3.5.20), (3.5.27), and (3.5.30) for $n = 1,3,5,...,\infty$. This is accomplished using the technique of Gaussian elimination [17].

Gaussian elimination is a technique to solve a matrix equation of the form

$$PX = Q (4.1.2)$$

where P is a given square matrix and Q is a given column matrix and X is the unknown column matrix to be determined. The technique is based on a theorem which states that P may be factored into a dot product of a lower triangularized matrix L and an upper triangularized matrix u, i.e.,

$$P = LU (4.1.3)$$

where

$$L = \begin{bmatrix} L_{1,1} & 0 & \cdots & 0 & 0 \\ L_{1,2} & L_{2,2} & \cdots & 0 & 0 \\ \vdots & \vdots & \ddots & \vdots & \vdots \\ L_{n-1,1} & L_{n-1,2} & \cdots & L_{n-1,n-1} & 0 \\ L_{n,1} & L_{n,2} & \cdots & L_{n,n-1} & L_{n,n} \end{bmatrix}$$
(4.1.4)

and

$$U = \begin{bmatrix} u_{1,1} & u_{1,2} & \cdots & u_{1,n-1} & u_{1,n} \\ 0 & u_{2,2} & \cdots & u_{2,n-1} & u_{2,n} \\ \vdots & \vdots & & \vdots & \vdots \\ 0 & 0 & \cdots & u_{n-1,n-1} & u_{n-1,n} \\ 0 & 0 & \cdots & 0 & u_{n,n} \end{bmatrix}.$$
 (4.1.5)

Defining a new unknown column matrix

$$y = UX \tag{4.1.6}$$

equation (4.1.2) may be written as

$$Ly = Q.$$
 (4.1.7)

Equation (4.1.7) is a set of equations that may be solved simply by back substitution. Once y is determined X may readily be determined from equation (4.1.6) by a similar procedure.

In theory the Gaussian elimination technique will give an exact solution to the set of equations (4.1.2), but in practice the solution must be obtained by use of a computer. This leads to errors due to the fact that the computer carries only a finite number of significant figures. Errors are obtained whenever the individual terms in equation (4.1.2) that are to be added together

differ by more than m orders of magnitude where m is the number of significant figures carried by the computer being used.

In our work we found that the solution for the G_n s to be very accurate in all cases judged on comparison of our results for spherical antennas in free space with those of Ramo, Whinnery, and Van Duzer [13]. The solutions for the $\mathbf{A}_{\mathbf{n}}$ s and $\mathbf{B}_{\mathbf{n}}$ s used in the calculation of the input admittance were found to be accurate only for antennas which are of the order of 0.1 wavelengths in radius. For smaller antennas surrounded by a lossless plasma, the input conductance calculated from equation (3.6.10) differed from the conductance calculated from the power radiated, equation (3.6.8), which is known to be correct in the limit of the plasma density going to zero. was probably due to numerical difficulties because the matrix M was nearly singular for small antennas. larger antennas, we were unable to keep enough terms in the series (3.6.10) to obtain a reasonable result. For an antenna radius of 0.1 wavelengths it was found that only the first term of the series (3.6.10) was needed to obtain five significant figure agreement with the conductance calculated from the power radiated for a lossless plasma layer. The power radiated was calculated retaining the first five terms, n = 1,3,5,7,9, in the infinite series in all our calculations. The susceptances for the graphs to be described later were calculated

keeping the first three terms, n = 1,3,5, which for a spherical antenna in free space give a result 27% less than the result given in the above reference [13].

As a conclusion we can say that the results given for the power radiated and the input conductance should be very accurate and the results for the input susceptance are accurate to within an order of magnitude for the cases plotted.

The Hankel functions required in the matrix M are calculated for n = 0,1 using the formulas [15]

$$H_{n+\frac{1}{2}}^{(1)}(z) = \sqrt{\frac{2z}{\pi}} j^{-n-1} z^{-1} e^{jz} \sum_{k=0}^{n} \frac{(n+k)!}{k! (n-k)!} (-2jz)^{-k}$$

$$H_{n+\frac{1}{2}}^{(2)}(z) = \sqrt{\frac{2z}{\pi}} j^{n+1} z^{-1} e^{-jz} \sum_{k! (n-k)!} \frac{(n+k)!}{k! (n-k)!} (2jz)^{-k}$$

(4.1.9)

(4.1.8)

and higher order Hankel functions, i.e., n = 2,3,... are calculated from the results for n = 0 and n = 1 for a given complex argument z = x + jy by a recurrence relation [15]

$$f_{n+1}(z) = (2n+1)z^{-1} f_n(z) - f_{n-1}(z)$$
 (4.1.10)

where f_n can be $\sqrt{\pi/2}z$ $H_{n+\frac{1}{2}}^{(1)}(z)$ or $\sqrt{\pi/2}z$ $H_{n+\frac{1}{2}}^{(2)}(z)$. The above formulas gave very good results for all values of

purely real or purely imaginary arguments that could be checked with Abramowitz and Stegun [15] for order up to n = 11.

The associated Legendre functions are calculated using [16]

$$P_1^{1}(\cos\theta) = -\sin\theta \tag{4.1.11}$$

$$P_2^{1}(\cos\theta) = -3 \sin\theta \cos\theta \qquad (4.1.12)$$

and the recurrence relation

$$n P_{n+1}^{1}(\cos\theta) = (2n+1) \cos\theta P_{n}^{1}(\cos\theta)$$

$$- (n+1) P_{n-1}^{1}(\cos\theta). \qquad (4.1.13)$$

These formulas gave very good numerical results.

All the numerical calculations were carried out on the CDC 6500 computer using single precision arithmetic (fifteen significant figures) except the calculation of the Hankel functions where double precision (twenty-nine significant figures) arithmetic was used.

The radiated power and the input admittance of a spherical antenna surrounded by a concentric layer of hot lossy plasma have been numerically calculated as a function of the antenna radius and the plasma parameters. In a realistic situation, the presence of the plasma sheath is taken into account by the adoption of a concentric dielectric layer which separates the plasma from

the metallic surface of the antenna. This adoption may also be used to account for an actual dielectric coating of the antenna. The thickness of a usual plasma sheath may be of the order of a few Debye lengths. In the present numerical calculation, the sheath is assumed to be an electron-free region extending from r=a to r=b. A convenient parameter to describe the thickness of the sheath is the dimensionless quantity s defined by $b-a=(V_e/\sqrt{3}\omega_e)$ s. It is to be noted that $(V_e/\sqrt{3}\omega_e)$ is of the order of a Debye length in the plasma and thus, s may be regarded as the "Debye thickness" of the sheath [12]. The permittivity of the sheath is assumed to be the same as that of free space, i.e., $\epsilon_d=\epsilon_0$.

4.2 Numerical Results

The results of the numerical calculations for various parameters for a spherical antenna surrounded by a finite layer of a hot lossy plasma are given in Figures 4.1 thru 4.20. The calculations were performed assuming an oxygen gas plasma so that $m_i = 2.67 \times 10^{-20}$ kilograms. The electrons and the ions were assumed to be in thermal equilibrium so that $T_e = T_i$ and the average thermal velocity of the electrons was assumed to be 0.01 times the speed of light. The antenna was assumed to be driven by a one-volt time varying source. Except where otherwise noted the sheath was assumed to be about one Debye length thick, i.e., $b = a + V_e/\sqrt{3}\omega_e$ and the ratio of the

ion-neutral particle collision frequency to the electronneutral particle collision frequency was taken equal to the ratio of the ion thermal velocity over the electron thermal velocity, i.e.,

$$\gamma_{i} = \gamma_{e} \frac{V_{i}}{V_{e}} = \gamma_{e} \sqrt{\frac{m_{e}}{m_{i}}}$$
 (4.2.1)

Unless otherwise noted we shall state only the electron-neutral particle collision frequency with the ion-neutral particle collision frequency being specified by equation (4.2.1). The values of the susceptance that are plotted in this chapter are calculated by matching the magnetic field to the current on the spherical antenna at $\theta_1 = 5^\circ$ or $\theta = 85^\circ$. This procedure was suggested by Infeld [14]. It is to be noted that for $1^\circ \le \theta_1 \le 7^\circ$ essentially the same results are obtained.

Figures 4.1, 4.2, and 4.3 plot the radiated power, the input conductance, and the input susceptance, respectively of a spherical antenna of radius 0.1λ , where λ is the free space electromagnetic wavelength, surrounded by a layer of hot plasma 0.03λ thick as a function of the plasma density, i.e., ω_e^2/ω^2 . The running parameter in each figure is the electron-neutral particle collision frequency. The range of ω_e^2/ω^2 considered in these figures is from 0.0 to 2.6 which corresponds to a high frequency or a low plasma density region. It should be noted that all plots over this range are actually

independent of the ion-neutral particle collision frequency because for high frequencies the ions are essentially immobile. The vertical scales in Figure 4.1 are 10 log (P/P_o) where P is the power radiated by the spherical antenna surrounded by a plasma layer as a function of ω_e^2/ω^2 and P_O is the power radiated by the same antenna without a plasma layer. In Figure 4.2 the vertical scales are 10 log (G/G_O) where G is the input conductance as a function of ω_e^2/ω^2 and G_o is the conductance of a spherical antenna in free space. Figure 4.3 is a series of plots of the input susceptance in mhos of a spherical antenna as a function of $\omega_{p}^{2}/\omega^{2}$. A study of these figures indicates that the inclusion of the electroacoustic wave in the theory gives rise to effects in all three figures for $\omega_e^2/\omega^2 < 1.0$ and $\gamma_e/\omega = 0.0$ in the form of troughs and peaks very close together whenever

$$c - b = N \frac{\pi}{Re(k_2)} = N \frac{\lambda_e}{2}$$
 (4.2.2)

where k_2 is the electroacoustic propagation constant and λ_e is the electroacoustic wavelength. The trough and peak pairs are labeled with the appropriate N in the plots. Physically, this says that the electroacoustic wave has a large effect whenever the parameters of the plasma layer are such that the electroacoustic wave may set up a standing wave of length N $\lambda_e/2$ in the plasma layer. For other

points the inward and outward traveling electroacoustic waves are out of phase and thus the total fields due to the waves are small. When losses are introduced into the plasma, the effects due to the electroacoustic wave are smaller because the standing wave pattern set up in the plasma layer will attenuate as one nears the outer surface. For $\gamma_{e}/\omega = 0.01$, effects due to standing waves of integer order in length are lost but standing waves of half integer order in length still have an effect. case of γ_e/ω = 0.1 all effects due to the electroacoustic wave are damped out. It is observed that the regions on these plots that cannot be related to the electroacoustic parameters are largely unaffected by the varying collision frequencies and therefore we assert that these results are due mainly to the electromagnetic wave. The effect of the plasma on the electromagnetic wave is to reduce the radiated power, the input conductance, and input susceptance as the antenna driving frequency, ω , is reduced to the neighborhood of the plasma frequency. After the plasma frequency exceeds the antenna frequency the radiated power and the input conductance build up to a value larger than the corresponding free space value. This phenomenon has been called enhanced radiation [1, 2, 3]. The input susceptance for ω_e^2/ω^2 > 1.0 shows some odd effects which we cannot attribute to any physical phenomena and may well be due to numerical problems. No further attempt was made to

find the source of the irregularities. It should be noted that the curves for the input conductance, which can also be considered as plots of the relative power radiated by the spherical antenna by itself, are always greater than or equal to the power radiated by the spherical antenna together with the surrounding plasma layer, the difference being the power absorbed by the lossy plasma due to collision effects. The losses are large only when the power radiated is affected by the electroacoustic wave.

Figures 4.4, 4.5, and 4.6 show the power radiated from progressively larger spherical antennas surrounded by hot, lossy $(\gamma_e/\omega = 0.01)$ plasmas of varying thicknesses as a function of $\omega_{\alpha}^{2}/\omega^{2}$. In these plots we again consider the high frequency region, i.e., $0 \le \omega_e^2/\omega^2 \le 2.6$. studying the three figures for one thickness of the plasma layer it is evident that the effects due to the electroacoustic wave become relatively weaker for the larger antennas. Looking at the plots for varying plasma layer thicknesses, particularly the $a = 0.01\lambda$ case, we can see that as the plasma layer becomes thicker the effect of the electroacoustic wave is observed in more regions and for large values of N. Also looking at any one figure we can see that the thickness of the plasma layer affects the power radiated due to the electromagnetic wave. Particularly for $\omega_e^2/\omega^2 > 1.0$ it can be seen that the thicker plasma layer decreases the power radiated due to the electromagnetic wave.

In Figure 4.7 the radiated power from a spherical antenna of radius 0.1 λ surrounded by a hot, lossy $(\gamma_e/\omega=0.01)$ plasma of thickness 0.03 λ is plotted as a function of ω_e^2/ω^2 . The region of enhanced radiation is seen to extend from $\omega_e^2/\omega^2=1.3$ to about $\omega_e^2/\omega^2=40.0$ for the parameters chosen. In this figure the effects due to the electroacoustic wave and to the pseudosonic wave which will soon be discussed are ignored.

Figures 4.8 and 4.9 are comparisons of our theory with some experimental results obtained by Lin [2] and Lin and Chen [3]. Power radiated is plotted as a function of plasma density for two different size antennas. The outer radius of the plasma layer is assumed to be nearly constant at about 7 cm. The electron-neutral particle collision frequency is assumed to be 0.12 GH_z in our theory and the running parameter in each figure is the antenna driving frequency. Good agreement between the theoretical and experimental results is observed.

Figure 4.10 shows three curves for the power radiated by a spherical antenna of radius 0.1λ surrounded by a hot plasma of thickness 0.03λ as a function of ω_e^{-2}/ω^2 . The range of ω_e^{-2}/ω^2 , $28400 \le \omega_e^{-2}/\omega^2 \le 30400$, corresponds to a high density plasma or a low frequency antenna source. The running parameter in the figure is the electronneutral particle collision frequency with the ion-neutral particle collision frequency set equal to zero in this

figure only. The peaks observed in these plots are due to the excitation of a pseudosonic wave in the plasma as verified by the fact that peaks occur whenever

$$c - b = N \frac{\pi}{Re(k_1)} = N \frac{\lambda p}{2}$$
 (4.2.3)

where \mathbf{k}_1 is the pseudosonic propagation constant and λp is the pseudosonic wavelength. It is observed that increasing the electron-neutral particle collision frequency decreases the maximum amplitude of the peaks indicating that the electrons contribute significantly to the propagation of the pseudosonic wave. Figure 4.11 differs from Figure 4.10 only in that the ion-neutral particle collision is now determined by equation (4.2.1). Comparison of Figures 4.10 and 4.11 shows that the ions in the plasma contribute more significantly than the electrons to the propagation of the pseudosonic wave.

Figures 4.11, 4.12, and 4.13 are identical to Figures 4.1, 4.2, and 4.3 except that the first mentioned figures are plots of the power radiated, the input conductance, and the input susceptance for low antenna frequency or high plasma density, i.e., $28400 \le \omega_e^{-2}/\omega^2 \le 30400$. The main point to note is that effects due to the inclusion of the pseudosonic wave in the theory are observed in all three figures for values of ω_e^{-2}/ω^2 that satisfy equation (4.2.3). Losses in the plasma layer decrease the effect

of the pseudosonic wave on the plotted quantities. physical interpretation here is that the pseudosonic wave has an effect on the quantities considered whenever the parameters of the plasma layer are such that a pseudosonic standing wave of a half integer pseudosonic wavelength in length may be set up in the plasma layer, i.e., in the vicinity where equation (4.2.3) holds. At other points the pseudosonic standing wave is either seriously attenuated or cannot be efficiently excited. Note that the values of the relative radiated power are always less than or equal to the values of the relative input conductance for corresponding loss terms, the difference being the amount of power absorbed by the plasma layer. The input susceptance plots in Figure 4.13 show effects that cannot obviously be related to the electromagnetic wave or the pseudosonic wave, i.e., the effects at $\omega_{p}^{2}/\omega_{\approx}^{2}$ 28550, 29900, No attempt was made to interpret the effect.

Figure 4.14 is a series of plots of the power radiated by a spherical antenna of radius 0.1 λ , surrounded by a hot lossy (γ_e/ω = 0.01) plasma of varying thicknesses as a function of ω_e^{-2/ω^2} . Comparing the upper and center plots, we notice that there are more peaks due to the pseudosonic wave for the thicker layer but these peaks are smaller in amplitude. This trend is continued in the lower plot. Here the effects due to the pseudosonic wave are so small that they cannot be seen on the scale used.

The radiated power from spherical antennas of varying radiuses surrounded by a hot lossy ($\gamma_e/\omega=0.01$) plasma which is 0.03λ thick as a function of ω_e^2/ω^2 in the low frequency region is shown in a series of plots in Figure 4.15. The only effect to be noted here is that the relative radiated power is greater for the smaller antennas.

In Figures 4.16, 4.17, and 4.18 we show the radiated power, the input conductance, and the input susceptance of a spherical antenna of radius 0.1% surrounded by a hot lossy (γ_e/ω = 0.01), plasma of thickness 0.03 λ plotted as a function of the dielectric sheath thickness in Debye lengths. Plots are given for $\omega_{\rm e}^{2}/\omega^{2}=0.31$, 0.85, and 1.5 in the high frequency region and for $\omega_{\rm p}^2/\omega^2$ = 29655, 29700, and 29900 in the low frequency region. $\omega_{\rm p}^2/\omega^2 = 0.31$ and 29655 represent points where the electroacoustic and the pseudosonic waves, respectively, contribute significantly to the quantities considered. The other values of ω_e^2/ω^2 plotted are those where the radiated power is due mostly to the electromagnetic wave. These figures indicate that the sheath thickness has very little effect on the power radiated and the input conductance for the system that we are considering. For the input susceptance the high frequency curves also show very little change due to the varying thickness of the dielectric sheath. frequency plots for the input susceptance do show a

considerable variance with changing sheath thickness. No further interpretation of these results will be attempted at this time.

In Figure 4.19 the radiated power from a very small antenna is plotted versus $\omega_e^{\ 2}/\omega^2$. The antenna is assumed to be of radius 0.00067 λ and the plasma layer thickness is 0.00004 λ . The relative radiated power is given for four collision factors, i.e., $\gamma_e/\omega=0.0$, 0.01, 0.1, and 10.0. This case is of interest if we are operating an antenna five meters in radius which is surrounded by a plasma layer, 20 cm thick, with an electron density equivalent to $f_e\approx 0.3~{\rm GH_Z}$. In this case, if we operate the antenna at a frequency $f=6\times 10^5$, Figure 4.19 predicts that the power radiated will be much greater than if the same antenna is operated without the plasma layer around it for all but the highest collisional losses. The plasma layer in the above described circumstances is approximately one-half of a pseudosonic wavelength thick.

Figure 4.20 is for the same situation as Figure 4.19 except the antenna is much larger. The result is that the plasma layer affects the radiated power very little except where equation (4.2.3) holds for N = 1.

4.3 Conclusions

From the discussion of the numerical results we can draw four conclusions:

- The propagation of a pseudosonic wave through a plasma layer covering a spherical antenna can, under proper conditions, strongly affect the radiated power, the input conductance, and the input susceptance of the antenna.
- The propagation of an electroacoustic wave through a plasma layer covering a spherical antenna can, under proper conditions, strongly affect the radiated power, the input conductance, and the input susceptance of the antenna.
- 3. As has been discussed by others [1, 2, 3], the propagation of the electromagnetic wave through the plasma layer can, under the proper conditions, strongly affect the radiated power of the antenna and, in addition, as we have shown, the input conductance and susceptance.
- 4. The thickness of the dielectric sheath has little effect on the radiated power and input conductance of a spherical antenna surrounded by a layer of hot lossy plasma.

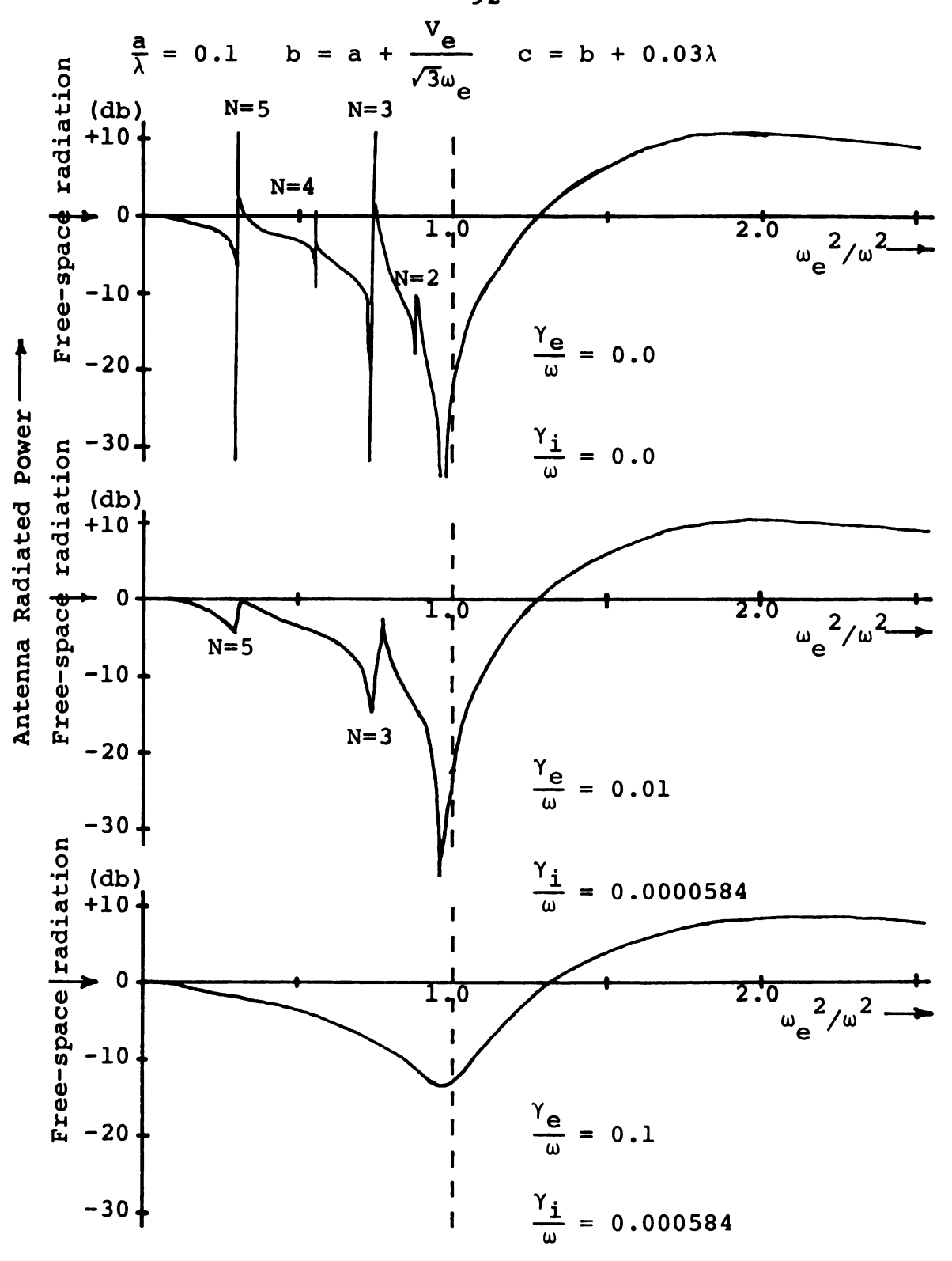


Figure 4.1. Theoretical power radiated by a spherical antenna in a hot ($V_e/C=0.01$) plasma as a function of plasma density for various collision frequencies.

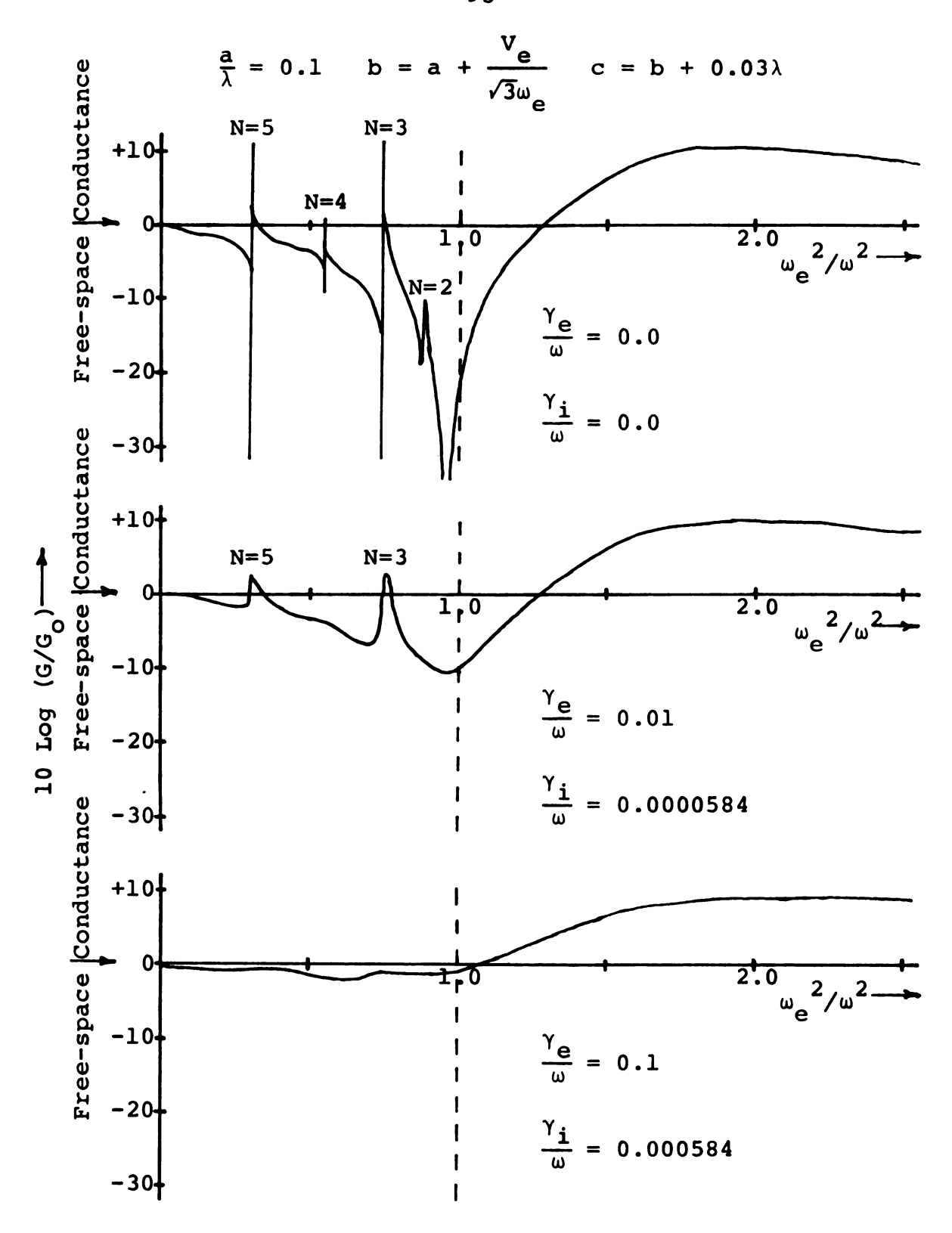


Figure 4.2. Theoretical input conductance of a spherical antenna in a hot ($V_e/C = 0.01$) plasma as a function of plasma density for various collision frequencies.

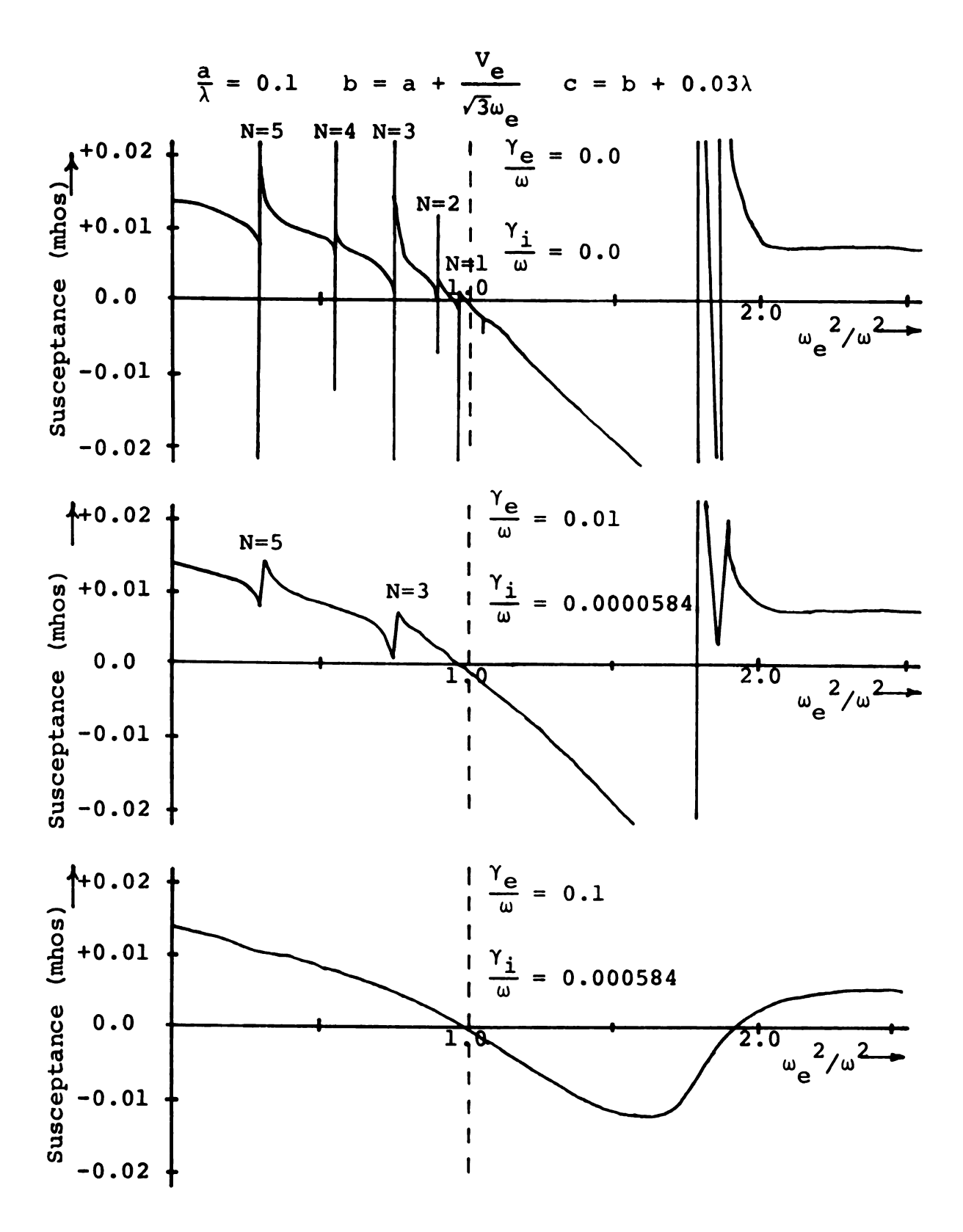


Figure 4.3. Theoretical input susceptance of a spherical antenna in a hot ($V_e/C=0.01$) plasma as a function of plasma density for various collision frequencies.

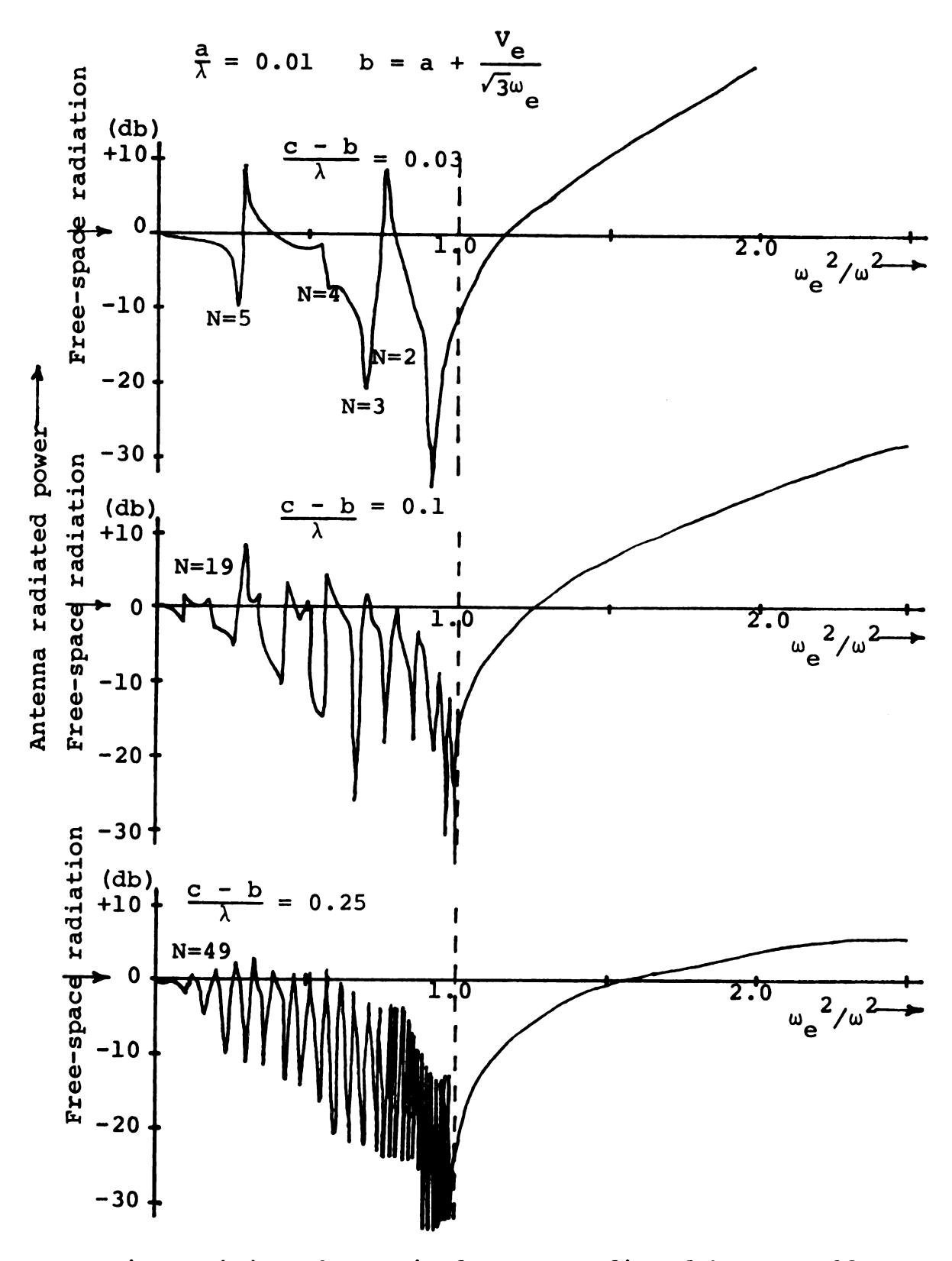


Figure 4.4. Theoretical power radiated by a small spherical antenna in a hot ($V_e/C=0.01$), lossy ($\gamma_e/\omega=0.01$, $\gamma_i/\omega=0.0000584$) plasma as a function of plasma density for various thicknesses of the plasma layer.

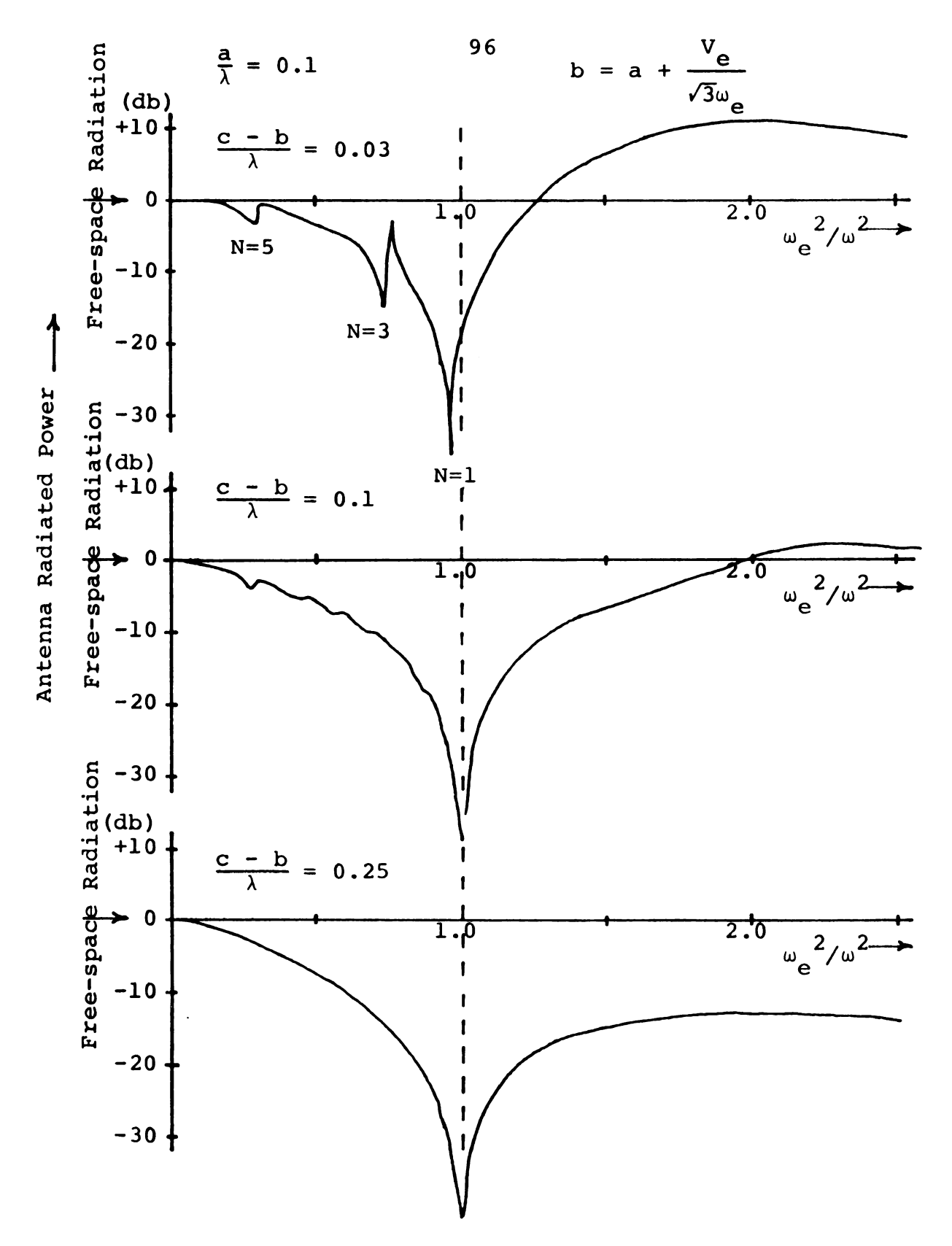


Figure 4.5. Theoretical power radiated by a spherical antenna in a hot ($V_e/C = 0.01$), lossy ($\gamma_e/\omega = 0.01$, $\gamma_i/\omega = 0.0000584$) plasma as a function of plasma density for various thicknesses of the plasma layer.

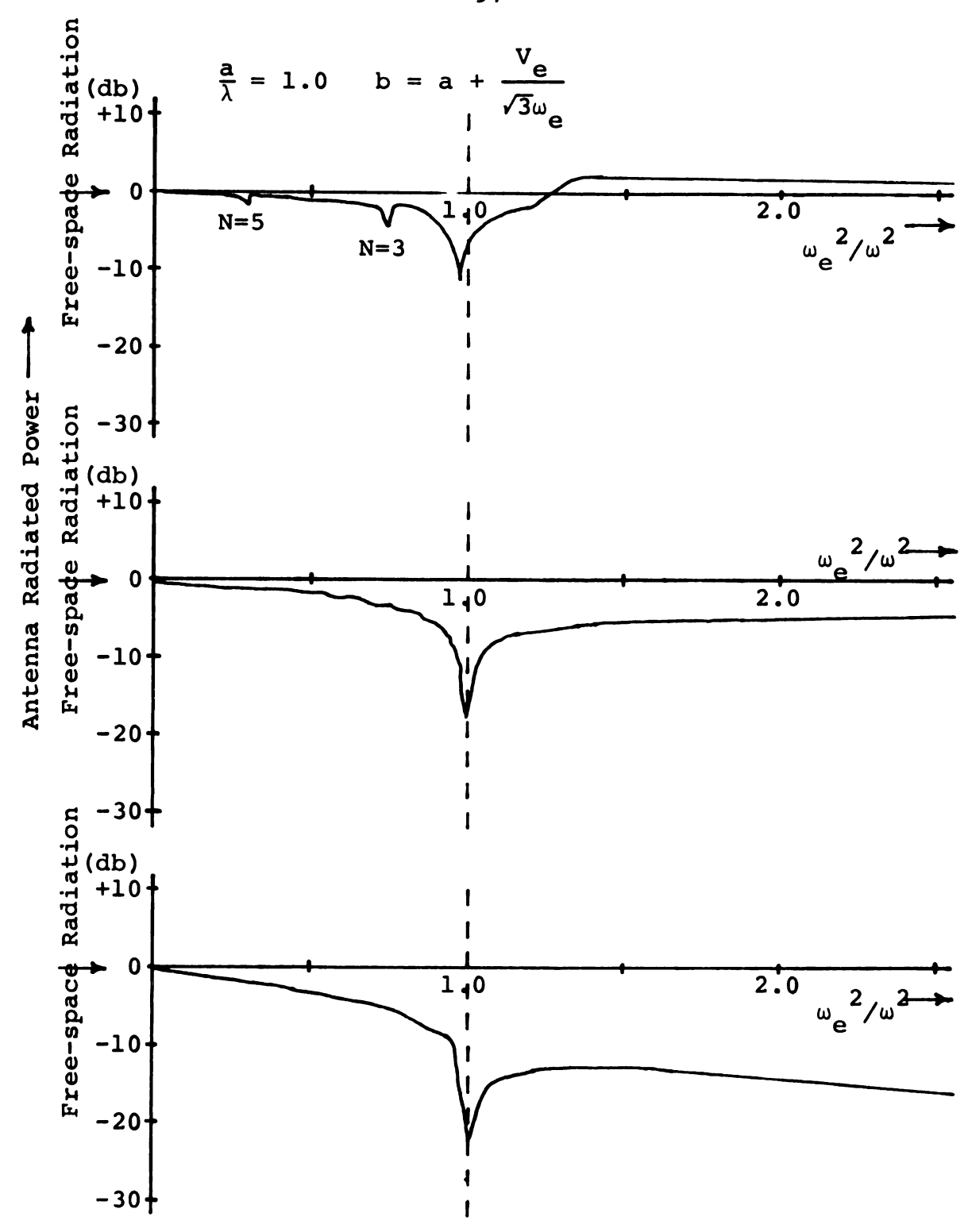
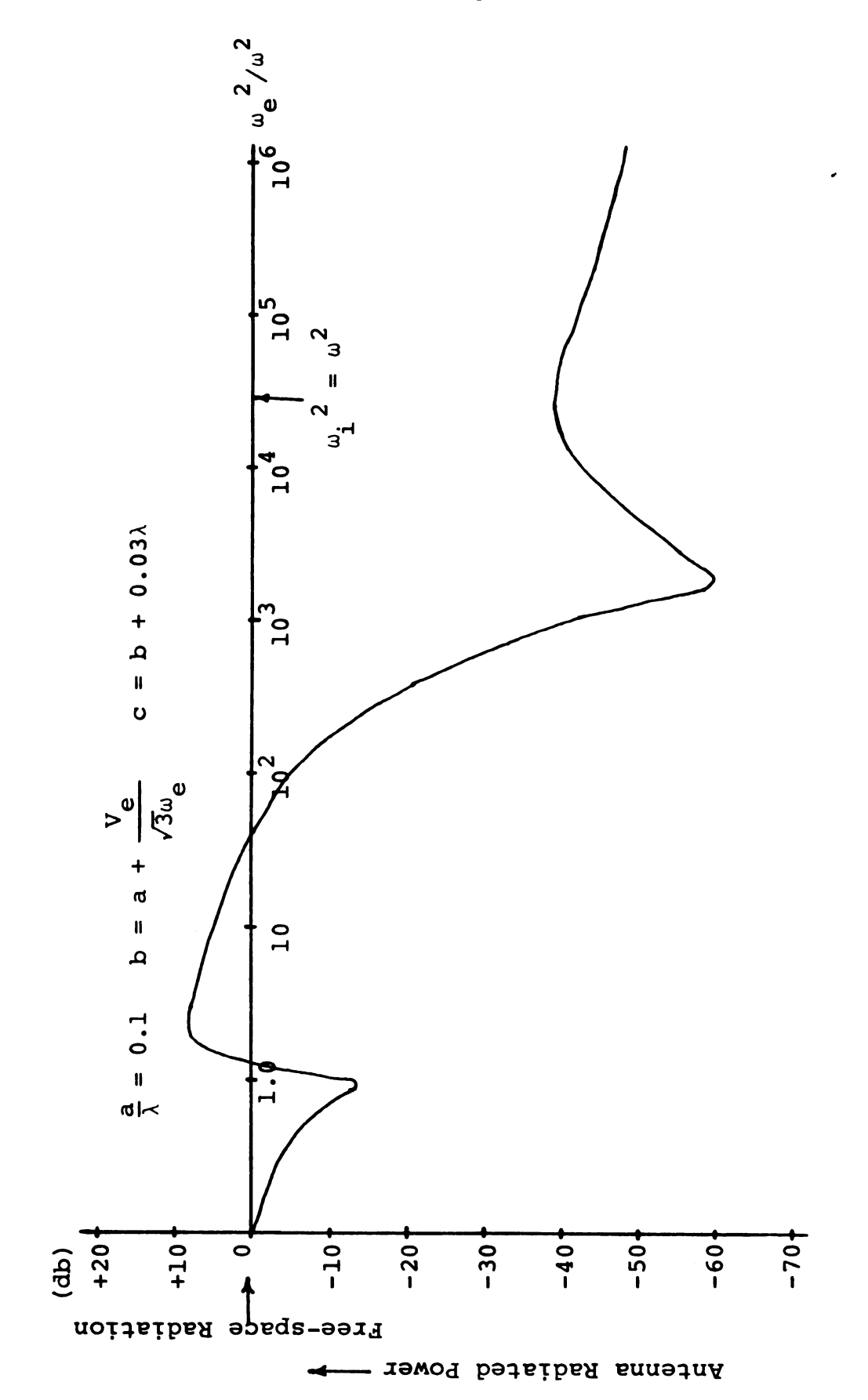


Figure 4.6. Theoretical power radiated by a large spherical antenna in a hot ($V_e/C = 0.01$), lossy ($\gamma_e/\omega = 0.01$, $\gamma_i/\omega = 0.0000584$) plasma as a function of plasma density for various thicknesses of the plasma layer.



Theoretical power radiated by a spherical antenna in a lossy $(\gamma_e/\omega$ = 0.1, γ_1/ω = 0.000584) plasma as a function Figure 4.7. hot $(V_e/C = 0.01)$, of plasma density.



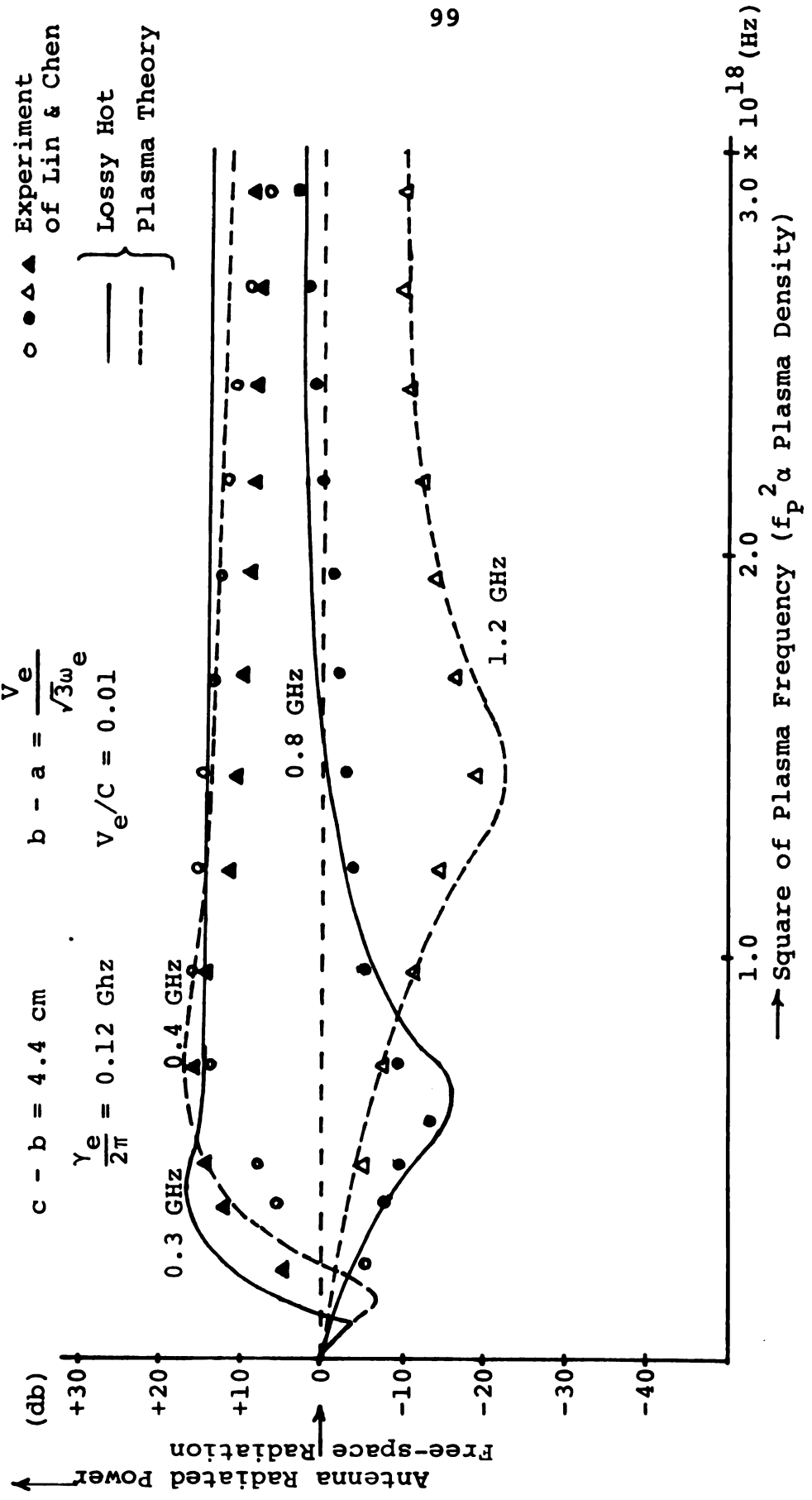
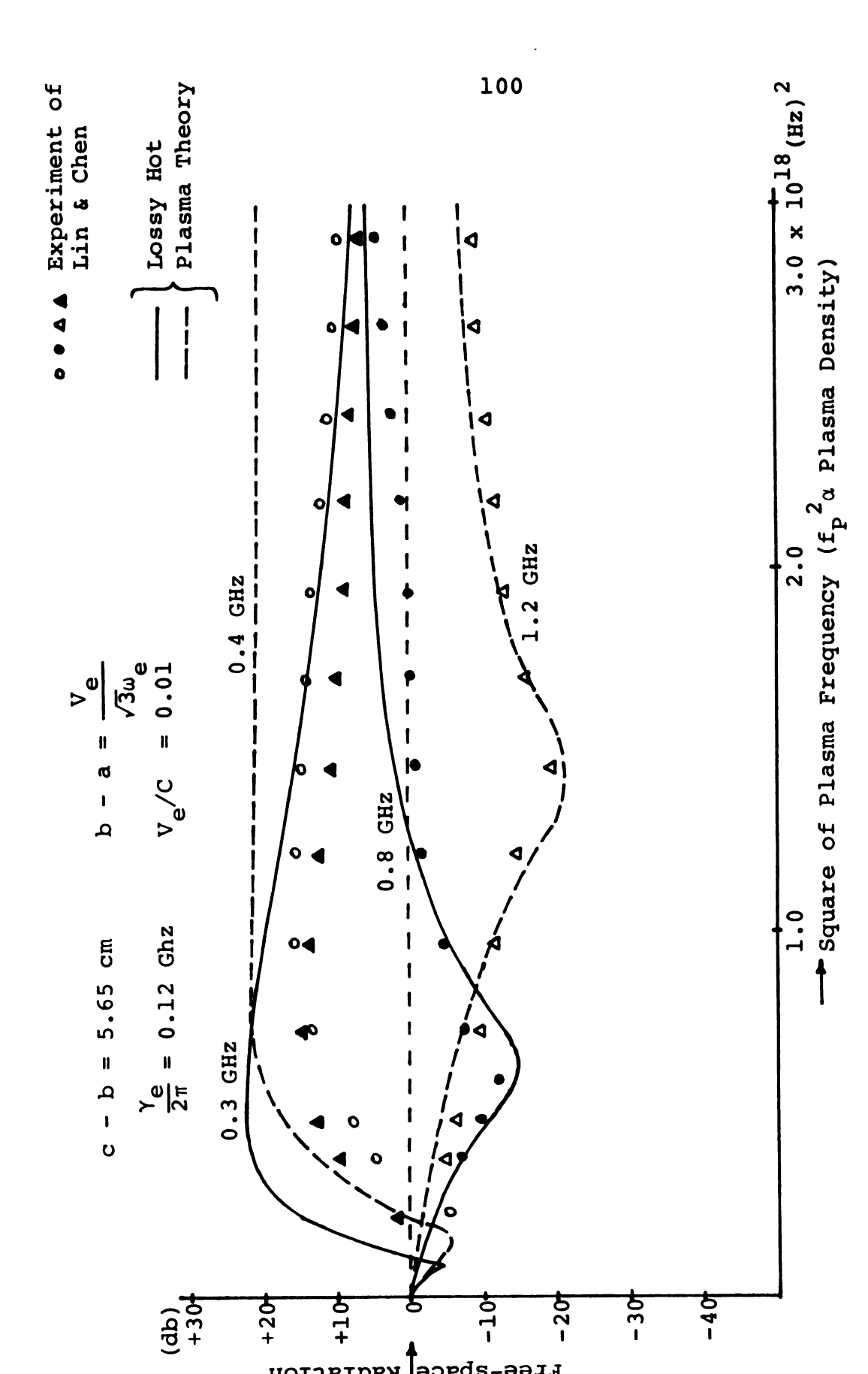


Figure 4.8. Comparison of experimental values by Lin and Chen [2,3] with our theoretical radiation of a spherical antenna ($a=2.54~{\rm cm}$) in a hot lossy plasma driven at various frequencies as a function of plasma density.



Radiated Power

Antenna

Figure 4.9. Comparison of experimental values by Lin and Chen [2,3] with our theoretical radiation of a spherical antenna $(a=1.27~\rm cm)$ in a hot lossy plasma driven at various frequencies as a function of plasma density.

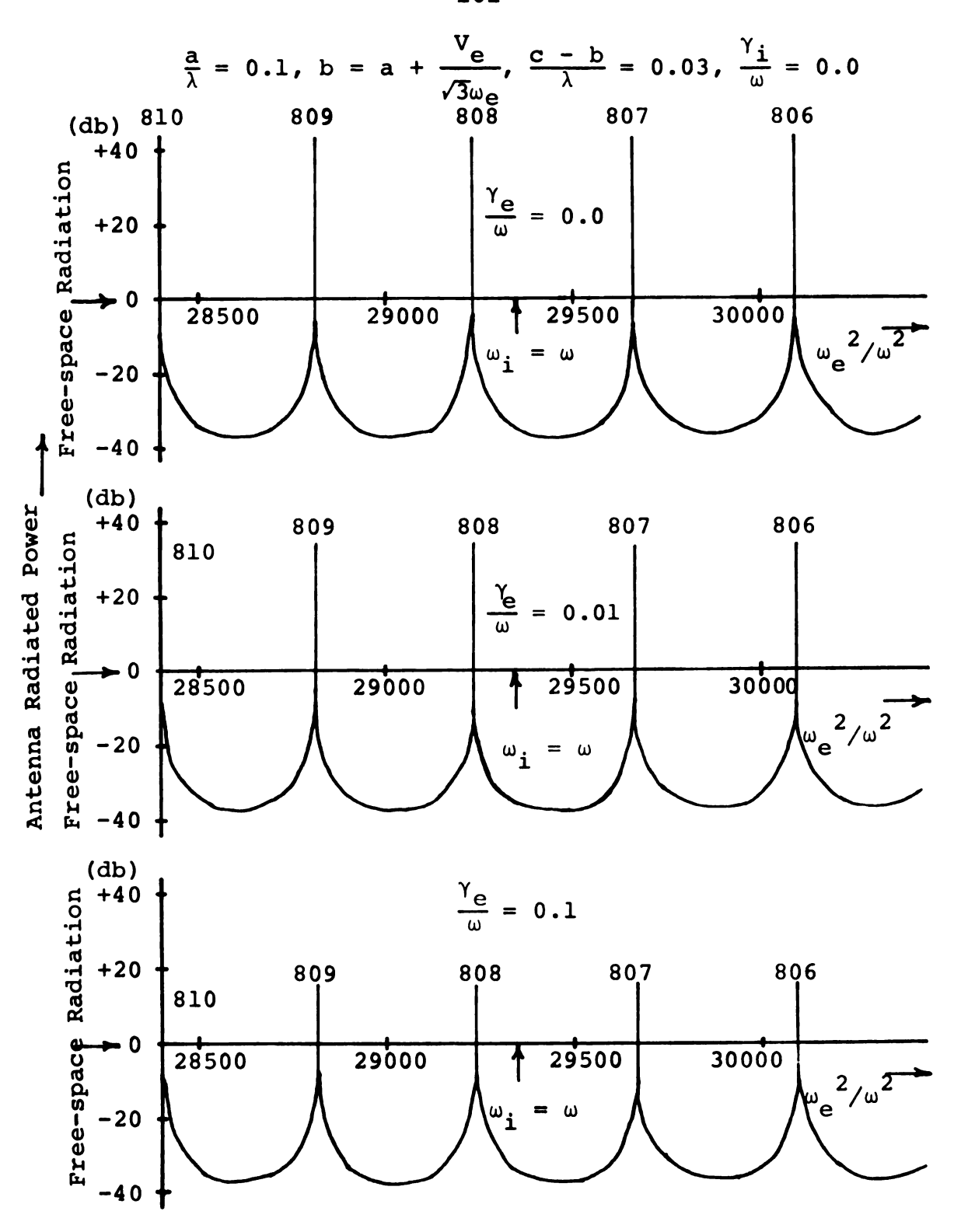


Figure 4.10. Theoretical power radiated by a spherical antenna in a hot ($V_e/C = 0.01$) plasma as a function of plasma density for various electron collision frequencies with the ion collision frequency set equal to zero.

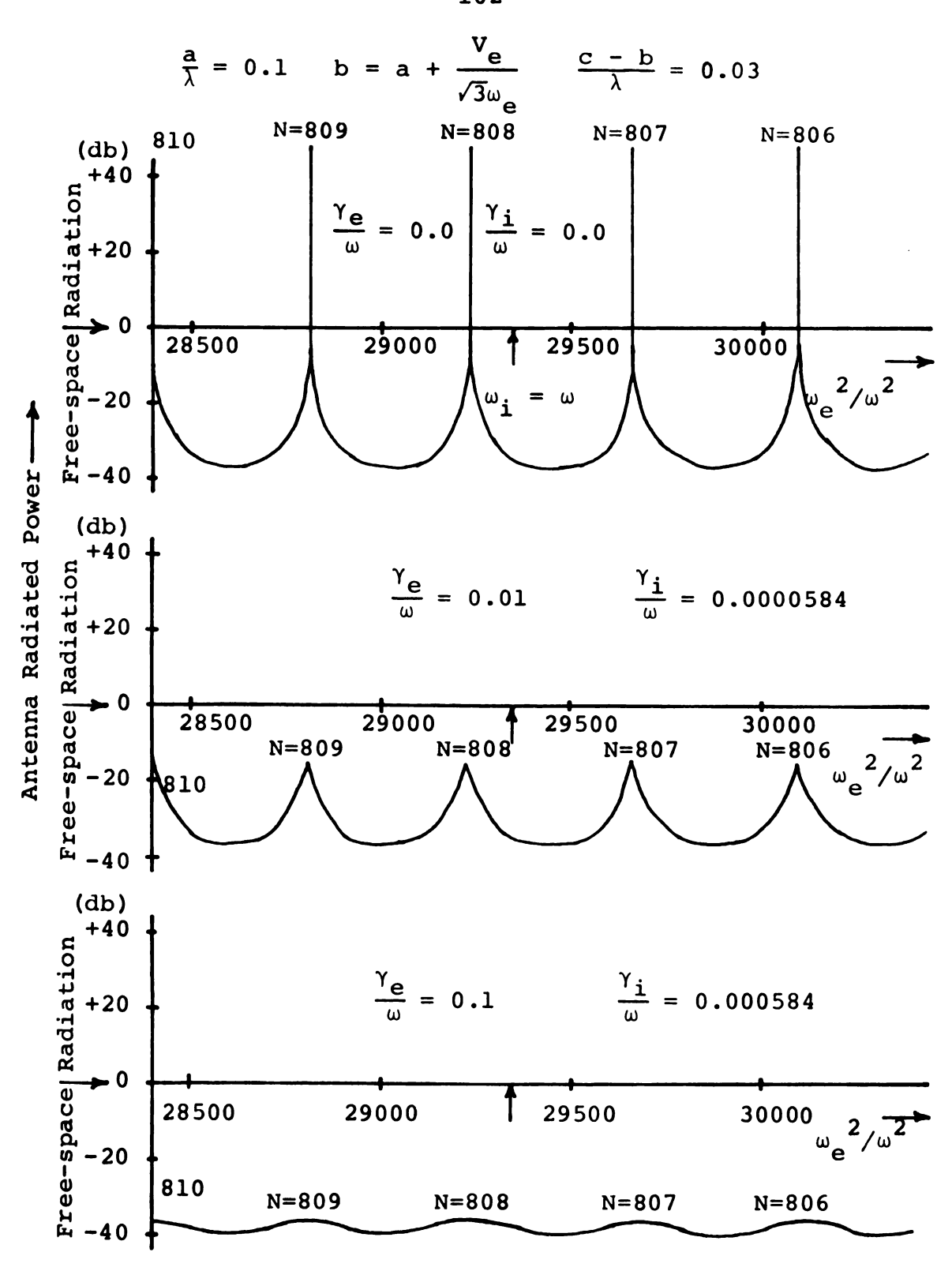


Figure 4.11. Theoretical power radiated by a spherical antenna in a hot ($V_e/C = 0.01$) plasma as a function of plasma density for various collision frequencies.

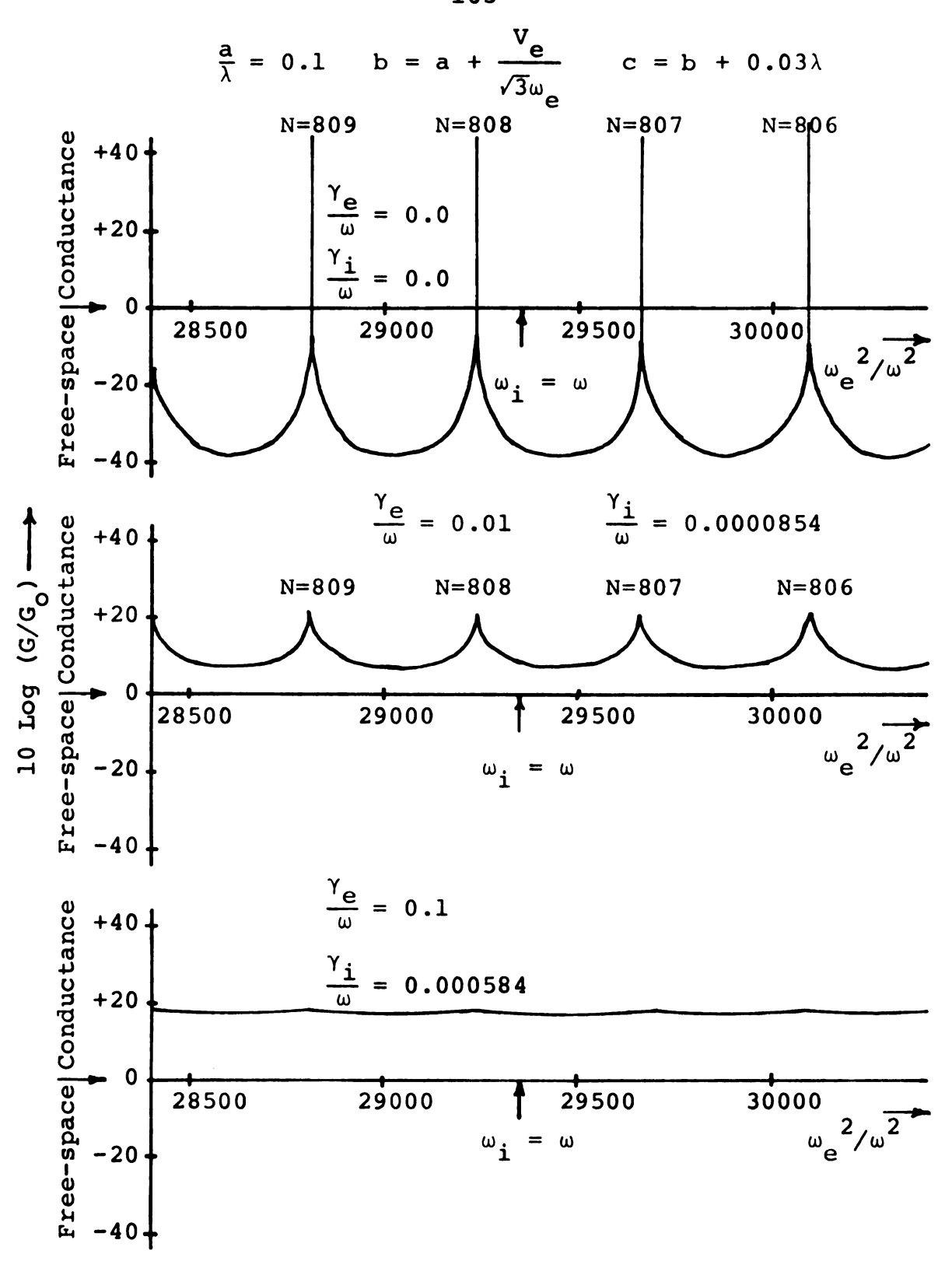


Figure 4.12. Theoretical input conductance of a spherical antenna in a hot ($V_e/C=0.01$) plasma as a function of plasma density for various collision frequencies.

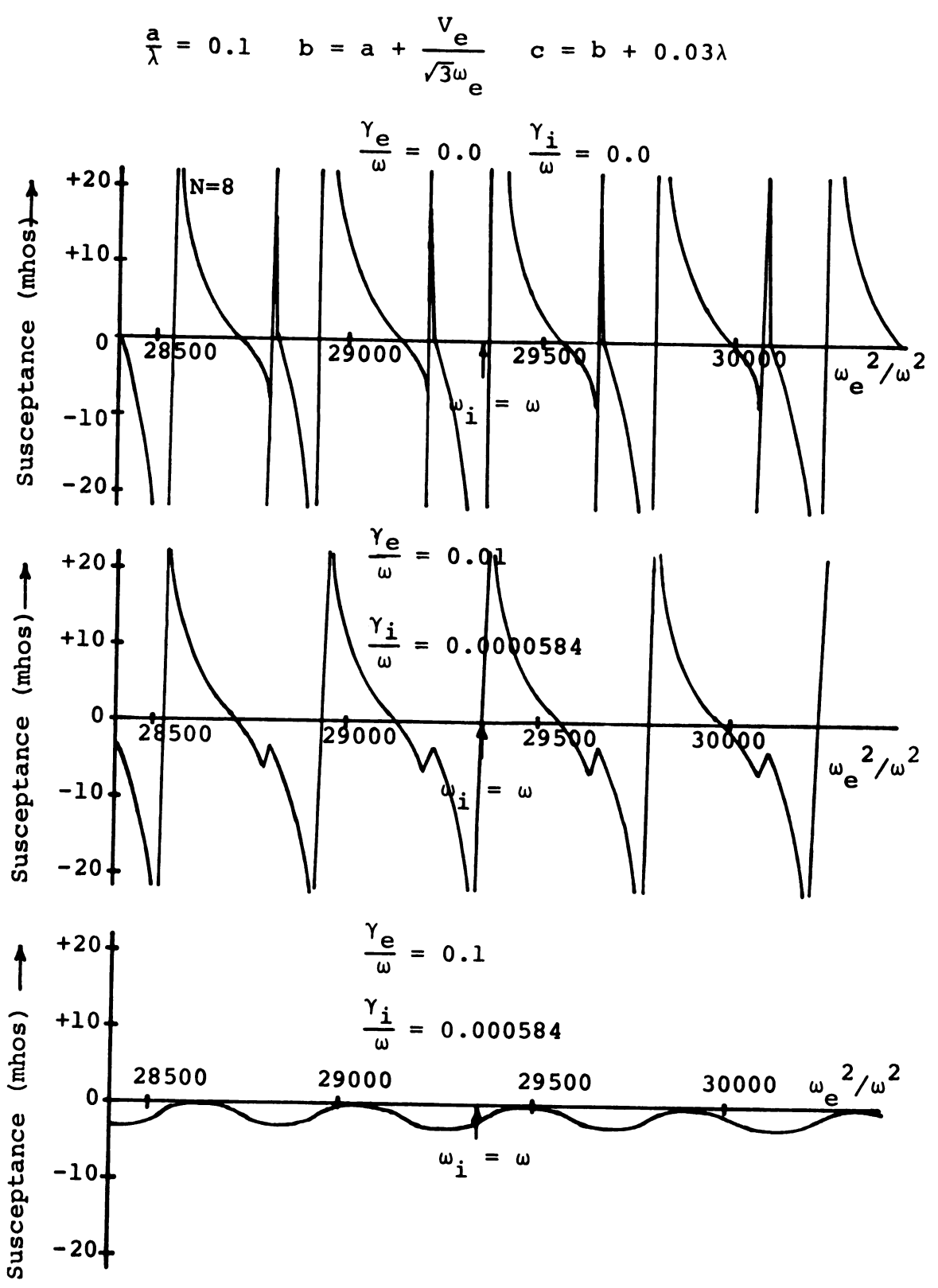


Figure 4.13. Theoretical input susceptance of a spherical antenna in a hot $(V_{\rm e}/C=0.01)$ plasma as a function of plasma density for various collision frequencies.

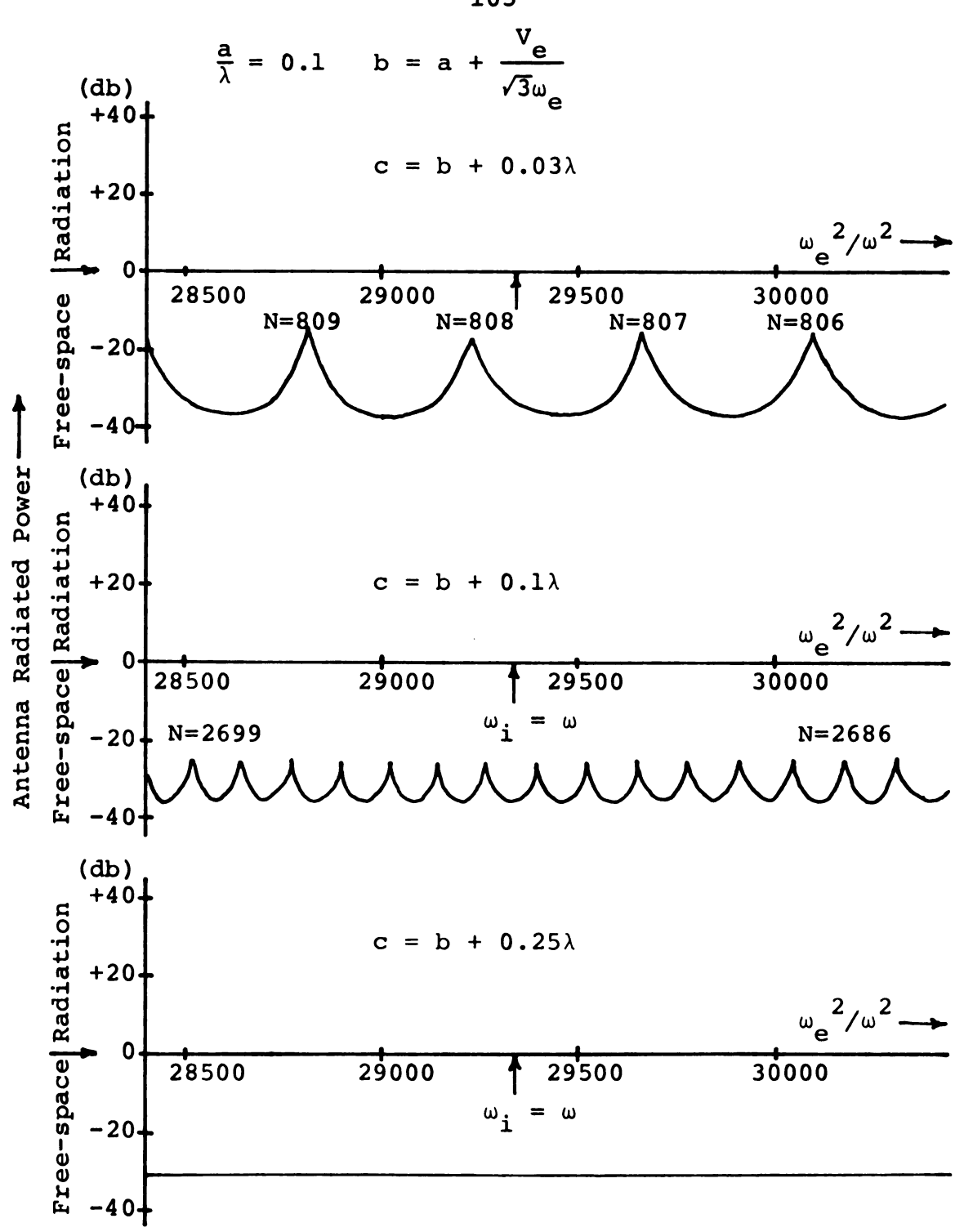


Figure 4.14. Theoretical power radiated by a spherical antenna in a hot ($V_e/C = 0.01$), lossy ($\gamma_e/\omega = 0.01$, $\gamma_i/\omega = 0.0000584$) plasma as a function of plasma density for various thicknesses of the plasma layer.

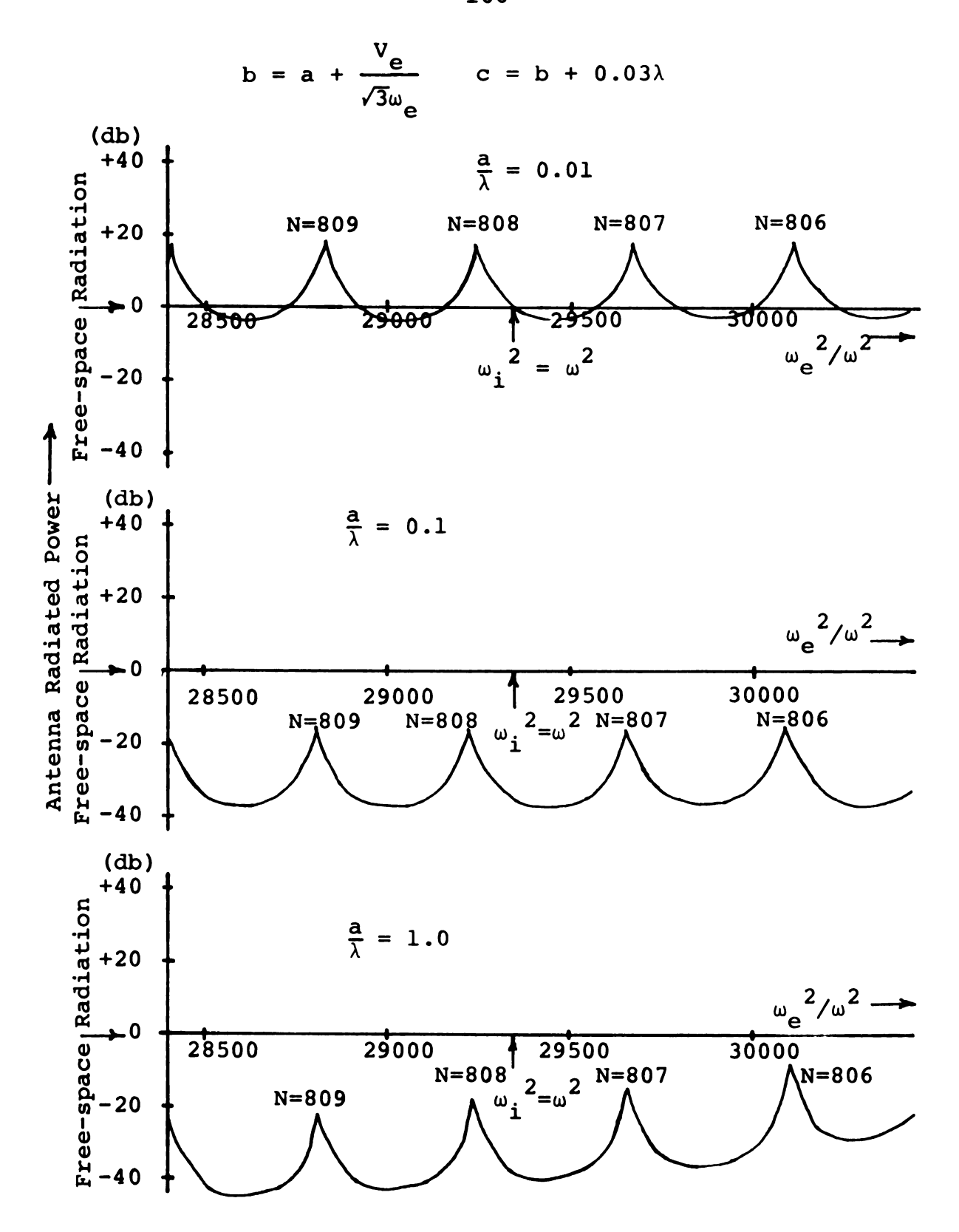
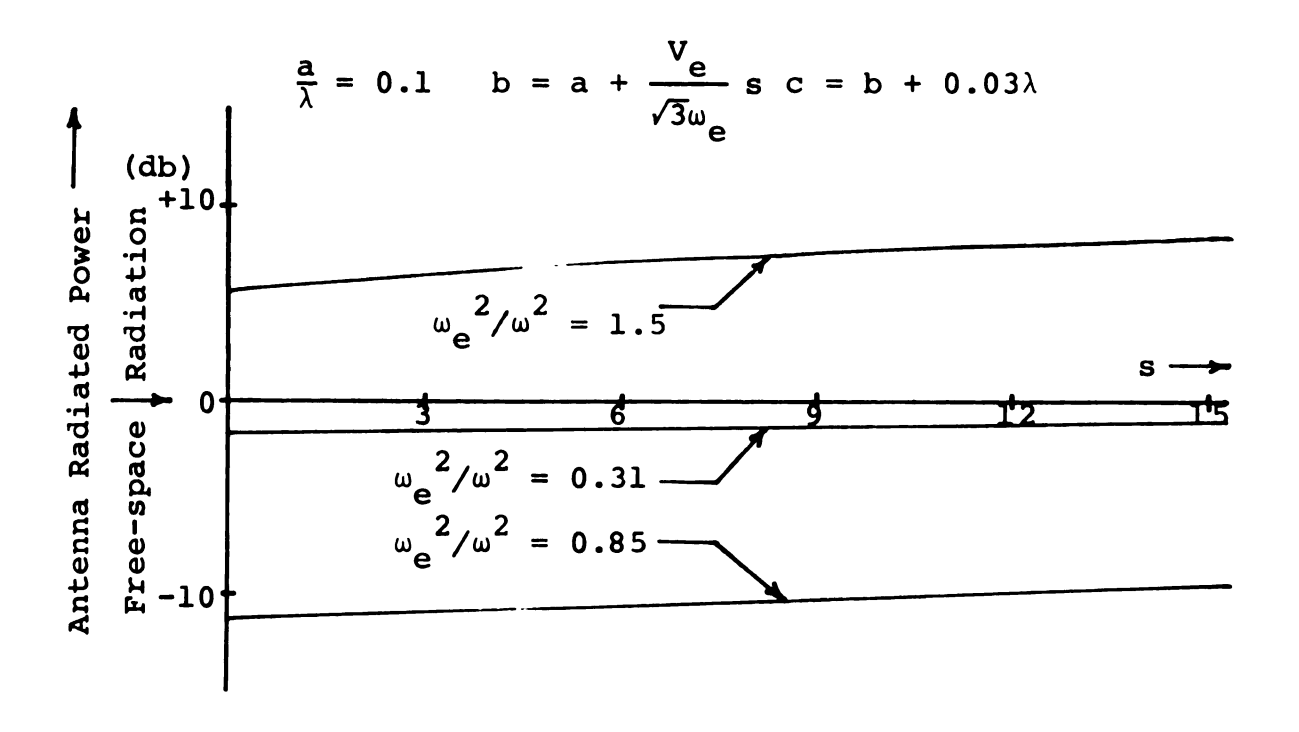


Figure 4.15. Theoretical power radiated by a spherical antenna in a hot ($V_e/C = 0.01$), lossy ($\gamma_e/\omega = 0.01$, $\gamma_i/\omega = 0.0000584$) plasma as a function of plasma density for different size antennas.



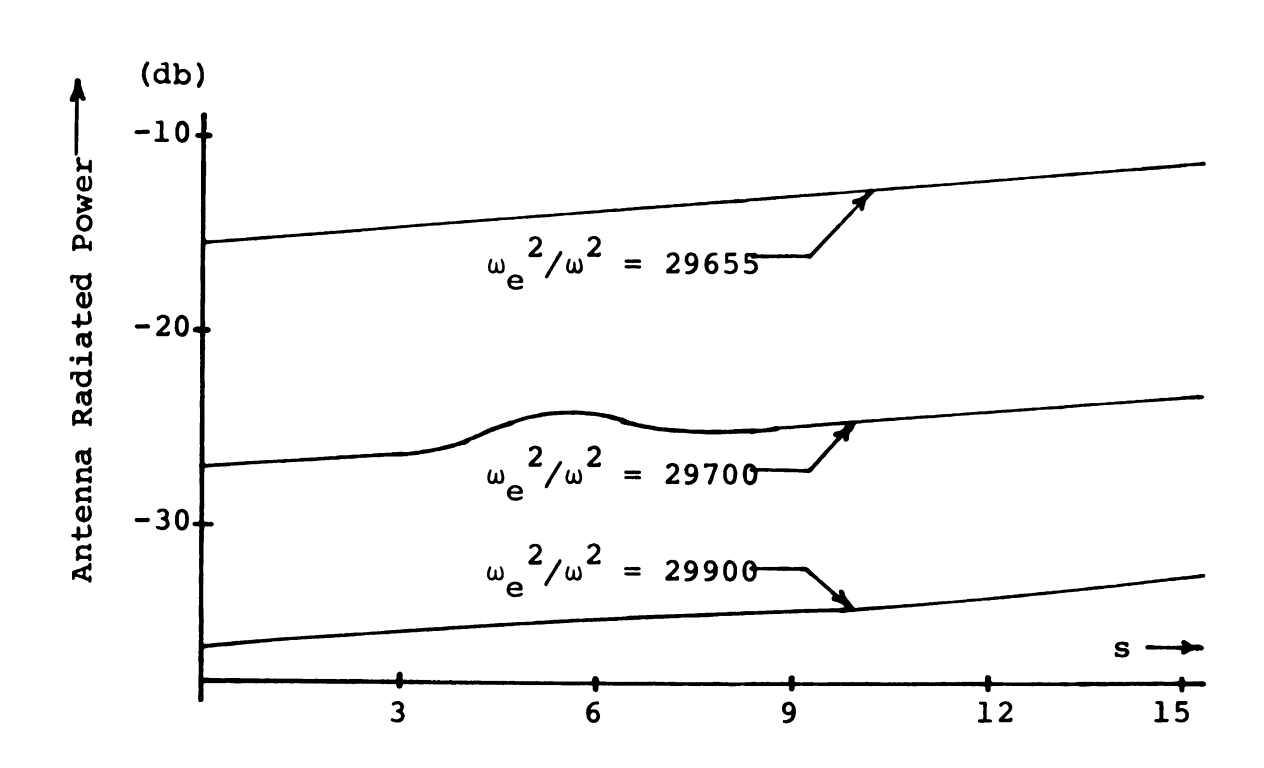
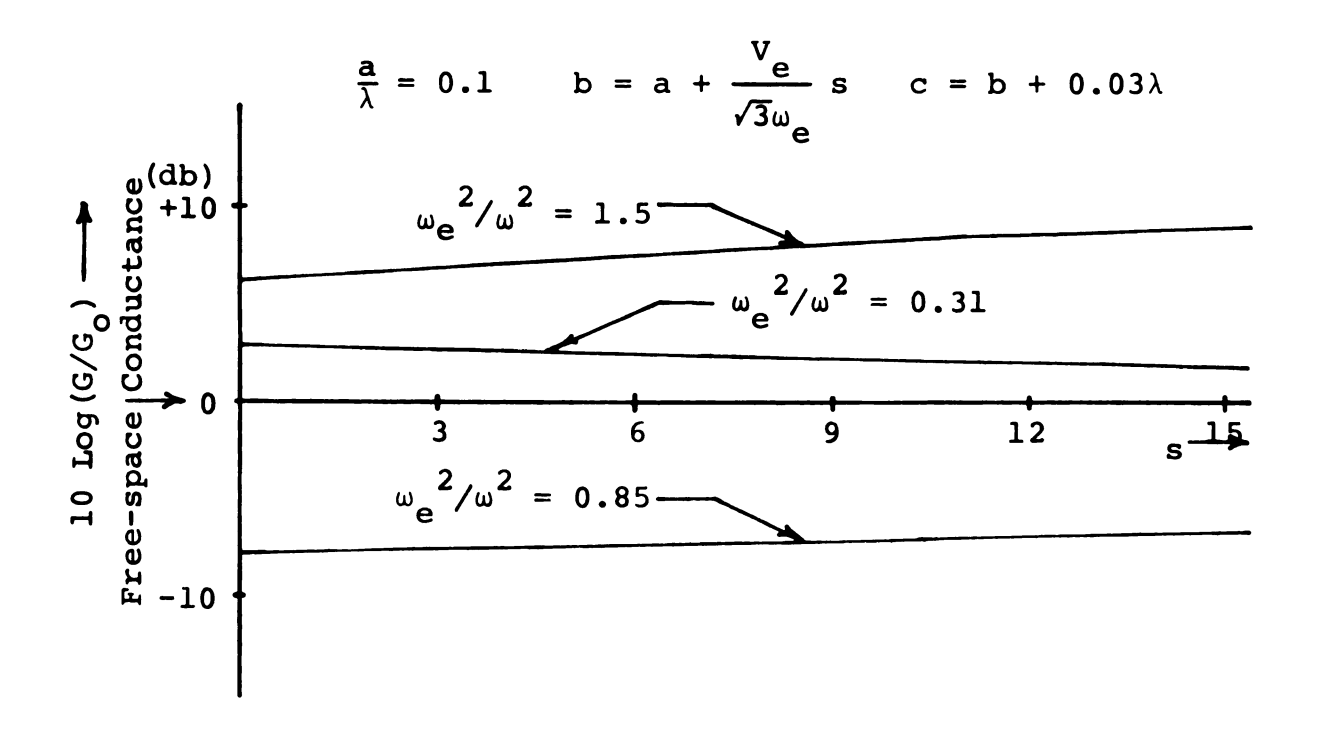


Figure 4.16. Theoretical power radiated by a spherical antenna in a hot ($V_e/C=0.01$) lossy ($\gamma_e/\omega=0.01$, $\gamma_i/\omega=0.0000584$) plasma as a function of dielectric layer thickness for various plasma densities.



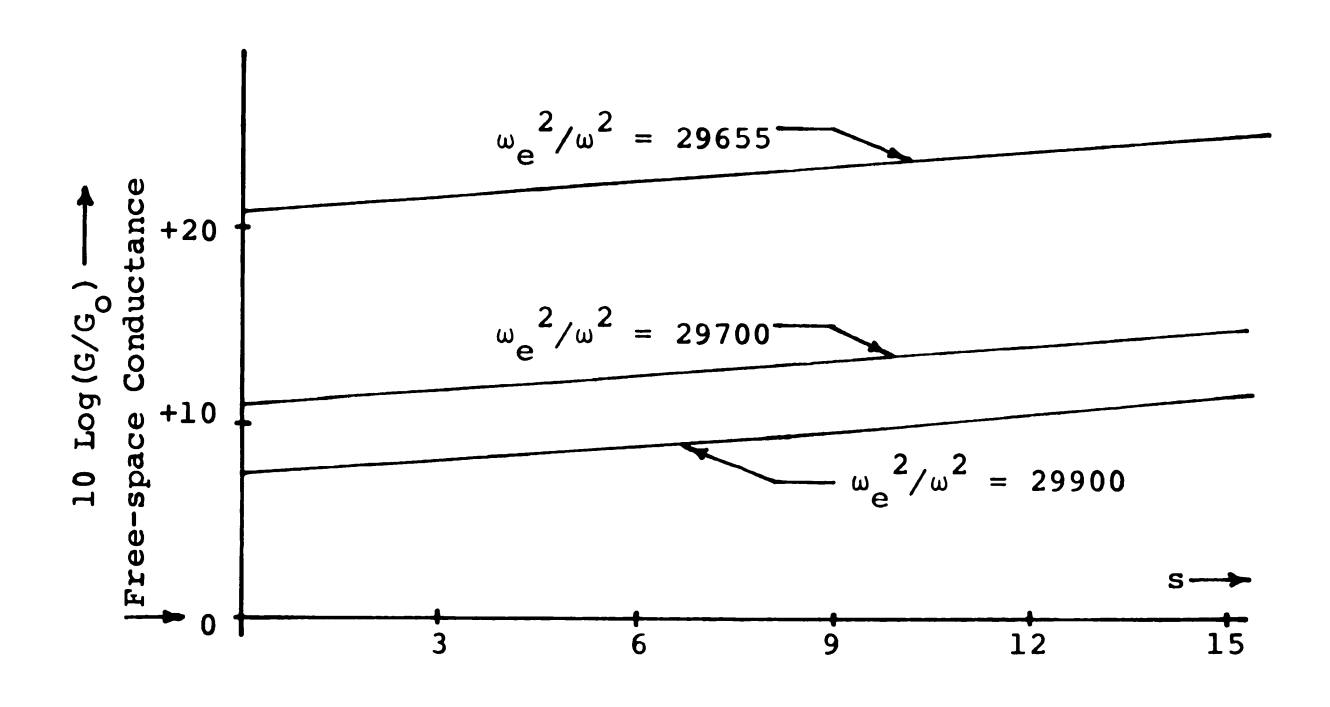
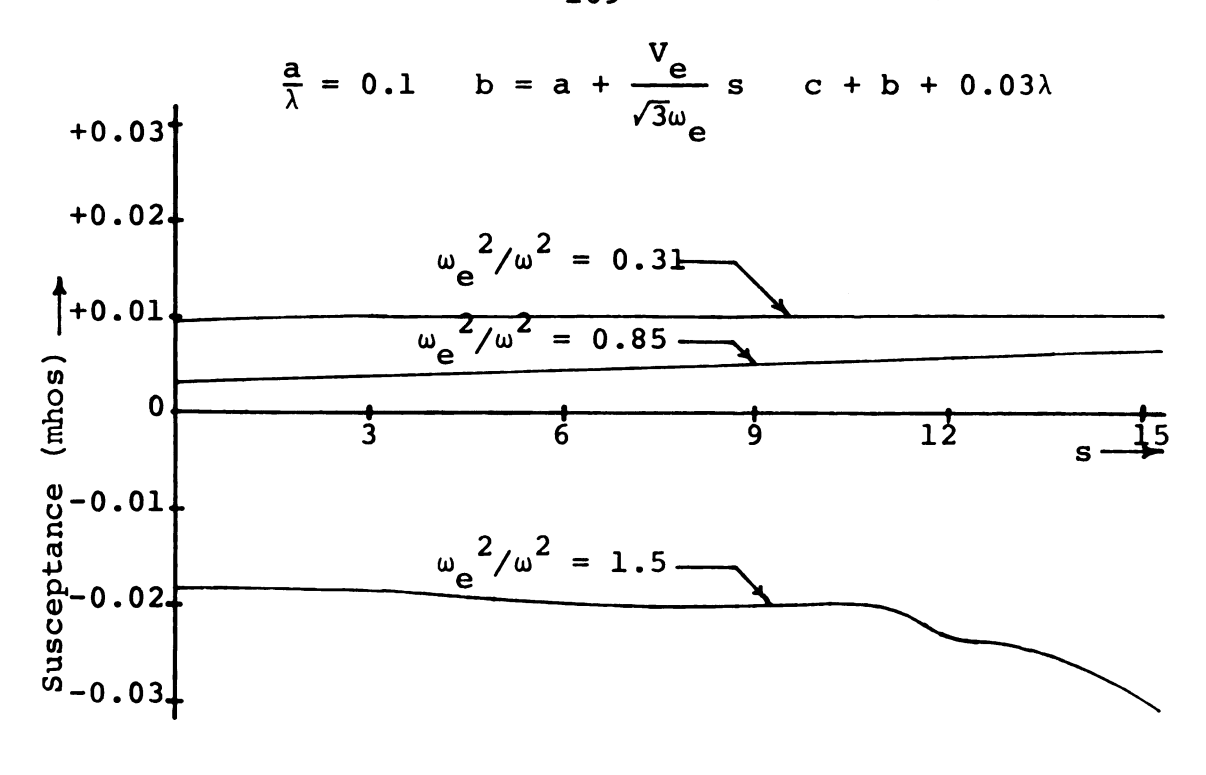


Figure 4.17. Theoretical input conductance of a spherical antenna in a hot $(V_e/C=0.01)$ lossy $(\gamma_e/\omega=0.01,\,\gamma_i/\omega=0.0000584)$ plasma as a function of dielectric layer thickness for various plasma densities.



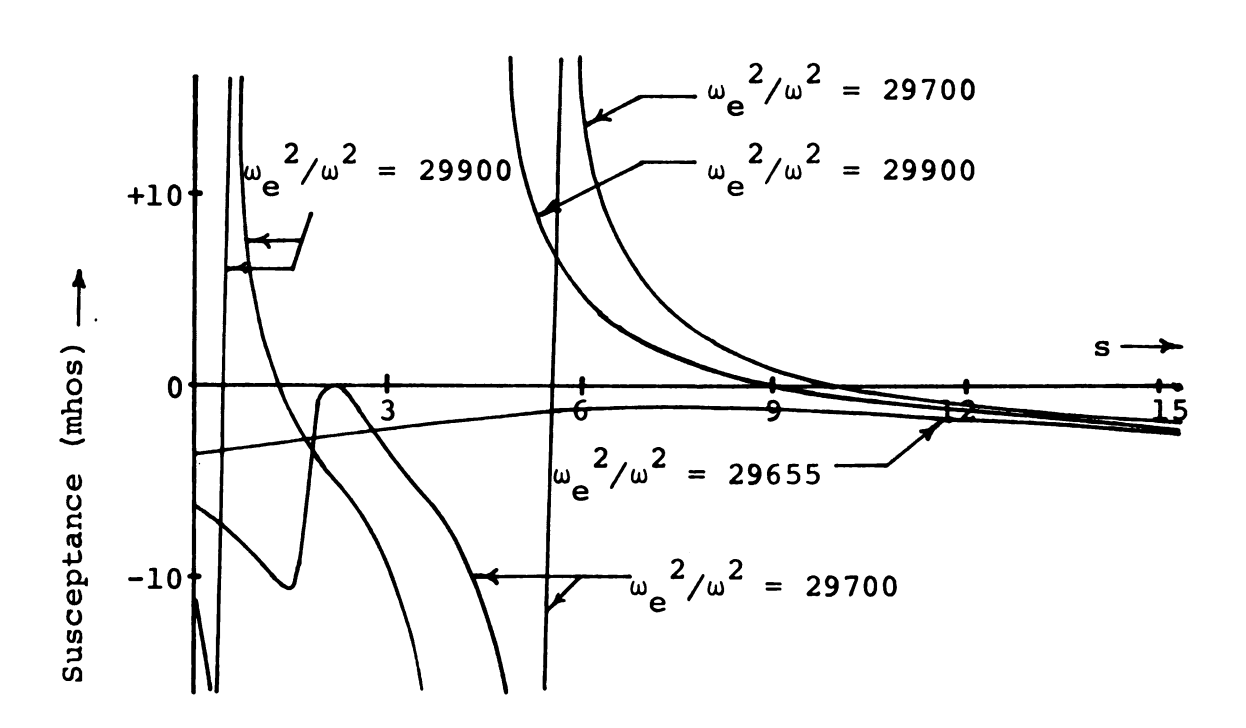


Figure 4.18. Theoretical input susceptance of a spherical antenna in a hot ($V_e/C = 0.01$) lossy ($\gamma_e/\omega = 0.01$, $\gamma_i/\omega = 0.0000584$) plasma as a function of dielectric layer thickness for various plasma densities.

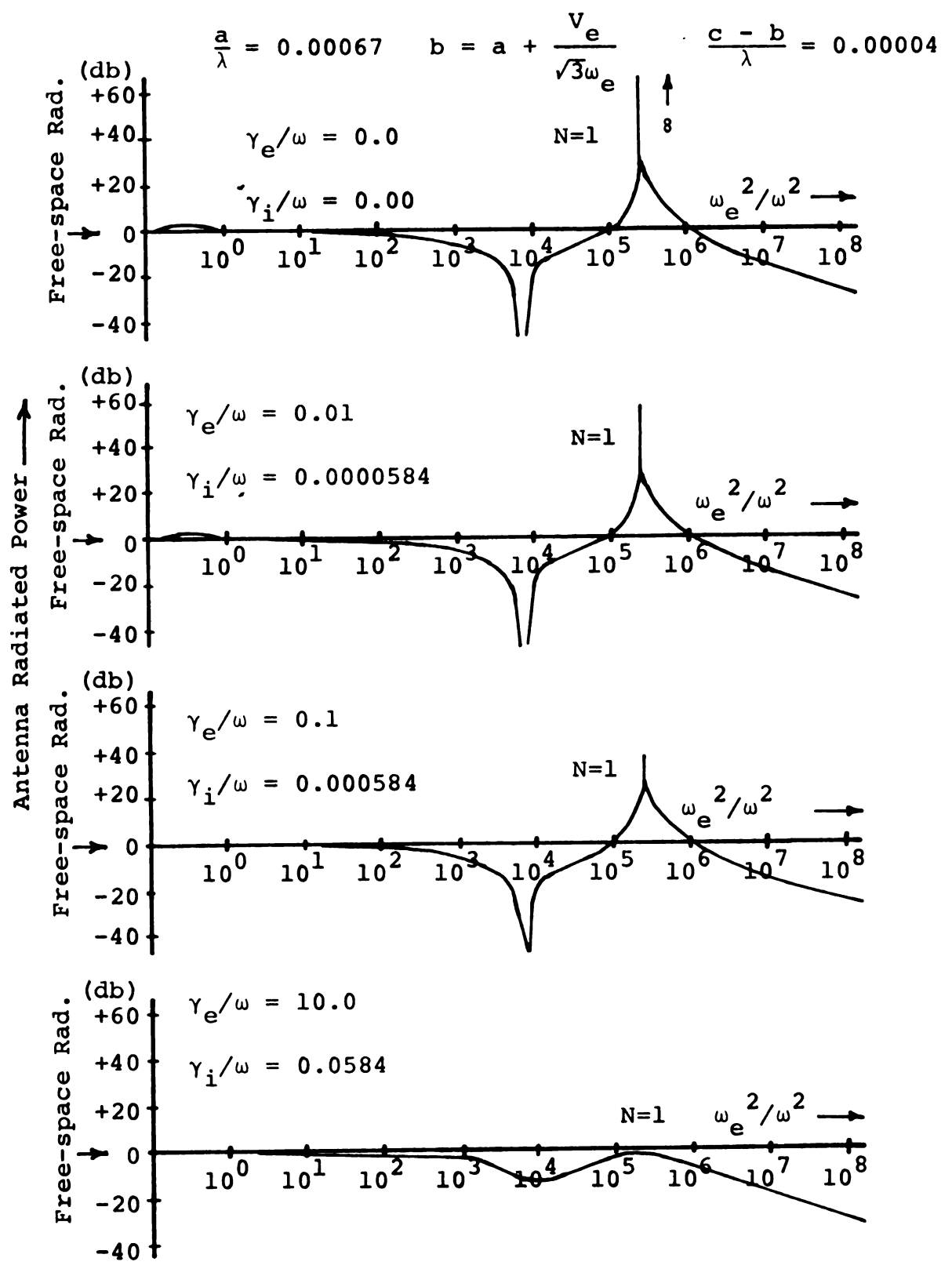


Figure 4.19. Theoretical power radiated by a small spherical antenna surrounded by a thin layer of a hot ($V_e/C=0.01$) plasma as a function of plasma density for various collision frequencies.

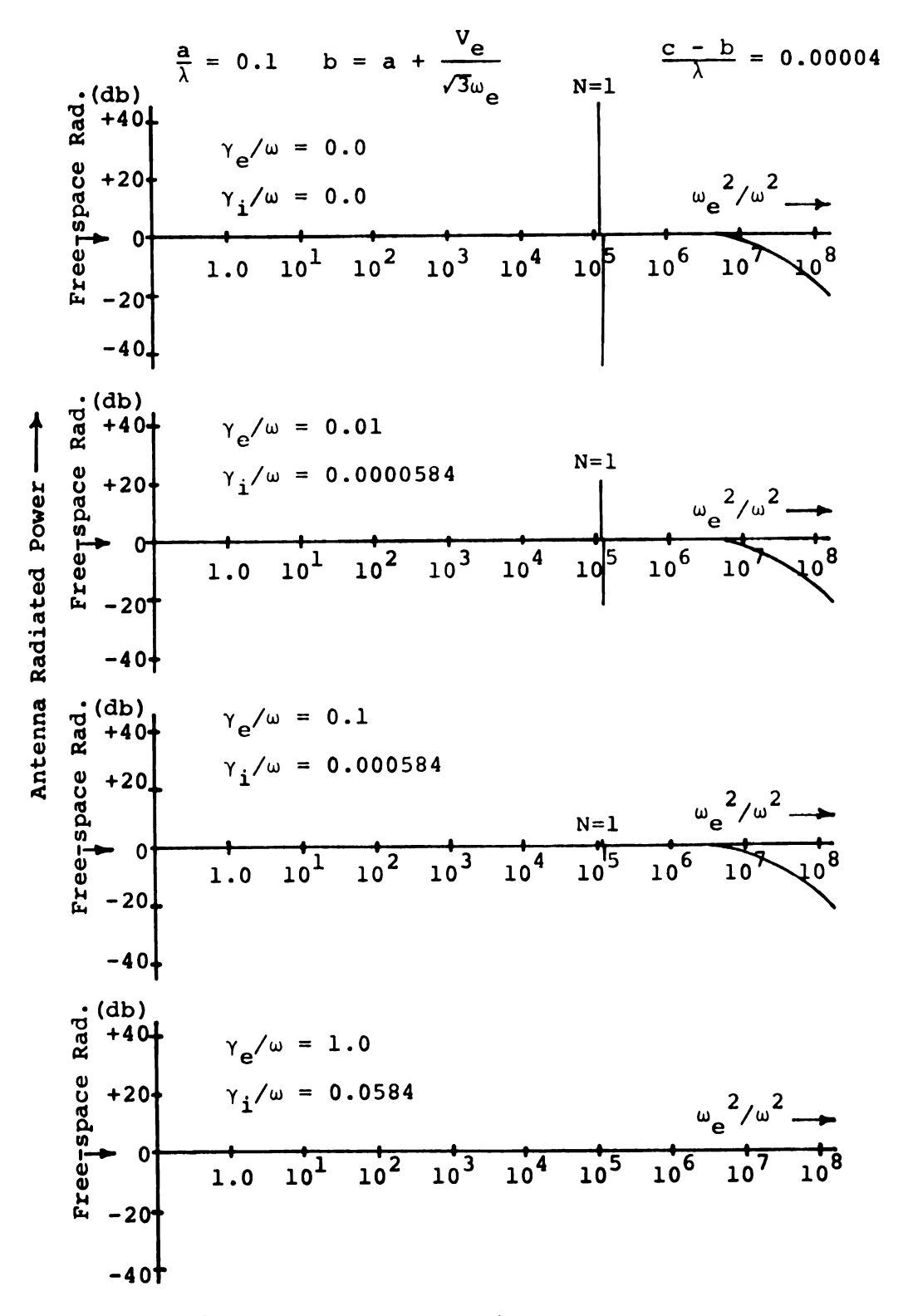


Figure 4.20. Theoretical power radiated by a spherical antenna surrounded by a thin layer of a hot $(V_e/C=0.01)$ plasma as a function of plasma density for various collision frequencies.

PART II

RADIATION OF A CYLINDRICAL ANTENNA IN A

COMPRESSIBLE PLASMA INCLUDING THE

EFFECT OF AN ELECTROACOUSTIC

WAVE

CHAPTER V

INTRODUCTION

Advances in space technology in the last few years have led to an increased utilization of antennas, operated in a plasma medium, as ionospheric probes to determine the state of the plasma, and for communication purposes. Thus it is important to be able to predict the effect that a plasma medium will have on the electrical properties of an antenna. In this part of the dissertation the electrical properties of a cylindrical antenna immersed in a hot lossy plasma of infinite extent are studied.

5.1 Historical Development

There is an abundance of literature dealing with the effect of a plasma upon the operating characteristics of a linear antenna. Varying assumptions have been made in order to simplify the problem. These assumptions typically involve one or more of the following; neglect the sheath region entirely [18-32], neglect the temperature effects of the electrons and ions [28,29], neglect the ions [12, 18, 20-42], neglect losses [18-22, 24-27, 30-32, 34-37, 39, 41], assume a sheath profile [40, 41], replace the

sheath region by an electron free sheath region [22, 32, 12, 34-38], assume a short filamental antenna with either a sinusoidal or triangular current distribution [19-21, 23, 25, 26, 33].

Prior to 1961, the theoretical considerations of the influence of a plasma on the characteristics of a linear antenna neglected collisions and the temperature of the plasma. Thus the plasma was regarded as a cold, nonlossy medium, which is equivalent to regarding the plasma medium as a lossless dielectric.

In 1961, King, Harrison, and Denton [28] solved the problem of a short, linear antenna immersed in a cold, lossy plasma. In the same month, Hessel and Shmoys [18] presented their paper dealing with the behavior of a Hertzian dipole operated in a warm, lossless plasma. Their results indicated, for the proper frequency range and acoustic velocity, a large acoustic wave off the ends of the antenna, in addition to the usual electromagnetic wave off the sides of the antenna.

In 1963, Whale [43] observed experimentally a larger real part of the input impedance of a short antenna used as an ionospheric probe than predicted by using the cold, lossless plasma theory. He attributed this to the electroacoustic wave.

Chen [23], in 1964, studied the problem of a thin cylindrical antenna of finite length with a sinusoidal

current distribution in a hot plasma. Balmain [33] treated the problem of an electrically short antenna with a triangular current distribution immersed in a hot plasma. Both papers gave the antenna resistance only for $\omega_{\rm s}/\omega$ < 1 where $\omega_{\rm s}$ and ω are the plasma and antenna frequencies. Later, Kuehl [25, 26] studied the same problem, but solved the Boltzmann equation instead of using the simpler linearized hydrodynamic equations. An interesting result of his work is the existence of an antenna resistance for $\omega_0/\omega > 1$. The antenna reactance was not determined in these papers. Meltz, Freyheit and C. D. Lustig [44] investigated an infinite cylindrical antenna covered by a set of coaxial plasma layers, based on a variational formulation. They were able to deduce both the antenna resistance and the antenna reactance for a wide range of ω_{Δ}/ω .

Compared to the wealth of theoretical papers produced, only a few reports have presented experimental results dealing with the electrical properties of linear antennas in plasmas. Some have measured the impedance of short dipoles in the ionosphere [43, 45, 46] and in a laboratory plasma [47]. More recently, impedance measurements of relatively long antennas in laboratory DC impulse discharges [48, 49, 52] and in an RF discharge [50] have been reported. Also, measurements of the current distribution on relatively long monopoles in sustained laboratory plasmas has been reported [51, 59].

5.2 Outline of the Investigation

To the best of our knowledge, no theoretical paper which accurately determines the complete input impedance of a cylindrical antenna of finite length in a hot lossy plasma has been published.

In Chapter VI, an integral equation for the current on a linear antenna in a hot lossy plasma is formulated. The antenna is assumed to support a two-dimensional surface current so that antennas of diameters comparable to the electroacoustic wavelength may be considered. An assumed form for the current distribution is introduced and then knowing the impressed voltage, the zeroth order input impedance is derived. The sheath is not considered.

In Chapter VII, numerical solutions for the zeroth order input impedance and current distribution are calculated and compared to experimental results. These solutions are also compared to theoretical and experimental results obtained by other workers.

CHAPTER VI

THEORETICAL DEVELOPMENT OF THE INTEGRAL EQUATION FOR THE CURRENT ON A LINEAR ANTENNA IN A HOT LOSSY PLASMA AND THE ZEROTH ORDER SOLUTION FOR THE CURRENT DISTRIBUTION AND

INPUT IMPEDANCE

The objective of this chapter is to derive an integral equation for the current distribution on a gap-excited linear antenna immersed in an infinite, isotropic, homogeneous, compressible plasma. The known function in the integral equation will be the tangential electric field intensity on the surface of the antenna. This function is known from the boundary condition on the tangential electric field on the surface of a perfect conductor and the idealization of the excitation (an assumed constant electric field in the gap). A zeroth order current distribution is proposed and a zeroth order input impedance is obtained.

6.1 Geometry and Basic Equations

The geometry of the linear cylindrical antenna is shown in Figure 6.1. The antenna is taken to have a

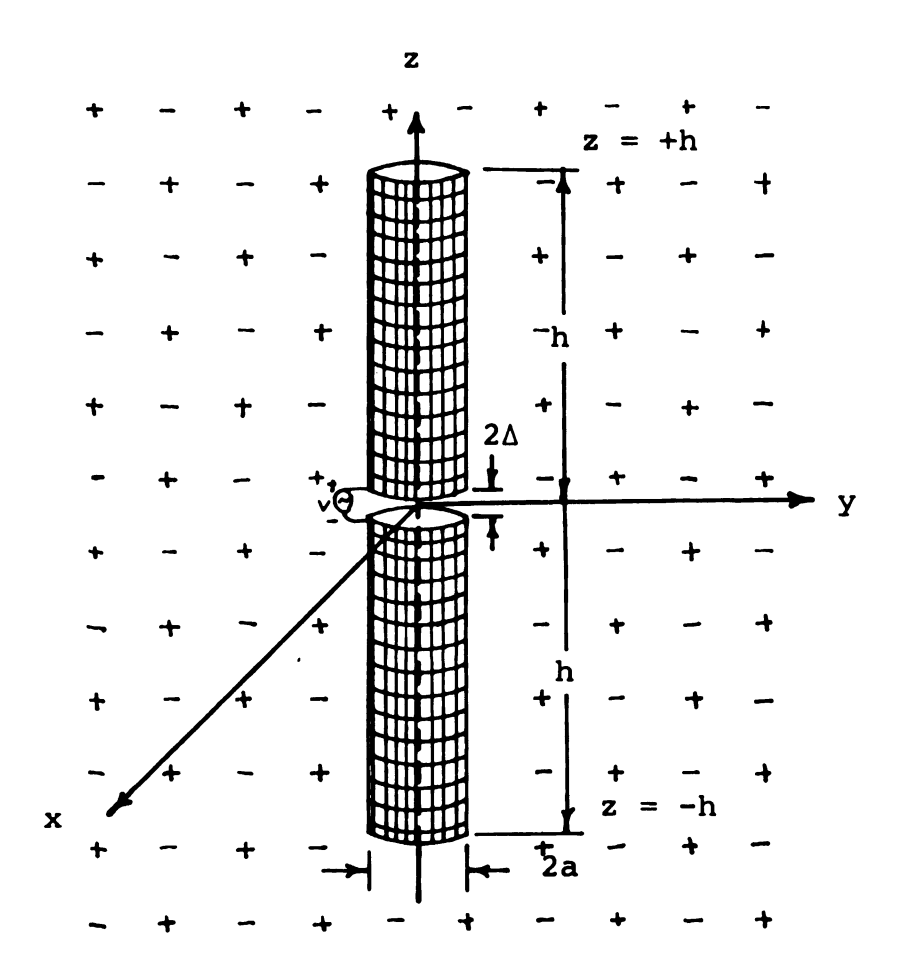


Figure 6.1 . A cylindrical antenna of radius a and half length h immersed in an unbounded hot lossy plasma.

half length h and radius a. It is assumed to lie along the z axis of a cylindrical coordinate system and to be excited at its center (z=0) by a harmonic voltage V with angular frequency ω . The gap of width 2Δ in the cylinder at z=0 is assumed to be very small so that $2\Delta\to 0$, corresponding to a point (or, what is termed, a slice) generator with rotational symmetry. The antenna is assumed to be constructed of a perfectly conducting screen or mesh-like material, with the spacing of the conductors being much less than the smallest characteristic dimensions of the system, so that the surface is penetrable to electrons and ions. This assumption eliminates the need to consider the formation of a sheath and to impose a boundary condition on the particle velocities at the surface of the antenna making the problem tractable.

The antenna is immersed in an unbounded weakly ionized gas which consists of equal numbers of free electrons and singly ionized positive atoms and a much larger number of neutral atoms. It is assumed that the generator frequency ω is sufficiently high to neglect ion motion so that the ions act as a uniform background of positive charge.

The basic equations that govern this system (source and plasma) are Maxwell's equations and the linearized hydrodynamic equations (see Chapter I),

$$\nabla \times \underbrace{\mathbf{E}}_{\sim}(\mathbf{r}) = -j\omega\mu_{\mathbf{O}} \underbrace{\mathbf{H}}_{\sim}(\mathbf{r}) \tag{6.1.1}$$

$$\nabla \times H(r) = J^{S}(r) - en_{O_{\sim}^{v}(r)} + j\omega \varepsilon_{O_{\sim}^{E}(r)}$$
 (6.1.2)

$$\varepsilon_{O}[\nabla \cdot E(r)] = \rho^{S}(r) - en(r)$$
 (6.1.3)

$$\nabla \cdot H(r) = 0 \tag{6.1.4}$$

$$n_{\mathcal{O}}[\nabla \cdot \mathbf{v}(\mathbf{r})] + j\omega n(\mathbf{r}) = 0$$
 (6.1.5)

$$(j\omega + \gamma) v(r) = -\frac{e}{m} E(r) - \frac{v_o^2}{n_o} \nabla n(r)$$
 (6.1.6)

$$\nabla \cdot J^{S}(\mathbf{r}) + j\omega \rho^{S}(\mathbf{r}) = 0$$
 (6.1.7)

where

E(r) = electric field

H(r) = magnetic field

 μ_{O} = permeability of free space

 $\epsilon_{_{\rm O}}$ = permittivity of free space

-e = charge on the electron

m = mass of the electron

 n_0 = equilibrium electron density

n(r) = perturbed electron density

 $J^{S}(r)$ = source current density

 $\rho^{S}(r)$ = source charge density

v(r) = average perturbed electron density

γ = electron-neutral particle collision frequency

$$v_{o} = \sqrt{\frac{3kT}{m}}$$
 = average thermal velocity of the electrons

where k is Boltzmann's constant and T is the average temperature of the electrons. The suppressed time dependence is assumed to be of the form $e^{j\omega t}$ and rationalized MKS units have been used throughout.

6.2 Integral Equation Formulation

The curl of equation (6.1.2) is

$$\nabla \times \nabla \times H = \nabla \times J^{S} - en_{O} \nabla \times v + j\omega \epsilon_{O} \nabla \times E.$$
 (6.2.1)

Using the vector identity $\nabla \times \nabla \times \mathbb{R} = \nabla (\nabla \cdot \mathbb{R}) - \nabla^2 \mathbb{R}$, equation (6.2.1) becomes

$$\nabla (\nabla \cdot \mathbf{H}) - \nabla^2 \mathbf{H} = \nabla \times \mathbf{J}^S - \operatorname{en}_O \nabla \times \mathbf{v} + \mathrm{j} \omega \varepsilon_O \nabla \times \mathbf{E}. \quad (6.2.2)$$

Substituting the curl of equation (6.1.6) and equations (6.1.1) and (6.1.4) into equation (6.2.2) gives after simplification,

$$\nabla^{2} H + \omega^{2} \varepsilon_{0} \mu_{0} \left[1 - \frac{\omega_{e}^{2}}{\omega^{2} + \gamma^{2}} - j \frac{\omega_{e}^{2} \gamma}{\omega(\omega^{2} + \gamma^{2})} \right] H = - \nabla \times J^{S}$$
(6.2.3)

where $\omega_e^2 = e^2 n_0 / m \epsilon_0$. If we define a complex permittivity as

$$\xi = \varepsilon_0 \left[1 - \frac{\omega_e^2}{\omega^2 + \gamma^2} - j \frac{\omega_e^2 \gamma}{\omega(\omega^2 + \gamma^2)} \right], \qquad (6.2.4)$$

equation (6.2.3) can be written as an inhomogeneous wave equation of the form

$$\nabla^2 \mathbf{H} + \mathbf{k_e}^2 \mathbf{H} = - \nabla \times \mathbf{J}^S$$
 (6.2.5)

where

$$k_e^2 = \omega^2 \mu_0 \xi.$$
 (6.2.6)

Consider the equation

$$(\nabla^2 + k_e^2) A(r) = - J^S(r)$$
. (6.2.7)

It can be shown (by straight-forward, but tedious, vector manipulations) that

$$(\nabla^2 + k_e^2) \nabla \times A = - \nabla \times J^S. \tag{6.2.8}$$

Comparing equation (6.2.8) with equation (6.2.5) and recalling that equation (6.1.4) holds for all space, we can say that H must be the curl of some vector field A or

$$\mathbf{H} = \nabla \mathbf{x} \mathbf{A}. \tag{6.2.9}$$

The solution for the inhomogeneous wave equation, equation (6.2.7), may be obtained using standard procedures [53, 54, 55]. Thus

$$\underset{\sim}{\mathbf{A}}(\mathbf{r}) = \frac{1}{4\pi} \int_{\mathbf{V}} \mathbf{J}^{\mathbf{S}}(\mathbf{r}') G_{\mathbf{e}}(\mathbf{r},\mathbf{r}') dV' \qquad (6.2.10)$$

$$G_{e}(r,r') = \frac{e^{-jk_{e}|r-r'|}}{|r-r'|}$$
(6.2.11)

and r is a vector from the origin to the field point, r' is a vector from the origin to the source point, and the integration is over all source points. Finally

$$\underset{\sim}{H}(\underline{r}) = \frac{1}{4\pi} \nabla x \int_{V} J^{S}(\underline{r}') G_{e}(\underline{r},\underline{r}') dV'. \qquad (6.2.12)$$

Taking the divergence of equation (6.1.6) and solving for ∇ • E yields

$$\nabla \cdot \mathbf{E} = -\frac{\mathbf{m}}{\mathbf{e}}(\mathbf{j}\omega + \gamma)\nabla \cdot \mathbf{v} - \frac{\mathbf{e}}{\mathbf{m}} \frac{\mathbf{v_o}^2}{\mathbf{n_o}} \nabla^2 \mathbf{n}. \tag{6.2.13}$$

Substituting equation (6.2.13) into equation (6.1.3) and using equation (6.1.5) yields upon rearrangement

$$\nabla^{2} n(\underline{r}) + \frac{\omega^{2}}{v_{o}^{2}} \left[1 - \frac{\omega_{e}^{2}}{\omega^{2}} - j \frac{\gamma}{\omega}\right] n(\underline{r}) = -\frac{\omega_{e}^{2}}{e v_{o}^{2}} \rho^{S}(\underline{r})$$

$$(6.2.14)$$

or

$$\nabla^{2} n + k_{p}^{2} n = -\frac{\omega_{e}^{2}}{e v_{o}^{2}} \rho^{S}$$
 (6.2.15)

$$k_p^2 = \frac{\omega^2}{v_0^2} \left[1 - \frac{\omega_e^2}{\omega^2} - j \frac{\gamma}{\omega} \right].$$
 (6.2.16)

Equation (6.2.15) is an inhomogeneous wave equation for the average perturned electron density n(r) which has a standard solution

$$n(r) = \frac{\omega_e^2}{4\pi e v_o^2} \int_{V} \rho^S(r') G_p(r,r') dV' \qquad (6.2.17)$$

where

$$G_{p}(r,r') = \frac{e^{-jk_{p}|r-r'|}}{|r-r'|}$$
(6.2.18)

where \underline{r} and \underline{r}' and the range of integration are the same as in equation (6.2.10). Using the continuity equation for the sources, equation (6.1.7), equation (6.2.17) can be written as

$$n(\underline{r}) = \frac{j\omega_e^2}{4\pi e v_0^2 \omega} \int \nabla' \cdot \underline{J}^S(\underline{r}') G_p(\underline{r},\underline{r}') dV' \qquad (6.2.19)$$

where $\nabla' \cdot J^S(\underline{r}')$ is the divergence of J^S with respect to the source coordinates.

The electric field $\mathbb{E}(\mathbf{r})$ at any non-source point can be derived by eliminating \mathbf{v} from equations (6.1.2) and (6.1.6) and rearranging to give

$$E = \frac{1}{j\omega\xi} \nabla x + \frac{ev_o^2}{\omega\xi(\omega-j\gamma)} \nabla n. \qquad (6.2.20)$$

 \forall x H can be calculated by taking the curl of equation (6.2.9)

$$\nabla \times H = \nabla \times \nabla \times A = \nabla (\nabla \cdot A) - \nabla^2 A. \qquad (6.2.21)$$

Equation (6.2.7) in a source free region implies that

$$-\nabla^2 \mathbf{A} = \mathbf{k_e}^2 \mathbf{A} \tag{6.2.22}$$

so equation (6.2.21) becomes

$$\nabla \times H = \nabla (\nabla \cdot A) + k_e^2 A. \qquad (6.2.23)$$

Using this result, equation (6.2.20) can be rewritten as

$$E = -\frac{j}{\omega \xi} \left[\nabla \left(\nabla \cdot \mathbf{A} \right) + k_e^2 \mathbf{A} \right] + \frac{e v_o^2}{\omega \xi \left(\omega - j \gamma \right)} \nabla n \qquad (6.2.24)$$

where the vector field $\mathbf{A}(\mathbf{r})$, the perturbed electron density $\mathbf{n}(\mathbf{r})$, and the complex permittivity ξ are given by equations (6.2.10), (6.2.17), and (6.2.4), respectively.

The current density on the surface of the cylindrical antenna can be represented as

$$J^{S}(r) = \hat{z}\delta(r-a)I_{z}(z)/2\pi a$$
 (6.2.25)

where \hat{z} is the unit vector in the z direction and $\delta(x)$ is the Dirac delta function. Very near the antenna surface

the tangential component of E(r) can then be written as $E_{z}(z)\hat{z}$ where

$$E_{z}(z) = -\frac{j}{\omega \xi} \left[\frac{\partial^{2} A_{z}(z)}{\partial z^{2}} + k_{e}^{2} A_{z}(z) \right] + \frac{e v_{o}^{2}}{\omega \xi (\omega - j \gamma)} \frac{\partial n(z)}{\partial z}$$
(6.2.26)

where using equation (6.2.25)

$$A_{z}(z,\phi) = \frac{1}{4\pi} \int_{-h}^{h} I_{z}(z') \left[\frac{1}{2\pi a} \int_{-\pi}^{\pi} \frac{e^{-jk}e^{R}}{R} ad\phi' \right] dz'$$
(6.2.27)

and

$$n(z,\phi) = \frac{j\omega_e^2}{4\pi e v_o^2 \omega} \int_{-h}^{h} \frac{\partial I_z}{\partial z'} \left[\frac{1}{2\pi a} \int_{-\pi}^{\pi} \frac{e^{-jk} p^R}{R} ad\phi' \right] dz'$$
(6.2.28)

where R is the distance between the source point \underline{r} and the field point \underline{r} . From Figure 6.2 it can be seen that R can be expressed as

$$R = |r - r'| = \{2a^{2}[1-\cos(\phi-\phi')] + (z-z')^{2}\}^{\frac{1}{2}}$$
(6.2.29)

where the primed coordinates are the source points on the antenna surface and the unprimed coordinates are the field points very near the surface of the antenna. Since the antenna is rotationally symmetric, A(r) and n(r) cannot

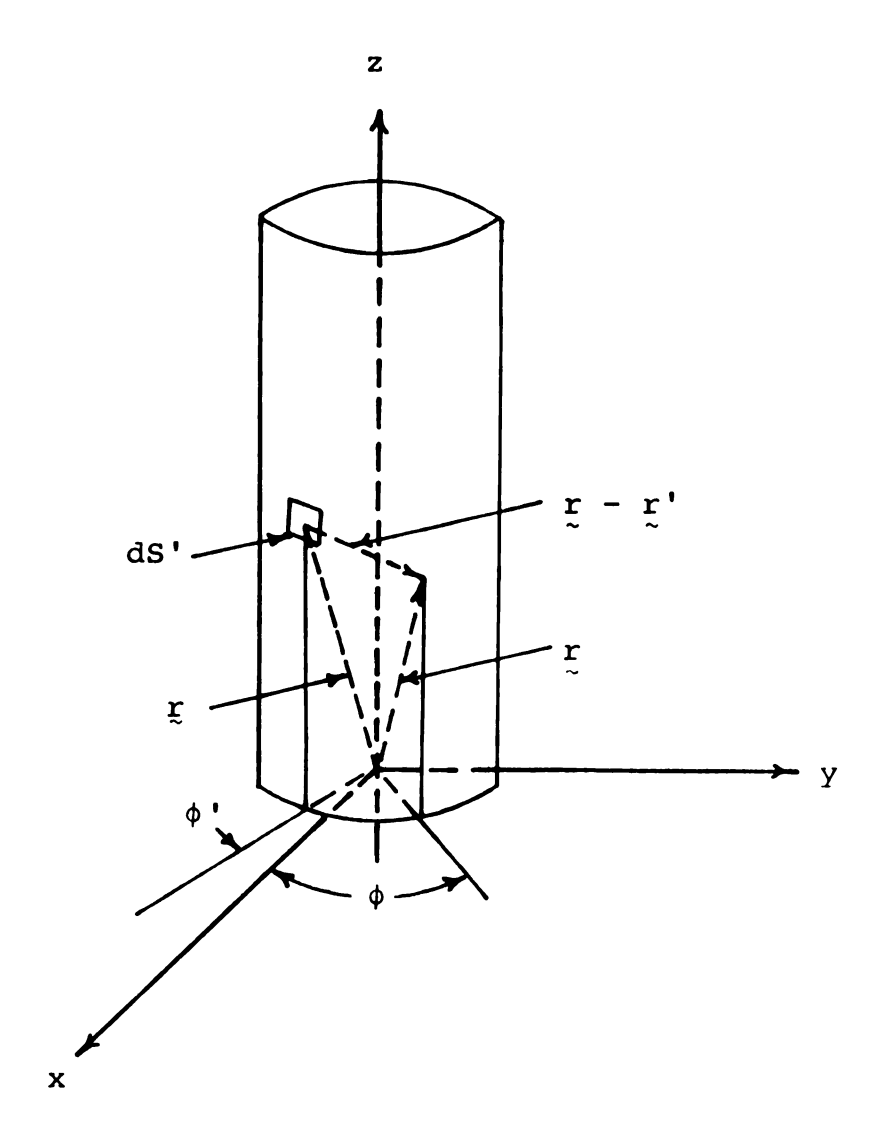


Figure 6.2. Source and field points on or near the surface of the antenna.

depend on ϕ , so we can arbitrarily set ϕ equal to zero. Therefore,

$$R = [2a^{2}(1-\cos\phi')^{2} + (z-z')^{2}]^{\frac{1}{2}}$$

$$= [(2a \sin \frac{\phi'}{2})^{2} + (z-z')^{2}]^{\frac{1}{2}}.$$
(6.2.30)

On the conducting surface of the antenna, the electric field is zero and in the gap at z=0, $E_z=-V/2\Delta$ or, in general, on the cylindrical surface, from $-h \le z \le h$ and at r=a we can say that

$$E_{z}(z) = -V\delta(z)$$
. (6.2.31)

Combining equations (6.2.26) and (6.2.31) gives an integral differential equation of the form

$$-V\delta(z) = -\frac{j}{\omega\xi} \left[\frac{\partial^2 A_z(z)}{\partial z^2} + k_e^2 A_z(z) \right] + \frac{ev_o^2}{\omega\xi(\omega - j\gamma)} \frac{\partial n(z)}{\partial z}$$
(6.2.32)

or

$$\frac{\partial^2 A_z(z)}{\partial z^2} + k_e^2 A_z(z) = f(z)$$
 (6.2.33)

where

$$f(z) = -j\omega\xi V\delta(z) - j \frac{ev_o^2}{\omega - j\gamma} \frac{\partial n(z)}{\partial z}$$
 (6.2.34)

which is valid on the surface of the antenna. The solution to the inhomogeneous differential equation, equation (6.2.33) is given by

$$A_z(z) = A_z^{C}(z) + A_z^{P}(z)$$
 (6.2.35)

where $A_z^{\ C}(z)$ in the complementary function and $A_z^{\ P}(z)$ is the particular integral. The complementary function is the solution to the homogeneous differential equation and is

$$A_z^{C}(z) = B \sin k_e z + C \cos k_e z.$$
 (6.2.36)

From symmetry requirements, i.e., $I_z(z) = I_z(-z)$, B must equal to zero. By the method of the variation of parameters, the particular integral for an equation of the form of equation (6.2.33) is given by

$$A_z^P(z) = \frac{1}{k_e} \int_0^z f(z') \sin k_e(z-z')dz'$$
 (6.2.37)

Thus

$$A_{z}(z) = \frac{1}{k_{e}} \int_{0}^{z} f(z') \sin k_{e}(z-z')dz' + C \cos k_{e}z$$
(6.2.38)

where f(z) is given by equation (6.2.34) and C is an arbitrary constant yet to be calculated.

Writing equation (6.2.37) out gives

$$A_{z}^{P}(z) = -j \frac{\omega \xi V}{k_{e}} \int_{0}^{z} \delta(z') \sin k_{e}(z-z') dz'$$

$$-j \frac{ev_{o}^{2}}{k_{e}(\omega-j\gamma)} \int_{0}^{z} \frac{\partial n(z')}{\partial z'} \sin k_{e}(z-z') dz'$$

$$= -j \frac{\omega \xi V}{2k_{e}} \sin k_{e} |z|$$

$$-j \frac{ev_{o}^{2}}{k_{e}(\omega-j\gamma)} \int_{0}^{z} \frac{\partial n(z')}{\partial z'} \sin k_{e}(z-z') dz'.$$

$$(6.2.39)$$

The integral on the right-hand side of equation (6.2.39) can be integrated by parts to give

$$\int_{0}^{z} \frac{\partial n(z')}{\partial z'} \sin k_{e}(z-z')dz' = n(z')\sin k_{e}(z-z') \begin{vmatrix} z'=z \\ z'=0 \end{vmatrix}$$

$$+ k_{e} \int_{0}^{z} n(z')\cos k_{e}(z-z')dz'$$

$$= -n(0)\sin k_{e}z + k_{e} \int_{0}^{z} n(z')\cos k_{e}(z-z')dz'.$$
(6.2.40)

But if we define R' = $[z'^{2} + (2a \sin \frac{\phi'}{2})^{2}]^{\frac{1}{2}}$

$$n(0) = j \frac{\omega_e^2}{4\pi e v_o^2 \omega} \int_{-h}^{h} \frac{\partial I_z(z')}{\partial z'} \left[\frac{1}{2\pi a} \int_{-\pi}^{\pi} \frac{e^{-jk_p R'}}{R'} ad\phi' \right] dz'$$

$$= 0 \qquad (6.2.41)$$

since the integrand is an odd function over the interval integrated. Thus

$$A_{z}^{P}(z) = -j \frac{\omega \xi V}{2k_{e}} \sin k_{e} |z|$$

$$-j \frac{ev_{o}^{2}}{\omega - j \gamma} \int_{0}^{z} n(z') \cos k_{e}(z-z') dz' \qquad (6.2.42)$$

Substituting n(z) from equation (6.2.19) into the integral on the right-hand side of equation (6.2.42) yields

$$\int_{0}^{z} n(z')\cos k_{e}(z-z')dz'$$

$$= j \frac{\omega_{e}^{2}}{4\pi e v_{o}^{2} \omega} \int_{0}^{z} \cos k_{e}(z-z') \int_{-h}^{h} \frac{\partial I_{z}(z'')}{\partial z''}$$

$$\times G_{p}'(z',z'')dz''dz' \qquad (6.2.43)$$

where

$$G_{p}'(z',z'') = \frac{1}{2\pi} \int_{-\pi}^{\pi} \frac{e^{-jk}p^{R''}}{R''} d\phi''$$
 (6.2.44)

where

$$R'' = \left[(z'-z'')^2 + (2a \sin \frac{\phi''}{2})^{\frac{1}{2}} \right]^{\frac{1}{2}}.$$

Noting that

$$\int_{-h}^{h} \frac{\partial I_{z}(z'')}{\partial z''} G_{p}'(z',z'')dz' = I_{z}(z'')G_{p}'(z',z'') \begin{vmatrix} z''=h \\ z''=-h \end{vmatrix}$$

$$- \int_{-h}^{h} I_{z}(z'') \frac{\partial}{\partial z''} G_{p}'(z',z'')dz''$$

$$= - \int_{-h}^{h} I_{z}(z'') \frac{\partial}{\partial z'''} G_{p}'(z',z'')dz'', (6.2.45)$$

based on the assumption that $I_z(z''=\pm h)=0$. Equation (6.2.43) can be rewritten as

$$\int_{0}^{z} n(z') \cos k_{e}(z-z') dz'$$

$$= - j \frac{\omega_{e}^{2}}{4\pi e v_{o}^{2} \omega} \int_{0}^{z} \cos k_{e}(z-z') \int_{-h}^{h} I_{z}(z'')$$

$$\times \frac{\partial}{\partial z'''} G_{p}'(z',z'') dz'' dz''$$

$$= - j \frac{\omega_{e}^{2}}{4\pi e v_{o}^{2} \omega} \int_{-h}^{h} I_{z}(z'') \int_{0}^{z} \cos k_{e}(z-z')$$

$$\times \frac{\partial}{\partial z'''} G_{p}'(z',z'') dz'' dz'' \qquad (6.2.46)$$

The interchange of the order of integration of equation (6.2.46) is legal because $I_z(z^*)$, $\cos k_e(z-z^*)$, and $G_p'(z^*,z^*)$ are continuous functions of z^* and z^* in the range of integration. Since

$$\frac{\partial}{\partial z^{\dagger}} G_{\mathbf{p}}'(z',z'') = -\frac{\partial}{\partial z^{\prime\prime}} G_{\mathbf{p}}'(z',z'') \qquad (6.2.47)$$

equation (6.2.46) can be expressed as

$$\int_{0}^{z} n(z') \cos k_{e}(z-z') dz'$$

$$= j \frac{\omega_{e}^{2}}{4\pi e v_{o}^{2} \omega} \int_{-h}^{h} I_{z}(z'') \int_{0}^{z} \cos k_{e}(z-z')$$

$$\times \frac{\partial}{\partial z'} G_{p'}(z',z'') dz'' dz''$$

$$= j \frac{\omega_{e}^{2}}{4\pi e v_{o}^{2} \omega} \int_{-h}^{h} I_{z}(z'') \int_{0}^{z} \cos k_{e}(z-z'')$$

$$\frac{\partial}{\partial z'''} G_{p'}(z'',z'') dz'' dz'''. (6.2.48)$$

Then $A_z(z)$ can be written as

$$A_{z}(z) = -j \frac{\omega \xi V}{2k_{e}} \sin k_{e} |z| + C \cos k_{e} z$$

$$+ \frac{\omega_{e}^{2}}{4\pi\omega(\omega - j\gamma)} \int_{-h}^{h} I_{z}(z')K'(z,z')dz' \qquad (6.2.49)$$

where

$$K'(z,z') = \int_{0}^{z} \cos k_{e}(z-z'') \frac{\partial}{\partial z''} G_{p}'(z'',z')dz''$$
 (6.2.50)

Combining equations (6.2.27) and (6.2.49) and rearranging yields an integral equation for $I_z(z)$ as follows

$$\int_{-h}^{h} I_{z}(z')K(z,z')dz' = -j \frac{\omega \xi V}{2k_{e}} \sin k_{e} |z|$$

$$+ C \cos k_{e}z \qquad (6.2.51)$$

$$K(z,z') = \frac{1}{4\pi} \left[G_{e'}(z,z') - \frac{\omega_{e}^2}{\omega(\omega-j\gamma)} K'(z,z') \right]$$
 (6.2.52)

where

$$G_{e}'(z,z') = \frac{1}{2\pi} \int_{\pi}^{-\pi} \frac{e^{-jk}e^{R}}{R} d\phi'$$
 (6.2.53)

where $R = [(z-z')^2 + (2a \sin \phi'/2)^2]^{\frac{1}{2}}$ and K'(z,z') is given by equation (6.2.50).

Now we must solve for the arbitrary constant C. Evaluating equation (6.2.51) at z=h and solving for C yields

$$C = \sec k_e h \int_{-h}^{h} I_z(z')K(h,z')dz' + j \frac{\omega \xi V}{2k_e} \tan k_e h$$

$$(6.2.54)$$

Substituting equation (6.2.54) back into equation (6.2.51) and rearranging gives us the final form for a Hallén type integral equation for the current $I_z(z)$ as follows:

$$\int_{-h}^{h} I_{z}(z') \left[\cos k_{e} h K(z,z') - \cos k_{e} z K(h,z')\right] dz'$$

$$= j \frac{\omega \xi V}{2k_e} \sin k_e (h-|z|) \qquad (6.2.55)$$

$$K(z,z') = \frac{1}{4\pi} \left[G_{e}'(z,z') - \frac{\omega_{e}^{2}}{\omega(\omega-j\gamma)} \int_{0}^{z} \cos k_{e}(z-z'') \right]$$

$$\times \frac{\partial}{\partial z''} G_{p}'(z'',z') dz'''$$

$$= \frac{1}{4\pi} \left\{ G_{e}'(z,z') - \frac{\omega_{e}^{2}}{\omega(\omega-j\gamma)} \left[\cos k_{e}(z-z'') \right] \right\}$$

$$\times G_{p}'(z'',z') \left| z'' = z \right|$$

$$z'' = 0$$

$$- k_{e} \int_{0}^{z} \sin k_{e}(z-z'') G_{p}'(z'',z') dz''' \right]$$

or

$$K(z,z') = \frac{1}{4\pi} \left\{ G_{e'}(z,z') - \frac{\omega_{e}^{2}}{\omega(\omega-j\gamma)} \middle| G_{p'}(z,z') \right\}$$

$$- \cos k_{e}z G_{p'}(0,z')$$

$$- k_{e} \int_{0}^{z} \sin k_{e}(z-z'') G_{p}(z'',z') dz'' \right\}.$$

$$(6.2.56)$$

6.3 Zeroth Order Current and Input Impedance

The results of Section 6.2 can be summarized as follows: the integral equation for the antenna current is

$$\int_{-h}^{h} I_{z}(z') [\cos k_{e}h K(z,z') - \cos k_{e}z K(h,z')]dz'$$

$$= j \frac{V\omega\xi}{2k_e} \sin k_e (h-|z|) \qquad (6.3.1)$$

where

$$K(z,z') = \frac{1}{4\pi} \left\{ G_{e'}(z,z') - \frac{\omega_{e}^{2}}{\omega(\omega-j\gamma)} \left[G_{p'}(z,z') - \cos k_{e}z G_{p'}(0,z') - k_{e} \int_{0}^{z} \sin k_{e}(z-z'') \right] \right\}$$

$$\times G_{p'}(z'',z') dz'' \right\} \qquad (6.3.2)$$

where

$$G_{e}'(z,z') = \frac{1}{2\pi} \int_{-\pi}^{\pi} \frac{e^{-jk}e^{R}}{e^{R}} d\phi'$$
 (6.3.3)

$$G_{p}'(z,z') = \frac{1}{2\pi} \int_{-\pi}^{\pi} \frac{e^{-jk}p^{R}}{e^{R}} d\phi'$$
 (6.3.4)

where

$$R = \left[(z-z') + (2a \sin \frac{\phi'}{2})^{\frac{1}{2}} \right]^{\frac{1}{2}}$$
 (6.3.5)

$$k_e^2 = \omega^2 \mu_0 \epsilon_0 \left[1 - \frac{\omega_e^2}{\omega^2 + \gamma^2} - j \frac{\omega_e^2 \gamma}{\omega(\omega^2 + \gamma^2)} \right]$$
 (6.3.6)

$$k_{p}^{2} = \frac{\omega^{2}}{v_{o}^{2}} \left[1 - \frac{\omega_{e}^{2}}{\omega^{2}} - j \frac{\gamma}{\omega} \right].$$
 (6.3.7)

The right-hand side of equation (6.3.1) varies with $\sin k_e(h-|z|)$ so a reasonable zeroth order current distribution on the surface of the antenna which also varies with wave number k_a is

$$I_{z}(z) = \begin{cases} I_{0} \sin k_{e}(h-|z|) & -h \leq z \leq h \\ 0 & \text{otherwise} \end{cases}$$
 (6.3.8)

It is noted that equation (6.3.8) for the assumed current distribution satisfies the required boundary conditions, i.e., $I_z(\pm h) = 0$ and $I_z(z) = I_z(-z)$.

If the zeroth order current distribution, equation (6.3.8), is substituted into equation (6.3.1), the following result is obtained

$$I_{0-h}^{\int_{-h}^{h} \sin k_e(h-|z'|)[\cos k_e h K(z,z')]}$$

- $\cos k_e z K(h,z')]dz'$

=
$$j \frac{V\omega\xi}{2k_e} \sin k_e(h-|z|)$$
. (6.3.9)

Evaluating equation (6.3.9) at z = 0 and solving for I_0 yields

$$I_{0} = j \frac{V\omega\xi}{2k_{e}} \frac{\sin k_{e}h}{\int_{-h}^{h} \sin k_{e}(h-|z'|)[\cos k_{e}h K(0,z') - K(h,z')]dz'}$$
(6.3.10)

so now equation (6.3.8) for the assumed current distribution is completely specified.

The input impedance of an antenna is defined as the driving point voltage divided by the driving point current, i.e.,

$$z_{in} = \frac{V}{I_z(z=0)}$$
 (6.3.11)

Therefore

$$Z_{in} = \frac{V}{I_0 \sin k_e h}$$

$$= -j \sqrt{\frac{\mu_0}{\xi}} \frac{2}{\sin^2 k_e h} \int_{-h}^{h} \sin k_e (h-|z'|) [\cos k_e h]$$

$$\times K(0,z') - K(h,z')] dz' \qquad (6.3.12)$$

Equation (6.3.12) is the result that we require and will be solved numerically in Chapter VII.

CHAPTER VII

NUMERICAL AND EXPERIMENTAL RESULTS

In this chapter, numerical solutions to equations (6.3.12) and (6.3.8) for the input impedance and current distribution of a cylindrical antenna immersed in a hot, lossy plasma of infinite extent are displayed for various plasma and antenna parameters. The numerical results are compared to values obtained for a cylindrical monopole immersed in DC laboratory plasma. Also, the numerical results are compared to experiments performed by Graf and Jassby [48] and with the theoretical results of Lin and Mei [56], and Wunsch [58] for very small antennas. It is also shown that this theory under appropriate approximations agrees with that of Chen (23) who calculated the input resistance by a Poynting vector method.

7.1 Numerical Techniques

The equation to be numerically solved is from Chapter VI

$$z_{in} = -j \sqrt{\frac{\mu_o}{\xi}} \frac{2}{\sin^2 k_e h} \int_{-h}^{h} \sin k_e (h-|z'|)$$

$$\times [\cos k_e h K(0,z') - K(h,z')]dz'$$
 (7.1.1)

$$K(z,z') = \frac{1}{4\pi} \left\{ G_{e}'(z,z') - \frac{\omega_{e}^{2}}{\omega(\omega-j\gamma)} \left[G_{p}(z,z') - \cos k_{e}z G_{p}'(0,z') \right] - \cos k_{e}z G_{p}'(0,z') - k_{e} \int_{0}^{z} \sin k_{e}(z-z'') G_{p}'(z'',z') dz'' \right\}$$

$$(7.1.2)$$

where

$$G_{e}'(z,z') = \frac{1}{2\pi} \int_{-\pi}^{\pi} \frac{e^{-jk}e^{R}}{e^{R}} d\phi'$$
 (7.1.3)

$$G_{p}'(z,z') = \frac{1}{2\pi} \int_{-\pi}^{\pi} \frac{e^{-jk_{p}R}}{e^{R}} d\phi'$$
 (7.1.4)

and where μ_0 , ξ , k_e , h, ω_e , ω , γ , and R are defined in Chapter VI. Equation (7.1.1) can be separated into five integrals each of which must be integrated numerically. These integrals are

$$I_{1} = \int_{-h}^{h} \sin k_{e}(h-|z'|)G_{e}'(0,z')dz' \qquad (7.1.5)$$

$$I_2 = \int_{-h}^{h} \sin k_e (h-|z'|) G_e'(h,z') dz'$$
 (7.1.6)

$$I_{3} = \int_{-h}^{h} \sin k_{e}(h-|z'|)G_{p}'(h,z')dz' \qquad (7.1.7)$$

$$I_{4} = \int_{-h}^{h} \sin k_{e} (h-|z'|) G_{p}'(0,z') dz'$$
 (7.1.8)

and

$$I_{5} = \int_{-h}^{h} \sin k_{e} (h-|z'|) \begin{bmatrix} h \\ \int \sin k_{e} (h-z'') \\ 0 \end{bmatrix}$$

$$\times G_{p}'(z'',z') dz'' dz''. \qquad (7.1.9)$$

Numerical integration is accomplished using a Simpson's rule formulation which insures that the numerical result approximates the true value by successive iteration until the difference between two succeeding results is within some prescribed limits. The limit in all cases except one to be noted later is taken to be 5%.

It was found by actually performing the numerical integration on the computer that the integral, equation (7.1.3), could very accurately be approximated by

$$G_{e'}(z,z') = \frac{e^{-jk_{e}R'}}{R'}$$
 (7.1.10)

where

$$R' = [(z-z')^2 + a^2]^{\frac{1}{2}}$$
 (7.1.11)

for the plasma and antenna parameters of interest. Using equation (7.1.10), integrals I_1 , and I_2 reduce to single integrations of a continuous function over the interval considered. These integrals are thus evaluated directly using the Simpson's rule technique.

The last three integrals, I_3 , I_4 , and I_5 are not handled as simply because the integration in equation (7.1.4) must be retained in all three cases.

By a change of variables, y = h - z', I_3 becomes

$$I_3 = \frac{1}{\pi} \int_0^{2h} \sin k_e (h-|h-y|) \int_0^{\pi} \frac{e^{-jk_p R''}}{R''} d\phi' dy$$
 (7.1.12)

where

$$R'' = \left[y^2 + (2a \sin \frac{\phi'}{2})^2 \right]^{\frac{1}{2}}.$$
 (7.1.13)

 I_3 in the form given in equation (7.1.12) is easily integrated using a nested Simpson's rule technique where the inner integral over ϕ ' is integrated for each value of y required in the outer integration. It is found numerically that I_3 is always four or five orders of magnitude smaller than I_A .

 I_{Δ} can be rewritten as

$$I_4 = \frac{2}{\pi} \int_0^h \sin k_e (h-z') \left[\int_0^{\pi} \frac{e^{-jk_p R'''}}{R'''} d\phi' \right] dz'$$

R''' =
$$\left[z'^2 + (2a \sin \frac{\phi'}{2})^2\right]^{\frac{1}{2}}$$
. (7.1.15)

Note that at z'=0 and $\phi'=0$ the integrand is singular. I_4 can be evaluated by the method of the auxiliary integral described in Appendix C. Using this method we can write I_4 as

$$I_{4} = \frac{4}{\pi} \sin k_{e} h \left[\frac{h}{2a} \sinh^{-1} \frac{2a}{h} + \sinh^{-1} \frac{h}{2a} \right] + \frac{2}{\pi} \int_{0}^{h} \int_{0}^{\pi} \frac{\sin k_{e} (h-z')e^{-jk_{p}R'''}}{R'''} - \sin k_{e} h \cos \frac{\phi'}{2} d\phi' dz'$$

$$(7.1.16)$$

where the second integral is well behaved at z' = 0 and $\phi' = 0$. Thus, the integral I_4 can be easily be evaluated on the computer.

The integral I_5 is the most difficult to evaluate on the computer because it involves a triple integral that requires a lot of computer time. The procedures for evaluating I_5 are similar to those used in evaluating the first four integrals, namely the method of the auxiliary integral is used to remove the singularity that occurs in the integral over z" and the Simpson's rule integrations are nested to obtain the required result. For I_5 the convergence limit is required to be only 10% in order to save computer time.

All numerical calculations were carried out on the CDC 6500 computer.

7.2 Numerical Results

Except where noted, the electron velocity, V_e , is assumed to be one one-hundredth of the speed of light, c, and the antenna dimensions are measured in terms of the free space electromagnetic wavelength λ_o , where λ_o = $2\pi c/\omega$ and ω is the angular driving frequency. All calculations have been made for a one volt gap voltage.

The input impedance and current distribution of a cylindrical dipole antenna as expressed in equations (6.3.12) and (6.3.8) have been numerically calculated as a function of the antenna dimensions and plasma parameters. The theoretical results on the input impedances of cylindrical monopole antennas of various lengths and diameters are taken to be $Z_{in}/2$ and are graphically shown in Figures 7.2, 7.4, 7.6, and 7.8. The input impedance is plotted as a function of ω_e^2/ω^2 with γ/ω as the running parameter. The value of $\omega_{\alpha}^{2}/\omega^{2}$ is directly proportional to the plasma density when the antenna frequency is kept constant and γ/ω is the ratio between electron collision frequency and the antenna frequency. The current distributions given by equation (6.3.8) are plotted in Figures 7.3, 7.5, 7.7, and 7.9 as a function of position along the antenna for various values of $\omega_{\rm p}^2/\omega^2$ and γ/ω .

phase, ϕ , of each current distribution which is very nearly constant along the length of the antennas considered is also given in these figures.

In the figures depicting the antenna impedances, the solid lines represent the antenna input resistances while the dashed lines stand for the antenna input reactances. From these figures, the effects of the collision frequency on the antenna input impedance can be summarized as follows:

- 1. For low plasma density $(\omega_e^2/\omega^2 < 0.4)$, the antenna input resistance remains nearly constant while the input reactance becomes slightly more negative. There is little effect due to the varying collision frequencies.
- 2. For 0.4 < ω_e^2/ω^2 < 0.8, the input resistance increases monotonically as the plasma density is increased. The antenna reactance decreases at a faster rate than in case (1) as the plasma density is increased. Over this range a larger collision frequency causes a larger input resistance and makes the input reactance less negative.
- 3. In the range of 0.8 < ω_e^2/ω^2 < 1.2, there are sharp peaks in the antenna resistance and a change from capacitive to inductive for the antenna reactance when the plasma frequency

approaches the antenna driving frequency. The maximum value of the antenna resistance is reduced considerably by larger collision frequencies.

4. For $\omega_e^2/\omega^2 > 1.2$, both antenna resistance and reactance decrease as the plasma density is increased.

The significant findings are that: (1) the peaking of the antenna input resistance at $\omega \sim \omega_e$, and (2) the change in sign of the reactance at $\omega \sim \omega_e$.

The main observation to be noted from a study of the antenna current distributions is that the amplitude of the current is larger for greater collision frequencies, this effect being more evident in the vicinity of $\omega \sim \omega_e$. This result can also be determined from the impedance plots. For $\omega_e^2/\omega^2=0.6$ and 1.2 the magnitude of the input current depends mainly on the magnitude of the reactance which is smaller for larger values of the collision frequency. At $\omega_e^2/\omega^2=0.95$ the magnitude of the input current is determined largely by the magnitude of the input resistance which is smaller for larger values of the collision frequency.

In Appendix D it is shown that the antenna input resistance from equation (6.3.12) under the assumptions of a line current flowing down the center of a very thin (a+0) antenna immersed in a hot lossless plasma reduces

to precisely the result obtained by Chen [23] using a poynting vector method. Further, the resistance under the above limitations may be broken into a part denoted by R_e due to the excitation of an electromagnetic wave in the plasma medium and a second part, call it R_p , due to the excitation of an electroacoustic wave in the plasma. R_e in our theory is derived from the integrals I_1 and I_2 of Section 7.1 while R_p arises from integrals I_3 , I_4 , and I_5 . Figure 7.10 is a plot of R_e , R_p , and $R_{in} = R_e + R_p$ evaluated using equation (6.3.12) for a one-dimensional current distribution. In addition to equation (7.1.10), it is assumed that

$$G_{p}'(z,z') = \frac{e^{-jk_{p}R}}{R}$$
 (7.2.1)

where

$$R = [(z-z')^2 + a^2]^{\frac{1}{2}}, \qquad (7.2.2)$$

for an antenna of half length $h = 0.25\lambda_{O}$ and radius $a = 0.001\lambda_{O}$ immersed in a hot lossless plasma. Also plotted are resistances calculated using Chen's results. The agreement between the two theories is almost exact. Figure 7.11 is a plot of X_{e} , X_{p} , and $X_{in} = X_{e} + X_{p}$, which are defined analogously to R_{e} , R_{p} , and R_{in} , calculated using our theory for the same parameters used in Figure 7.10. It is noted that Chen was unable to calculate reactances using his poynting vector method.

Figure 7.12 is a comparison of current distributions calculated using our theory and those measured by Judson, Chen, and Lundquist [51] in a finite DC laboratory plasma for an antenna of half length, h = 5.9 cm and radius, a = 0.615 cm, driven with a frequency of 1.25 GHZ. The collision frequency in the theory is assumed to be $\gamma/\omega = 0.12$. The agreement between our theory and their experiment is good.

Figures 7.13 and 7.14 are comparisons of our theoretical input impedances with experimental values measured by Graf and Jossby [48] for two different size cylindrical antennas immersed in a hot lossy ($\gamma/\omega = 0.2$) plasma. Our theory is found to give much better agreement with their experimental values than the cold lossy plasma theory that Graf and Jossby used.

In Figures 7.15 and 7.16 we compare our theory to that of Lin and Mei [36] which is limited to very short antennas on the order of an electroacoustic wavelength long. For these two figures the plasma is considered to be hot $(V_e/C = 0.001)$ and lossless. In Figure 7.15 our theory predicts impedances very close to the values calculated by Lin and Mei for an antenna of half length $h = \lambda_e/4$ and radius $a = \lambda_e/75$ where

$$\lambda_{e} = 2\pi \frac{V_{e}}{\omega} \left(1 - \frac{\omega_{e}^{2}}{\omega^{2}}\right)^{-\frac{1}{2}}$$
 (7.2.3)

Also plotted is the input impedance of an antenna of dimensions $h = \lambda_{e0}/4$ and $a = \lambda_{e0}/75$ where $\lambda_{e0} = 2\pi V_e/\omega$ which do not vary with plasma density. This is a more physical case to consider because the actual dimensions of a real antenna do not change as ω_e^2/ω^2 is varied. Figure 7.16 is a comparison of the two theories for an antenna of dimensions $h = 3.84\lambda_D$ and $a = 0.204\lambda_D$, where λ_D is on the order of a Debye length. In both figures excellent agreement between the two different theories is observed. It is noted that Lin and Mei's theory is restricted to an extremely short antenna while our theory can be used to calculate the input impedance and current distribution of longer antennas with practical dimensions. The reason is that our theory is based on a much simpler formulation.

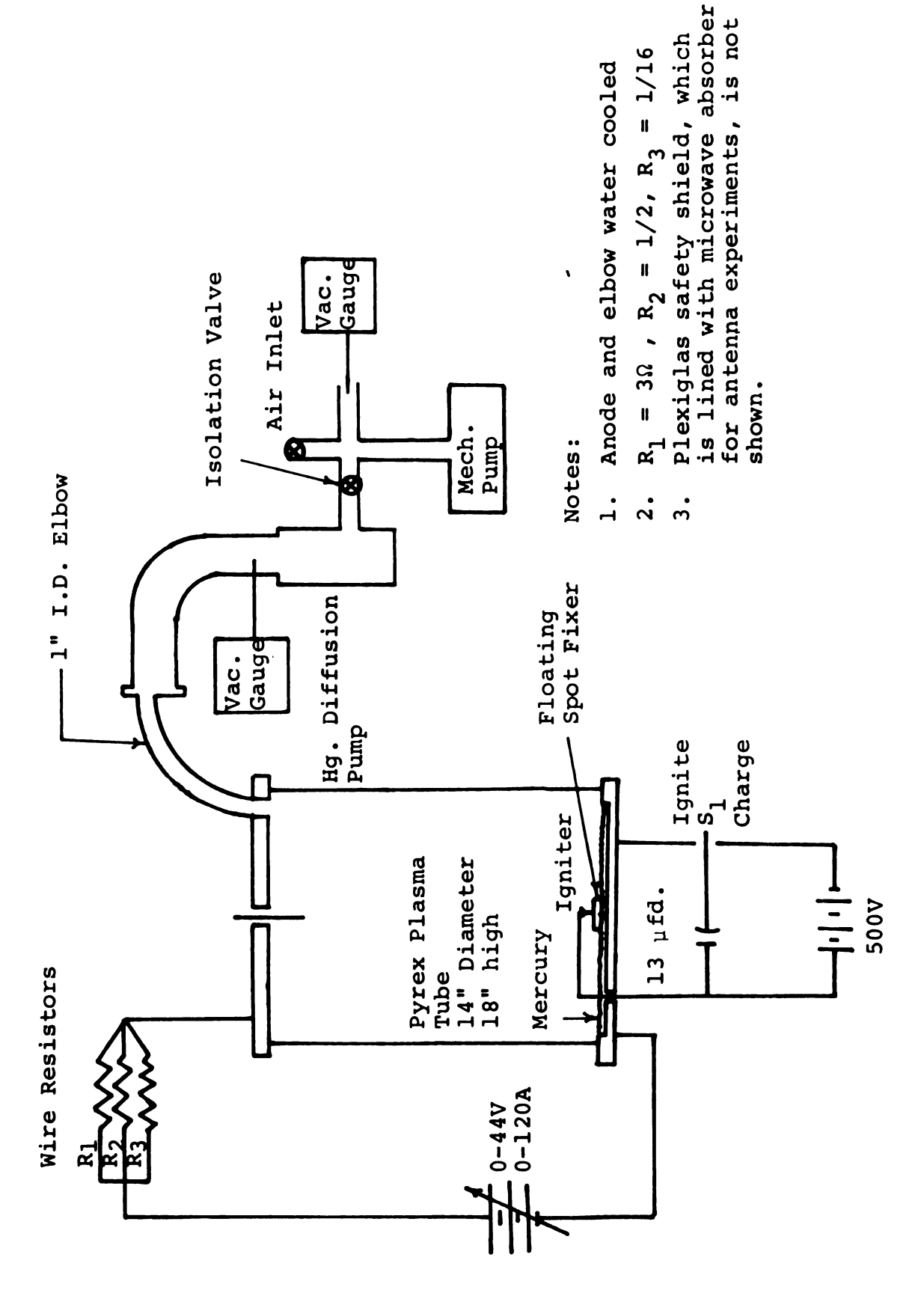
Figure 7.17 compares the input admittance of a dipole of half length $h = 9\pi/2$, $V_e/\sqrt{3}\omega_e$ and radius a = h/60 calculated by Wunsch [58] using Balmain's theory [33] with the input admittance calculated using our theory. The plasma is considered to be hot $(V_e/C = 0.001)$ and lossless. Fair agreement between the two theories is observed.

7.3 Experimental Results

The radiation of a cylindrical antenna in a plasma medium has been studied theoretically by many researchers. As mentioned before, only a few workers have attempted to

measure the properties of antennas in plasmas experimentally. Because of the availability of a large volume of a stable, high density plasma in our laboratory [60], we have performed an experiment that measured the input impedances of cylindrical antennas in a plasma medium.

The schematic diagram of the experimental setup for the antenna impedance is shown in Figure 7.1. The plasma tube is made of an open-end Pyrex bell jar with dimensions 14 inches in diameter and 18 inches in length. The upper end of the tube is a circular metal plate used as an anode in the excitation of the plasma and as a ground plane for a cylindrical monopole antenna feeding through the center of the plate. The lower end of the tube is the cathode which consists of a pool of mercury contained in a metal dish. A floating metallic ring is placed at the center of the mercury pool to fix the moving hot spots of the mercury arc discharge. An ignition circuit is installed in the mercury pool for the purpose of starting the plasma. A DC power supply circuit is connected between the anode and the cathode of the tube. Under normal operating conditions the discharge currents range from 0 to 120 amperes which corresponds to a range of from DC to 3GHZ for the plasma frequency, $\omega_{o}/2\pi$. The vacuum pumping system consists of a mechanical pump and a mercury diffusion pump. The tube is continuously pumped during the experiment and the pressure in the tube is maintained at



Experimental setup for the measurement of impedance of a Figure 7.1. cylindrical antenna.

about 10⁻³ mm Hg. The antenna input impedance is measured by using the standard SWR method.

The experimental results for the input impedance of various size cylindrical antennas are shown in Figures 7.18 to 7.26. In each figure we have also plotted theoretical results calculated from equation (6.3.12) for the input impedance for the corresponding size antenna and for a hot $(V_e/C=0.01)$, lossy $(\gamma/\omega=0.12)$ plasma. The antennas actually used in the experiments were 2.2 cm, 3.2 cm, and 4.7 cm in length and 0.12 cm in radius. The driving frequencies were 1.6GHZ, 1.8GHZ, and 2.0GHZ for each antenna size yielding experimental results for antennas of nine different electrical lengths. In each figure the solid lines and the circular points are the theoretical and experimental resistances respectively, while the dashed lines and square points are the theoretical and experimental reactances, respectively.

A study of Figures 7.18 to 7.26 yields the following observations:

1. For low plasma density $(\omega_e^2/\omega^2 < 0.6)$ the theoretical and experimental resistances are nearly constant and in good agreement. The experimental reactance tends to become more negative faster than the theoretical values as the plasma density is increased.

- 2. For $0.6 < \omega_e^2/\omega^2 < 1.0$ the antenna resistances increases monotonically and reaches a peak at $\omega \sim \omega_e$ for both the experimental and theoretical curves and the reactances reach a large negative value and then increase in value until the reactances are nearly zero at $\omega \sim \omega_e$.
- 3. In the range 1.0 $< \omega_e^2/\omega^2 <$ 1.6 the antenna resistances both experimentally and theoretically decrease monotonically with the theoretical values decreasing at a faster rate than the experimental values. The antenna reactances are inductive in this range and reach a maximum and then begin to decrease as the plasma density is increased.

In general good qualitative agreement between theory and experiment is observed with the resistances reaching a maximum at ω ~ ω_e and the reactances changing from capacitative to inductive at ω ~ ω_e .

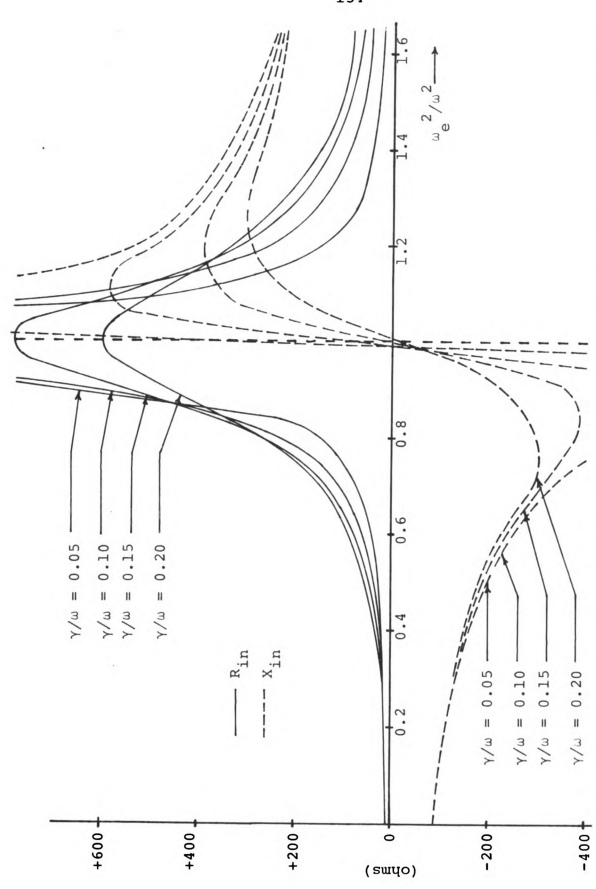
7.4 Conclusions

A theory has been developed and an experiment performed to evaluate the input impedance of a cylindrical antenna immersed in a hot lossy plasma. Good qualitative agreement between theory and experiment was observed. To the best of our knowledge our theory is the first that is able to predict the input resistance for $\omega_{\rm p}^{\ 2}/\omega^2 > 1.0$

and the input reactance over the entire range (0 < ω_e^2/ω^2 < 2.6) for an antenna on the order of a free space wavelength in length immersed in a hot lossy plasma.

The theoretical effect of collisional losses on the input impedances has been demonstrated.

Further, it has been shown that our theory is compatible with that of Chen [23] who used a poynting vector method and with the theories of Lin and Mei [56] and Wunsch [58] whose solutions were limited to antennas on the order of an electroacoustic wavelength in length. It has been shown that our theory is in good agreement with the experimental results of Graf and Jassby [48] and it has been demonstrated that the form of our assumed current distribution, equation (6.3.8) is in good agreement with experimentally measured current distributions of Judson, Chen, and Lundquist [52].



7.2. Theoretical input impedance of a monopole $(h/\lambda_0=0.147,~a/\lambda_0=0.008)$ /C = 0.01) lossy plasma as a function of plasma density. Figure 7.2. in a hot $(V_{\Delta}/C = 0)$

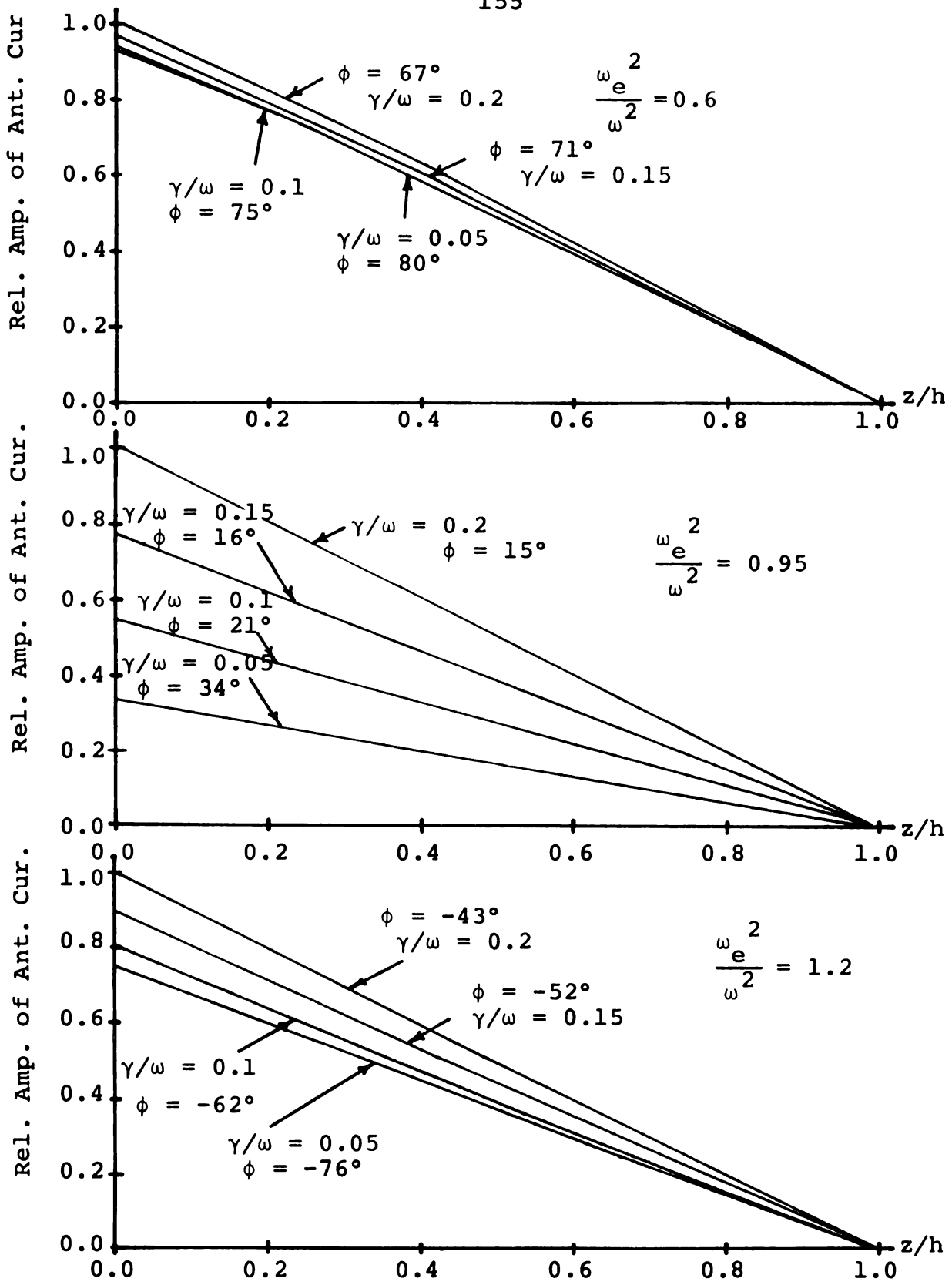


Figure 7.3. Current distributions on a dipole with $h/\lambda_0=0.147$ and $a/\lambda_0=0.0072$ for various values of ω_e^2/ω^2 and γ/ω as a function of z/h.

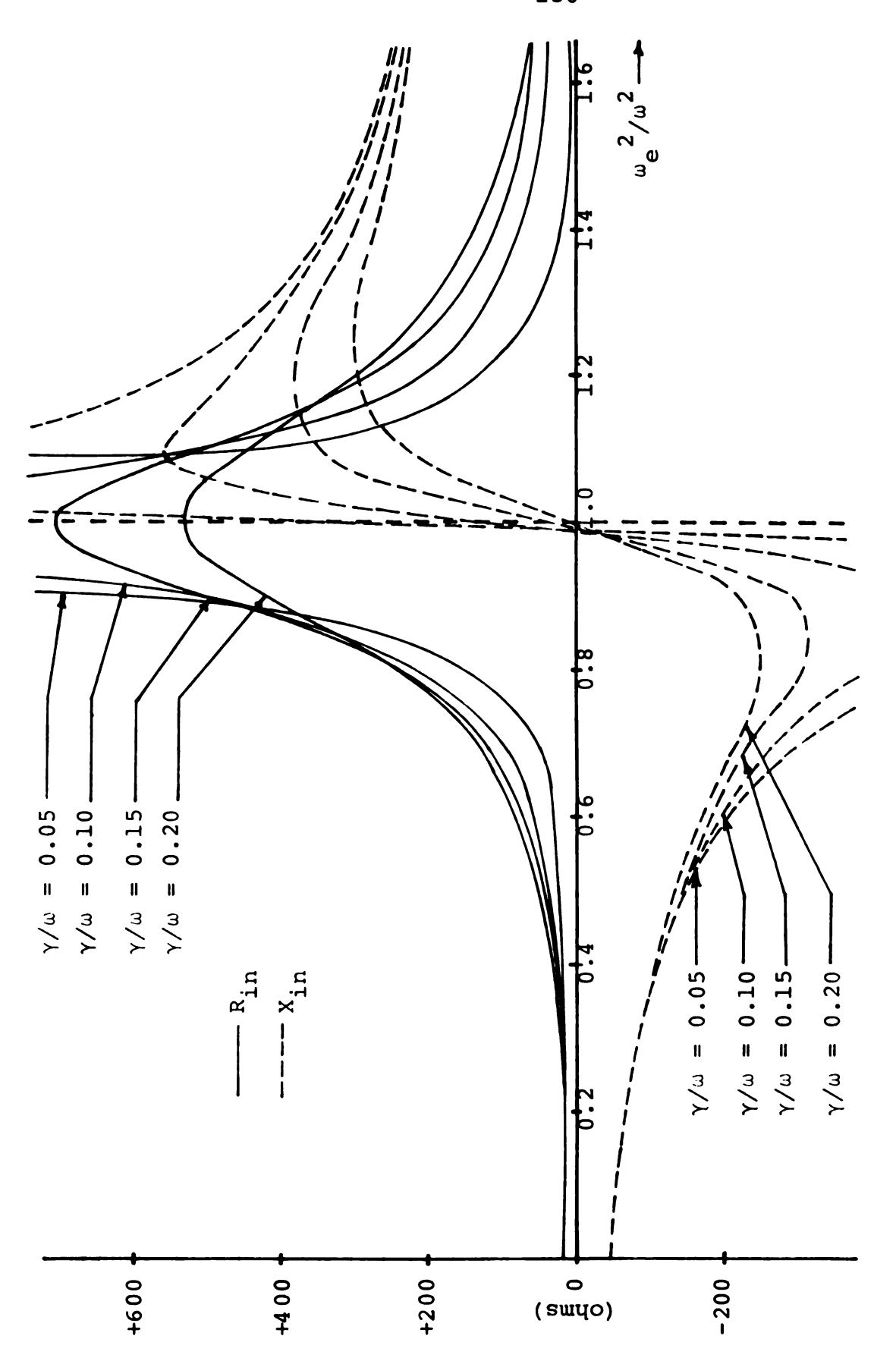


Figure 7.4. Theoretical input impedance of a monopole $(h/\lambda_O=0.192,~a/\lambda_O=0.0072)$ in a hot $(V_{\rm e}/C=0.01)$ lossy plasma as a function of plasma density.

Figure 7.5. Current distributions on a dipole with $h/\lambda_O=0.192$ and $a/\lambda_O=0.0072$ for various values of $\omega_e{}^2/\omega^2$ and γ/ω as a function of z/h.

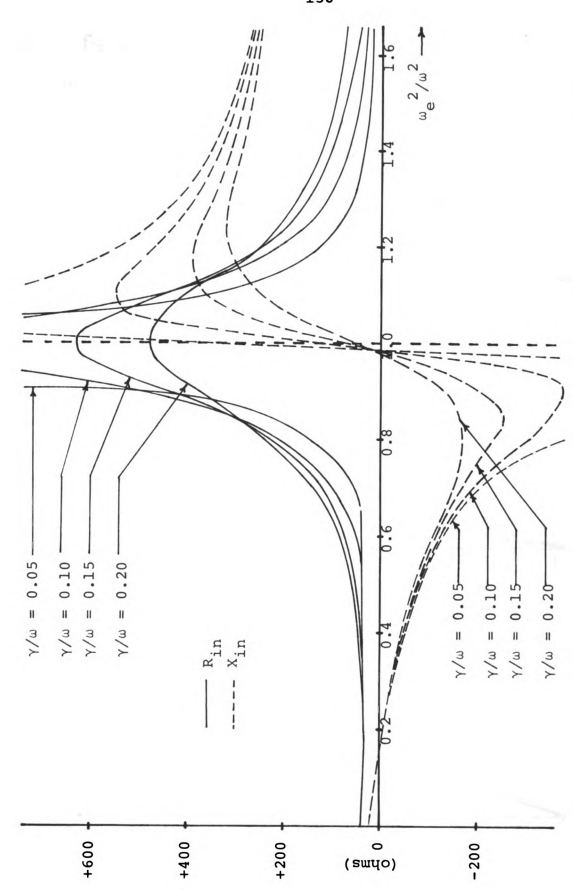


Figure 7.6. Theoretical input impedance of a monopole $(h/\lambda_0=0.251,~a/\lambda_0=0.0064)$ in a hot $(V_e/C=0.01)$ lossy plasma as a function of plasma density.

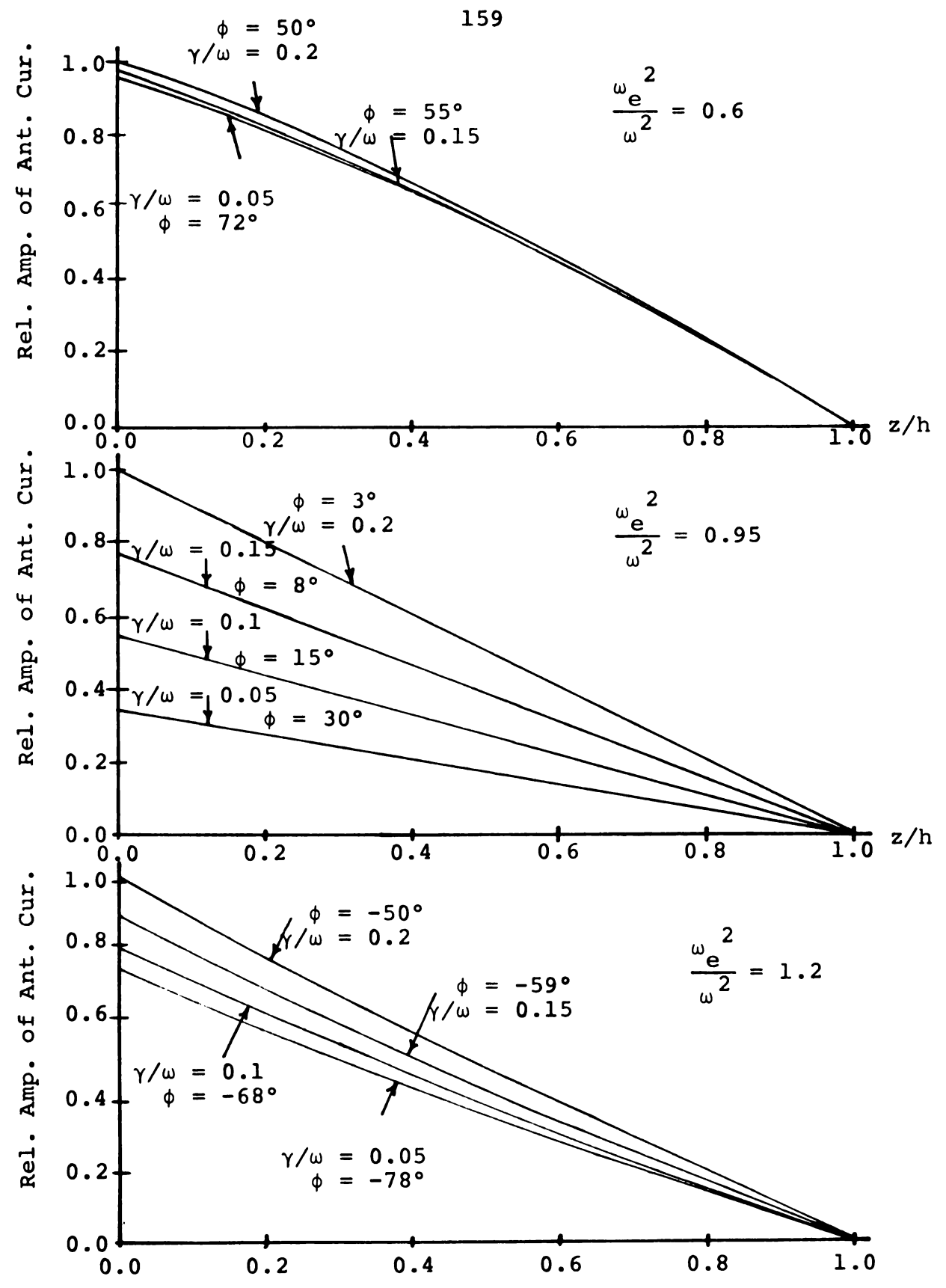
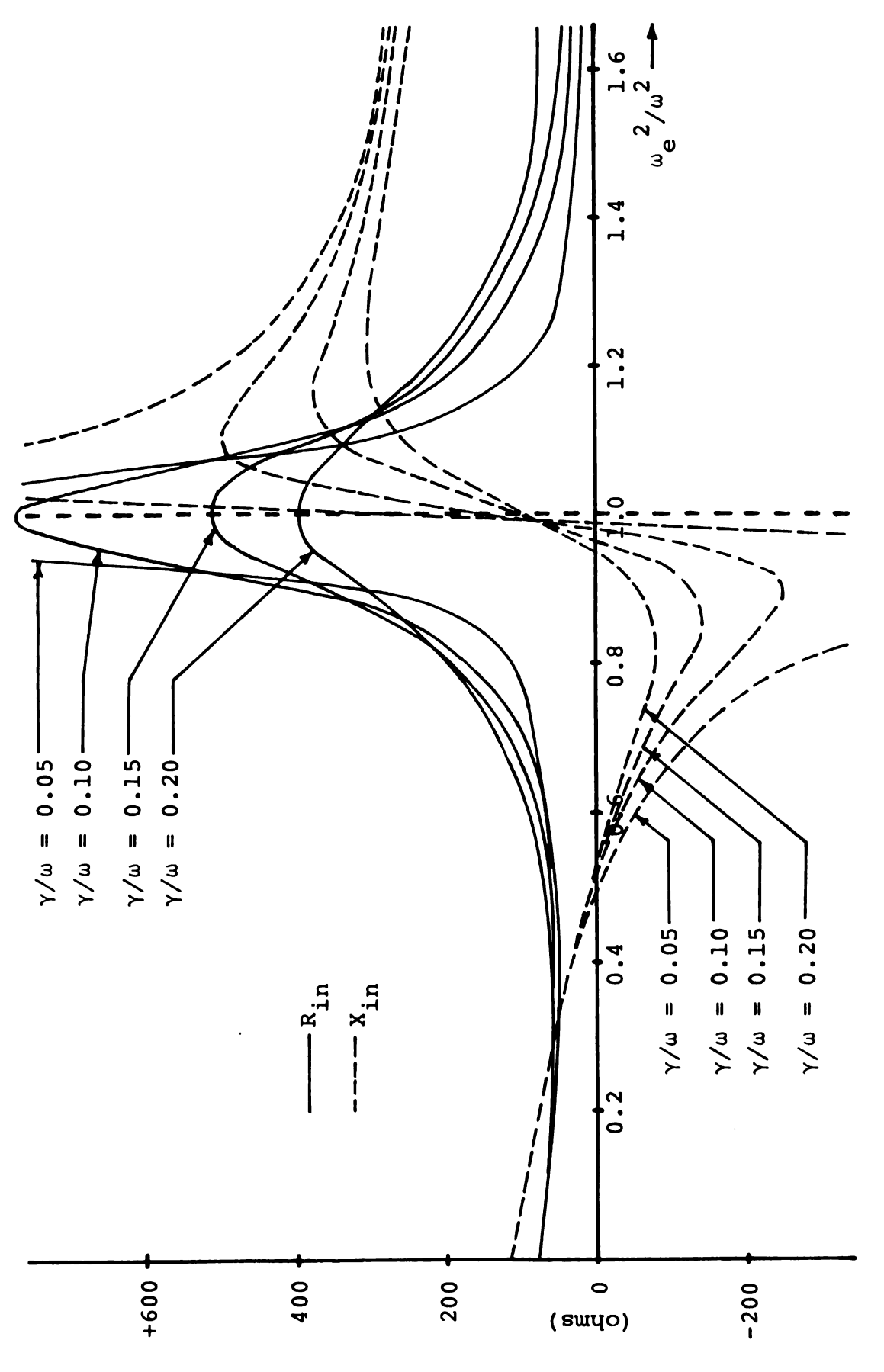


Figure 7.7. Current distributions on a dipole with $h/\lambda_0=0.251$ and $a/\lambda_0=0.0064$ for various values of ω_e^2/ω^2 and γ/ω as a function of z/h.



Theoretical input impedance of a monopole $(h/\lambda_O=0.313,~a/\lambda_O=0.008)$ 01) lossy plasma as a function of plasma density. Figure 7.8. Theoretical input impedance of a in a hot ($V_e/C = 0.01$) lossy plasma as a function of

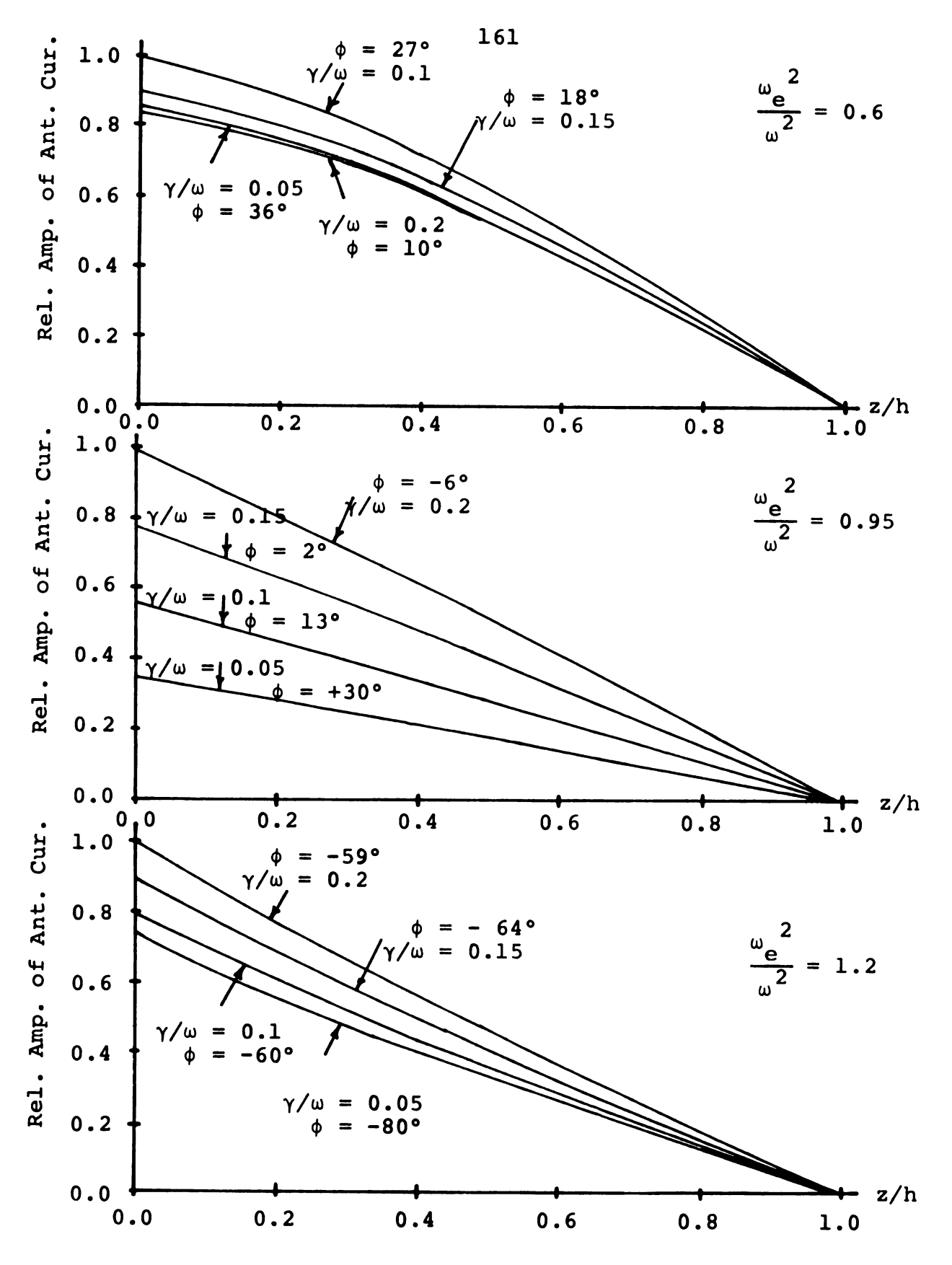
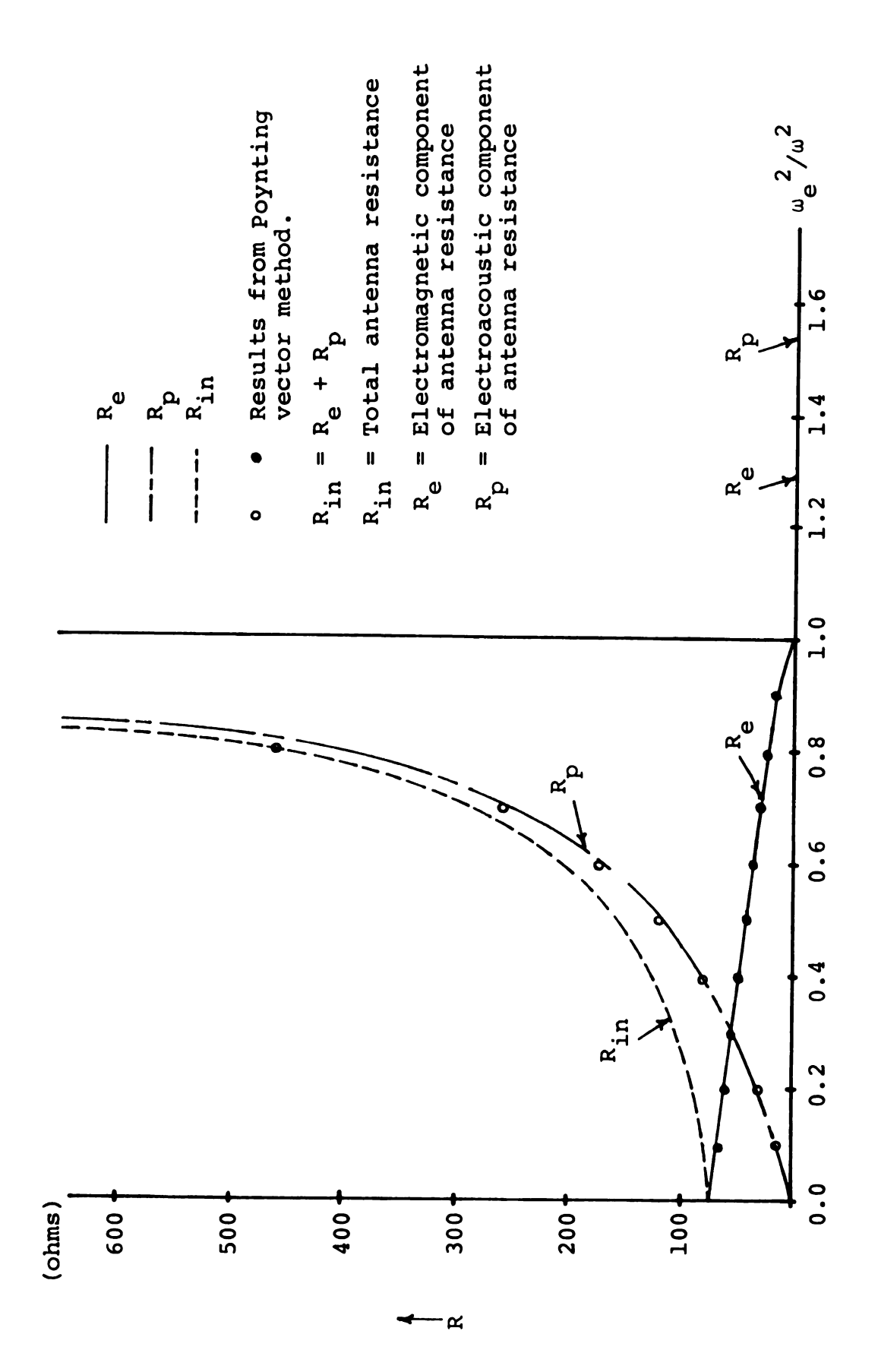


Figure 7.9. Current distributions for a dipole with $h/\lambda_0=0.313$ and $a/\lambda_0=0.008$ for various values of ω_e^{2/ω^2} and γ/ω as a function of z/h.



Antenna resistance of a cylindrical antenna (half length = 0.25 λ_{o} , in a hot (Ve/C = 0.01) lossless plasma as a function of plasma Figure 7.10. radius = 0.001 $\lambda_{\rm O}$) density.

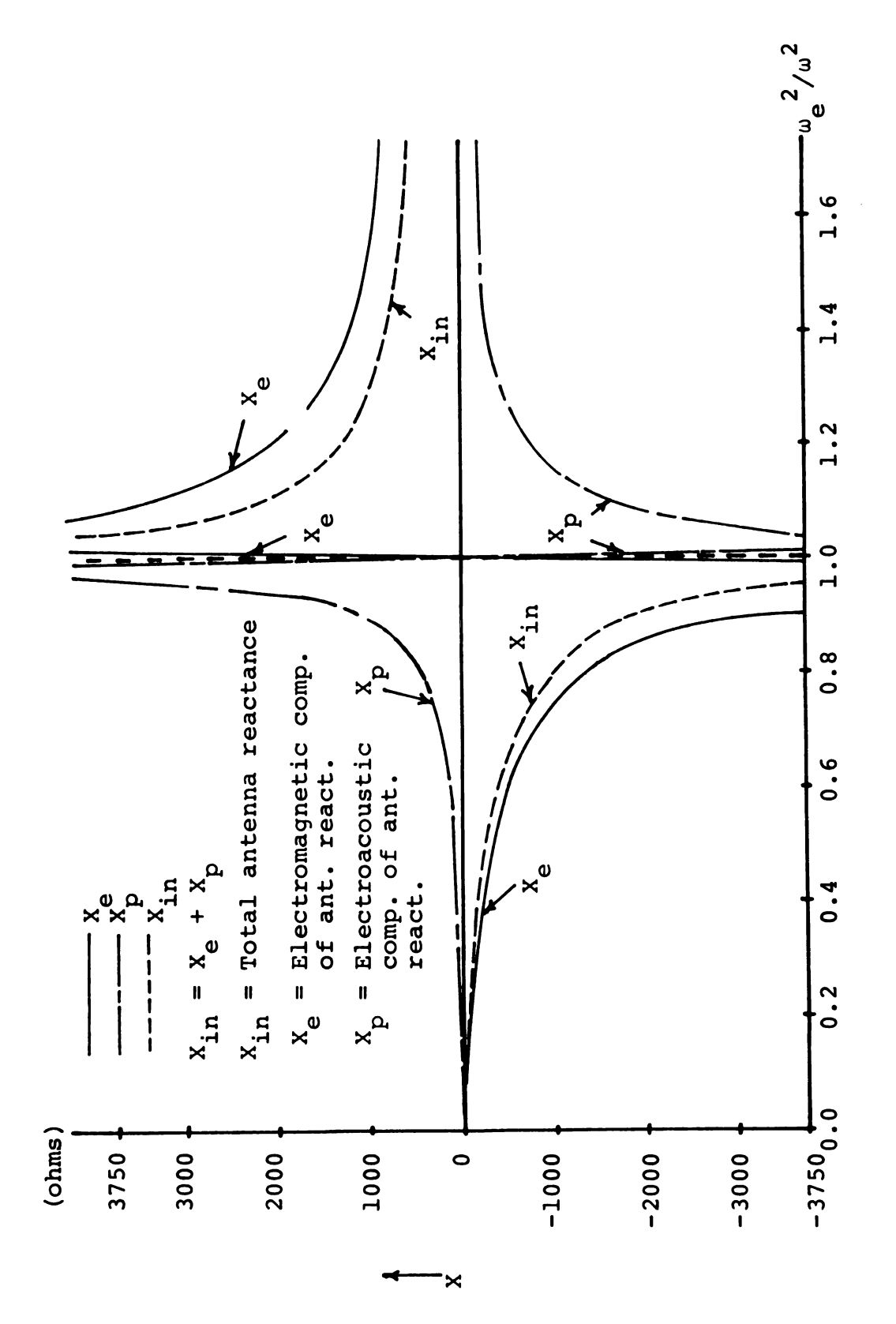


Figure 7.11. Antenna reactance of a cylindrical antenna (half length = 0.25 λ_0 , radius = 0.001 λ_0) in a hot (V_e/C = 0.01) lossless plasma as a function of plasma density.

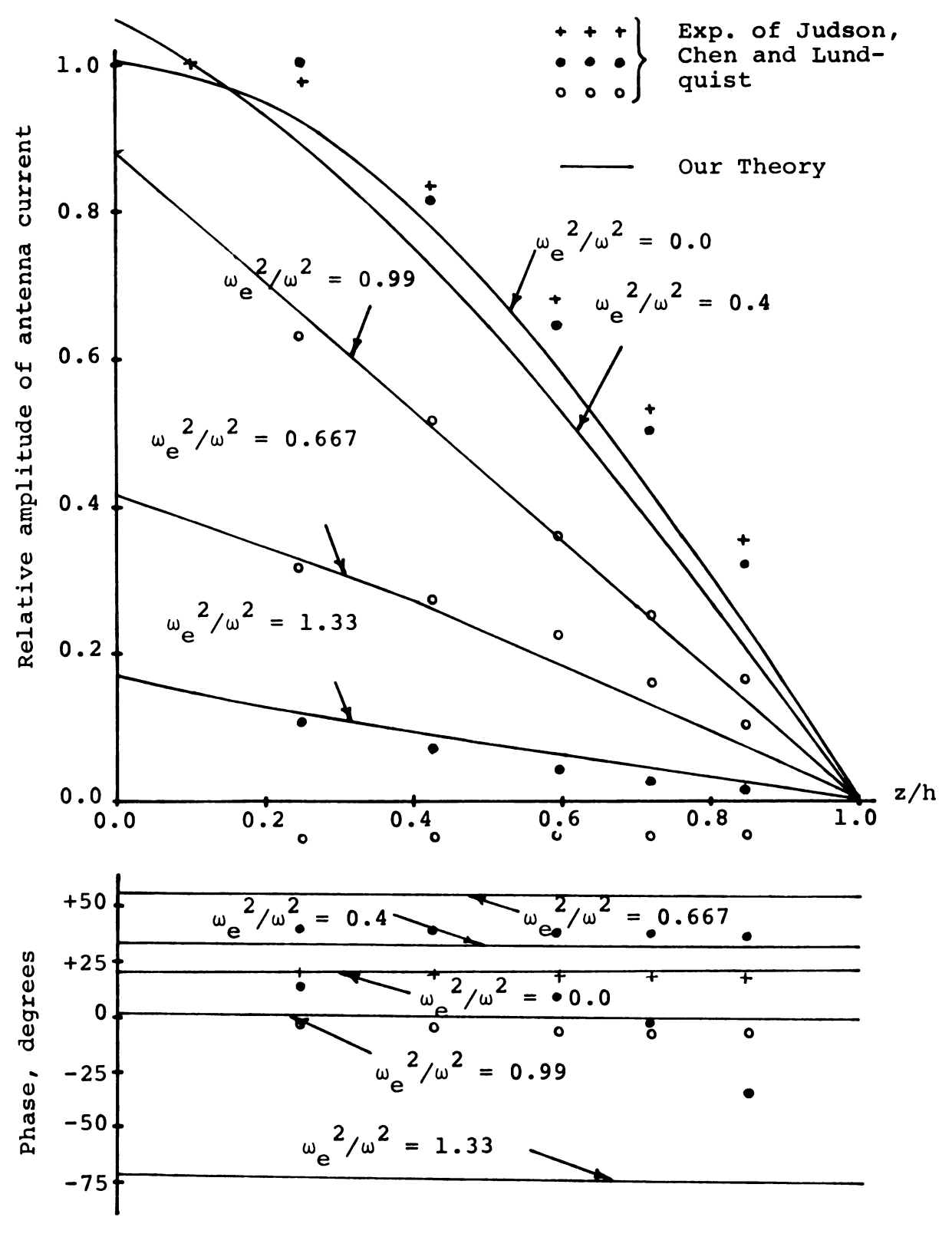


Figure 7.12. Comparison of theoretical and experimental current distributions on a monopole with β oh = 1.54 and a = 0.615 cm for various values of ω_e^2/ω^2 . The driving frequency in the experiment was 1.25 GHZ.

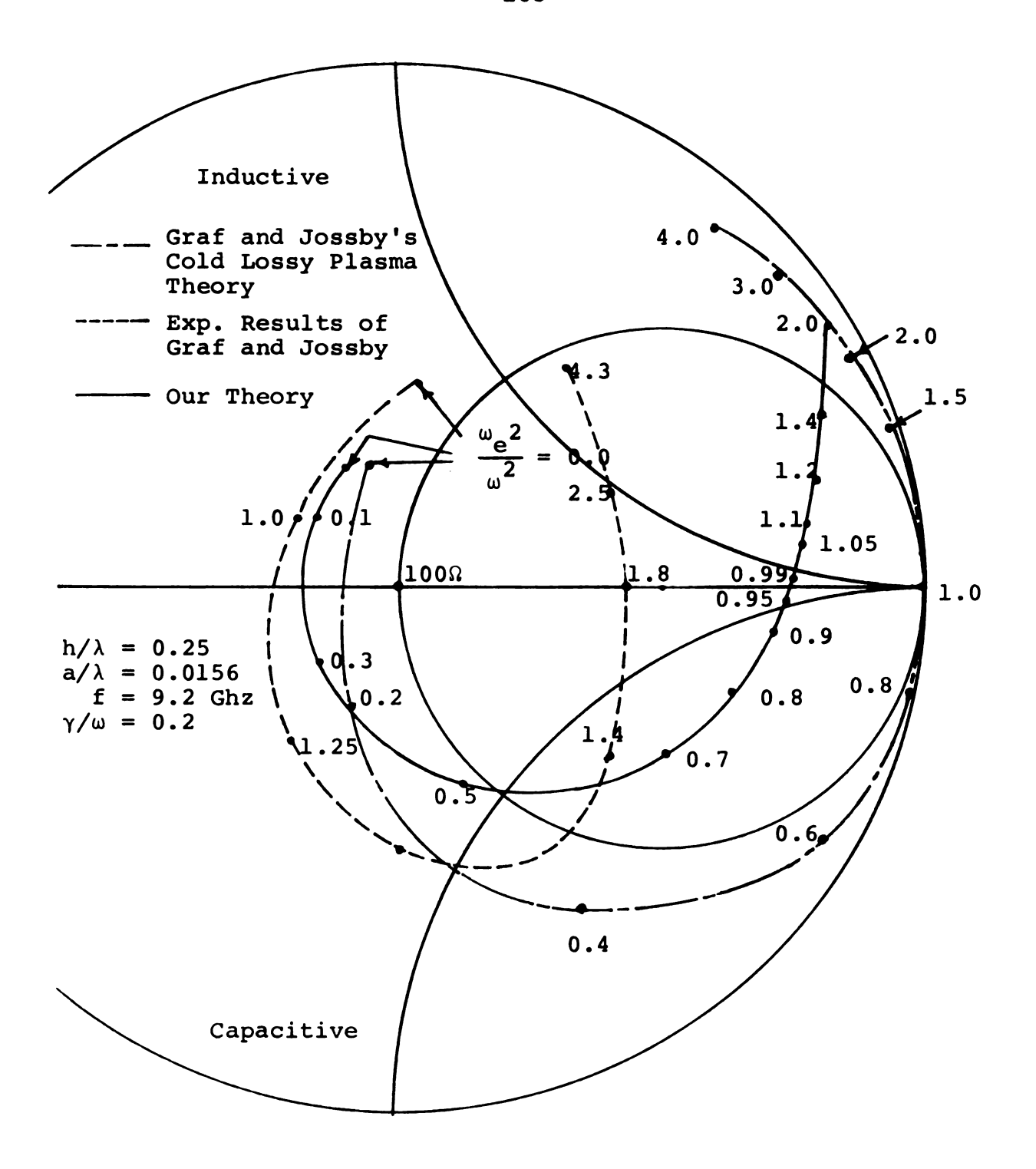


Figure 7.13. Input impedance of a dipole of half length $h/\lambda_0=0.25$ normalized to 100Ω . Normalized electron density $(\omega_e^{\ 2}/\omega^2)$ values are indicated.

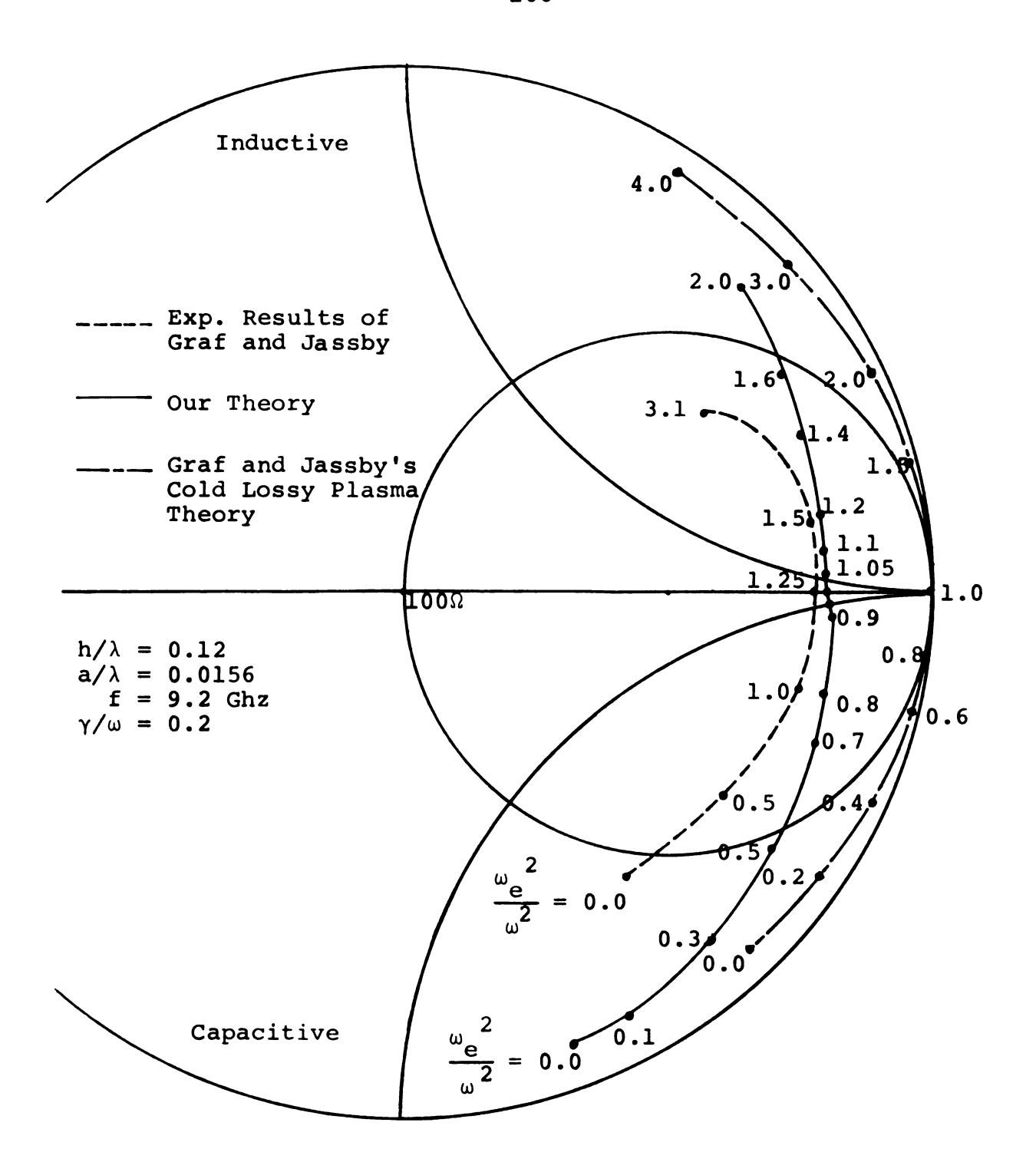


Figure 7.14. Input impedance of a dipole of half length $h/\lambda_0 = 0.12$ normalized to 100Ω . Normalized electron density (ω_e^2/ω^2) values are indicated.

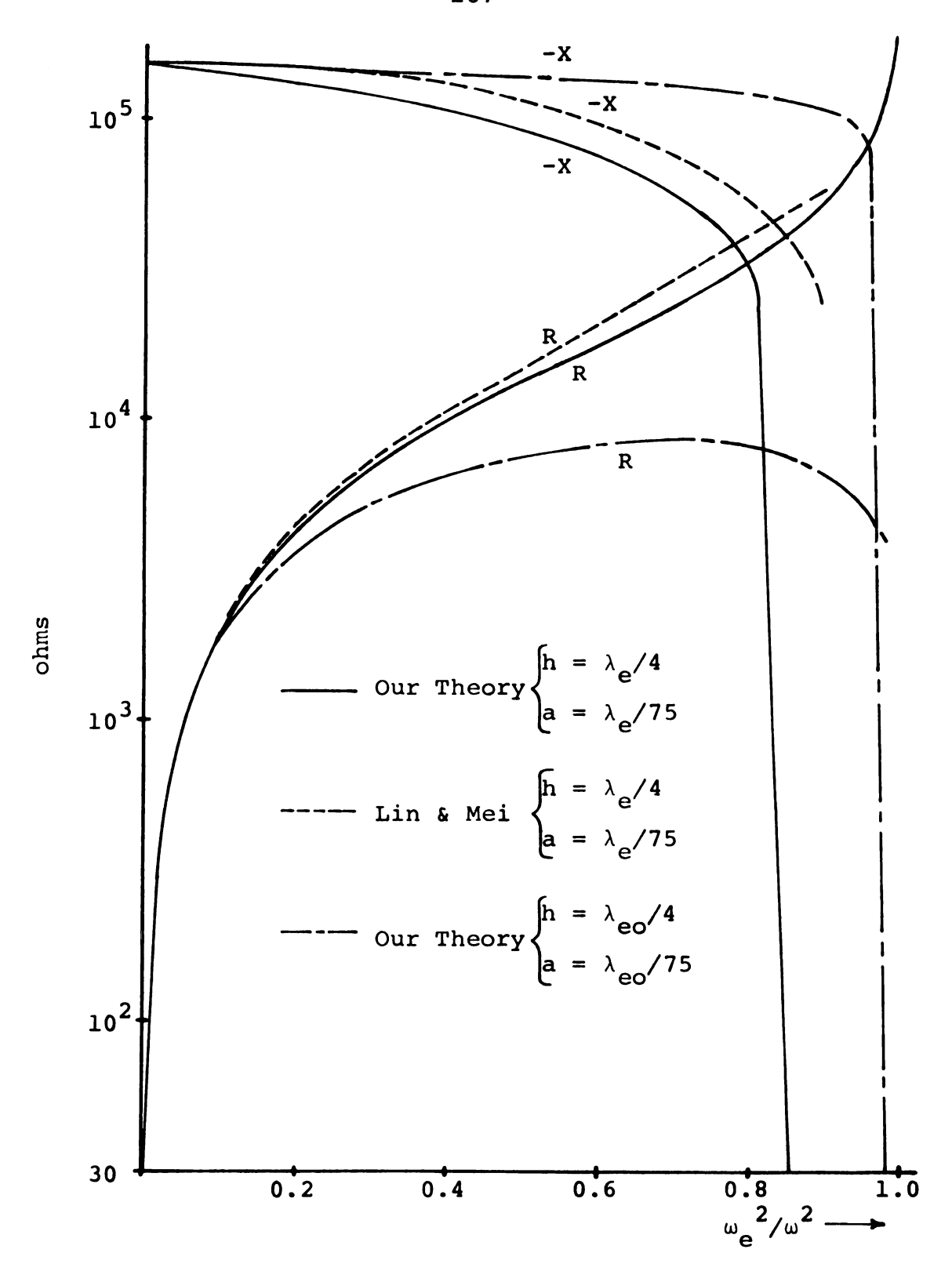


Figure 7.15. Input impedance of a short dipole antenna in a hot ($V_{\rm e}/C$ = 0.001) lossless plasma as a function of plasma density.

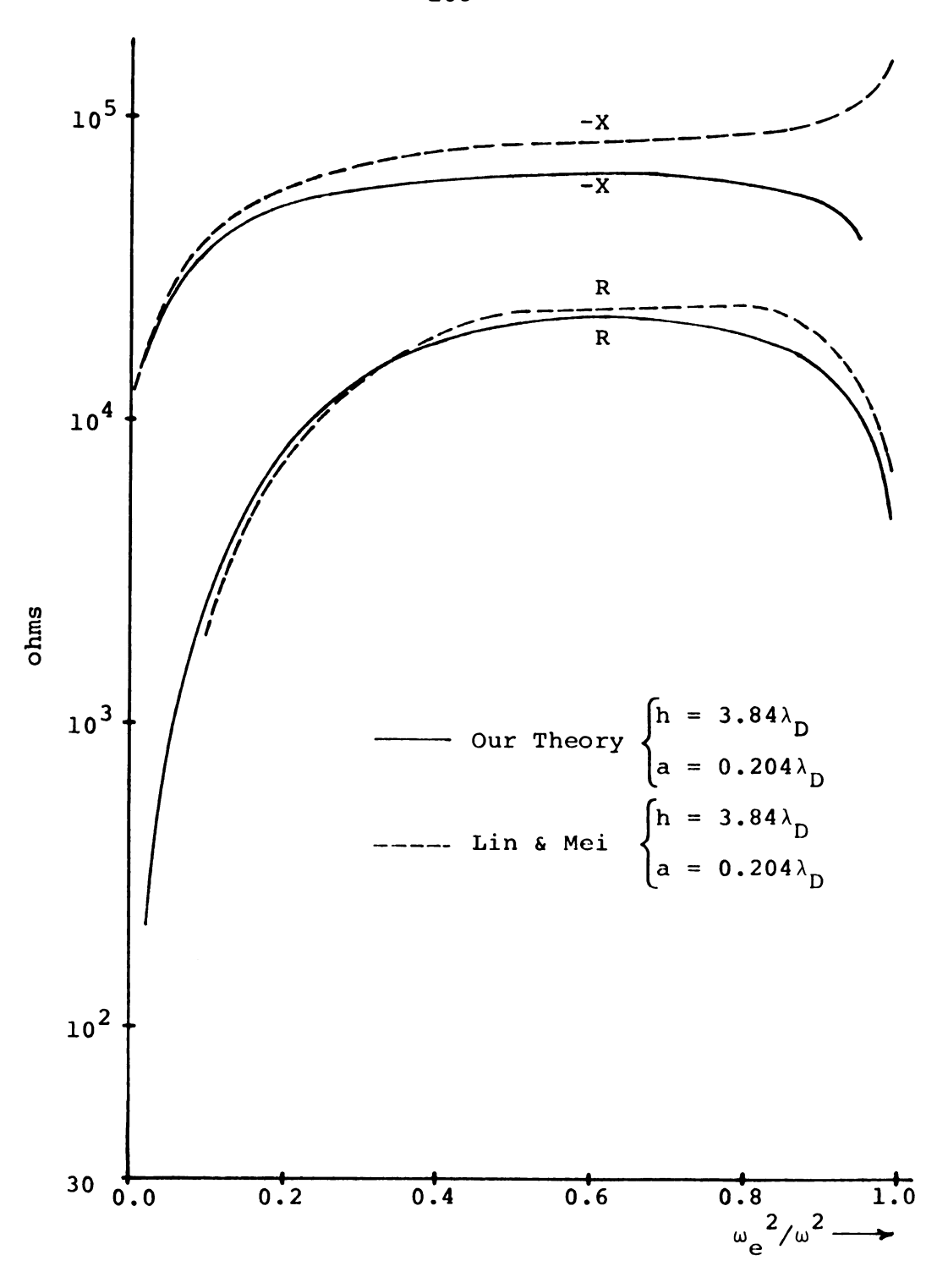


Figure 7.16. Input impedance of a short dipole antenna in a hot ($V_{\rm e}/C$ = 0.001) lossless plasma as a function of plasma density.

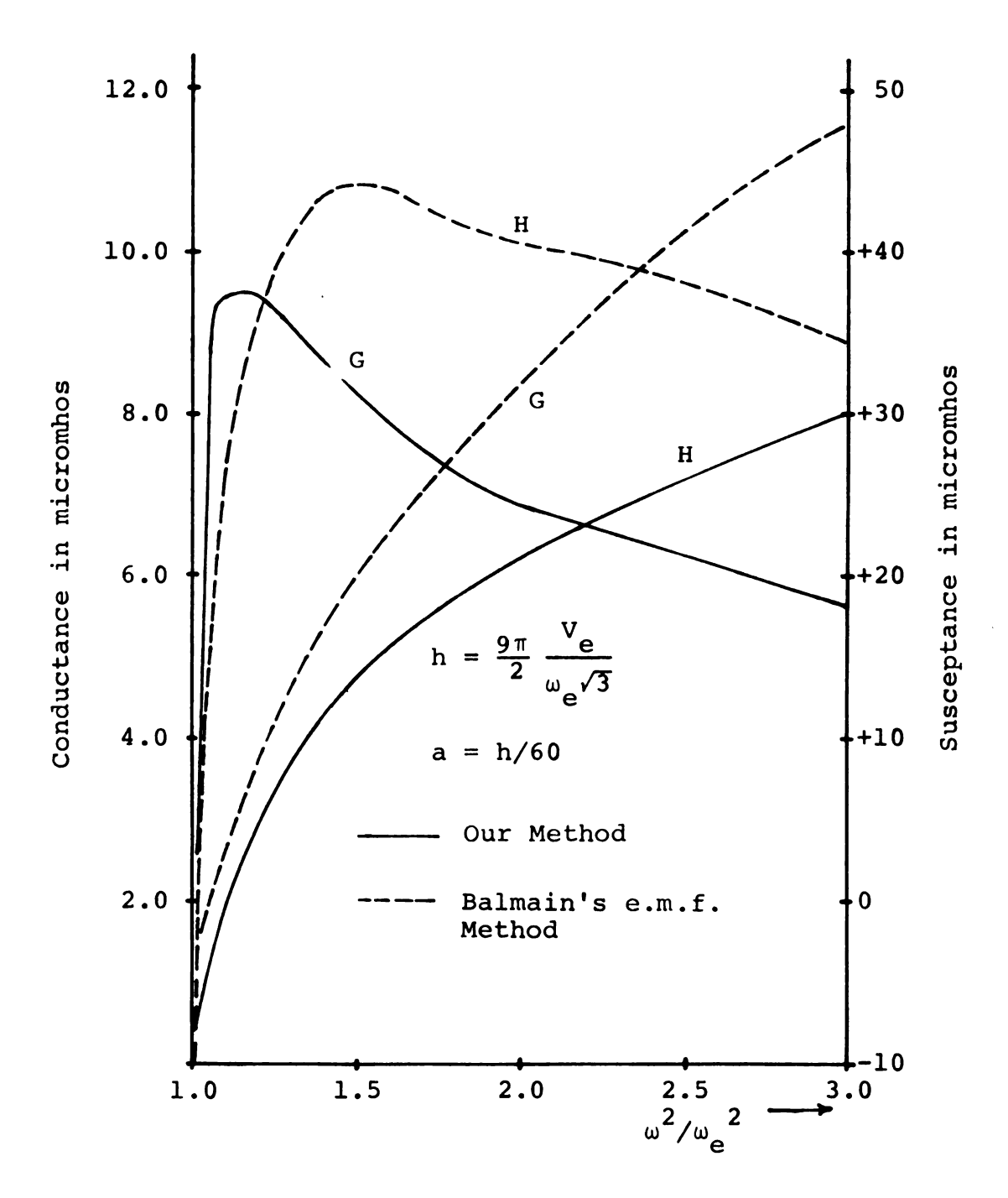


Figure 7.17. Input admittance (y = G + jH) of a dipole antenna in a hot ($V_{\rm e}/C$ = 0.001) lossless plasma as a function of the plasma density.

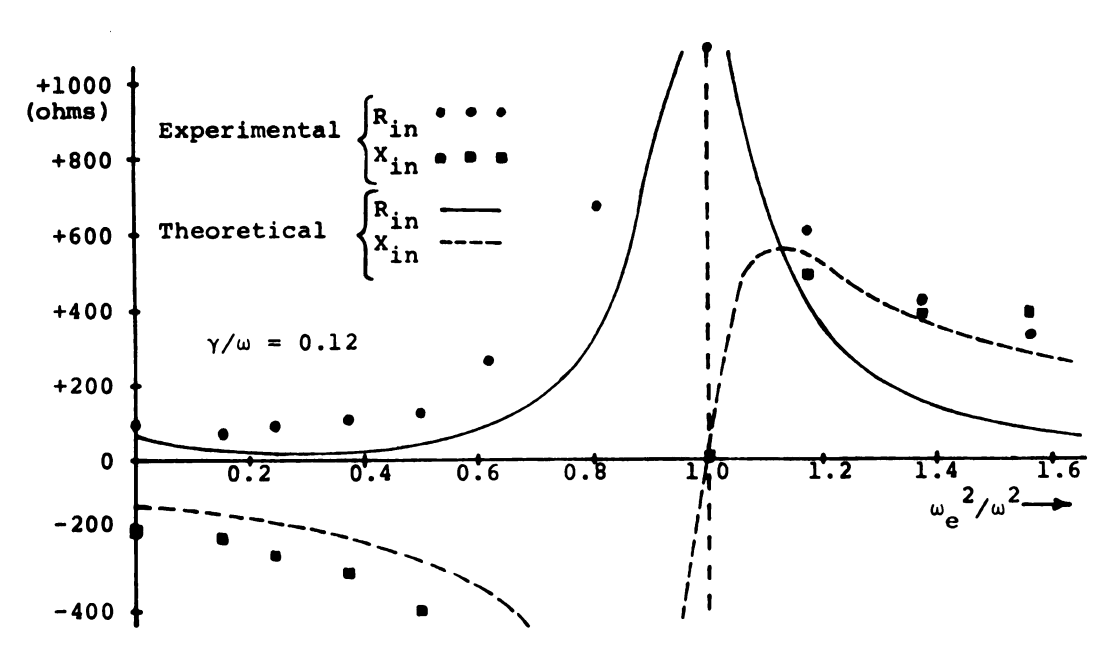


Figure 7.18. Experimental and theoretical input impedance of a monopole (h/ λ_0 = 0.117, a/ λ_0 = 0.0064) in a hot lossy plasma as a function of plasma density.

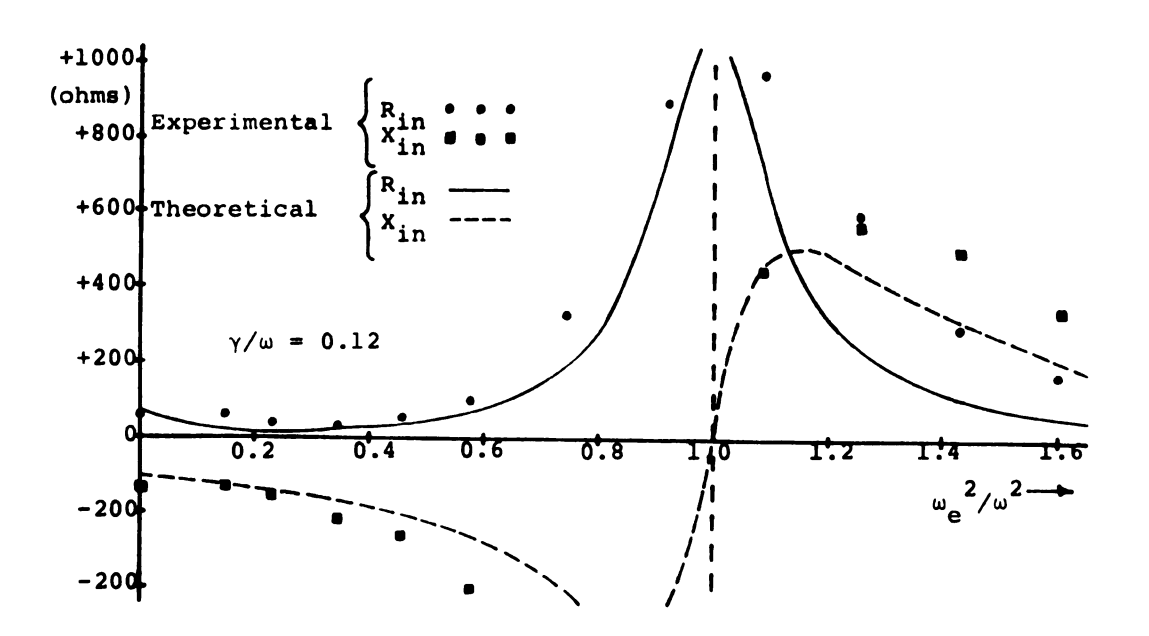


Figure 7.19. Experimental and theoretical input impedance of a monopole ($h/\lambda_0=0.132$, $a/\lambda_0=0.0072$) in a hot lossy plasma as a function of plasma density.

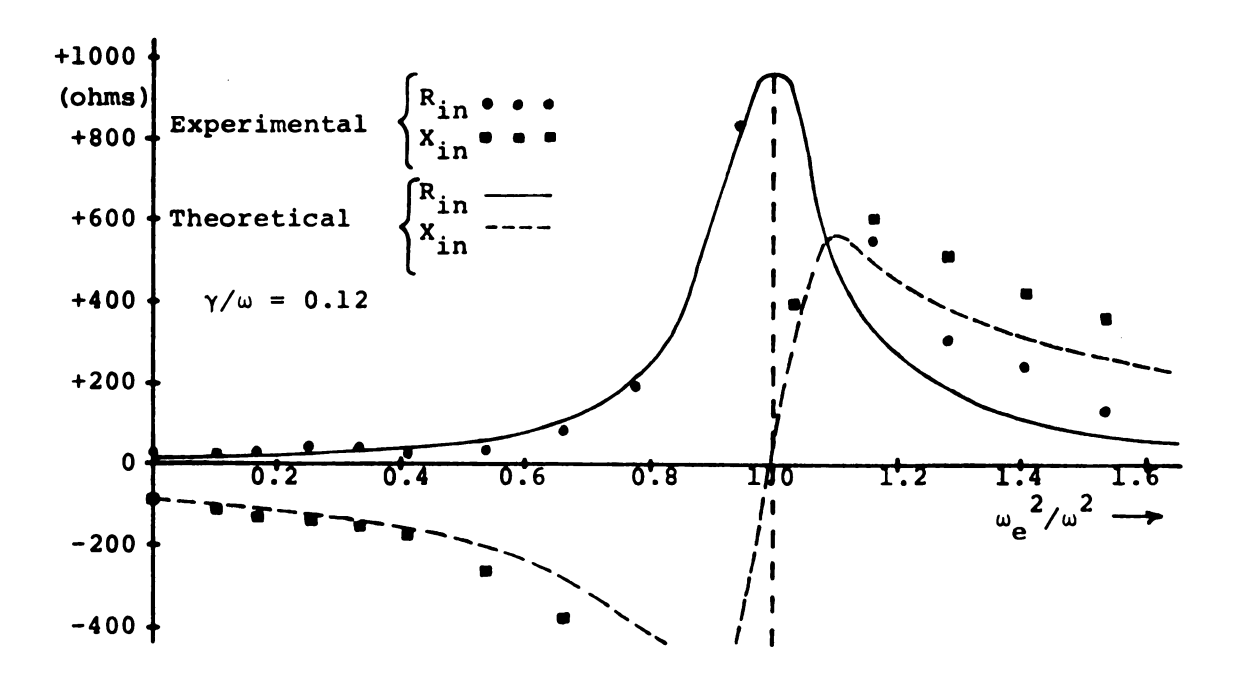


Figure 7.20. Experimental and theoretical input impedance of a monopole (h/ $\lambda_{\rm O}$ = 0.147, a/ $\lambda_{\rm O}$ = 0.008) in a hot lossy plasma as a function of plasma density.

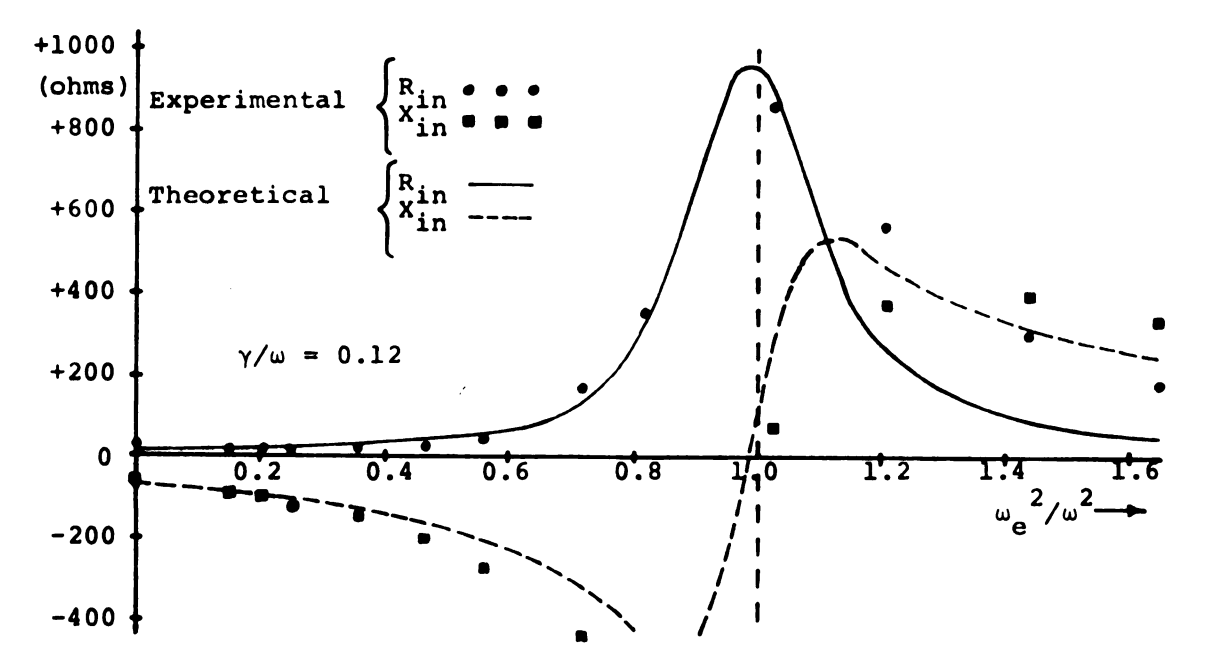


Figure 7.21. Experimental and theoretical input impedance of a monopole ($h/\lambda_0 = 0.171$, $a/\lambda_0 = 0.0064$) in a hot lossy plasma as a function of plasma density.

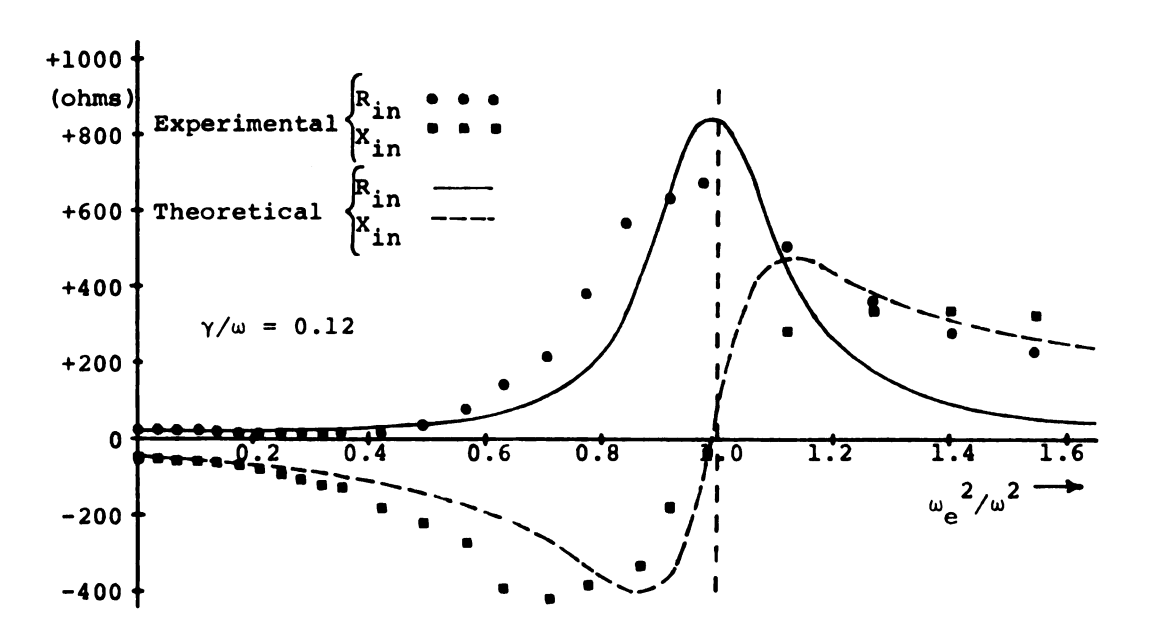


Figure 7.22. Experimental and theoretical input impedance of a monopole ($h/\lambda_0=0.192$, $a/\lambda_0=0.0072$) in a hot lossy plasma as a function of plasma density.

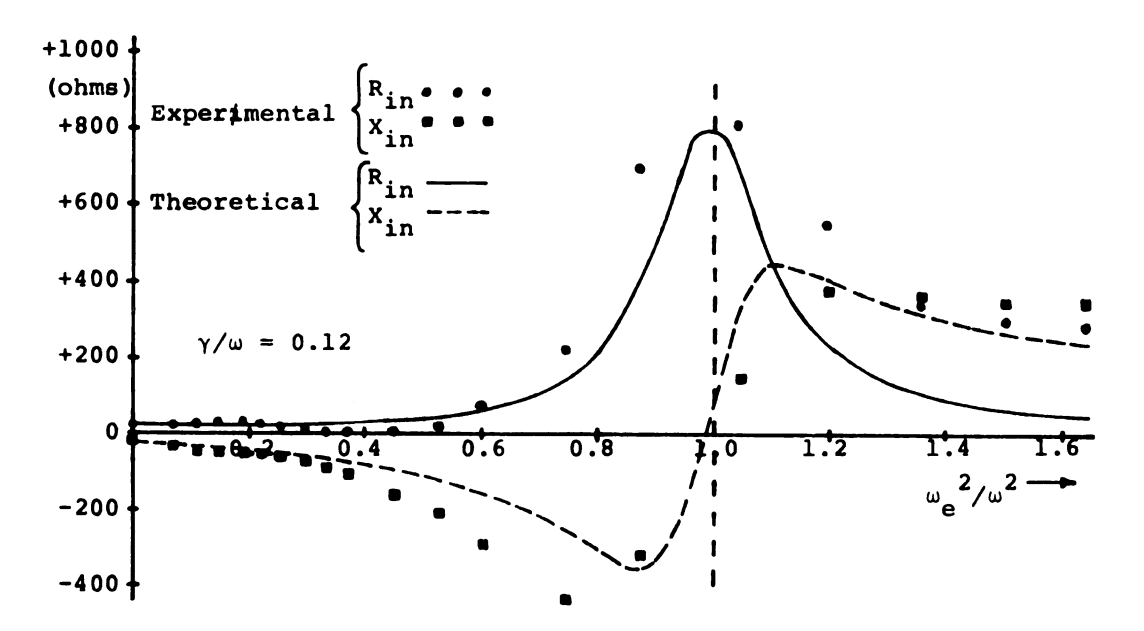


Figure 7.23. Experimental and theoretical input impedance of a monopole ($h/\lambda_0 = 0.213$, $a/\lambda_0 = 0.008$) in a lossy hot plasma as a function of plasma density.

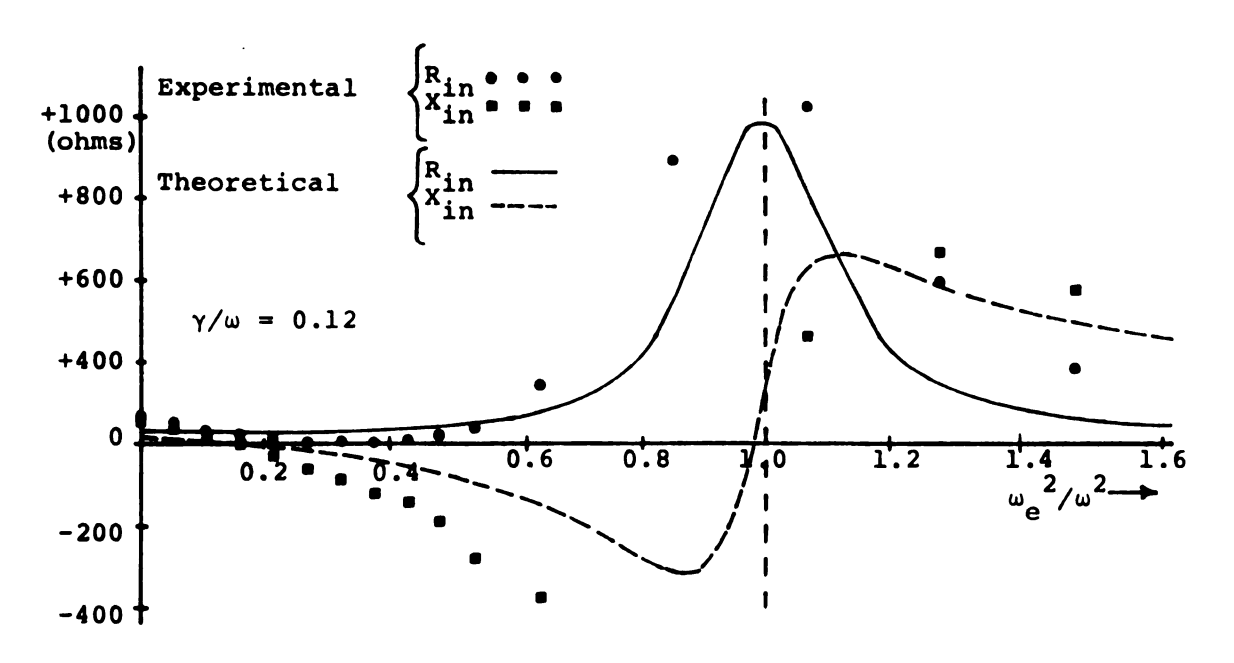


Figure 7.24. Experimental and theoretical input impedance of a monopole (h/ λ_0 = 0.251, a/ λ_0 = 0.0064) in a hot lossy plasma as a function of plasma density.

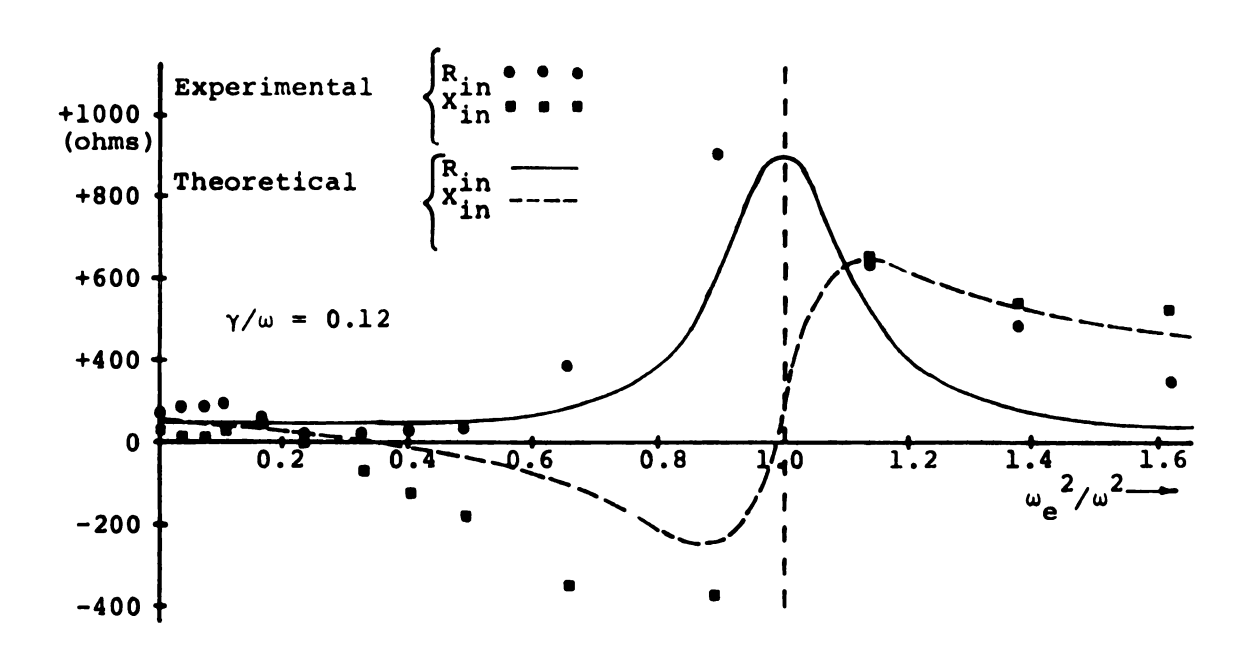


Figure 7.25. Experimental and theoretical input impedance of a monopole ($h/\lambda_0 = 0.282$, $a/\lambda_0 = 0.0072$) in a hot lossy plasma as a function of plasma density.

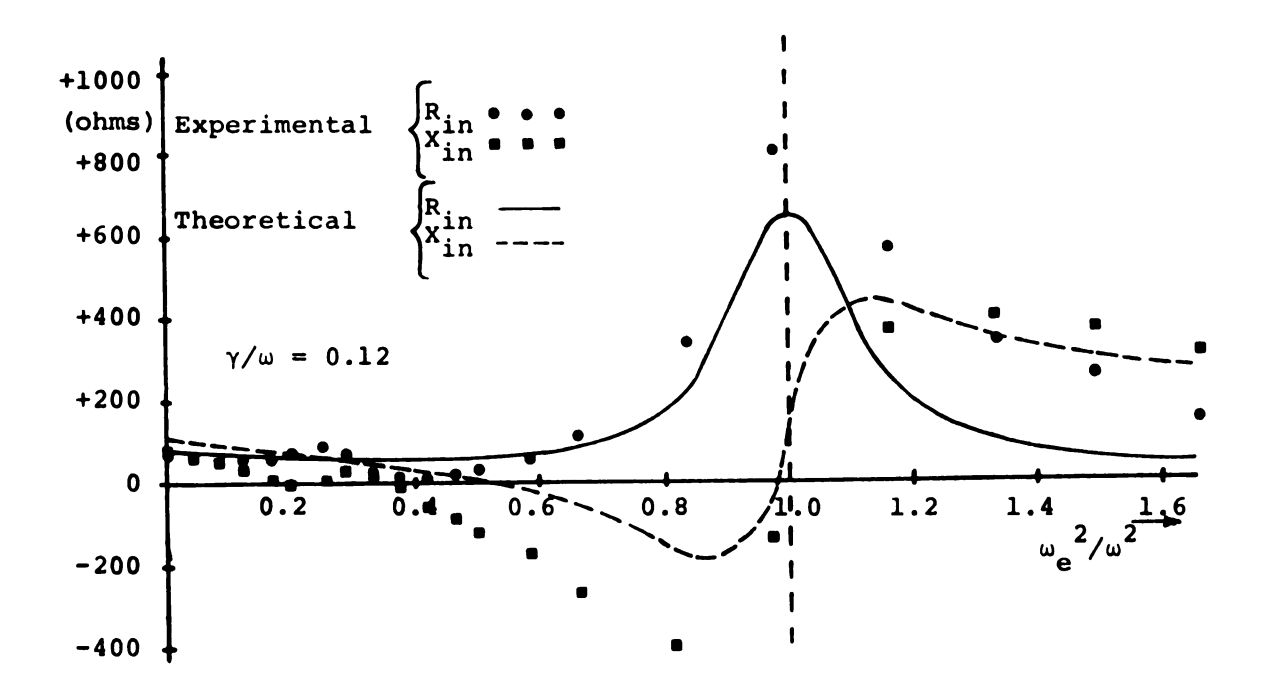


Figure 7.26. Experimental and Theoretical input impedance of a monopole (h/ λ_0 = 0.313, a/ λ_0 = 0.008) in a hot lossy plasma as a function of plasma density.

REFERENCES

REFERENCES

- 1. A. M. Messiaen and P. E. Vandenplas, "Theory and Experiments of the Enhanced Radiation from a Plasma-Coated Antenna," <u>Electronics Letters</u>, Vol. 3, 26, (1967).
- 2. C. C. Lin, "Radiation of Spherical and Cylindrical Antennas in Imcompressible and Compressible Plasmas," Ph.D. Thesis, Michigan State University, (1969).
- 3. C. C. Lin and K. M. Chen, "Effect of Electroacoustic Wave on the Radiation of a Plasma Coated Spherical Antenna," IEEE Trans GAP, Vol. AP-18, No. 6, 831, (1970).
- 4. L. Tonks and I. Langmuir, "Oscillations in Ionized Gases," Physical Review, Vol. 33, 195, (1929).
- 5. R. W. Revans, "The Transmission of Waves Through an Ionized Gas," Physical Review, Vol. 44, 798, (1933).
- 6. P. J. Barret and P. F. Little, "Externally Excited Waves in Low-Pressure Plasma Columns," Physical Review Letters, Vol. 14, 356, (1965).
- 7. I. Alexeff, W. D. Jones, and K. Lonngren, "Excitation of Pseudowaves in a Plasma Via a Grid," <u>Physical Review Letters</u>, Vol. 21, 878, (1968).
- 8. K. R. Cook and R. B. Buchanan, "Radiation Characteristics of a Slotted Ground Plane into a Two Fluid Compressible Plasma," Proc. of the Conf. on Environmental Effects on Antenna Performance, 122, (1969).
- 9. T. H. Stix, <u>Theory of Plasma Waves</u>, McGraw-Hill, Chapter 7, (1962).
- 10. R. A. Tanenbaum, <u>Plasma Physics</u>, McGraw-Hill, 169, (1967).

- 11. L. Oster, "Linearized Theory of Plasma Oscillations," Reviews of Modern Physics, Vol. 32, 141, (1960).
- 12. J. R. Wait, "Theory of a Slotted-Sphere Antenna Immersed in a Compressible Plasma, Part II," Radio Sci. J. Res. NBS 68D, No. 10, 1137, (1964b).
- 13. Ramo, Whinnery, and Van Duzer, <u>Fields and Waves in Communications Electronics</u>, John Wiley and Sons, Inc., 701, (1965).
- 14. L. Infeld, "The Influence of the Width of the Gap Upon the Theory of Antennas," Quart. Appl. Math, Vol. 5, 113, (1947).
- 15. M. Abramowitz and I. A. Stigun, <u>Handbook of Mathematical Functions</u>, Dover, Chapter 10, (1968).
- 16. M. Abramowitz and I. A. Stigun, <u>Handbook of</u>
 <u>Mathematical Functions</u>, Dover, Chapter 8, (1968).
- 17. G. Forsythe and C. B. Moles, <u>Computer Solution of Linear Algebraic Systems</u>, Prentice-Hall, Chapters 9 and 17, (1967).
- 18. A. Hessel and J. Shmoys, "Excitation of Plasma Waves by a Dipole in a Homogeneous Isotropic Plasma,"

 Proc. of the Symposium on Electromagnetics and Fluid Dynamics of Gaseous Plasmas, Interscience, 173, (1961).
- 19. S. R. Seshadri, "Radiation from Electromagnetic Sources in a Plasma," IEEE PGAP, Vol. 13, 79, (1965).
- 20. Marshall H. Cohen, "Radiation in a Plasma, III, Metal Boundaries," Phys. Rev., Vol. 126, 398, (1962).
- 21. James R. Wait, "On Radiation of Electromagnetic and Electroacoustic Waves in a Plasma," Appl. Sci. Res., Sect. B, Vol. 11, 423, (1965).
- 22. James R. Wait, "On Radiation of Electromagnetic and Electroacoustic Waves in a Plasma, Part II," Appl. Sci. Res., Sect. B, Vol. 12, 130, (1965).
- 23. Kun-Mu Chen, "Interaction of a Radiating Source with a Plasma," Proc. IEE, Vol. 11, 1668, (1964).
- 24. K. R. Cook and B. C. Edgar, "Current Distribution and Impedance of a Cylindrical Antenna in an Istropic Compressible Plasma," Radio Science, Vol. 1, 13, (1966).

- 25. H. H. Kuehl, "Resistance of a Short Antenna in a Warm Plasma," Radio Science, Vol. 1, 971, (1966).
- 26. H. H. Kuehl, "Computations of the Resistance of a Short Antenna in a Warm Plasma," Radio Science, Vol. 2, 73, (1967).
- 27. James R. Wait, "Theories of Prolate Spheroidal Antennas," Radio Science, Vol. 1, 475, (1966).
- 28. R. W. P. King, C. W. Harrison, Jr., and D. H. Denton, Jr., "The Electrically Short Antenna as a Probe for Measuring Free Electron Densities and Collision Frequencies in an Ionized Region," <u>Journ. Of Res. of NBS</u>, Sect. D., Radio Prop., Vol. 65, 371, (1961).
- 29. R. W. P. King, "Dipoles in Dissipative Media," <u>Electromagnetic Waves</u>, edited by R. E. Langer, University of Wisconsin Press, 199, (1961).
- 30. James R. Wait, "Theory of a Slotted-Sphere Antenna Immersed in a Compressible Plasma, Part I," Radio Science, Vol. 68D, 1127, (1964).
- 31. A. D. Wunsch, "Current Distribution on a Dipole Antenna in a Warm Plasma," <u>Electronics Letters</u>, Vol. 3, 320, (1967).
- 32. S. R. Seshadri, "Propagation Coefficient for the Current Distribution Along a Cylindrical Antenna Immersed in a Warm Plasma," Proc. IEE, Vol. 112, 877, (1965).
- 33. K. G. Balmain, "Impedance of a Short Dipole in a Compressible Plasma," Radio Science, Vol. 69D, 559, (1965).
- 34. James R. Wait and Kenneth P. Spies, "Theory of a Slotted-Sphere Antenna Immersed in a Compressible Plasma, Part III," <u>Radio Science</u>, Vol. 1, 21, (1966).
- 35. J. Carlin and R. Mittia, "Acoustic Waves and Their Effects on Antenna Impedance," <u>Canadian Journ. of Phys.</u>, Vol. 45, 1251, (1967).
- 36. J. W. Carlin and R. Mittia, "Terminal Admittance of a Thin Biconical Antenna in an Isotropic Compressible Plasma," <u>Electronics Letters</u>, Vol. 2, 199, (1966).
- 37. S. R. Seshadri, "Radiation in a Warm Plasma from an Electric Dipole with a Cylindrical Column of Insulation," IEEE PGAP, Vol. 13, 613, (1965).

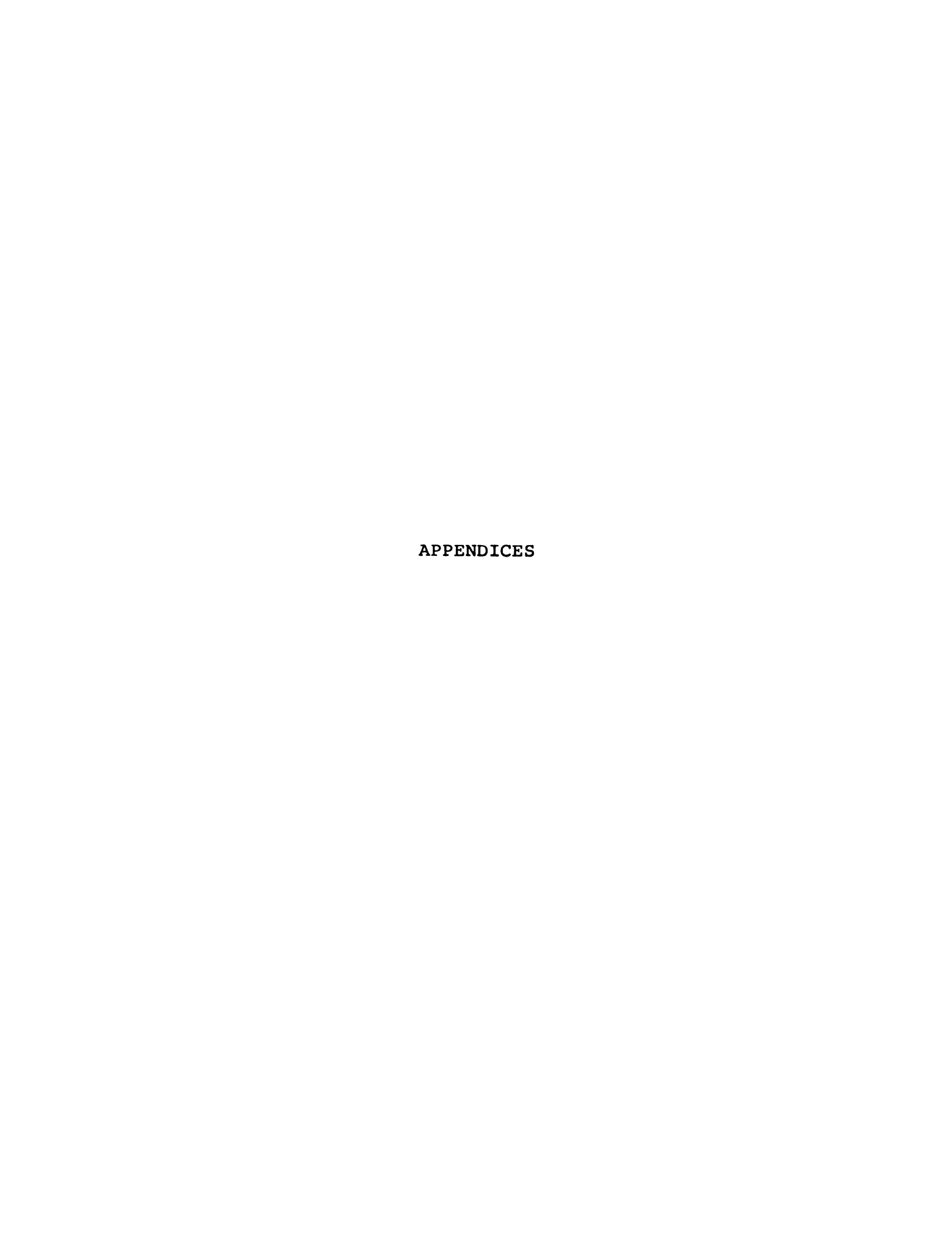
- 38. James R. Wait, "Radiation from Sources Immersed in Compressible Plasma Media," Canadian Journ. of Phys., Vol. 42, 1760, (1964).
- 39. A. Hessel, N. Marcuvitz, and J. Shmoys, "Scattering and Guided Waves at an Interfare Between Air and a Compressible Plasma," IRE PGAP, Vol. 10, 48, (1962).
- 40. Edmund K. Miller, "The Admittance of the Infinite Cylindrical Antenna in a Lossy, Isotropic, Compressible Plasma," Univ. of Mich., Col. of Eng. Rept. 05627-10-S, (1967).
- 41. Ronal W. Larson, "A Study of an Inhomogeneously Sheath Spherical-Dipole Antenna in a Compressible Plasma," Univ. of Mich., Radiation Lab. Rept. 7000-25-T, (1966).
- 42. S. Chen and C. T. Tai, "The Input Impedance of Thin Biconical Antennas Immersed in a Dissipative or an Ionized Medium," Ohio State Univ., Antenna Lab. Tech. Rept. 1021-14, (1962).
- 43. H. A. Whale, "The Excitation of Electroacoustic Waves by Antennas in the Ionosphere," J. Geophys. Res., Vol. 68, 415, (1963).
- 44. G. Meltz, P. J. Freyheit, and C. D. Lustig, "Admittance of a Plasma-Covered Cylindrical Antenna," Radio Science, Vol. 2, No. 2, 203, (1966).
- 45. J. A. Kane, J. E. Jackson, H. A. Whale, "RF Impedance Probe Measurements of Ionospheric Electron Densities," J. Res. NBS (Radio Prop.), Vol. 66D, 641, (1962).
- 46. R. G. Stone, R. R. Weber, and J. K. Alexander, "Measurement of Antenna Impedance in the Ionosphere-I. Observing Frequency Below the Electron Gyrofrequency," Planet. Space Sci., Vol. 14, 631, (1966).
- 47. K. G. Balmain, "The Impedance of a Short Dipole Antenna in a Magnetoplasma," IEEE Trans. Antennas and Propagation, Vol. AP-12, 605, (1964).
- 48. K. A. Graf and D. L. Jassby, "Measurements of Dipole Antenna Impedance in an Isotropic Laboratory Plasma,"

 <u>IEEE Trans. Antennas and Propagation</u>, Vol. AP-15,

 681, (1967).

- 49. D. L. Jassby, "Experimental Impedance of a Quarter-Wave Monopole in an Isotropic Plasma," <u>IEEE Trans</u>.

 Antennas and Propagation, Vol. AP-16, 282, (1968).
- 50. C. Ancona, "Antenna Impedance Measurements and Sheath Effects in an R.F. Generated Plasma," <u>IEEE Trans. Antennas and Propagation</u>, Vol. AP-19, 237, (1971).
- 51. H. Judson, K. M. Chen, R. Lundquist, "Measurement of the Current Distribution on Monopoles in a Large Volume of Hot Plasma," <u>Electronics Letters</u>, Vol. 4, 289, (1968).
- 52. K. M. Chen, H. Judson, and C. C. Lin, "Experimental Study of an Electroacoustic Wave Excited by an Antenna in a Hot Plasma," Proc. IEEE, Vol. 55, No. 9, 1656, (1967).
- 53. C. C. Johnson, Field and Wave Electrodynamics, McGraw-Hill, Chapter 1, (1965).
- 54. J. D. Jackson, <u>Classical Electrodynamics</u>, John Wiley and Sons, Chapters 6 and 9, (1962).
- 55. J. A. Stratton, <u>Electromagnetic Theory</u>, McGraw-Hill, Chapter 8, (1941).
- 56. S. H. Lin and K. K. Mei, "Numerical Solution of Dipole Radiation in a Compressible Plasma," IEEE Trans. Antennas and Propagation, Vol. AP-16, 235, (1968).
- 57. F. E. Hohn, Elementary Matrix Algebra, Macmillan, Chapter 8, (1964).
- 58. A. David Wunsch, "The Finite Tubular Antenna in a Warm Plasma," Radio Science, Vol. 1, 901, (1968).
- 59. H. Judson and K. M. Chen, "Measurement of Antenna Current Distribution in a Hot Plasma," <u>IEEE Proceedings</u>, Vol. 56, 753, (1968).
- 60. H. Judson and K. M. Chen, "Construction and Operating Characteristics of a Large-Volume Mercury Arc Plasma Tube," <u>IEEE Trans. Antennas and Propagation</u>, Vol. AP-16, 144, (1968).



APPENDIX A

UNCOUPLING THE DIFFERENTIAL EQUATIONS
FOR THE ELECTRONS AND THE IONS

APPENDIX A

UNCOUPLING THE DIFFERENTIAL EQUATIONS FOR THE ELECTRONS AND THE IONS

From Chapter II the differential equations to be considered are

$$\nabla^{2} \left[\frac{\mathbf{v}_{e}}{\mathbf{\omega}_{e}} \, \mathbf{n}_{e} \right] + \beta_{e}^{2} \left[\frac{\mathbf{v}_{e}}{\mathbf{\omega}_{e}} \, \mathbf{n}_{e} \right] + \frac{\mathbf{\omega}_{e}^{\omega_{\mathbf{i}}}}{\mathbf{v}_{e}^{\mathbf{v}_{\mathbf{i}}}} \left[\frac{\mathbf{v}_{\mathbf{i}}}{\mathbf{\omega}_{\mathbf{i}}} \, \mathbf{n}_{\mathbf{i}} \right] = -\frac{\mathbf{\omega}_{e}}{\mathbf{v}_{e}} \, \frac{\rho^{S}}{e}$$
(A-1)

and

$$\nabla^{2} \left[\frac{\mathbf{v_{i}}}{\omega_{i}} \; \mathbf{n_{i}} \right] + \beta_{i}^{2} \left[\frac{\mathbf{v_{i}}}{\omega_{i}} \; \mathbf{n_{i}} \right] + \frac{\omega_{e}^{\omega_{i}}}{\mathbf{v_{e}}^{v_{i}}} \left[\frac{\mathbf{v_{e}}}{\omega_{e}} \; \mathbf{n_{e}} \right] = \frac{\omega_{i}}{\mathbf{v_{i}}} \; \frac{\rho^{S}}{e}$$
(A-2)

where

$$\beta_e^2 = \frac{\omega^2}{v_e^2} \left(1 - \frac{\omega_e^2}{\omega^2} - j \frac{\gamma_e}{\omega} \right)$$
 (A-3)

$$\beta_{i}^{2} = \frac{\omega^{2}}{v_{i}^{2}} \left[1 - \frac{\omega_{i}^{2}}{\omega^{2}} - j \frac{\gamma_{i}}{\omega} \right].$$
 (A-4)

The objective of this section is to uncouple equations (A-1) and (A-2) and obtain two independent linear differential equations for the variables n_1 and n_2 which are linear combinations of n_e and n_i . This can be accomplished by using eigenvalue techniques. The uncoupled equations, the relationship between the variables n_e and n_i , and the variables n_1 and n_2 , and the high and low frequency limits of all pertinent coefficients will be developed and presented in this section.

Equations (A-1) and (A-2) can be written compactly as a matrix equation

$$\nabla^2_n + \beta_n = S_n = \frac{\rho^S}{e}$$
 (A-5)

where

$$n = \begin{bmatrix} \frac{v_e}{\omega_e} & n_e \\ \frac{v_i}{\omega_i} & n_i \end{bmatrix},$$

$$\beta = \begin{bmatrix} \beta_e^2 & \frac{\omega_e^{\omega_i}}{v_e v_i} \\ \frac{\omega_e^{\omega_i}}{v_e v_i} & \beta_i^2 \end{bmatrix},$$

and

$$S = \begin{bmatrix} -\frac{\omega_e}{v_e} \\ \frac{\omega_i}{v_i} \end{bmatrix}$$
 (A-6)

Define a new vector N such that

where T is specified to be an orthonormal transformation. The substitution of equation (A-7) into equation (A-5) gives

$$\nabla^2 \underset{\sim}{\mathbf{T}} \underset{\sim}{\mathbf{N}} + \underset{\sim}{\beta} \underset{\sim}{\mathbf{T}} \underset{\sim}{\mathbf{N}} = \underset{\sim}{\mathbf{S}} \frac{\rho^{\mathbf{S}}}{\mathbf{e}} . \tag{A-8}$$

At this point it is assumed that the determinant of T, denoted by det T, is not zero (this is verified later). Then the inverse of T, denoted by T^{-1} , is defined by

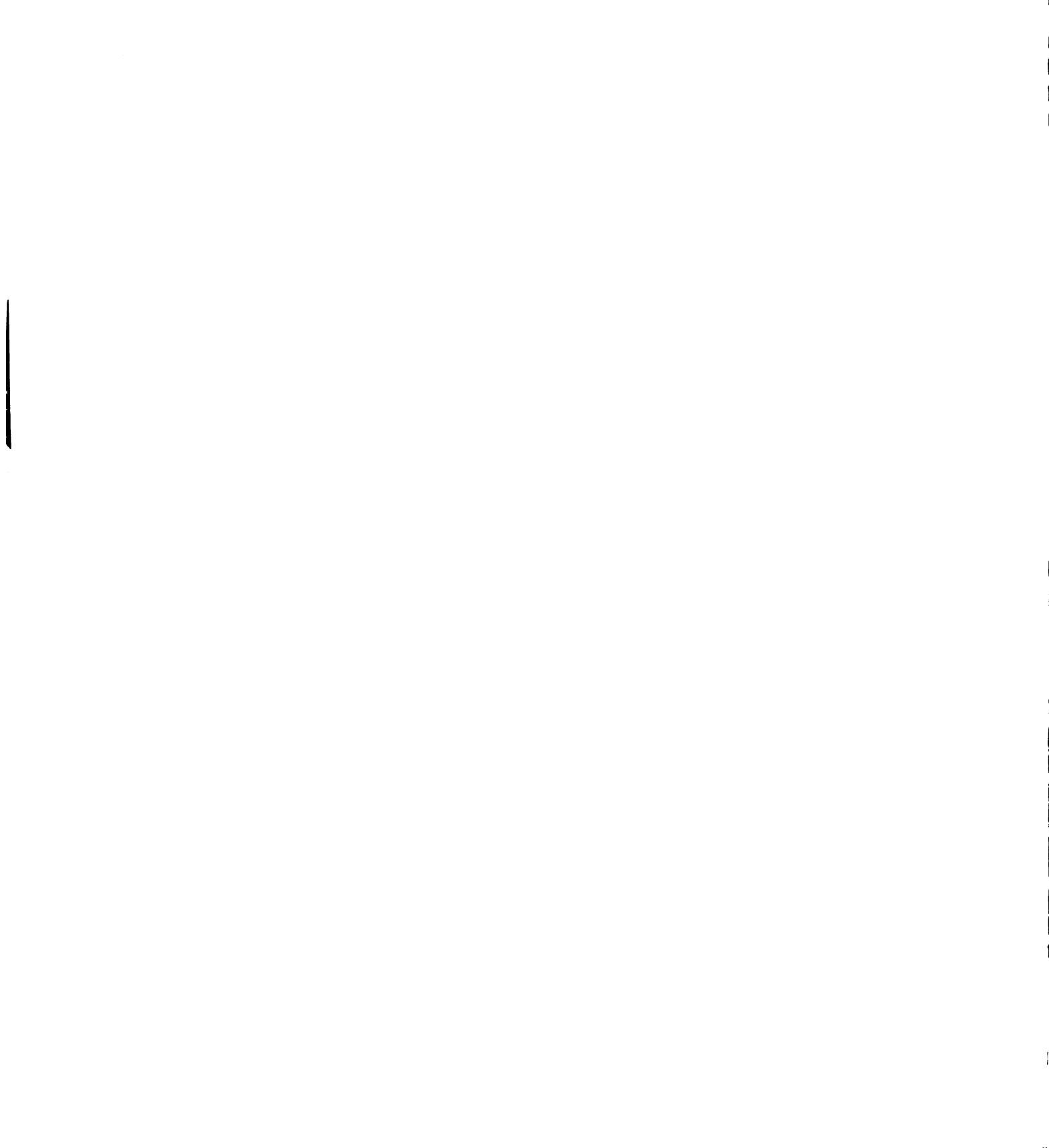
$$T_{\stackrel{\sim}{\approx}} T^{-1} = T^{-1} T_{\stackrel{\sim}{\approx}} = I_{\stackrel{\sim}{\approx}}$$
(A-9)

where I is a 2 x 2 unit matrix. Premultiplying equation (A-8) by T^{-1} gives

$$\mathbf{T}^{-1} \quad \nabla^2 \quad \mathbf{T} \quad \mathbf{N} \quad + \quad \mathbf{T}^{-1} \quad \mathbf{S} \quad \mathbf{T} \quad \mathbf{N} \quad = \quad \mathbf{T}^{-1} \quad \mathbf{S} \quad \frac{\mathbf{o}^{\mathbf{S}}}{\mathbf{e}} \quad . \tag{A-10}$$

Assuming that $\underset{\approx}{\mathtt{T}}$ is independent of space coordinates, it follows that

$$\mathbf{T}^{-1} \quad \nabla^2 \quad \mathbf{T} \quad \mathbf{N} = \mathbf{T}^{-1} \quad \mathbf{T} \quad \nabla^2 \quad \mathbf{N} = \nabla^2 \mathbf{N} \quad . \tag{A-11}$$



Therefore equation (A-10) becomes

$$\nabla^2 \mathbf{N} + \mathbf{T}^{-1} \quad \beta \quad \mathbf{T} \quad \mathbf{N} = \mathbf{T}^{-1} \quad \mathbf{S} \quad \frac{\rho^{\mathbf{S}}}{\mathbf{e}} . \tag{A-12}$$

Equation (A-12) reduces to two uncoupled differential equations for n_1 and n_2 if T is an orthonormal transformation that transforms β into a diagonalized form. The procedure associated with determining T is the subject of the next few paragraphs.

The eigenvalues of $\underset{\alpha}{\beta}$ are solutions to characteristic equation of $\underset{\alpha}{\beta}$

$$\lambda^{2} - (\beta_{e}^{2} + \beta_{i}^{2})\lambda + \beta_{e}^{2}\beta_{i}^{2} - \frac{\omega_{e}^{2}\omega_{i}^{2}}{v_{e}^{2}v_{i}^{2}} = 0$$
 (A-13)

or

$$\lambda_{1,2} = \frac{1}{2}(\beta_e^2 + \beta_i^2) + \frac{1}{2}\sqrt{(\beta_e^2 - \beta_i^2)^2 + 4\frac{\omega_e^2\omega_i^2}{v_e^2v_i^2}}.$$
(A-14)

The problem now is to find the transformation T such that

$$\mathbf{T}^{-1} \underset{\approx}{\beta} \mathbf{T} = \begin{bmatrix} \lambda_1 & 0 \\ 0 & \lambda_2 \end{bmatrix} \tag{A-16}$$

From the theory of matrix algebra

$$\mathbf{T} = \begin{bmatrix} \mathbf{T}_{11} & \mathbf{T}_{12} \\ \mathbf{T}_{21} & \mathbf{T}_{22} \end{bmatrix} = \begin{bmatrix} \mathbf{T}^1 & \mathbf{T}^2 \end{bmatrix}$$

where \underline{T}^1 and \underline{T}^2 are the eigenvectors associated with λ_1 and λ_2 , respectively. \underline{T}^1 and \underline{T}^2 are solutions to the matrix equations

$$\left(\beta - \lambda_{1}\right) \quad \tau^{1} = 0 \tag{A-16}$$

and

$$\left(\beta - \lambda_{2z}\right) \quad z^2 = 0 \quad . \tag{A-17}$$

Equations (A-16) and (A-17) reduce to one relationship each for the two unknowns of the eigenvectors \mathbf{T}^1 and \mathbf{T}^2 , respectively. In order to completely specify the transformation we choose to normalize the eigenvectors, i.e.,

$$T^{i} \cdot T^{i} = T_{1i}^{2} + T_{2i}^{2} = 1, i = 1, 2.$$
 (A-18)

In what follows a commonly reoccurring term will be specified by $\mathbf{A}_{\mathbf{O}}$ where

$$A_{O} = \sqrt{(\beta_{i}^{2} - \beta_{e}^{2})^{2} + 4 \frac{\omega_{e}^{2} \omega_{i}^{2}}{v_{e}^{2} v_{i}^{2}}}.$$
 (A-19)

The matrix equation (A-16) reduces to the single relationship

$$T_{21} = -\frac{1}{2} \frac{V_e V_i}{\omega_e \omega_i} [\beta_e^2 - \beta_i^2 - A_o] T_{11}$$
 (A-20)

which together with equation (A-18) defines T_{11} and T_{21} as follows

$$T_{11} = \frac{1}{\sqrt{1 + \frac{1}{4} \frac{v_e^2 v_i^2}{\omega_e^2 \omega_i^2} \left[\beta_e^2 - \beta_i^2 - A_o\right]^2}}$$
 (A-21)

$$T_{21} = -\frac{1}{2} \frac{v_{e}v_{i}}{\omega_{e}\omega_{i}} \frac{\beta_{e}^{2} - \beta_{i}^{2} - A_{o}}{\sqrt{1 + \frac{1}{4} \frac{v_{e}^{2}v_{i}^{2}}{\omega_{\omega}^{2} \left[\beta_{e}^{2} - \beta_{i}^{2} - A_{o}\right]^{2}}}.$$
(A-22)

Similarly, equations (A-17) and (A-18) define \mathbf{T}_{12} and \mathbf{T}_{22} as follows

$$T_{12} = \frac{1}{\sqrt{1 + \frac{1}{4} \frac{v_e^2 v_i^2}{\omega_e^2 \omega_i^2} \left[\beta_e^2 - \beta_i^2 + A_o\right]^2}}$$
 (A-23)

$$T_{22} = -\frac{1}{2} \frac{v_e v_i}{\omega_e \omega_i} \frac{\beta_e^2 - \beta_i^2 + A_o}{\sqrt{1 + \frac{1}{4} \frac{v_e^2 v_i^2}{\omega_e^2 \omega_i^2} \left[\beta_e^2 - \beta_i^2 + A_o\right]^2}}.$$

(A-24)

For this development it is necessary that det $\mathbf{T} \neq 0$ as assumed earlier. We are now able to calculate det \mathbf{T} as follows:

$$\det T = T_{11} T_{22} - T_{12} T_{12} = -1$$
 (A-25)

Therefore T^{-1} exists and can be written as

$$\mathbf{T}^{-1} = \begin{bmatrix} -\mathbf{T}_{22} & \mathbf{T}_{12} \\ \mathbf{T}_{21} & -\mathbf{T}_{11} \end{bmatrix}$$
 (A-26)

 $^{n}\mathrm{e}$ and $^{n}\mathrm{i}$ can now be written in terms of $^{n}\mathrm{l}$ and $^{n}\mathrm{2}$ and visa versa as follows

$$n_e = \frac{\omega_e}{V_e} (T_{11}n_1 + T_{12}n_2)$$
 (A-27)

$$n_{i} = \frac{\omega_{i}}{V_{i}} (T_{21}n_{1} + T_{22}n_{2})$$
 (A-28)

and

$$n_1 = -\frac{v_e}{\omega_e} T_{22} n_e + \frac{v_i}{\omega_i} T_{12} n_i$$
 (A-29)

$$n_2 = \frac{v_e}{\omega_e} T_{21}^n e - \frac{v_i}{\omega_i} T_{11}^n i$$
 (A-30)

Equation (A-12) can now be written as two linear uncoupled differential equations

$$\nabla^2 n_1 + k_1^2 n_1 = s_1 \frac{\rho^S}{e}$$
 (A-31)

$$\nabla^2 n_2 + k_2^2 n_2 = S_2 \frac{\rho^S}{e}$$
 (A-32)

where

$$k_1^2 = \frac{1}{2} [\beta_e^2 + \beta_i^2 + A_o],$$
 (A-33)

$$k_2^2 = \frac{1}{2} [\beta_e^2 + \beta_i^2 - A_o],$$
 (A-34)

$$s_1 = + T_{22} \frac{\omega_e}{V_e} + T_{12} \frac{\omega_i}{V_i}$$
, (A-35)

and

$$s_2 = -T_{21} \frac{\omega_e}{V_e} - T_{11} \frac{\omega_i}{V_i}$$
 (A-36)

Equations (A-27), (A-28), (A-31), (A-32), (A-33), (A-34), (A-35), and (A-36) are a tractable set of equations whose solutions specify the electron and ion perturbations in an infinite homogeneous plasma due to charge density source ρ^{S} immersed in the plasma. The conclusion is that two independent particle waves are able to propagate in an infinite plasma.

Let us look at the forms of T_{11} , T_{12} , T_{21} , T_{22} , k_1^2 , and k_2^2 in the high frequency and in the low frequency limits. For simplicity, let the ion- and electron-neutral particle collision frequencies equal zero, i.e., $\gamma_e = \gamma_i = 0$.

(a) High Frequency Limit ($\omega^2 > \omega_e^2 >> \omega_i^2$)

$$\beta_{e}^{2} \rightarrow \frac{\omega^{2}}{v_{e}^{2}} \left[1 - \frac{\omega_{e}^{2}}{\omega^{2}} \right], \quad \beta_{i}^{2} \rightarrow \frac{\omega^{2}}{v_{i}^{2}}$$

$$A_0 \rightarrow \frac{\omega^2}{v_1^2} - \frac{\omega^2}{v_2^2} - \frac{\omega_e^2}{v_2^2}$$
.

In this limit

$$k_{1}^{2} \approx \frac{1}{2} \left[\frac{\omega^{2}}{v_{1}^{2}} + \frac{\omega^{2}}{v_{e}^{2}} \left[1 - \frac{\omega_{e}^{2}}{\omega^{2}} \right] + \frac{\omega^{2}}{v_{1}^{2}} - \frac{\omega^{2}}{v_{e}^{2}} \left[1 - \frac{\omega_{e}^{2}}{v_{e}^{2}} \right] \right]$$

$$= \frac{\omega^{2}}{v_{1}^{2}} \qquad (A-37)$$

$$k_{2}^{2} \approx \frac{1}{2} \left[\frac{\omega^{2}}{v_{1}^{2}} + \frac{\omega^{2}}{v_{e}^{2}} \left(1 - \frac{\omega_{e}^{2}}{\omega^{2}} \right) - \frac{\omega^{2}}{v_{1}^{2}} + \frac{\omega^{2}}{v_{e}^{2}} \left[1 - \frac{\omega_{e}^{2}}{v_{e}^{2}} \right] \right]$$

$$= \frac{\omega^{2}}{v_{e}^{2}} \left[1 - \frac{\omega_{e}^{2}}{\omega^{2}} \right] \qquad (A-38)$$

$$\beta_{e}^{2} - \beta_{1}^{2} + A_{o} \approx \frac{\omega^{2}}{v_{e}^{2}} \left[1 - \frac{\omega_{e}^{2}}{\omega^{2}} \right] - \frac{\omega^{2}}{v_{1}^{2}} + \frac{\omega^{2}}{v_{1}^{2}}$$

$$- \frac{\omega^{2}}{v_{e}^{2}} \left[1 - \frac{\omega_{e}^{2}}{\omega^{2}} \right] \approx 0 \quad .$$

 $\beta_e^2 - \beta_i^2 - A_o \approx 2 \left[\frac{\omega^2}{v_o^2} \left[1 - \frac{\omega_e^2}{\omega^2} \right] - \frac{\omega^2}{v_o^2} \right]$

Hence

$$T_{11} \approx 0$$

$$T_{21} \approx -1$$

$$T_{12} \approx 1$$

$$T_{22} \approx 0$$

From equations (A-29) and (A-30)

$$n_{1} \approx \frac{v_{i}}{\omega_{i}} n_{i} \tag{A-39}$$

$$n_2 \approx -\frac{V_e}{\omega_e} n_e \tag{A-40}$$

So in the high frequency limit n_1 is wave consisting of ion motion only and propagates with a phase velocity V_i which is the thermal velocity of the ions. Similarly, n_2 is an electron wave which propagates with the thermal velocity of the electrons.

(b) Low Frequency Limit (
$$\omega^2 << \omega_i^2 << \omega_e^2$$
)

$$\beta_e^2 = \frac{1}{v_e^2} (\omega^2 - \omega_e^2) \qquad \beta_i^2 = \frac{1}{v_i^2} (\omega^2 - \omega_i^2)$$

$$(\beta_{i}^{2} - \beta_{e}^{2})^{2} = \beta_{e}^{4} - 2\beta_{e}^{2}\beta_{i}^{2} + \beta_{i}^{2}$$

$$= \frac{1}{v_e^4} [\omega^4 - 2\omega^2 \omega_e^2 + \omega_e^4] - \frac{2}{v_e^2 v_i^2} [\omega^4]$$

$$- (\omega_{e}^{2} + \omega_{i}^{2})\omega^{2} + \omega_{e}^{2}\omega_{i}^{2} + \frac{1}{v_{i}^{4}} \left[\omega^{4} - 2\omega^{2}\omega_{i}^{2} + \omega_{i}^{4} \right]$$

$$= \left[\frac{\omega_{e}^{2}}{v_{e}^{2}} - \frac{\omega_{i}^{2}}{v_{i}^{2}} \right]^{2} - 2\omega^{2} \left[\frac{\omega_{e}^{2}}{v_{e}^{4}} - \frac{\omega_{e}^{2} + \omega_{i}^{2}}{v_{e}^{2}v_{i}^{2}} + \frac{\omega_{i}^{2}}{v_{i}^{4}} \right]$$

$$+ \omega^{4} \left[\frac{1}{v_{e}^{4}} - \frac{1}{v_{i}^{4}} \right]^{2}$$

where the first term on the right hand side is of the zeroth order in ω , the second term is of the 2nd order in ω , and the third term is of 4th order in ω .

Noting that $\omega_e^2 >> \omega_i^2$ and dropping 4th order terms in ω yields

$$(\beta_{i}^{2} - \beta_{e}^{2})^{2} \approx \left[\frac{\omega_{e}^{2}}{v_{e}^{2}} - \frac{\omega_{i}^{2}}{v_{i}^{2}}\right]^{2} - 2\omega^{2}\left[\frac{\omega_{e}^{2}}{v_{e}^{4}} - \frac{\omega_{e}^{2}}{v_{e}^{2}v_{i}^{2}} + \frac{\omega_{i}^{2}}{v_{i}^{4}}\right]$$

Therefore

$$A_{o} \approx \frac{1}{v_{e}^{2}v_{i}^{2}} \left[\left(\omega_{e}^{2}v_{i}^{2} + \omega_{i}^{2}v_{e}^{2} \right)^{2} - 2\omega^{2} \left(\omega_{e}^{2}v_{i}^{4} - \omega_{e}^{2}v_{e}^{2}v_{i}^{2} \right)^{2} + \omega_{i}^{2}v_{e}^{4} \right]^{\frac{1}{2}}$$

$$\approx \frac{\omega_{e}^{2}v_{i}^{2} + \omega_{i}^{2}v_{e}^{2}}{v_{e}^{2}v_{i}^{2}} \left[1 - 2\omega^{2} \frac{\omega_{e}^{2}v_{i}^{4} - \omega_{e}^{2}v_{e}^{2}v_{i}^{2} + \omega_{i}^{2}v_{e}^{4}}{\left(\omega_{e}^{2}v_{i}^{2} + \omega_{i}^{2}v_{e}^{2} \right)^{2}} \right]$$

$$\frac{\omega_{e}^{2} v_{i}^{4} - \omega_{e}^{2} v_{e}^{2} v_{i}^{2} + \omega_{i}^{2} v_{e}^{4}}{(\omega_{e}^{2} v_{i}^{2} + \omega_{i}^{2} v_{e}^{2})^{2}} = \frac{1}{\omega_{i}^{2}} \frac{T_{e}^{2} - T_{i} T_{e} + T_{i}^{2} \frac{m_{e}}{m_{i}}}{(T_{e} + T_{i})^{2}}$$

$$\leq \frac{1}{\omega_{i}^{2}}$$

where the underlined term is small and therefore it is dropped in the remaining calculations. By definition $\omega^2/\omega_i^2 << 1$, so using the binomial expansion and keeping only the first two terms

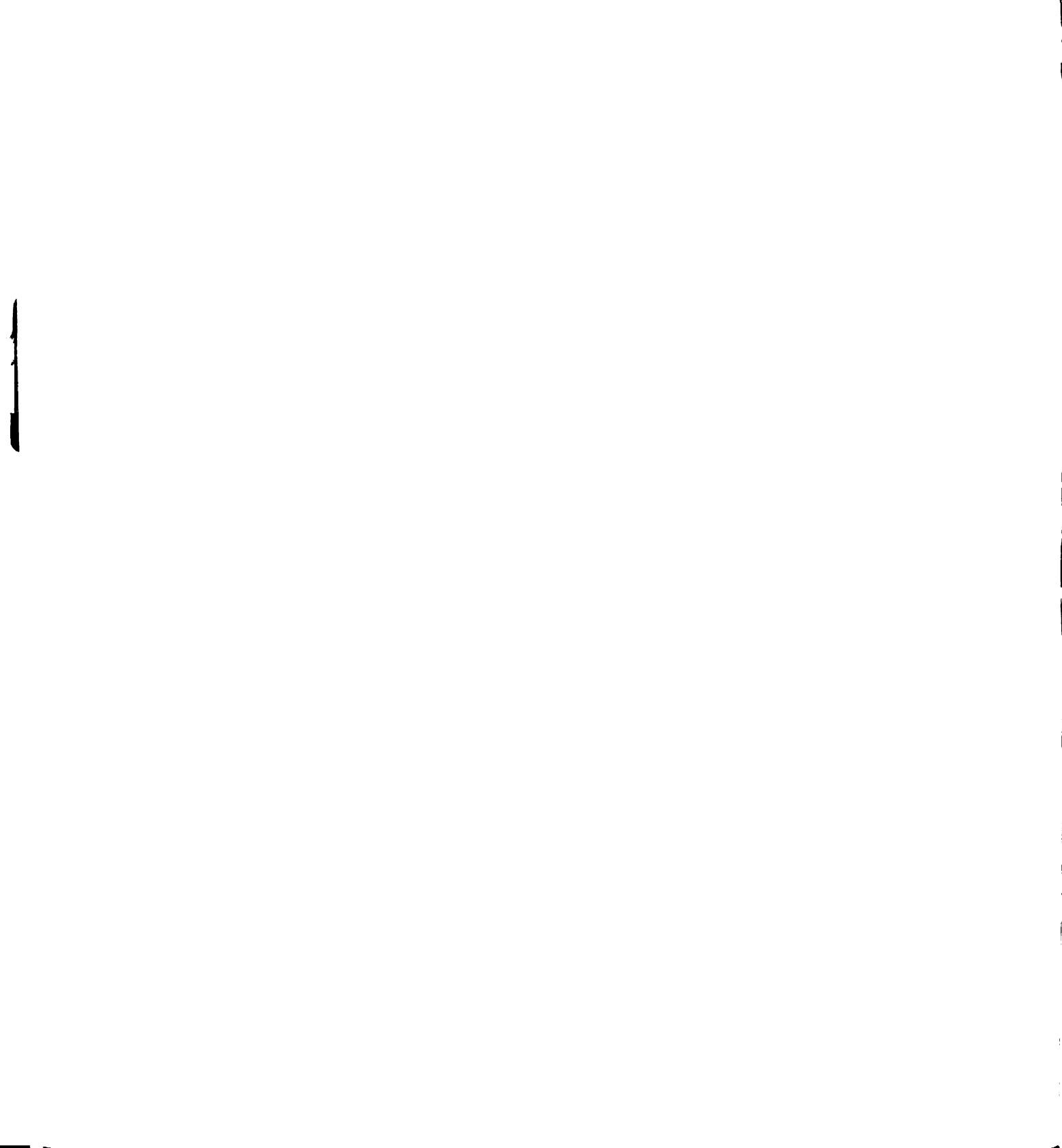
$$A_{O} \approx \frac{\omega_{e}^{2} v_{i}^{2} + \omega_{i}^{2} v_{e}^{2}}{v_{e}^{2} v_{i}^{2}} \left[1 - \omega^{2} \frac{\omega_{e}^{2} v_{i}^{4} - \omega_{e}^{2} v_{e}^{2} v_{i}^{2} + \omega_{i}^{2} v_{e}^{4}}{(\omega_{e}^{2} v_{i}^{2} + \omega_{i}^{2} v_{e}^{2})^{2}} + \dots \right]$$

Then

$$k_{1}^{2} = \frac{1}{2} \left\{ \frac{\omega^{2}}{v_{e}^{2}} - \frac{\omega_{e}^{2}}{v_{e}^{2}} + \frac{\omega^{2}}{v_{i}^{2}} - \frac{\omega_{i}^{2}}{v_{i}^{2}} + \frac{\omega_{e}^{2}}{v_{e}^{2}} + \frac{\omega_{i}^{2}}{v_{i}^{2}} - \frac{\omega_{i}^{2}}{v_{e}^{2}} + \frac{\omega_{e}^{2}}{v_{i}^{2}} + \frac{\omega_{i}^{2}}{v_{i}^{2}} - \frac{\omega_{i}^{2}}{v_{e}^{2}} + \frac{\omega_{i}^{2}}{v_{i}^{2}} + \frac{\omega_{i}^{2}}{v_{e}^{2}} + \frac{\omega_{i}^{2}}{v_{i}^{2}} + \frac$$

or

$$k_{1}^{2} \approx \frac{\omega^{2}}{2 v_{e}^{2} v_{i}^{2}} \left[\frac{v_{i}^{2} v_{e}^{2} v_{i}^{2} + \omega_{e}^{2} v_{i}^{2} v_{e}^{2} + \omega_{e}^{2} v_{e}^{2} v_{i}^{2}}{\omega_{e}^{2} v_{i}^{2} + \omega_{i}^{2} v_{e}^{2}} \right]$$



or dropping the small underlined term

$$k_1^2 \approx \frac{\omega^2 \omega_e^2}{\omega_e^2 v_i^2 + \omega_i^2 v_e^2} = \omega^2 / \left(v_i^2 + \frac{\omega_i^2}{\omega_e^2} v_e^2 \right)$$
 (A-41)

So the phase velocity of the n_1 wave is

$$v_{ph}^{1} = \sqrt{v_{i}^{2} + \frac{\omega_{i}^{2}}{\omega_{e}^{2}}} v_{e}^{2}$$

$$= \sqrt{\frac{3k(T_{i} + T_{e})}{m_{i}}}$$
(A-42)

$$k_{2}^{2} = \frac{1}{2} \left[\frac{\omega^{2}}{v_{e}^{2}} - \frac{\omega_{e}^{2}}{v_{e}^{2}} + \frac{\omega^{2}}{v_{i}^{2}} - \frac{\omega_{i}^{2}}{v_{i}^{2}} - \frac{\omega_{e}^{2}}{v_{e}^{2}} - \frac{\omega_{i}^{2}}{v_{i}^{2}} \right]$$

$$+ \frac{\omega^{2}}{v_{e}^{2}v_{i}^{2}} \frac{\omega_{e}^{2}v_{i}^{4} - \omega_{e}^{2}v_{e}^{2}v_{i}^{2} + \omega_{i}^{2}v_{i}^{2}v_{e}^{4}}{\omega_{e}^{2}v_{i}^{2} + \omega_{i}^{2}v_{e}^{2}}$$

$$k_2^2 \approx -\left[\frac{\omega_e^2}{v_e^2} + \frac{\omega_i^2}{v_i^2}\right]$$
 (A-43)

where the underlined terms are small and again they are dropped. k_2 is purely imaginary and hence the n_2 wave will not propagate in the low frequency limit.

$$\beta_e^2 - \beta_i^2 + A_o \approx 2 \frac{\omega_i^2}{V_i^2}$$

$$\beta_e^2 - \beta_i^2 - A_0 \approx -2 \frac{\omega_e^2}{V_e^2}$$

$$T_{11} \approx \frac{1}{\sqrt{2}} \frac{V_e^{\omega} i}{\omega_e V_i}$$

$$T_{12} \approx \frac{1}{\sqrt{2}}$$

$$T_{21} \approx \frac{1}{\sqrt{2}}$$

$$T_{22} \approx -\frac{1}{\sqrt{2}} \frac{V_e}{\omega_e} \frac{\omega_i}{V_i}$$
.

In an equilibrium plasma $(T_e = T_i)$

$$n_1 = \frac{1}{\sqrt{2}} \left[\frac{v_e}{\omega_e} n_e + \frac{v_i}{\omega_i} n_i \right]$$
 (A-44)

$$n_2 = \frac{1}{\sqrt{2}} \left[\frac{V_e}{\omega_e} \ n_e - \frac{V_i}{\omega_i} \ n_i \right]. \tag{A-45}$$

From equations (A-41), (A-43), (A-44), and (A-45) we see that in the low frequency limit only the n_1 wave exists and it consists of both electron and ion motion.

APPENDIX B

SOME PROPERTIES OF LEGENDRE FUNCTIONS

APPENDIX B

SOME PROPERTIES OF LEGENDRE FUNCTIONS

Some properties of the associated and ordinary Legendre functions that are useful in this thesis are listed below.

- (1) P_n^1 (cos θ) is zero at $\theta = \frac{\pi}{2}$ if n is even.
- (2) P_n^1 (cos θ) is maximum at $\theta = \frac{\pi}{2}$ if n is odd and the value of this maximum is given by

$$P_{n}^{1}(0) = \begin{cases} \frac{2}{\sqrt{\pi}} \frac{\Gamma(\frac{n}{2} + 1)}{\Gamma(\frac{n}{2} + \frac{1}{2})} & \text{for } n = 1,5,9,\dots \\ -\frac{2}{\sqrt{\pi}} \frac{\Gamma(\frac{n}{2} + 1)}{\Gamma(\frac{n}{2} + \frac{1}{2})} & \text{for } n = 3,7,11,\dots \end{cases}$$
(B-1)

or

$$[P_n^1(0)]^2 = \frac{4}{\pi} \left[\frac{\Gamma(\frac{n}{2} + 1)}{\Gamma(\frac{n}{2} + \frac{1}{2})} \right]^2$$
 for n odd (B-2)

where $\Gamma(x)$ is the Gamma function with argument x.

(3) The associated Legendre functions have orthogonality properties,

$$\int_{-1}^{+1} P_n^1(x) P_m^1(x) dx = \begin{cases} 0 & \text{for } n \neq m \\ \\ \frac{2n(n+1)}{2n+1} & \text{for } n = m. \end{cases}$$
 (B-3)

(4) A recurrence formula for the ordinary Legendre functions is

$$\frac{d}{dx} P_{n+1}(x) - x \frac{d}{dx} P_n(x) - (n+1) P_n(x) = 0$$
 (B-4)

and a relationship between associated Legendre functions and ordinary Legendre functions is

$$P_n^m(x) = (-1)^m (1-x^2)^{m/2} \frac{d^m P_n(x)}{dx^m}$$
 (B-5)

For m = 1, equation (B-5) becomes

$$P_n^1 (\cos \theta) = \frac{d}{d\theta} P_n (\cos \theta).$$
 (B-6)

Combining equations (B-4) and (B-6) we obtain

$$\frac{1}{\sin\theta} \left[\cos\theta P_{\mathbf{n}}^{1}(\cos\theta) - P_{\mathbf{n}+1}^{1}(\cos\theta) \right] = (\mathbf{n}+1) P_{\mathbf{n}}(\cos\theta).$$
(B-7)

(5) A differentiation formula for the associated Legendre functions is

$$\frac{d}{d\theta} \left[P_n^1(\cos\theta) \right] = \frac{1}{\sin\theta} \left[n \ P_{n+1}^1(\cos\theta) - (n+1)\cos\theta P_n^1(\cos\theta) \right].$$
(B-8)

APPENDIX C

METHOD OF THE AUXILIARY INTEGRAL

APPENDIX C

METHOD OF THE AUXILIARY INTEGRAL [56]

In the numerical solution of input impedance Z in Chapter 7, singular integrals of the form

$$I_{O} = \int_{-\pi}^{\pi} \int_{0}^{h} \frac{e^{-jkR}}{R} \cos\phi \, dzd\phi \qquad (C-1)$$

where

$$R = [z^{2} + 4a^{2} \sin^{2} \frac{\phi}{2}]^{\frac{1}{2}}$$

$$a > 0 , h > 0$$
(C-2)

are often encountered. Integrals of this form can be handled using the method of the auxiliary integral.

Consider the result from an integration table

$$I_{1} = \int_{-\pi}^{\pi} \int_{0}^{h} \frac{\cos \frac{\phi}{2}}{R} dz d\phi$$

$$= 4 \left[\frac{h}{2a} \sinh^{-1} \frac{2a}{h} + \sinh^{-1} \frac{h}{2a} \right]$$
 (C-3)

which is called the auxiliary integral. Equation (C-1) can be rewritten as

$$I_0 = I_1 + (I_0 - I_1) = I_1 + I_2$$
 (C-4)

where

$$I_2 = \int_{-\pi}^{\pi} \int_0^h \frac{e^{-jkR} \cos\phi - \cos\frac{\phi}{2}}{R} dz d\phi \qquad (C-5)$$

The integrand of I, is nonsingular since

$$\lim_{R\to 0} \left[\frac{e^{-jkR} \cos \phi - \cos \frac{\phi}{2}}{R} \right] = -jk. \tag{C-6}$$

Therefore the numerical integration of I_2 , hence I_0 , can readily be carried out on the computer. Other singular integrals encountered in Chapters VI and VII are handled in the same manner.

APPENDIX D

THE INPUT RESISTANCE OF A VERY THIN CYLINDRICAL ANTENNA IN A HOT LOSSLESS PLASMA

APPENDIX D

THE INPUT RESISTANCE OF A VERY THIN CYLINDRICAL ANTENNA IN A HOT LOSSLESS PLASMA

In this appendix, we consider the solution for the zeroth order input resistance to a cylindrical antenna immersed in an infinite plasma. It is shown that, under appropriate assumptions, this resistance is the same as that derived by Chen [23] using a poynting vector method. The resistance can, under these assumptions, be broken into a component due to the electromagnetic wave and a component due to the electroacoustic wave.

From Chapter VI

$$R_{in} = \text{Real} \left\{ -j \sqrt{\frac{\mu_{o}}{\xi}} \frac{2}{\sin^{2} k_{e} h} \int_{-h}^{h} \sin k_{e} (h-|z'|) \right\}$$

$$\times \left[\cos k_{e} h K(0,z') - K(h,z') \right] dz' \qquad (D-1)$$

where

$$K(z,z') = \frac{1}{4\pi} \left\{ G_{e}(z,z') - \frac{\omega_{e}^{2}}{\omega(\omega-j\gamma)} \left[G_{p}(z,z') \right] \right\}$$

-
$$\cos k_e zG_p(0,z')$$

$$-k_{e} \int_{0}^{z} \sin k_{e}(z-z'')G_{p}(z'',z')dz'''$$

where

$$G_{e}(z,z') = \frac{1}{2\pi} \int_{-\pi}^{\pi} \frac{\exp[-jk_{e}R_{a}]}{R_{a}} d\phi'$$
 (D-3)

$$G_{p}(z,z') = \frac{1}{2\pi} \int_{-\pi}^{\pi} \frac{\exp[-jk_{p}R_{a}]}{R_{a}} d\phi'$$
 (D-4)

where

$$R_a = \sqrt{(z-z')^2 + (2a \sin \frac{\phi'}{2})^2}$$
 (D-5)

$$k_e^2 = \omega^2 \mu_0 \varepsilon_0 \left[1 - \frac{\omega_e^2}{\omega^2 + \gamma^2} - j \frac{\omega_e^2 \gamma}{\omega(\omega^2 + \gamma^2)} \right]$$
 (D-6)

$$k_{p}^{2} = \frac{\omega^{2}}{V_{0}^{2}} \left[1 - \frac{\omega_{e}^{2}}{\omega^{2}} - j \frac{\gamma}{\omega} \right].$$
 (D-7)

An assumption that we will make is that the antenna is very thin so that a line current is assumed to flow along the axis and the radius of the antenna, a, goes to zero. A second assumption is that the plasma is lossless, i.e., $\gamma = 0$.

With these assumptions, equations (D-2) through (D-7) become

$$K(z,z') = \frac{1}{4\pi} \left\{ G_{e}(z,z') - \frac{\omega_{e}^{2}}{\omega^{2}} \left[G_{p}(z,z') \right] \right\}$$

-
$$\cos k_e^{zG_p(0,z')}$$

$$-k_{e} \int_{0}^{z} \sin k_{e}(z-z'')G_{p}(z'',z')dz'' \bigg]$$
 (D-8)

$$G_{e}(z,z') = \frac{\exp[-jk_{e}R_{a}]}{R_{a}}$$
 (D-9)

$$G_{p}(z,z') = \frac{\exp(-jk_{p}R_{a})}{R_{a}}$$
 (D-10)

$$R_{a} = |z - z'| \tag{D-11}$$

$$k_e^2 = \omega^2 \mu_o \varepsilon_o \left[1 - \frac{\omega_e^2}{\omega^2} \right]$$
 (D-12)

$$k_{\rm p}^2 = \frac{\omega^2}{v_{\rm o}^2} \left[1 - \frac{\omega \frac{2}{e}}{\omega^2} \right],$$
 (D-13)

and the input resistance, Rin, may be written as

$$R_{in} = -\sqrt{\frac{\mu_{o}}{\xi}} \frac{2}{\sin^{2} k_{e}h} \int_{-h}^{h} \sin k_{e}(h-|z'|)T(z')dz'$$
(D-14)

where

$$T(z') = \frac{1}{4\pi} \left\{ \cos k_{e} h \frac{\sin k_{e} z'}{z'} - \frac{\sin k_{e} (h-z')}{h-z'} + \frac{\omega_{e}^{2}}{\omega^{2}} \left[\frac{\sin k_{p} (h-z')}{h-z'} - \cos k_{e} h \frac{\sin k_{p} z'}{z'} - k_{e} \int_{0}^{h} \sin k_{e} (h-z'') \frac{\sin k_{p} (z''-z')}{(z''-z')} dz'' \right] \right\}.$$
(D-15)

Let us rewirte R $_{\mbox{in}}$ in terms of five separate integrals and then examine each of the integrals separately. With γ = 0

$$\sqrt{\frac{\mu_{o}}{\xi}} = \frac{\sqrt{\mu_{o}/\epsilon_{o}}}{\sqrt{1 - \omega_{e}^{2}/\omega^{2}}} = \frac{120\pi}{\sqrt{1 - \omega_{e}^{2}/\omega^{2}}}, \quad (D-15)$$

so

$$R_{in} = 60 \left[1 - \frac{\omega_e^2}{\omega^2} \right]^{\frac{1}{2}} \frac{1}{\sin^2 k_e h} \left\{ -\cos k_e h I_1 + I_2 - \frac{\omega_e^2}{\omega^2} \left[I_3 - \cos k_e h I_4 - k_e I_5 \right] \right\}$$
 (D-16)

where

$$I_1 = \int_{-h}^{h} \sin k_e (h-|z'|) \frac{\sin k_e z'}{z'} dz'$$
 (D-17)

$$I_2 = \int_{-h}^{h} \sin k_e(h - |z'|) \frac{\sin k_e(h-z')}{h-z'} dz'$$
 (D-18)

$$I_3 = \int_{-h}^{h} \sin k_e(h - |z'|) \frac{\sin k_p(h-z')}{h-z'} dz'$$
 (D-19)

$$I_4 = \int_h^h \sin k_e (h - |z'|) \frac{\sin k_p z'}{z'} dz'$$
 (D-20)

$$I_5 = \int_{-h}^{h} \sin k_e(h - |z'|) \int_{0}^{h} \sin k_e(h-z'')$$

$$\times \frac{\sin k_{p}(z"-z')}{(z"-z')} dz"dz'. \tag{D-21}$$

First, let us look at \mathbf{I}_1 . Using trigometric identities and making some changes of integration variables, \mathbf{I}_1 becomes

$$I_1 = \sin k_e h S_i(2k_e r) - \cos k_e h C_{in}(2k_e h)$$
 (D-22)

where the S_i and C_{in} functions are defined as

$$S_{i}(R) = \int_{0}^{R} \frac{\sin x}{x} dx \qquad (D-23)$$

and

$$C_{in}(R) = \int_0^R \frac{1 - \cos x}{x} dx$$
 (D-24)

Similarly, it can be shown that

$$I_{2} = \frac{1}{2} \sin 2k_{e}h \left[S_{i}(4k_{e}h) - S_{i}(2k_{e}h) \right]$$

$$+ \frac{1}{2}(1 + \cos 2k_{e}h) C_{in}(2k_{e}h)$$

$$- \frac{1}{2} \cos 2k_{e}h C_{in}(4k_{e}h), \qquad (D-25)$$

$$I_3 = \frac{1}{2} \sin 2k_e h \left[S_i(2k_p h) - S_i(k_p h) \right]$$
 (D-26)

$$I_4 = 2 \sin k_e h S_i(k_p h),$$
 (D-27)

and

$$I_{5} = S_{i}(k_{p}h) \left[h - \frac{1}{k_{e}} \sin 2k_{e}h + h \cos 2k_{e}h \right]$$

$$+ S_{i}(2k_{p}h) \left[\frac{1}{2k_{e}} \sin 2k_{e}h - h \cos 2k_{e}h \right] \qquad (D-28)$$

where we have assumed that $k_p >> k_e$ and $k_p >> 1$. Therefore

$$R_{in} = 60 \left[1 - \frac{\omega_{e}^{2}}{\omega^{2}} \right]^{-\frac{1}{2}} \frac{1}{\sin^{2} k_{e}h} \left(-\frac{1}{2} \cos 2k_{e}h C_{in}(4k_{e}h) + [1 + \cos 2k_{e}h] C_{in}(2k_{e}h) + \frac{1}{2} \sin 2k_{e}h[S_{i}(4k_{r}h) - 2S_{i}(2k_{e}h)]$$

$$+ \frac{\omega_{e}^{2}}{\omega^{2}} \left\{ \frac{1}{2} \sin 2k_{e}h \left[s_{i}(2k_{p}h) - s_{i}(k_{p}h) \right] \right.$$

$$+ \sin 2k_{e}h s_{i}(k_{p}h) + k_{e}s_{i}(k_{p}h) \left[h - \frac{1}{k_{e}} \sin 2k_{e}h \right]$$

$$+ h \cos 2k_{e}h + k_{e}s_{i}(2k_{p}h) \left[\frac{1}{2k_{e}} \sin 2k_{e}h \right]$$

$$- h \cos 2k_{e}h$$

$$- h \cos 2k_{e}h$$

$$+ \cos 2k_{e}h$$

$$+ \cos 2k_{e}h$$

$$+ \cos 2k_{e}h$$

$$+ \cos 2k_{e}h$$

For the system we are discussing, i.e., antennas of the order of $\omega\mu_0\epsilon_0h$ = 1, k_ph is a very large number. By definition

$$S_{i}(\infty) = \frac{\pi}{2} \tag{D-30}$$

so we can reasonably use the approximation

$$S_{i}(k_{p}h) \approx \frac{\pi}{2}$$
 (D-31)

With this approximation, equation (D-29) becomes

$$R_{in} = 30 \left[1 - \frac{\omega_{e}^{2}}{\omega^{2}} \right]^{-\frac{1}{2}} \frac{1}{\sin^{2} k_{e}h} \left\{ -\cos 2k_{e}h C_{in}(4k_{e}h) + 2\left[1 + \cos 2k_{e}h \right] C_{in}(2k_{e}h) + \sin 2k_{e}h \right.$$

$$\times \left[S_{i}(4k_{e}h) - 2S_{i}(2k_{e}h) \right] + \frac{\omega_{e}^{2}}{\omega^{2}} \frac{\pi}{2} \left[\sin 2k_{e}h + 2k_{e}h \right] \right\}. \tag{D-32}$$

Comparing equation (D-32) with the results of Chen [23] we can identify an electromagnetic component of the input resistance of a cylindrical dipole antenna as

$$R_{e} = 30 \left[1 - \frac{\omega_{e}^{2}}{\omega^{2}} \right]^{-\frac{1}{2}} \frac{1}{\sin^{2} k_{e}h} \left\{ -\cos 2k_{e}h C_{in}(4k_{e}h) + 2 \left[1 + \cos 2k_{e}h \right] C_{in}(2k_{e}h) + \sin 2k_{e}h \right]$$

$$\times \left[S_{i}(4k_{e}h) - 2 S_{i}(2k_{e}h) \right]$$
(D-33)

and a plasma component of the input resistance as

$$R_{p} = 15\pi \frac{\omega_{e}^{2}}{\omega^{2}} \left[1 - \frac{\omega_{e}^{2}}{\omega^{2}} \right]^{-\frac{1}{2}} \frac{1}{\sin^{2} k_{e}h} \left[2k_{e}h + \sin 2k_{e}h \right].$$
(D-34)

Equations (D-33) and (D-34) are exactly the form of the corresponding radiation resistances derived by Chen [23].

